AIRFLOW CHARACTERISTICS OF MODULATED LOUVERED WINDOWS WITH REFERENCE TO THE ROWSHAN OF JEDDAH, SAUDI ARABIA

Thesis submitted in accordance with the requirements of the University of Sheffield for the degree of Doctor of Philosophy by:

Amjed Abdulrahman Maghrabi

B. Arch., Umm Al-Qura University, Makkah, Saudi Arabia
M. Arch, University of Colorado at Denver, Colorado, USA

School of Architecture

University of Sheffield

August 2000

بسم الله الرحمن الرحيم

إهـــــــــــــــــداء

إلى اللذين سهرا من أجل راحتي

إلى اللذين ضحى بكل مالديهم من أجل تعليمي

إلى اللذين إحتملا غربتي عنهم كل هذه السنين

إلى أمّـــــي ... إلى أبـــــي

أهدي هذا العمل

أمجـد

Abstract

The main aim of this research project is to assess the potential of the modulated louvered windows (MLW) to provide ventilation as a cooling source to achieve thermal comfort inside buildings. It presents an intensive analysis of the characteristics of airflow as function of the various MLW parameters in order to provide designers with practical information about the performance of MLW in the control of natural ventilation inside the room. Some initial studies suggested the significance of adjustable horizontal louvered windows, or the MLW as they are referred to in this research, as an effective technique for the control of natural ventilation beside the other Environmental issues.

In Jeddah, Saudi Arabia, the shelter adaptation to the hot-humid climate was achieved by employing a number of passive solutions, one of which, the MLW constructed in the Rowshan, was considered a main elevation treatment. The Rowshan, a projected window bay, covered in this study is constructed with adjustable louvers in a number of sashes arranged in rows and columns to control and alter breeze to the desired level inside the room. The Rowshan is also credited with controlling other environmental factors and is supposed to reflect social necessities.

This thesis has investigated the airflow characteristics of the MLW with reference to the Rowshan of Jeddah, Saudi Arabia. After reviewing the previous efforts and prediction techniques concerned, the research has conducted a series of experiments including laboratory and computation fluid dynamics (CFD) appraisal stages. The laboratory stage included the evaluation of the pressure drop (ΔP) and the velocity drop ($v_i/v_e\%$) characteristics across the MLW. The pressure drop was examined under various airflow rates (Q) using the depressurising test chamber technique. The velocity drop ($v_i/v_e\%$) was examined under various prevailing wind conditions using the test chamber technique. This appraisal stage covered also the room configuration and its contribution to this effect. On the other hand, the CFD measurement has examined the viability of CFD coding to simulate airflow around the reviewed MLW. The predicted results obtained from CFD were compared against those obtained from the laboratory. Consequently, an intensive evaluation of airflow patterns of the common Rowshan configurations, including the plain and projected Rowshans, employed in Jeddah in conjunction with various outlet types was conducted.

From the literature review, it has been concluded that the MLW played a major role in the provision and the control of natural ventilation in the traditional architecture of Jeddah, Saudi Arabia. The various appraisal stages showed that parameters such as louver inclination, aperture between louver blades and the free area of the MLW were more significant variables than the depth of louver blades. Nevertheless, the major pressure and velocity drops were not due to individual variable but rather to the combination of variables that would comprehensively describe ΔP and $v_i/v_e\%$ across the MLW.

Practically, the design of the modulated louvered windows must give consideration to those variables that play an important role in altering airflow characteristics inside the room. It should also have an element of flexibility as this enables designers to approach their window treatments with a number of choices whilst retaining similar ventilation performances. Airflow velocities in a room containing an MLW result from an interaction of louver geometry, room geometry and prevailing wind conditions. As far as the Rowshan configuration was concerned, the plain Rowshan was generally better than the projected Rowshan. Yet the flow in the living zone could be enhanced by correctly sizing the projected Rowshan. Finally, CFD analysis has been successfully used to predict air velocities in the region close to the MLW side.

Acknowledgment

I am particularly indebted to my parents: my Father, Abdulrahman M. Maghrabi and my Mother, Zakiah A. Halwani. I believe that this achievement is the result of their continuous love, support and prayers for my success. Their consent to the absence of their son for a long period is greatly appreciated. I hope that I will shortly compensate them for some of this.

I am also particularly indebted to both Prof. S. Sharples, *my former supervisor*, and Prof. P.R. Tregenza, *my current supervisor*. Their constant assistance, supervision, and constructive criticism have played a significant role in the production of this thesis. I am also grateful to Dr. A. C. Pitts and Mr. I. C. Ward for their help at different phases of this research. I wish also to thank the staff, the technicians and my colleagues in the School of Architecture for their help.

My appreciation to many people who also helped me, with great patience and kindness, during the various phases of this research: Dr. O. Azhar, Dr. D. Suker, Arch. A. Khoj, Dr. F. Al-Shareef, Mr. M. Limb, Dr. D. Thiam, Dr. K. Al-Barrak, Dr. M. Gadi and others. I also owe a great deal to the continuous support, courage and advice of my brother Dr. Aimen Maghrabi. Likewise, I cannot forget the rest of my bothers and sisters Ms. Omaymah, Mr. Mahmoud, Ms. Eman, Mr. Hesham and Dr. Ashraf.

Last but not the least, I am indebted to my wife who has endured a lot to keep me relaxed and concentrated throughout in my PhD work. My children: Ammar, Abrrar, Abdulrahman, Albarra and loujayne, *in whom I see my future*, have also endured during my graduate studies, and I promise to compensate them for all of this in the near future.

TABLE OF CONTENTS

CHAPTER 5: THE MODULATED LOUVERED WINDOWS AND THE ROWSHAN PARAMETERS

CHAPTER 6: PRESSURE DROP ACROSS THE MODULATED LOUVERED WINDOWS

LIST OF TABLES

LIST OF FIGURES

LIST OF APPENDICES

Appendix A: Natural ventilation in Architecture

Appendix B: Pressure drop across the modulated louvered windows.

Appendix C: Velocity drop across the modulated louvered windows.

Appendix D: Computational Fluid Dynamics appraisal stage.

NOMENCLATURE

a	Constant proportional to the effective leakage area of the crack (m^3/s Pa),
A	Opening area (m^2) or Flow coefficient for fully developed laminar friction losses [(Pa s)/m^3] (depending on application).
A_f	Free area (m^2)
A_1	Inlet area (m^2)
A_2	Internal opening area (m^2)
A_n	Outlet area (m^2)
B	Coefficient of entry, exit and turbulent flow losses [(Pa s^2)/m^6].
C	Coefficient obtained from experimental measurements
C_ε	Turbulence model constant
C_d	Discharge coefficient of an opening.
C_p	Static pressure coefficient
C_{pl}	Leeward pressure coefficient
C_{pw}	Windward pressure coefficient
C_Q	Flow coefficient
d	Gap thickness between louver plates (m)
D	Summation of gaps between louvers $\sum_{n}^{1} d$ (m).
f	Expansion Factor
F_j	External body forces (N)
g	Gravitational acceleration (m/s^2)
G_κ	Rate of production of turbulent kinetic energy.
K	Head loss
L	Breadth of the plate or structure (depending on application) (m)
L_c	Segment length
mV	Mill-voltage signals
n	Number of openings in series or an exponent (depending on application).
N	Number of louvers
N_c	Number of cells in the segment
p	porosity percentage (%)
P	Pressure (Pa)
P_w	Wind pressure (Pa)
Q	Volumetric flow of air (m3/s)
Q_t	Flow rate due to infiltration (m^3/s).

Q_t Total flow rate including infiltration (m^3/s)

r^2 Coefficient of determination

R_d Room depth (m)

S_h Sash height (m)

S_l Sash length (m)

S_w Sash width (m)

t Time (s) or plate thickness(m) (depending on application)

T Temperature(C) or Summation of louver thickness (m) (depending on application)

T_i internal temperature(C)

T_o External (outside) temperature (C)

u Axial velocity (m/s)

v_e External air velocity (m/s)

v_i internal air velocity (m/s)

v_p Velocity reduction due to porosity of an MLW(m/s)

V_L Volume of louvers (m^3)

V_{new} Volume reduction due to louvers (m^3)

V Wind speed at opening level (m/s) or volume (m^3) (depending on application)

Vz Mean wind velocity at z height above the ground (roof level) (m/s)

$v_i/v_e\%$ Ratio of internal to external air velocity (%)

w_i Wind angle of incidence (“)

Y Factor depending on crack geometry.

z Plate length (m) or height above a horizontal reference datum (m) (depending on application)

Greek symbols

Δ Increment (dimensionless)

a Slope constant determined by the linear regression.

β Intercept constant determined by the linear regression.

c Intercept constant determined by the linear regression.

κ Thermal conductivity (W/m-K)

ρ Air density (Kg/m^3)

μ Dynamic viscosity (Kg/ms)

μ_t Turbulent viscosity (Kg/ms)

ɔ Shadow angle (“)

θ Inclination angle (^{o})

σ Stefan-Boltzmann constant (5.67×10^{-8} W/m^2-K^4)

ε Dissipation of κ (m^2/s^3)

Σ Summation of an element.

CHAPTER 1: INTRODUCTION

PAGE NUMBERING AS IN THE ORIGINAL THESIS

1.1. Preface

Architectural responses to climate have, throughout the history of building evolution, varied from one climatic zone to another. In hot humid climates, the environmental stresses and climatic hazards had influenced the architectural elements of the shelter into being more *responsive*. Techniques found in this climatic zone are of significance in producing comfort by using the natural means available in the environment. They were handed down through the generations and allowed to evolve through the process of elimination and adaptation. This man-made architecture was also governed by the social structure of the inhabitants and the availability of the natural resources in the settlement.

In modern architecture, people in the tropics have suffered from architectural solutions proposed by designers and engineers for whom the idea of respecting environment is quite alien. Those solutions were presumed to originate from the earlier forms, but the irony is that they turned out to be inappropriate for the climate. Nowadays, building production in the tropics is associated with a major increase in labour, materials, and huge energy waste to meet human standards of comfort, which in turn influences the environment and its quality.

Recently, the prevailing trend towards a sustainable environment has become a global task. People working in areas related to environment have been urged to review their approaches and methods to resolve the problems unintentionally caused to the environment. In architecture this task is implemented in the process of developing passive and low energy alternatives in the building engineering. Wind-induced natural ventilation is one of the alternatives to relieve climatic stress and at the same time to reduce energy

usage in hot humid climates. In the vast majority of the Arabian countries, the ongoing trend to implement old-fashioned techniques in the modern buildings started in the 1980's.

In hot humid climates allowing as much breeze as possible to cross through the enclosure of the building is the strategic technique for achieving thermal comfort requirements. The case study presented in this thesis in the city of Jeddah, Saudi Arabia reveals the same principles. Jeddah is one of the major coastal cities in Saudi Arabia and is located on the western border of the country. Traditionally, modulated louvered windows (MLW) are the common apertures that are employed in houses to cover part or the entire elevation in the form of split units or in the form of the Rowshan, a projected window bay. Some initial analysis suggested that this window accessory is believed to provide the optimum ventilation cooling to occupants indoors and to act as a protecting shield from direct solar radiation through its simple and yet magnificent geometry. Its application also reveals some sociological requirements. In this context, the design of this window treatment should be given the utmost attention in these climatic zones. Nevertheless, the body of literature pertaining to the MLW deals more with the anthropological developments, visual appearance and daylighting performances. On the other hand, the efforts made to exhibit the natural ventilation performance of this window type suggested the appropriateness of this technique to the warm and humid environments and specifically where cross ventilation is required. However, the amount of research that deeply investigates airflow characteristics as a function of the various MLW configurations is very limited in scope and therefore by no means complete. The literature review in this thesis has addressed the issue that this window system still lacks intensive scientific analysis and thus further comprehensive analysis is needed to highlight the contribution of MLW various parameters that govern airflow indoors.

This study sets out to ascertain that MLW was a major climatic control in hot humid climates to produce cross ventilation within various parts of the building and therefore the potential and the parametric performance of the MLW as a mean of alleviating airflow within in the traditional architecture of Jeddah, Saudi Arabia is needed to be investigated further.

1.2. Aims of the research

Two sources of wind-induced natural ventilation including the pressure drop (ΔP) and the velocity drop ($v_i/v_e\%$) across the MLW are the criterion element of this study. The research is assessing the potential of the modulated louvered windows to provide ventilation as a cooling source to achieve thermal comfort inside the buildings.

The research aims and objectives were divided into a number of areas as follow:

- **Encourage the use of natural ventilation techniques:**

    1. Review the methods to control natural ventilation that have been employed in the traditional house in Jeddah.
    2. Address the main architectural element that enhanced cross ventilation within the traditional house.

- **Present technical analysis of the potentials of the MLW:**

    1. Deeply investigate the various parameters of the modulated louvered windows (MLW) and their contribution to the governing of airflow characteristics indoors with respect to pressure and velocity drops.

2. The thorough investigation of the overall performance in relation to integrating all variables of the MLW.

- **Present practical information for the designers:**

1. Address the critical MLW geometry at which airflow characteristics would experience a significance reduction.
2. The velocity drop as function of prevailing wind conditions as well as the room depth up to certain distance behind louvers.
3. The schematic analysis of the patterns of airflow inside the room as function of the common Rowshan configurations employed in Jeddah is studied in conjunction with a number of outlet types. This is to find out the optimum configuration of the Rowshan from natural ventilation perspective.

The above aims and objectives of the investigation could not be accomplished without a suitable investigation and analysis tool. Therefore, within this context certain objectives are added:

1. To analyse the results obtained from the pressure drop appraisal stage using the two common model equations, the Power law and the Quadratic, and further to examine the coefficients embedded into them theoretically.
2. To examine the viability of using computational fluid dynamics (CFD) coding to simulate the airflow around the reviewed modulated louver windows.

1.3. Methodological approach

The author has followed the following methodological approach:

- Reviewed of climatic zones of Saudi Arabia and their diverse architectural responses. The climate and architecture of Jeddah was covered in detail and more emphasis was given to natural ventilation strategies and the bio-climatic needs to assess comfort in buildings.
- Reviewed the previous efforts and prediction techniques with direct relevance to the scope of this research. In this context, the fundamentals of airflow principles and natural ventilation in building were also reviewed.
- Visited a number of traditional buildings in Jeddah and performed direct measurements of the variety of modulated louvered windows configurations employed. Subsequently, a number of full-scale MLW models were constructed for further investigation. The model configurations corresponded to the most common configurations employed in Jeddah.
- Performed two experimental appraisal stages to evaluate the airflow characteristics across the MLW. Both appraisals took place at the University of Sheffield campus in the ventilation laboratory of the School of Architecture. The appraisals included the following:
    - Examining the pressure drop (ΔP) characteristics under various airflow rates (Q) using the depressurising test chamber technique.
    - Examining the velocity drop ($v_r/v_e\%$) characteristics under various prevailing wind conditions using the test chamber technique. This appraisal stage has also covered the room configuration and its contribution to this effect.
- The Rowshan structure is complex and its performance could not sufficiently be understood through physical measurements. This necessitated the use of another

technique in the field. The computational fluid dynamics (CFD) technique was then selected with an initial attempt to examine the viability of CFD coding to simulate the airflow around the reviewed modulated louver windows. Consequently, an intensive evaluation of the Rowshan components in conjunction of various outlet types was then studied.

- Drawn up conclusions and recommendations that will be guidelines for further research.

1.4. Research Approach

Chapter One is an introduction of the problem upon which the hypothesis is built. In this, the author is describing the scale of the problem in the modern architectural approaches in hot humid zones. The research aims and methodology is discussed in this chapter.

Chapter Two is devoted to highlighting the climatic adaptation to architecture for the regional context and in particular to natural ventilation approaches seeking to adapt the micro and macroclimate environments in Jeddah. It is believed that they would allow a better understanding of the bio-climatic environment and the thermal comfort requirements. The analysis of Rowshan's various components and configurations is also discussed in this chapter.

Chapter Three reviews the application of the modulated louvered windows in architecture and their preference over other window treatments. The literature review on the related research pertaining to the scope of current research along with its contributions and critiques are also discussed in the chapter. The conclusions derived from Chapter Two

and Chapter Three set the problem statement of the work in hand and stress the need for further analysis of this window treatment.

The principles in architectural aerodynamics including the common mathematical representations of wind-induced natural ventilation around and within buildings are established in Chapter Four. These will be taken as guidelines to establish the ground for further laboratorial and CFD appraisals carried out in the subsequent chapters.

Chapter Five sets out the various components of the MLW and the Rowshan obtained from the two visits to Jeddah conducted by the author as well from the available literature. Consequently, the various configurations of the full-scale MLW as well as the Rowshans that will be further examined are highlighted. The shading performance of the MLW examined and its effect on daylighting potentials based on solar data of sunpath diagram of Jeddah will be examined later in the chapter. A brief presentation of the reduction in the view angle as a function of the MLW configurations will then be followed. The chapter ends up with the arithmetical representations of each parameter as a function of the total reduction in volumetric flow.

The two laboratorial appraisals stages of pressure and velocity characteristics as functions of the reviewed MLW are placed respectively in Chapter Six and Chapter Seven of this thesis. Since the measuring technique was different, the experimental setup including calibrations of various instrumentations used and measuring principles will be discussed separately in each chapter. Similarly, the analysis and discussion of the contribution of MLW various parameters as well as the integration of the overall variables to this effect are discussed in details in each chapter.

Attempts to examine the CFD coding to simulate the airflow around the reviewed modulated louver windows is discussed in Chapter Eight. The first part of the chapter reviews the application of CFD in predicting airflow in buildings, the theory of numerical modelling, the range of CFD software packages used for simulation and justification of the selected CFD package. The second part is devoted to discussing the set up of MLW models configurations, the boundary conditions and the comparison of both CFD and velocity results obtained from Chapter Seven. This chapter ends up by highlighting the patterns of airflow within the room based on a number of common Rowshan configurations adapted in Jeddah.

The last chapter summarises the main conclusions and contributions of the thesis to the field of natural ventilation and emphasizes recommendations that are concluded from this research.

CHAPTER 2: THE REGIONAL CONTEXT

2.1. Introduction.

Wind-induced natural ventilation is a fundamental technique to achieve human comfort in humid climates. This chapter is devoted to highlighting the climatic adaptation of architecture to the regional context and in particular to natural ventilation approaches seeking to adapt the micro and macroclimate environments in Jeddah. A brief background is given first to the climatic features and their adaptations in the architecture of Saudi Arabia. Then comes the climate and architecture of Jeddah where the climatic variables are discussed more deeply since it is believed that they would allow a better understanding of the bio-climatic environment and its thermal comfort requirements. The traditional architecture and its distinguishing features will be discussed here, followed by the manipulation of natural ventilation approaches on the simple house scale as well as on the spatial structure of the entire settlement, i.e. macroclimate. The analysis of Rowshan's various components and configurations is discussed in the last section in this chapter as the main elevation treatment that served both climatic and social requirements.

2.2. The Climate and Architecture of Saudi Arabia

2.2.1. Geographical location

Saudi Arabia is one of the world's largest oil producers and exporters. It is one of the Middle-East countries and is located within the latitudes 16^{o} N to 32^{o} N at the border of the Asian continent near to Africa with an area of nearly 2,240,000sq.Km. Along the west border of Saudi Arabia there is the Red Sea which connects it to the African, European, North and South American continents. It is the longest border, approximately 1700Km, and extends from the Gulf of Aqaba in the north to Maydi in the south. To the East there is

the Arabian Gulf that extends from Ras-Mish'ab to Qatar and is 450Km long. Both northern and southern borders are land borders (Figure 2.1). Northern Saudi shares borders, which total 1300Km, with Jordan, Iraq and Kuwait. Oman and Yemen share the southern borders of Saudi Arabia which are 1200Km long. The geographical location and economical status of Saudi Arabia, added to its religious status as the home to Islam's two holiest shrines, shape its political agenda and give Saudi Arabia its uniqueness to the rest of the world.

Figure (2.1): The geographical map of Saudi Arabia, (Microsoft Encarta World Atlas, 1997)

2.2.2. Topography

Saudi Arabia is a tropical country that lies within the narrow belt between the Tropic of Cancer and the Tropic of Capricorn. It is mainly desert with few green spots and green areas with no permanent bodies of water or main rivers (Al Shareef, 1996). Regarding its topographical features, they are classified as follows:

2.2.2.1. Sarawat Mountains.

The mountains of Sarawat are located between Najd plateau and Tehamah plain. They are high mountains broken by great valleys such as Wadi-Fatimah and Wadi-Bishah. The Sarawat extend from the north with a height of 1,000m to the south near Asir where peaks rise up to 3,000m and stretch by the city of Madinah. They are the longest chain of mountains in Saudi Arabia.

2.2.2.2. Tehamah Plain.

This contains two plains; Tehamah and Hedjaz. This narrow plain is located along the western border of Saudi Arabia and lies parallel to the Red Sea. The maximum width of the plain is 40 miles in the south and narrows gradually, reaching 10 miles near the city of Al-Wajh in the north. The plain then extends towards The Gulf of Aqabah with a similar width. The plain and the mountains of Sarawat act as deflectors to the wind that is prevailing from the Red Sea (Al-Ansari et al. 1985).

2.2.2.3. *Najd Plateau.*

This is located in the middle of Saudi Arabia east of the Sarawat Mountains. Its peak reaches up to 2,000m above sea level with the elevation drops reaching nearly 700m

near Al-Dahna towards the Arabian Gulf. The plateau extends to the south towards Wadi Al-Dawaser and runs deep parallel to the Empty-Quarter (Al-Rubu Al-khali) (Figure2.1). More fertile lands are found on the Najd Plateau such as those in Qaseem, Kharj and Aflaj. To the north, the Najd Plateau extends for nearly 1500Km where there are a number of famous mountains such as the mountains of Aja, Salma and Towik. Further north stretch huge sandy hills, called the Al-Nufoud, which join the Iraqi and Jordanian borders.

2.2.2.4. Eastern Coastal Plain

This is a sandy plain that extends along the Arabian Gulf from north to south and shares borders with both Al-Dahna and the Empty-Quarter.

2.2.2.5. The Empty-Quarter (Al-Rubu Al-khali)

The world's largest area of continuous sand dunes is found in the Empty-Quarter (Al Shareef, 1996). It is a desert with no evidence of life as only minimum annual precipitation occurs.

2.2.3. Climatic zones and the architectural responses

Saudi Arabia is generally classified as a tropical climate where hot temperatures are predominant, "*Arid, desert land, with long, hot summers, and short, cool, winters*" (Al-Ansari et al. 1985).

The month of March marks the beginning of summer and October and November mark the beginning of winter (Al-Ansari et al. 1985). However, the distribution of land and sea masses and land heights has produced large varieties of climatic zones in Saudi

Arabia. The climatic zones, and hence the architectural responses to climate on dwelling and urban layout scales, are discussed here in brief.

2.2.3.1. Hot Dry Climatic Zone

2.2.3.1.1. The Climate

The desert that covers most parts of the region is mainly characterized by a hot dry climate. Arid and semi-arid desert climates are classified by the percentage of vegetation (Konya, 1980). Cities with hot dry and arid climates such as Riyadh and Makkah generally have two seasons; summer and winter. Humidity is low and temperatures range between 25 and 45°C during the day and night in summer, and between 20-30°C during winter. Skies are clear, no clouds most of the year and annual rainfall is insignificant. As a result, direct solar radiation is intense and is augmented by radiation reflected from barren, light-coloured terrain. The wind blows slowly during the morning; dust storms occur frequently in the afternoon.

2.2.3.1.2. The Architecture

Internal courtyards are constructed everywhere in hot arid regions (Winterhalter, 1982). A courtyard house simply acts as a central core connecting all other elements of the house. Besides privacy needs, the courtyard operates as a climate moderator as well as a natural lighting source. In a courtyard house, the daily temperature difference between inside and outside may reach up to 10°C (Maghrabi, 1993). This difference is crucial to the generation of an acceptable microclimate indoors when higher temperatures exist. In these regions, the body moisture evaporates easily since the relative humidity is very low, and hence, direct wind currents are not desirable (Evans, 1979). As stated by Kaizer

(1984), the courtyard in these climatic regions has three regular daily phases (Figure 2.2). The first occurs during night when cool air descends into the courtyard and fills surrounding rooms. As a result, walls, floors, columns, roofs, etc. remain cool until late afternoon. Then comes the second phase around noon. When the sun hits the courtyard floor, cool air sinks through surrounding rooms. While heat penetrates the thick walls, a pleasant and comfortable temperature is maintained inside. The last phase occurs in the afternoon when the courtyard and rooms become warmer. Then, as the sun sets in the

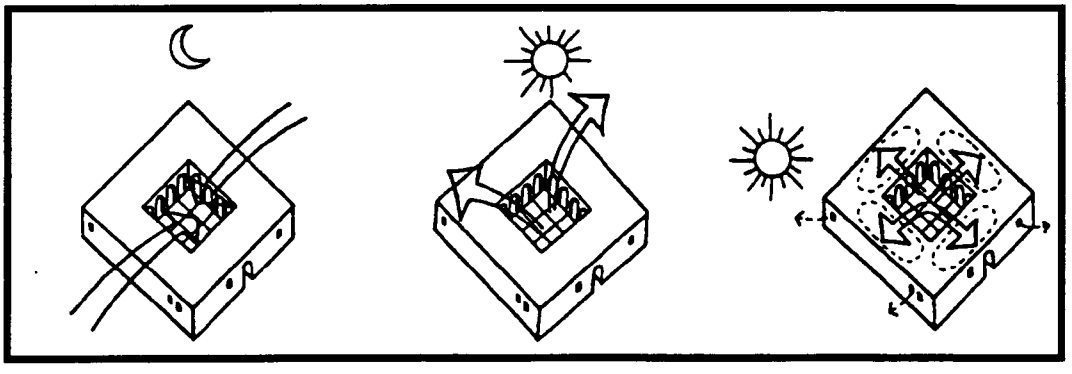

Figure (2.2): Diagrammatic illustrations of the three climatic phases (at night, noon and afternoon). (Kaizer, 1984)

desert, air temperature falls rapidly and colder air begins to flow. Thus, a new cycle begins. So, large interior openings overlooking the courtyard are found and smaller ones are located on exterior walls. An example of this could be found in Riyadh traditional dwellings (Hemeid, 1999). However, when larger openings are desired on exterior walls, such as those found in traditional dwellings in Makkah, Rowshans are used to allow cross ventilation, to provide privacy and to shelter occupants from direct sun radiations.

On the urban scale, several examples of compact urban form courtyard architecture can be found in Saudi Arabia. To shelter from solar radiation, courtyard houses are grouped together, sharing two or three walls with one another and forming narrow streets.

This arrangement allows walls to be less exposed to the sun. The compact urban form also helps reduce the effect of sand storms. In some cities, the neighbourhood is usually surrounded by a thick growth of palm trees which protect houses from sand storms (Figure 2.3)

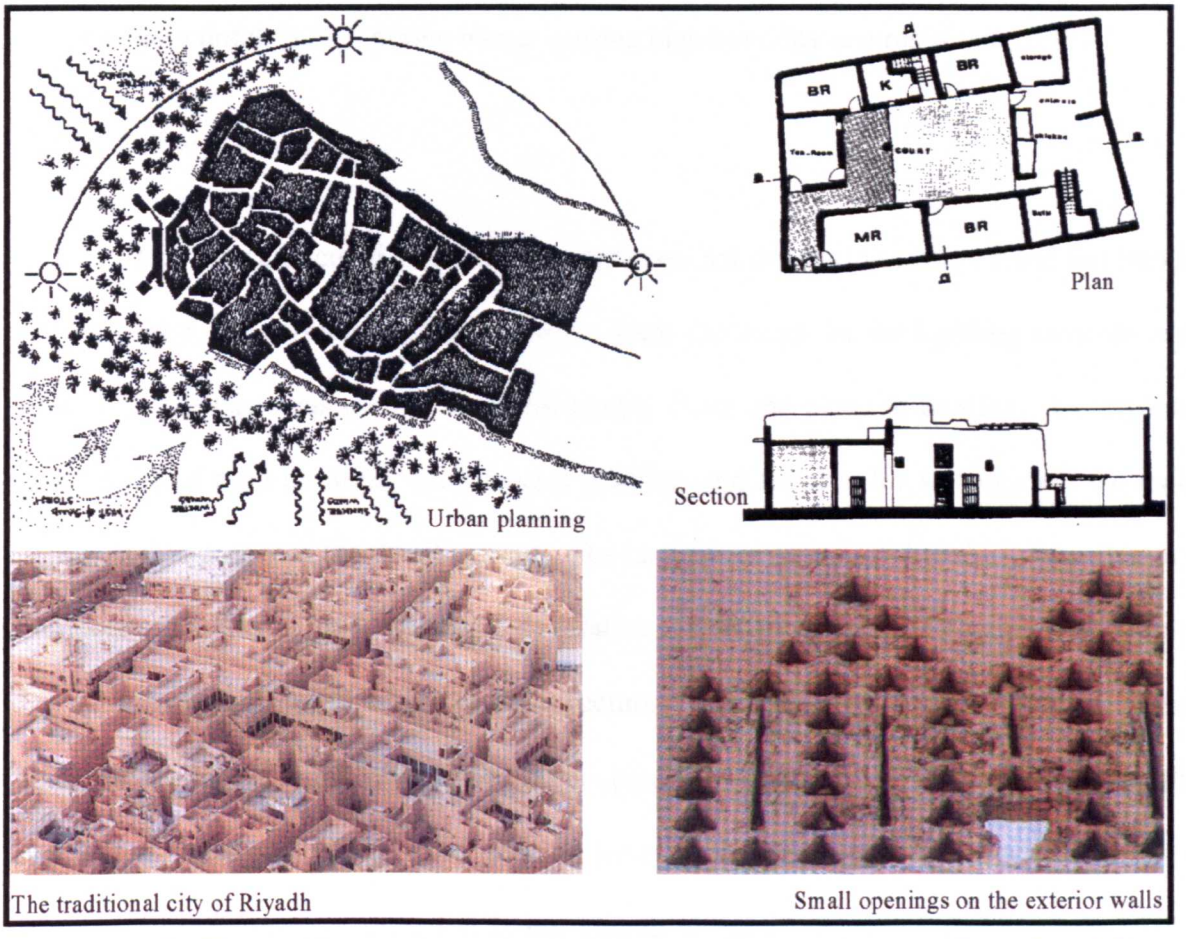

Figure (2.3): The architectural response to the hot arid climatic zone where found the courtyard house, smaller apertures on the exterior walls and the compact urban form surrounded by thick layers of palm trees to protect against frequent sandstorm. (Al-Hussaini and Al-Shoaibi 1989)

2.2.3.2. Composite Climatic Zone.

2.2.3.2.1. The Climate

Composite or monsoon climates are *" Neither consistently hot dry, nor warm and humid,"*, so they, *"Altering between long hot, dry periods to shorter periods of concentrated rainfall and high humidity"*(Koenigsberger et al. 1977). Eastern region of Saudi Arabia falls under this climatic zone where almost direct sun radiation with relatively low humidity during summer and rainfall is high during winter causing high humidity records(Kaizer, 1984).

2.2.3.2.2. The Architecture

Since climatic conditions fluctuate between hot dry during summer and hot humid during winter, the composite climate poses a great challenge for the building environment. Traditional design responses differ considerably from one place to another. Courtyards, thick walls of mud or stone, wind towers (badjirs) and terraces for sleeping are the main elements that compose the dwelling unit. The badjirs are meaningful to those who live in a composite climate. This is a vertical decorative element that works as cooling ventilators for both lower and upper levels of the structure. The mouth of a badjir usually extends some meters higher than the building and is opened towards the prevailing wind. From the ventilation point of view, wind towers have some preference over windows since prevailing wind speed or direction is not altered ahead of the tower (Al-Megren, 1987). The dampness occurring at lower floors is treated with cross ventilation through the Rowshans and other elevation apertures. For upper levels, which are usually the family living section, air entering through badjirs enhances comfort and reduces humidity (Figure 2.4). When natural ventilation is not desired, during extreme winter or summer conditions or sand storms, the badjir is closed with operable louvers or wooden boards.

The Iwan, a courtyard house surrounded by opening arcades, is another feature of a composite climate dwelling. Deep entrances and colonnaded passages around the courtyard provide cooling and shading. Providing cross ventilation in the dwelling has been considered essential. Enhanced cross ventilation throughout the building, particularly in lower levels, is an important consideration if the building is to last for centuries.

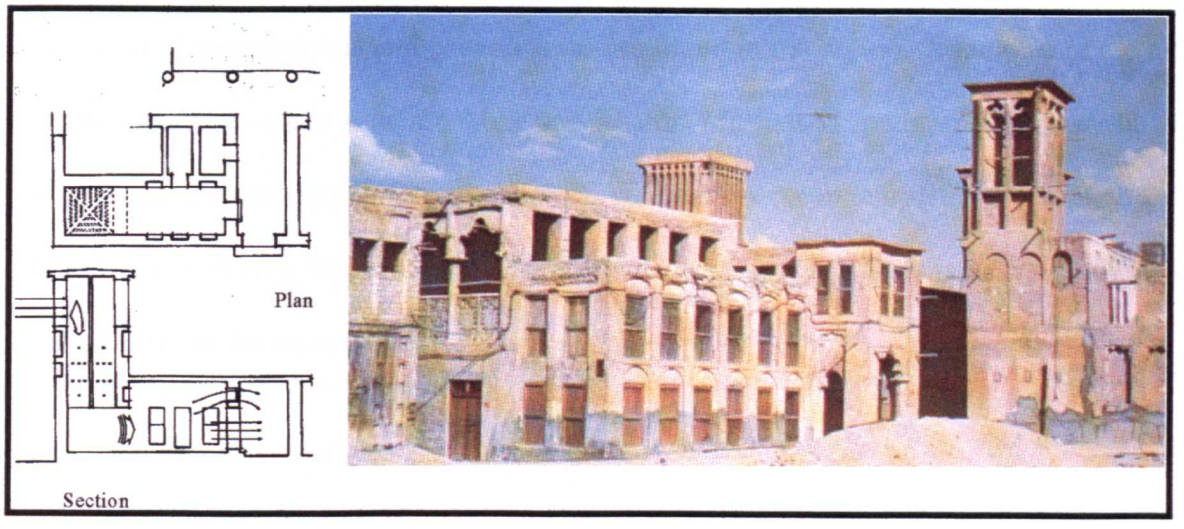

Figure (2.4): The Composite climatic zone where found the wind towers (badjirs) to catch the maximum breeze and direct it downwards. (Fathy & Sultan 1985; Unhwin 1981)

Due to the sun's radiation and sand storms that blow suddenly during the summer time, overhangs shelter outer spaces between buildings. Long and narrow streets are found. The traditional courtyard between buildings is protected from the sun by building heights and overhangs. Furthermore, the courtyard is naturally protected from unpleasant wind by narrow streets; pleasant cross-ventilated air moves slowly all day. The distribution of buildings and their surroundings is made to essentially protect most surfaces from direct sun radiation. A compact urban form has been considered to be the best solution for distribution of dwelling layout in this climatic zone (Kaizer, 1984).

2.2.3.3. Tropical Upland Climatic Zone

2.2.3.3.1. The Climate

This climate can be found in the southern region of Saudi Arabia. Although it is uncommon in the Arabian region, its influence on traditional architecture has been significant. Most of the zone lies at an average of 1,000-2,000m above sea level. Widespread mountainous and plateau areas are found in the region. Examples of the cities located in this climatic zone are Abha and Khamis Meshait in southern Saudi Arabia. The highest temperature might rise to over 40°C whereas the mean temperature is around 28°C. Due to considerable annual rainfall, humidity rises seasonally. Dew is heavy at night, and the ground has frosts in winter.

2.2.3.3.2. The Architecture

Despite the fact that the majority of the population has been concerned with farming, it is a wonder to see simple, yet magnificent traditional architecture in upland areas. Great similarity exists in building construction, materials, and urban planning of cities for those areas located in the tropical upland zone.

Tall buildings have been constructed due to climatic responses as well as for defensive purposes as shown in Figure 2.5. External windows in the upper floor are opened during summer to keep the house pleasantly cool. The upper floors are traditionally used for the family, while the lower floors are used for storage. Sun-dried bricks and adobe are commonly used for building construction providing strength and stability. Wall thickness of 0.6m provides insulation and stores heat during cool months. In the city of Abha, traditional builders have invented and developed a method to protect

thick adobe walls from regular heavy rainfalls. Flat stone pieces are put together in rows to protect mud walls from sun radiation during summer and from heavy rain in winter (Figure 2.5).

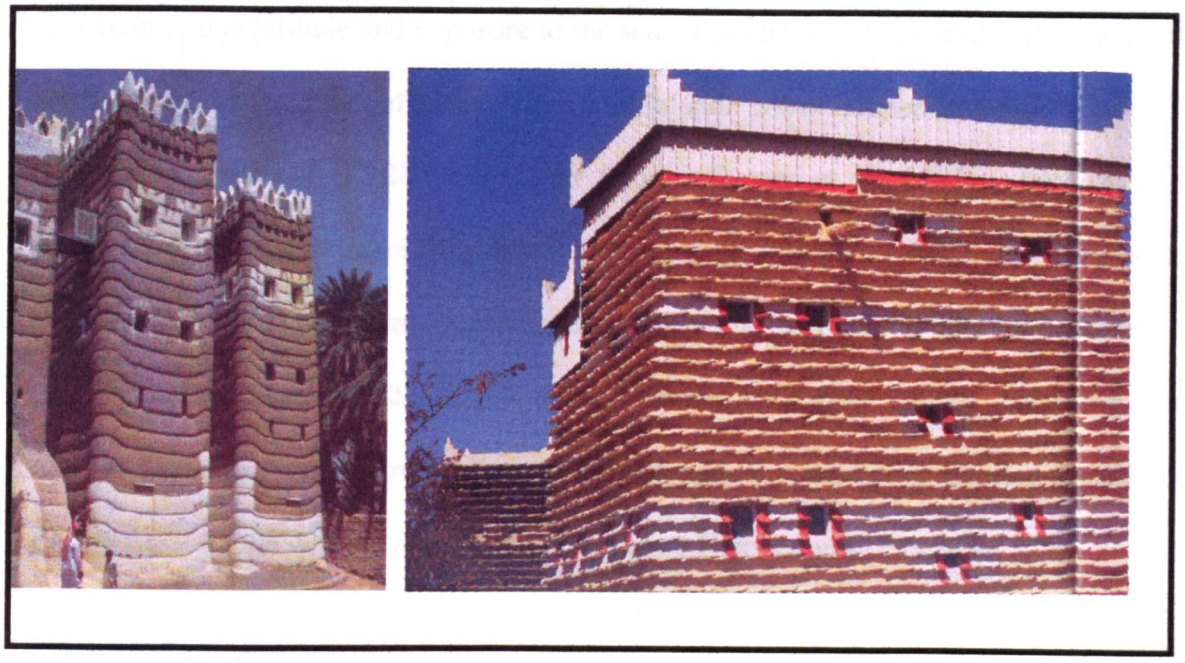

Figure (2.5): Typical houses in the tropical upland climatic zone where flat stone pieces are put together in rows to protect mud walls from solar radiation and from heavy rain in summer and winter seasons respectively. (Mauger 1996)

Classifying the urban planning of upland areas is difficult because it is affected by the presence of extensive hills and mountain slopes. Villages are small, sometimes containing five or six houses spread in a valley. Larger villages may be located on the slopes of a hill with the lower slopes used for farming while the hilltops are used for buildings. The character of tall buildings, 3 to 6 floors, in such villages creates narrow alleyways connected to one another through open spaces. Open spaces are usually shaded during the summer by high-rise buildings.

2.2.3.4. Hot Humid Climatic Zone.

2.2.3.4.1. The Climate

Coastal cities have widely different temperatures from one area to another, depending upon latitude and exposure to the sea. The climate of linear cities located on the seashore differs from that of cities that extend inland. Mean temperature falls between 25-38°C in summer and 17-28°C in winter (Koenigsberger et al. 1977). Because of the influence of the sea, relative humidity is very high, at 70-100%. Based on the percentage of relative humidity, annual rainfall varies from one location to another. Winds are stronger in settlements located on the seashore rather than those inland. The wind energy atlas of Saudi Arabia (Al-Ansari et al. 1985) indicates that the strongest wind speeds occur during April - June while the weakest occur during October and December.

2.2.3.4.2. The Architecture

The architecture in the hot humid climatic zone has traditionally followed three main construction practices including establishing tall ventilated structures that allow cross ventilation, constructing large openings covered by projected bay windows (Rowshans) and plastering walls with coral or gypsum for protection against heavy rain and humidity as gypsum works as a sealant for water proofing. The courtyard is replaced by a high, raised building (Kaizer, 1984). Three to six story buildings catch the offshore and onshore breezes near the sea. Large openings enhance cross ventilation through the structure as they are necessary to reduce humidity inside the building. Preferred orientation of structures has been towards the seaside. In some cases, a back or front yard serves the essential need for relaxation.

On the city urban planning scale, cities located in this climatic zone differ from those found in other climatic zones. The urban planning of hot humid climates has been developed through years of trial and error experience to enhance desirable wind penetration through and between buildings. The wider apertures oriented towards the sea create a remarkable wind movement. This solution helps considerably in reducing humidity and in cooling down streets temperatures. Unlike the compact urban form, wide and long streets separate buildings. This climatic zone will be discussed in more details in the following sections.

2.3. The Climate of Jeddah

2.3.1. Geographical location

Jeddah is one of the western region and coastal cities that is overlooking the Red Sea and is located at 21^{o} 19' north and 39^{o} 12' east with an elevation ranging from 3 to15m above sea level. The width of Tehamah Plain near Jeddah is approximately 30Km; it is relatively flat and rises gradually eastward from the sea. The Red Sea shapes the western border of Jeddah whilst continuous lines of foothills are found towards the East. Makkah, the city with the holiest shrine to all Muslims, is the nearest major city to Jeddah and is located 80Km eastwards. Therefore Jeddah shapes the access for most Muslims aiming to reach Makkah. Additionally, Jeddah is classed as the capital city of trade since its harbor is the link with the African, European and American continents. Figure 2.1 shows the location of Jeddah within Saudi Arabia.

2.3.2. The Climatic Environment

Jeddah has a maritime-desert climate (hot humid) and hence the relative humidity is reasonably high (Najib, 1987). The data recorded between 1970 and 1983 by the Meteorology and Environmental Protection Administration (MEPA) are used here to exhibit the climatic conditions in Jeddah (1983). The long-term data are much more comprehensive than the short-term data collection (Said and Al-Zaharnah, 1994). It is worth mentioning that the data collected did not include the year 1976, and hence the data in hand covered 1970-1975 and 1977-1983. The daily- 24 hours- records were averaged to yield mean monthly readings over 13 years.

2.3.2.1. Dry bulb air temperature

In Jeddah, the mean maximum temperature is recorded between June and August. The dry bulb temperature reaches up to 38°C daytime and falls to 26°C at night. These temperatures, added to the high percentages of relative humidity and direct solar radiation, are the source of discomfort during the summer seasons (MEPA, 1983). In winter season, the daytime temperature falls to about 28°C and nocturnal temperature falls to 18°C (Figure 2.6), (Table 2.1). The mean daily temperatures are recorded between December and February where the minimum temperatures are found all year-round. The diurnal temperature range does not suffer much variation, unlike the hot day climates where major variations are found. The mean diurnal ranges in summer and winter are 8°C and 14°C, respectively.

2.3.2.2. Relative humidity

The relative humidity is extremely high due to the presence of the sea and the maximum mean relative humidity is almost steady, being over 90% year-round. However, the minimum mean relative humidity reaches nearly 55% in the winter and summer. As shown in Figure 2.7 the diurnal relative humidity falls between 42-92% showing that humidity is fairly high.

2.3.2.3. Wind speed and directions

Air circulation over Saudi Arabia changes forming high-pressure and low-pressure zones seasonally as a function of temperature change (Al-Ansari et al. 1985). For instance, during spring the occurrence of low-pressure zone developed on the Arabian Gulf favours a strong wind from the Empty Quarter towards the north west of Saudi Arabia. *"These winds are caused by the meeting of north and south tropical winds"* (Al-Ansari et al. 1985). In summer, wind is affected by the high-pressure zone near the Mediterranean Sea and low-pressure on the Arabian Gulf as well as by the African low pressure (Figure 2.8). The wind behaviour lasts until the end of October, when it is then weakened and replaced by relatively humid cool currents. Lastly, in the winter the wind is *"dominated by high pressure over central Asia and Siberia, and low pressure over the African lakes and the Red Sea"* (Al-Ansari et al. 1985).

By examining the four seasonal maps of air circulation illustrated in Figure 2.8 and in conjunction with the wind rose of Jeddah, the year-round predomination of sea breeze blowing from the northwest and west seemed obvious. The maximum mean wind speed varies with seasons. While in warmer seasons the speed in Jeddah reaches to nearly 9m/s, it is just under 6m/s in winter as shown in Figure 2.9 (MEPA, 1983). In early mornings the

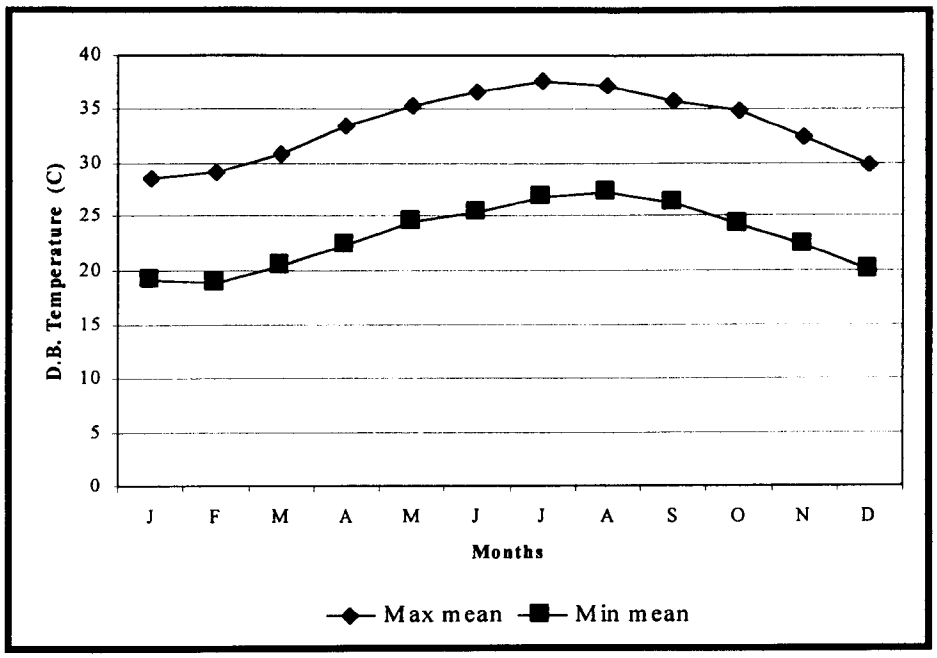

Figure (2.6): The Mean for the monthly maximum dry bulb temperatures in Jeddah. (MEPA 1983)

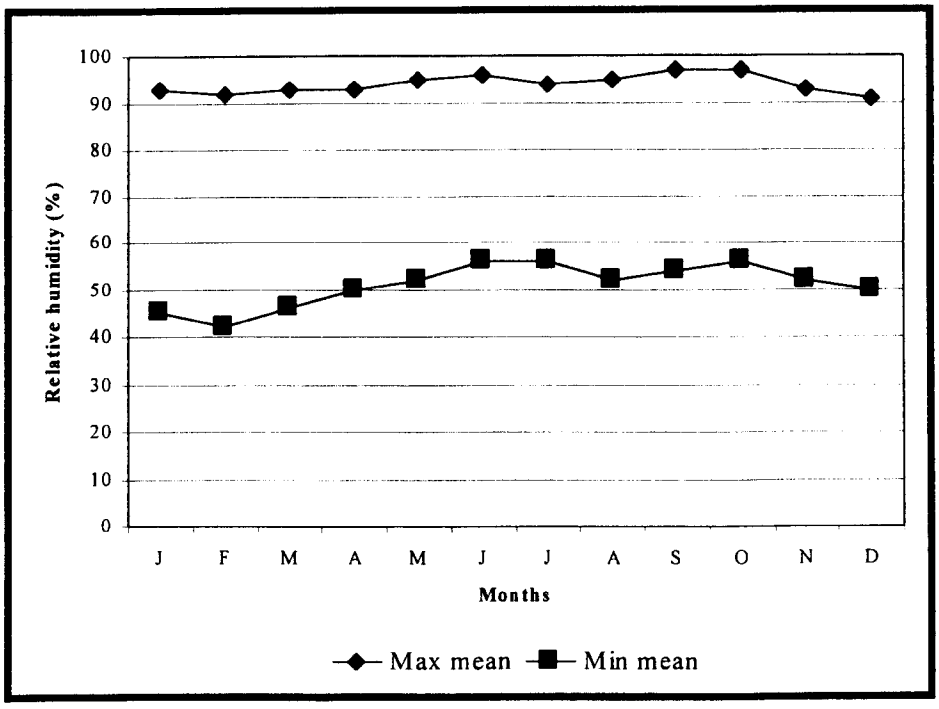

Figure (2.7): Mean monthly relative humidity in Jeddah. (MEPA 1983)

Table (2.1): Data record of climatic variables in Jeddah. The mean monthly readings over 13 years, (Weather data, 1970-1983), (Al-Lyaly, 1990).

Months	Dry Bulb Temperature (C)		Rel Humidity (%)		Wind Speed (m/s)		Sky Clarity (okta)		Rainfall (mm)
	Max Mean	Min Mean	Max Mean	Min Mean	Max Mean	Min Mean	Max Mean	Min Mean	
January	28.5	19	93	45	5.8	3.2	2	1	19.6
February	29.1	18.7	92	42	6	3.4	2	1	16.6
March	30.9	20.4	93	46	6.9	3.5	2	1	0
April	33.5	22.2	93	50	6.8	3.4	2	0	1.6
May	35.4	24.5	95	52	7.2	3.8	1	0	2.1
June	36.6	25.3	96	56	8.5	4.1	0	0	0
July	37.7	26.7	94	56	9	4.2	0	0	0
August	37.2	27.2	95	52	8.4	3	0	0	0
September	35.8	26.2	97	54	7.7	2.3	0	0	0
October	34.9	24.2	97	56	6.5	2.2	0	0	0.8
November	32.4	22.2	93	52	6	2.3	1	0	10
December	29.8	20	91	50	5.8	2.8	2	1	10.7
max	37.7	27.2	97	56	9	4.2	2	1	19.6
Annual Min	28.5	18.7	91	42	5.8	2.2	0	0	0
Mean	**33.48**	**23.05**	**94.08**	**50.92**	**7.05**	**3.18**			**5.12**

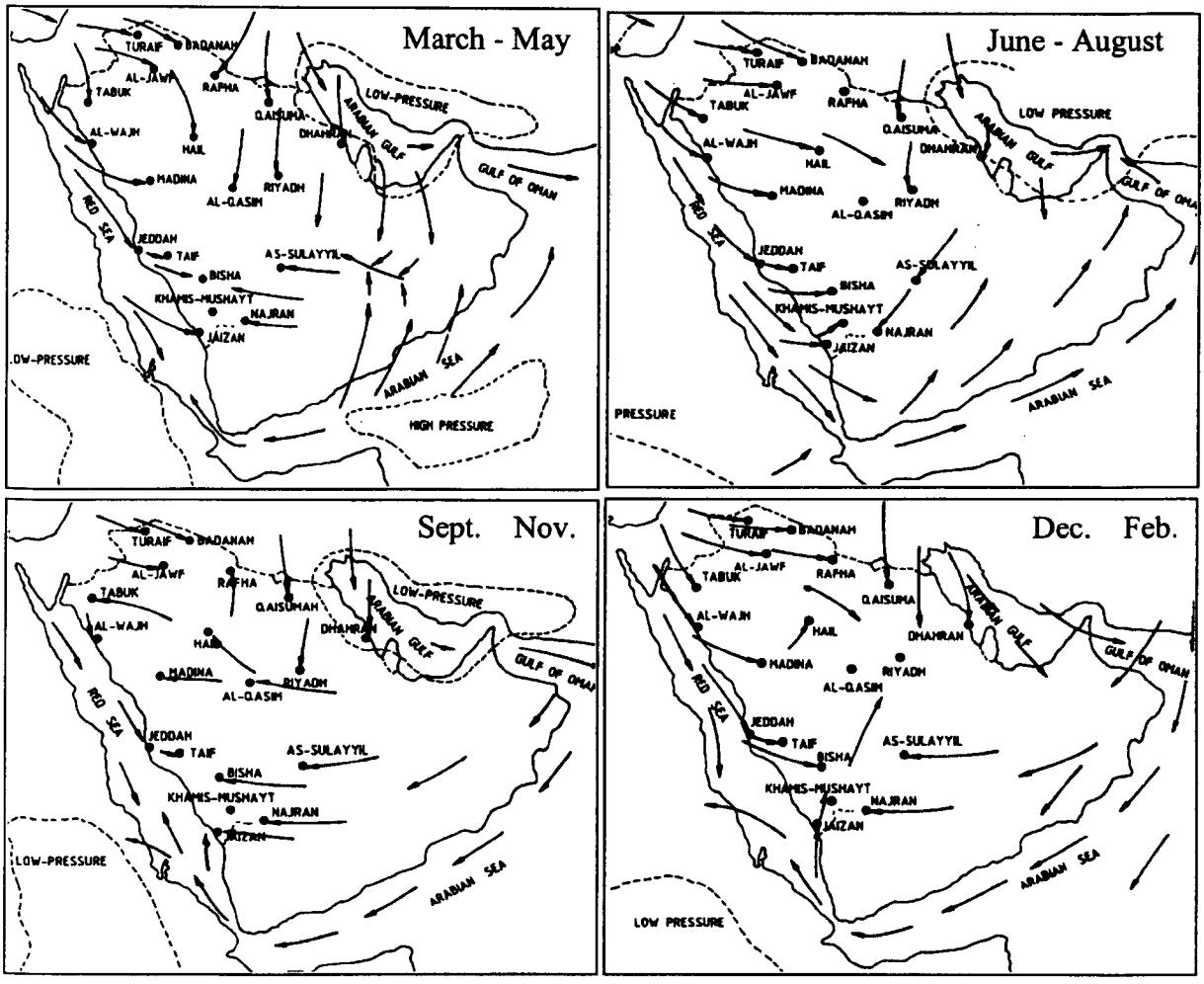

Figure (2.8): The four seasonal maps of air circulation over Saudi Arabia showing the year-round predomination of sea breeze blowing from the northwest and west in Jeddah. (Al-Ansari et al. 1985)

wind speed starts increasing and peaks at 3pm then starts decreasing (Al-Ansari et al. 1985). The predominant wind throughout the year prevails from the north and northwest directions. As shown from the wind rose (Figure 2.10) Jeddah falls under two directions of prevailing winds. The first is from the directions mentioned previously and is referred to the sea-land breeze. Wind also prevails from the opposite direction and is referred to as the land-sea breeze. These wind directions occur between daytime and nighttime cycles. During daytime the breeze flows from the sea towards the landside and vice versa. Najib noted (1987) that the winds prevailing from the south are usually accompanied with an increased temperature and humidity. On certain occasions, they blow suddenly causing thunderstorms with rainfall. Sand storms usually blow from the foothills located on eastern Jeddah. They are troublesome and are called Al-Samum as they refer to sand and dust storms accompanied by higher temperatures. Najib (1987) also stated that visibility in some days could fall to less than 1km.

2.3.2.4. Precipitation

No precipitation occurs during the warmer seasons, unlike the warm humid climates. The rainfall in the winter and autumn seasons is irregular and the maximum precipitation usually occurs in January when it reaches up to about 20mm (Figure 2.11), (Table 2.1). On certain occasions, it could happen that a number of years would pass without any records of precipitation (Bokhari, 1978).

2.3.2.5. Solar radiation

Jeddah lies at 21° 29'N latitude. As shown from the sunpath diagram for the 21° N latitude, the summer solstice occurs on June 21 where the Sun's azimuth arc totals 230° (Kukerja, 1978) (Figure 2.12). The noon altitude of the sun is 88° where the sunrise is at

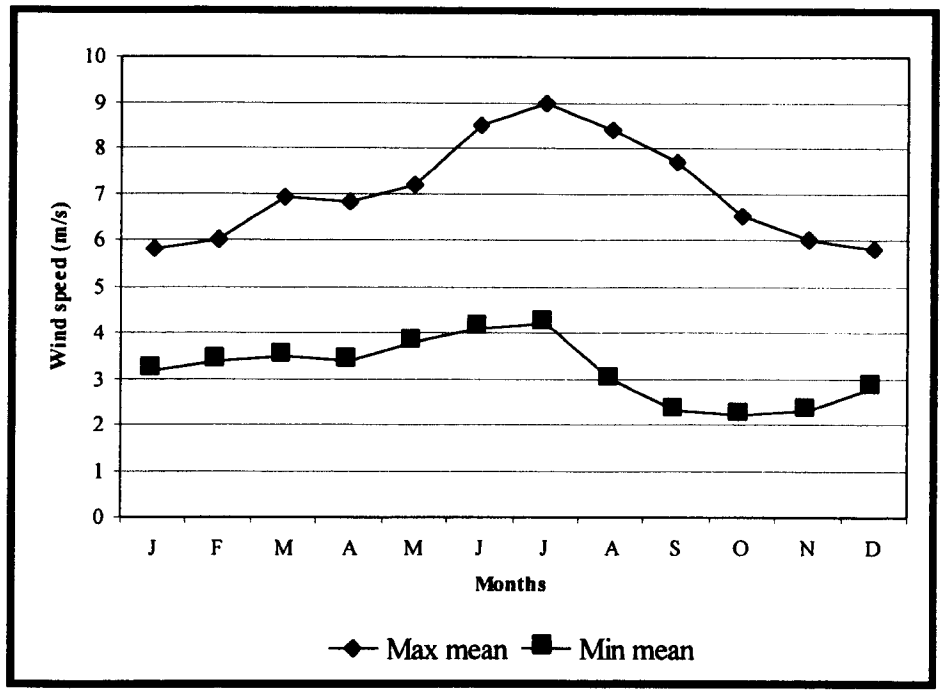

Figure (2.9): Mean monthly wind speeds in Jeddah. (MEPA 1983)

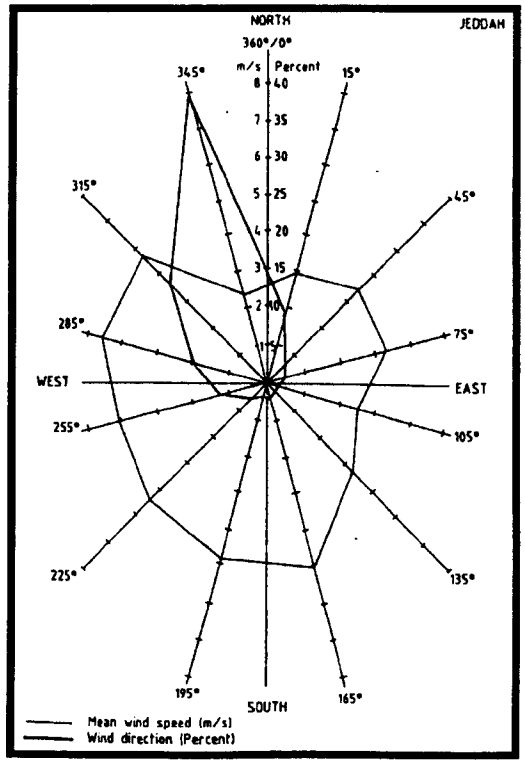

Figure (2.10): The wind rose of Jeddah. (Al-Ansari et al. 1985)

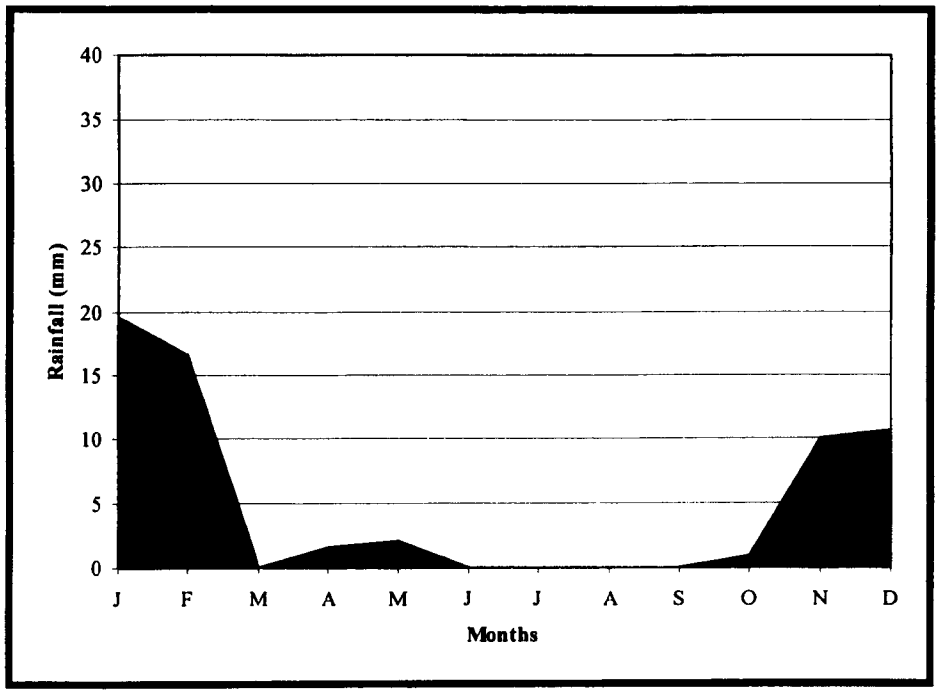

Figure (2.11): Mean monthly precipitations in Jeddah. (MEPA 1983)

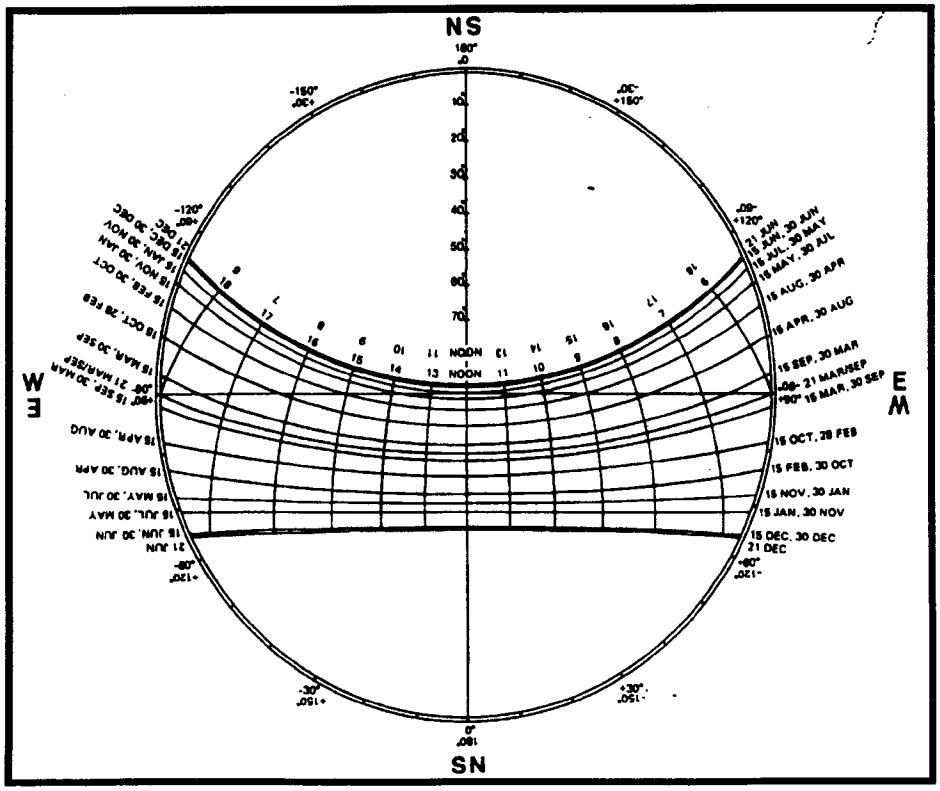

Figure (2.12): Sunpath diagram for 21°N latitude. (Kukreja 1978)

5:18am and sunset is 6:42pm, showing that daylight extends up to 13 hours and 18 minutes. The shortest day occurs on December 21 when daylight extends from 6:36am until 5:24pm; this is the winter solstice day where the sun's azimuth arc is 130° and noon solar altitude is 46°. The difference between the lengths of both days is approximately 2 hours and 30 minutes.

2.3.3. Isopleths charts of climatic variables

The method of transforming climatic variables into isopleths charts is used by many researchers (Olgyay and Olgyay, 1976), (Olgyay, 1963), (Koenigsberger et al. 1977), (Markus and Morris, 1980), (Givoni, 1981), (Said & Al-Zaharnah 1994) to extrapolate the data hidden in the climatic variables. It is essential to transform the long-term weather data into diagram forms, and hence, use them as design guidelines for building engineering as they reflect the environment adaptation to climate. The Jeddah's isopleths charts of dry bulb temperature, relative humidity, wind speed and directions are discussed here. These charts were developed by Al-Lyaly (1990) and represent the same period of data in hand; hence they are useful to refer to.

The temperature variations show that between June and August noon is the time of maximum temperature occurrence, at about 39°C, which then drops to about 30°C at midnight. Consequently, the diurnal changes are relatively small, being less than 10°C (Figure 2.13.a). The relative humidity at noontimes is less than 50% (Figure 2.13.b). This significant reduction in the relative humidity is coupled with higher wind speeds, about 8m/s, that prevail from the north and northwest (sea-land breeze) (Figure 2.13.c). Within building, the air movement acts as the *energy-free* cooling factor to occupants through conduction. At midnight, a land-sea breeze of nearly 3m/s comes from the northeast

direction and the relative humidity increases to nearly 85%. It is worth mentioning that the significant increase in temperature is found in hours of daytime up to 2:00-3:00pm. The temperature then drops off relatively slowly till late night. In winter seasons, the diurnal temperatures are less than 8°C. In a winter month like January, the temperature at noontime rises up to 26°C and midnight temperature may fall to less than 18°C as shown in Figure 2.13.a. The maximum relative humidity is found at sunrise and sunset and during winter seasons.

Noontime heat decreases in autumn and winter seasons. The increase between January and June is about 14°C at noon and the relative humidity decreases to 20%. While the wind direction never changes at noon, the wind in January decreases to about 4.5m/s which is almost one-half of its speed in summer. Conversely, mean wind speed at midnight ranges from 2.5m/s to 3.5m/s in winter and summer respectively, showing a relatively small increase. The wind speed in the daytime is notably more than that at nighttime. Wind from the west usually prevails in late afternoon till sunset, between 3:00pm and 7:00pm. This preferred wind rarely changes its direction and its speed varies from 3.5m/s to 6m/s from winter to summer respectively.

In general, the sea breeze seems to greatly affect the diurnal temperatures. For example when larger magnitudes of diurnal temperature are found that correspond to fairly slow and weak sea breezes. The development of sea breezes therefore significantly reduces the diurnal temperature changes (Edwards, 1987). In other words, the sea-land breeze works merely as a climate moderator since it suppresses both temperature and humidity levels. Similarly, the relative humidity is largely affected by the presence of sea breezes and diurnal temperature ranges. Lower temperature raises the relative humidity

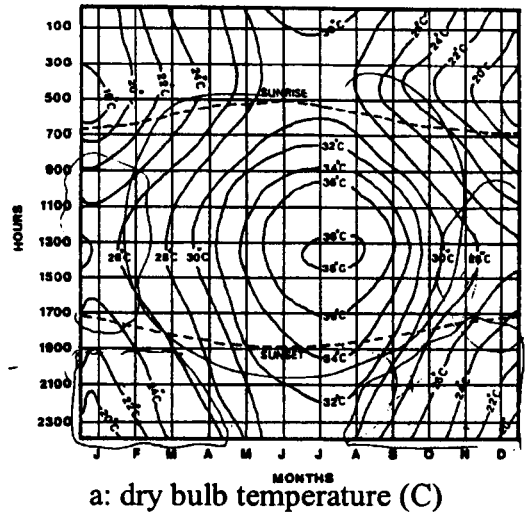

a: dry bulb temperature (C)

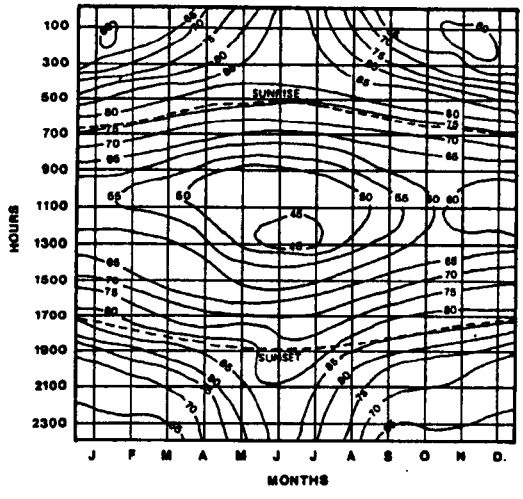

b: relative humidity (%)

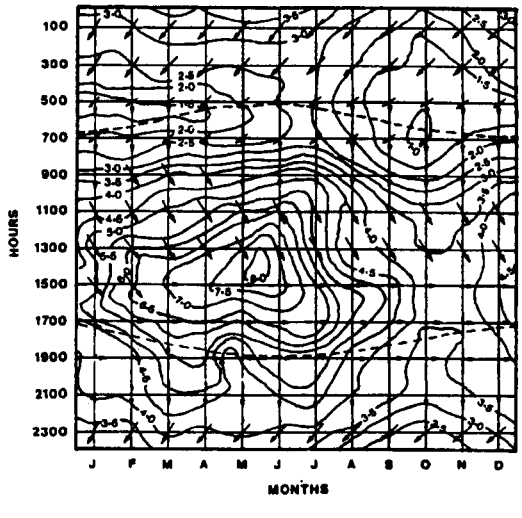

c: wind speed and direction (m/s)

Figure (2.13): The isopleths charts of various climatic variables, [a: dry bulb temperature (C)], [b: relative humidity (%)] , [c: wind speed and direction (m/s)]. (Al-Lyaly, 1990)

during evenings and nighttimes while lower relative humidity occurs at higher temperatures during the daytime.

2.3.4. The phenomenon of sea and land breezes

There is a widely known phenomenon of prevailing winds occurring at coastal settlements and referred to as sea and land breezes. Traditionally, the design of settlements at micro and macroclimate scales responds to this phenomenon (Koenigsberger et al. 1977). In Jeddah the sea-land breeze occurs during daylight hours and encounters higher wind speeds than those due to the land-sea breeze that occasionally arises after sunset (Figure 2.13.c and Figure 2.14). As mentioned earlier, the predominant wind directions prevail from the north and northwest. As it becomes noontime, the direction seems to be more from the northwest side and from the west by mid afternoon. This shows that the

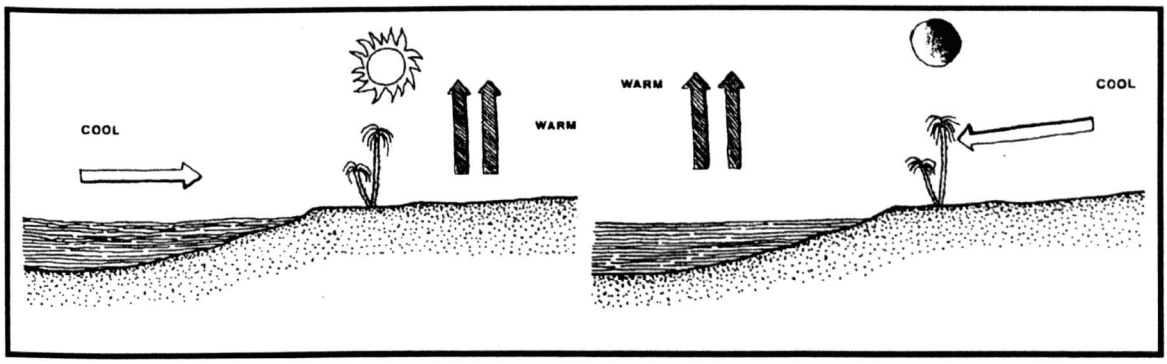

Figure (2.14): The phenomenon of sea and land breezes. (Sanderson, 1982)

wind deviates about 90° from sunrise to late afternoon. Sanderson (Sanderson, 1982) noted that wind force rarely extends to more than 32km inland and 500 to 1000m above the terrain. This mostly happens in the spring and summer seasons. During winter and autumn seasons the wind mainly blows from the north due to the effect of north winds (Al-Lyaly, 1990).

The land-sea breeze occurs during nighttime and prevails mainly from northeast and east. The directions are consistent and are not affected by the monthly climatic variations. The highest speed of wind does not exceed 4.5m/s with a mean of approximately 2.7m/s. Another land-sea wind direction blows from the south and southeast directions. While it rarely blows, the wind is always coupled with dust and storm and, therefore unwelcome.

2.4. The Architecture of Jeddah

2.4.1. Construction and decoration materials

Historically, Jeddah is well known for commerce, and hence, the flourishing trade in Jeddah exerts a direct influence on the architectural formation of the city. The architectural characteristics are greatly inspired by those originated in Turkey and Egypt (Mani', 1980). The skills and techniques were brought through migrations and gradually implemented in Jeddah during the Ottoman era (Al-Lyaly, 1990). Some building materials were also imported from abroad. For example the qandal, which is extensively used in Jeddah for construction and wall reinforcements, was the famous timber imported from India (Bokhari, 1978). Al-Lyaly (1990) suggested that the importing of this wood coincided with the construction of tall buildings since qandal increases the structural solidity and prevents uneven settling. Alternatively, the Jawi (teak wood) was mainly used for decoration. Its name refers to the country where it was brought from, Java. It is more expensive and of higher quality than the qandal and is widely used by craftsmen for decorating façades, main doors and windows. Rowshans that are mainly made with Jawi wood are believed to offer more resistance to humidity and insects (Bokhari, 1978). Wood

was the common architectural element used for exterior elevations. In certain circumstances the traditional house was entirely covered with wood.

Mangaby and Kasur are the coral stones used for construction. They are obtained locally, from Al-Manqabah lagoon, and sized into cubical shapes for construction purposes where clay serves as cement between them. Bokhari (1978) mentioned that clay is also applied to cover coral stones and to shape smoother edges.

2.4.2 Layout

The traditional houses in Jeddah are by no means identical but they share common features and characteristics. The typical house in Jeddah contains multi-stories ranging from 3 to 6 floors, and the rooms are distributed around the stairwell (Figure 2.15). The house usually contains front and back entrances. Females usually use the rear entrance while the main entrance is for males. The main entrance is connected with the entrance hall (dehleez) that acts as the transitional zone between outside and inside the house. Next to it is the guest room(s) (maqad) which is decorated with coloured rugs, soft cushions and comfortable mattresses for visitors. On the same floor near the back entrance there are usually some storerooms, toilets and small kitchen.

The middle floors are the family residential floors. The stairwell usually leads to a small hall (salah) or a narrow corridor which then connects it with the main family living rooms. At the front, there are usually two main living rooms; majlis and suffah while the facilities are located at the rear of the floor as illustrated in Figure 2.15. It is interesting to indicate that rooms serve various functions such as living, dining, studying, etc. The terraces and sleeping rooms share the top floors with some facilities like toilets, and kitchens.

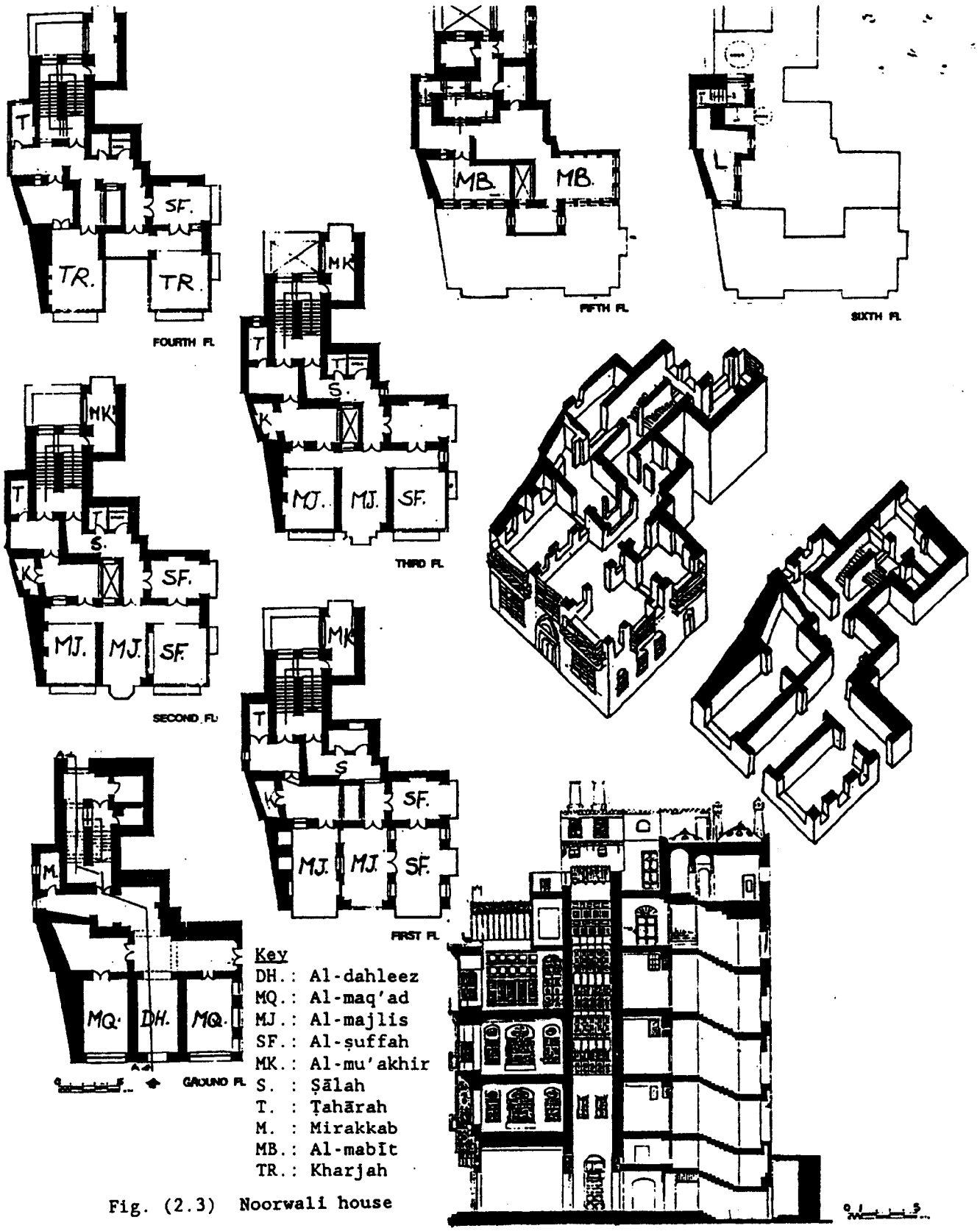

Fig. (2.3) Noorwali house

Figure (2.15): A typical traditional house in Jeddah (Noorwali house). (Al-Lyaly, 1990).

2.4.3. Elevations

In his journey over the Arabian Peninsula, Lawrence (Lawrence of Arabia) described Jeddah as a remarkable city (Khan, 1986). He wrote:

> *"The streets were alleys, wood roofed in the main bazaar, but elsewhere open to the sky in the little gap between the tops of the lofty white-walled houses. These were built four or five stories high, the coral rag tied with square beams and decorated by wide bow-windows running from the ground to (top) floor in gray wooden panel".*

The elevations in Jeddah are the main distinguishing feature of its architecture, from the remarkably carved wooden main doors to the astonishingly decorated windows representing what is locally known by Rowshans, mashrabiah and taqqat (Figure 2.16). The extensive decorations were made by the professional local craftsmen to reflect the family living standard. The Rowshan and mashrabiah are cantilever elements projecting from the walls to form a projected window bay jutting out of the main body of the building. The Rowshan is commonly used in Jeddah while the mashrabiah are mostly used in hot dry climates (Al Shareef, 1996). Al Shareef added:

> *" The name Mashrabiah is used for an opening with a wooden lattice screen composed of small wooden balusters that are circular in section and arranged at specific regular intervals, often in a decorative and intricate geometric patterns".*

The Rowshan configurations will be discussed in details later in this chapter. On the top floors are found the terraces which breakup the continuity of Rowshans that extend from the ground, shaping the staggered and uneven skylines of the structure elevation.

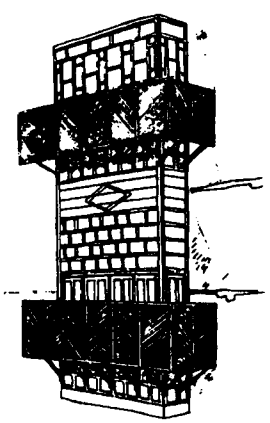

Mashrabiah

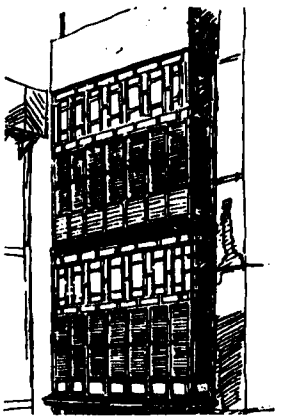

Projected Rowshan

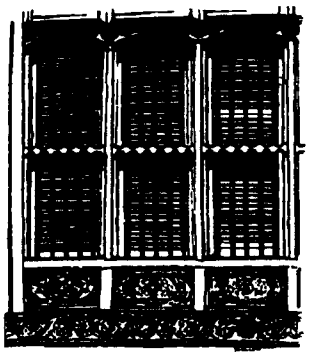

Plain Rowshan (Taqqat)

Figure (2.16): The main elevation treatments in Jeddah in all of which the modulated louvered windows are commonly used. (Khan, 1986).

2.4.4. Social influence on traditional buildings

Social values are given very significant consideration in the Islamic architecture, and hence, the traditional building in Jeddah reveals the same principles. Hospitality, neighbour-to-neighbour relations and the extended family structure shape the integrations between levels of privacy and are replicated in the traditional dwellings. The woman's status within the family is also given great importance.

Two dimensions of privacy are found within the traditional house, vertical and horizontal. The social obligations towards guests created a vertical dimension of privacy between the visitors and the rest of the family. As mentioned earlier, the house master's hospitality to guests and all the related facilities are situated on the ground floor (semi-private zone), whilst the upper floors are more private, as they are out of bounds for the guests. Within the upper floors is found another degree of privacy sanctioned in the segregation between the sleeping and living zones. The living zones are usually found in the middle floors, and the sleeping zone is located at the uppermost floors. The concept of the extended family structure also carries some levels of privacy. In the case of a married son living with his parents, he is usually allocated a certain floor or a quarter within the floor. This creates a specific zone of privacy that does not interfere with the daily activities of other family members. Parents would normally live above the floor of their married son (Al-Lyaly, 1990). The floor layout reveals some horizontal levels of privacy as well. For example the stairwell is usually located near the rear entrance to enable family members and women in particular to go to the upper floors freely and without passing by the guests. The small hall connecting the stairwell with other rooms provides a degree of privacy within the floor.

With regard to the apertures, their design reveals a strong social character. The Rowshan, mashrabiah and shish are meant to maintain privacy for the occupants whilst enabling them to look out. The terrace works also as an outdoor within the building enclosure since it is opened to the sky. The parapets around the terraces are above the height of the occupants and act as a shield from nearby neighbours.

2.5. Natural ventilation strategies in traditional dwellings

Wind-induced natural ventilation in Jeddah was given great consideration on the microclimate scale as well as the macroclimate scale as represented in the building orientations, street orientations, and the urban planning of the city. These will be highlighted in this section to trace the most important element for improving natural ventilation in the typical house in Jeddah, and thus, improve the indoor environment.

2.5.1. Layout of the floor plan

The typical layout of the floor plan in Jeddah contains bigger room sizes such as living and guest rooms at the front while other facilities such as toilets, kitchen and stores share back elevations. This was not merely due to their functions but also to benefit from the sea-land breezes. As a result, larger rooms are allocated on the front, facing towards the sea, north or northwest, with considerable aperture areas. Both northern and western elevations occupy the maximum number of apertures. Khan (1986) indicated that living rooms are more comfortable than other rooms on the same floor and are sometimes used as bedroom also. The aperture-to-wall ratio for a typical room may reach up to 50-100% as can be seen from the various floor plans shown in Figures 2.15 (Maghrabi, 1995). The openness to the outside provides not only spaces concerned with continuous ventilation but

it also enhances the ventilation of the other spaces on the same floor as seen in Figure 2.17. The large openings are usually covered by massive wooden elements called Rowshans, Mashrabiah or Taqqat. Within the dwelling, lattice wooden screens are provided above doors to enhance air circulation whilst maintaining occupants' privacy.

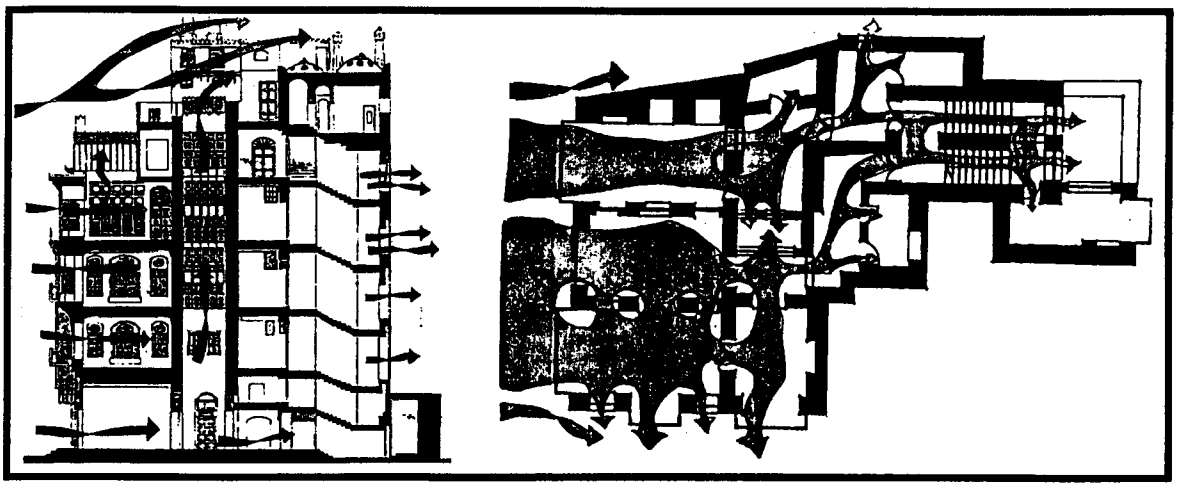

Figure (2.17): A sketch of the vertical and horizontal airflow patterns in a typical house in Jeddah. (Al-Lyaly 1990)

The other approach to the enhancement of air circulation is through stairwells and airshafts as shown in the Figure. The house in Jeddah normally consists of various elements distributed around the stairwell or vertical airshaft. As wind blows near the top of the airshaft and stairwell causing negative pressure at the top, the pressure difference between upper and lower zones creates upstream suction thus allowing ventilation to occur. The pressure difference between the windward and leeward sides could also cause air circulation within the house.

With the absence of substantial winds, air still circulates within the house through the stack effect (Al-Lyaly, 1990). The airshaft acts as a solar chimney where hot air at the top induces air from the rooms to flow upwards and to be replaced by external air. The top of the airshaft is usually open to let the airflow upwards easily.

2.5.2. Elevation treatment

The Rowshan is a main elevation treatment in Jeddah. It extends vertically or horizontally to cover part, or the whole, of the building's façade. Khan (1986) indicated that the use of Rowshans reflects the elegance of the house owner. Additionally he stated:

> *"Practically, the Rowshan is considered window to the external world, veil from the Sun's glare, source of ventilation in buildings and piece of furniture in the house which sometimes extends to cover a number of rooms."*

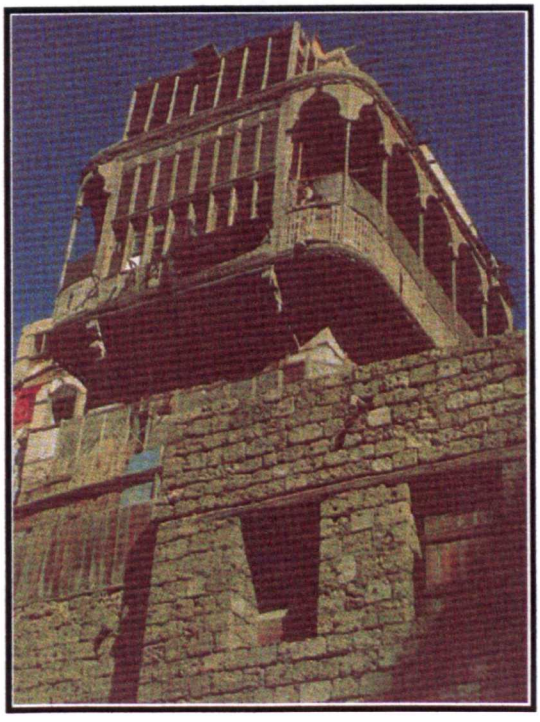

Figure (2.18): The uppermost floor (Al-Mabit) is normally covered with modulated louver windows. (Khan, 1986).

The above description reflects the importance of the Rowshan as the main source of cross ventilation in the buildings. It contains adjustable louvers which allow breeze to penetrate at the desired inclination. Occasionally, small screens are found near the top of the

Rowshan that serve another important role. When air penetrates through the screens it extracts the excessive humidity and heat near ceiling level.

The modulated louvered windows (MLW) are also employed on the top floors where the sleeping area and terrace are found. The sleeping rooms are surrounded by wooden louvers on two or three sides, giving the impression of an air pavilion as illustrated in Figure 2.18 (Al-Lyaly, 1990). This is merely made to favour continuous circulation of air within the room even at very low wind speed. The terraces located at the upper floors in Jeddah replace the central courtyard (Hariri, 1993). They are surrounded by high-perforated parapets and open to the sky, acting as an outdoor environment within the building.

2.5.3. Building orientation

Freestanding structures that are penetrated by a number of alleys to channel air through are one of the most favorable solutions in humid climates (Koenigsberger et al. 1977). Houses distributions and orientations in Jeddah have arisen from the same perception. Indeed the concept was optimized after long-term experience of trial and error technique (Al Shareef, 1996). The tall buildings rarely share any walls and are often surrounded by a number of alleys to enhance cross ventilation. As mentioned earlier, rooms located on the north and the west elevations are widely opened and facilitated with Rowshans while the house shares only a single wall with the neighbour. This was necessary since the inflowing air between buildings will take the moisture away. In turn, it increases the house's durability. The traditional dwellings therefore faced the seafront. Such orientation is certainly joyful to the occupants who benefit from the continuous breeze.

2.5.4. Urban planning layout

The distribution of buildings created channels for air to pass. They are irregular in width and yet they seemed to have a common character. This is noticeable when the urban planning of the traditional city shown in Figure 2.19 is carefully examined. Main streets radiate from the waterfront while secondary alleys are laid out along a north-south axis as shown from the Figure. In the light of what was previously noted regarding wind directions, one could acknowledge the climatic adaptations on the macro scale. As the sea

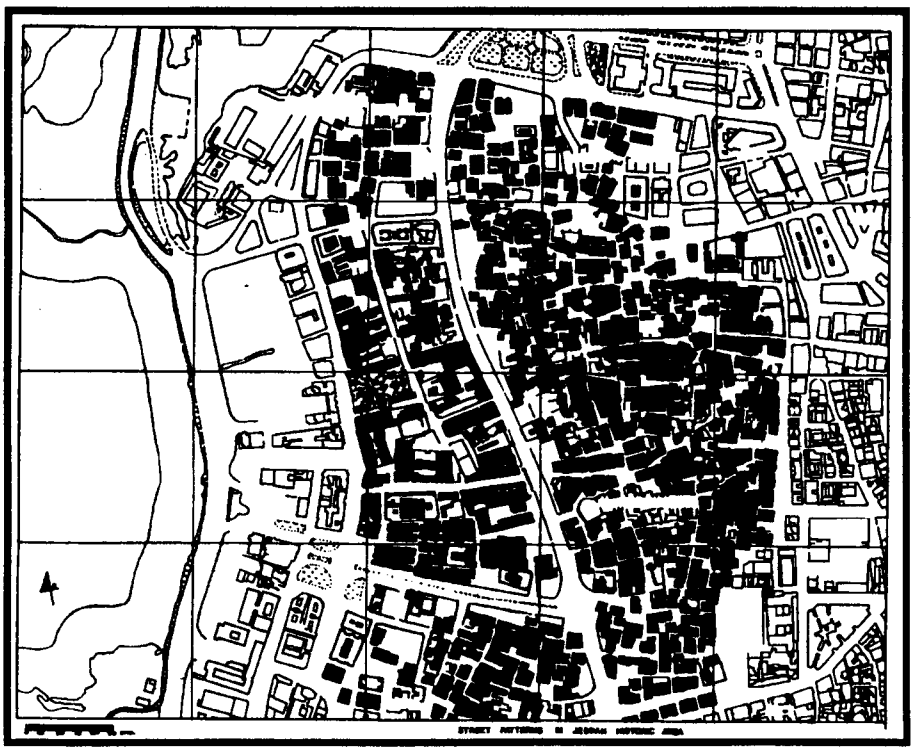

Figure (2.19): The master plan of old Jeddah. (Khan, 1986)

breeze prevails, the air travelling through the streets tends to generate more speed due to the occurrence of considerable reduction in volume (Awbi, 1991) (Al-Lyaly, 1990). The smaller alleys, that are not facing the seafront, on the leeward side would fall under low pressure which causes airflow through (Fathy, 1986). Interestingly, streets and alleys are

shaded all day by surrounding tall buildings that in turn tend to cool the air before it reaches the building. This advantage is not hypothetical but rather was confirmed during the evaluation of the temperature records of traditional and modern streets of the city referred to. Al-Lyaly (1990) carried out simultaneous hourly temperature measurements at both streets and found that the traditional street in Jeddah is approximately 3°C cooler than the modern street as shown in Figure 2.20.

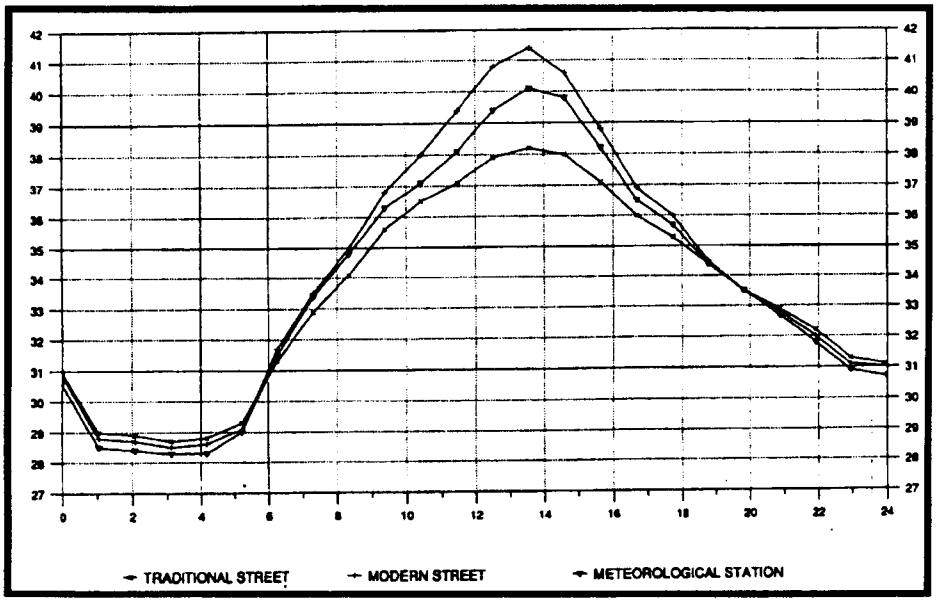

Figure (2.20): The hourly temperature variations obtained from Jeddah traditional street, modern street and the meteorological station on 18/7/1987. (Al-Lyaly, 1990).

2.6. The Rowshan

In the light of what was mentioned earlier, it is evident that the climate in Jeddah is not naturally comfortable. Nevertheless, people have adapted their architecture accordingly. Amongst all climatic variables, natural ventilation within building was the main source of relaxation and comfort, and thus, was given great attention from building to

the urban planning scale. The Rowshan is the major window type adopted in Jeddah as it answered the climatic and social needs of the occupants inside the dwelling. The Rowshan's origination, configuration, types and applications are discussed in the following subsections.

2.6.1. Historical background

The projected window bay- the Rowshan- does not only glorify the traditional architecture in Jeddah but it is rather a distinctive feature replicated in many structures across the world:

> "*The distinguishing external features of the old houses of the Red Sea and some other Islamic and Indian styles are the large casement windows jutting-out into the street to catch the slightest passing breeze,*" (Greenlaw, 1976).

Its name may differ but its role remains similar: an environmental modulator. In other words, it is a transition between harsh outdoor and comfortable indoor environments, acting as a shield against direct solar radiation and glare, insects, dust and undesired flows. Equally, it is designed to exploit natural breeze through its detailed apertures. Its development also reflects occupants' social values.

The origin of Rowshan is still debatable. Some refer it back to the ancient castles built thousands of years ago when Rowshans were used merely for defensive purposes, while others refer its origin to Turkey or India (Al Shareef, 1996). But according to Khan (1986), the Rowshan is primarily an Islamic technique that has been modified and adapted by many others later. This argument is also supported by some Islamic literature. Back in 1100AD, the prominent scholar Ibn AL-Qaim AL-Joziah (1997) cited the word

"Rowzanah" in one of his books and referred to it as a window. Such an argument could still be debated but what is of more relevance here is the widespread use of this type of window not only in the Middle East but worldwide, from as far east as India to as far west as south America (Danby, 1980), (Greenlaw, 1976). But Rowshans found elsewhere are much smaller in size and dimensions than those found in the traditional buildings of Jeddah (Khan, 1986).

2.6.2. Construction components and details

The configuration details of the Rowshans in Jeddah are left to the house owners' preferences. Yet the common theme among them is that they consist of repetitive horizontal and vertical patterns extended to cover part, or the whole, elevation. So they are either in the form of split units distributed in special arrangement or in the form of a whole unit covering the entire elevation as demonstrated in Figure 2.21. Additionally, Figure 2.22 illustrates the various components of the Rowshan that are as follows (Khan, 1986), (Al-Said, 1996), (Maghrabi, 1995), (Al Shareef, 1996), (Hariri, 1992), (Salloum, 1983):

1. Crown (Taj): located at the top of the Rowshan and consisting of fashionable decoration details. Sometimes this extends beyond the Rowshan's main body.
2. Pearl (Durah): located at the centre of the crown.
3. Upper belt (Hezam Foqani): The horizontal panel that is usually embellished with geometrical patterns. These patterns may sometimes contain porous wooden screens.
4. The sashes (deraf): These contain two sections, upper and lower. Each section consists of a single or more sashes. The upper sashes are fixed and

the one underneath moves up and down behind the sash above through side grooves and rests on two hinges leaving a complete aperture. Every sash contains a number of horizontal wooden slats (louver blades). These are

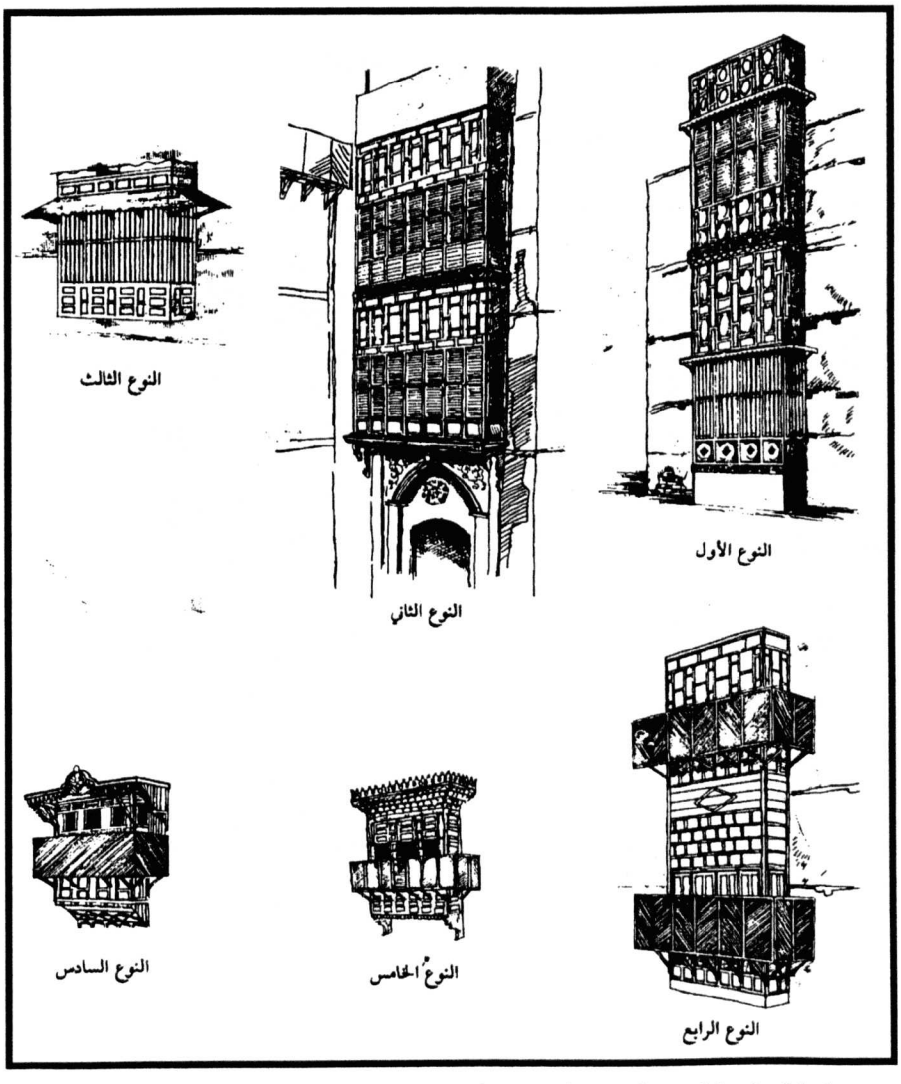

Figure (2.21): The various types of Rowshans found in Jeddah. (Khan, 1986).

movable in circular manner around their axes. They are called Qalaleeb, referring to the modulated louver windows (MLW). Al-Shareef (1996) indicated that every sash contains 12-18 louver blades.

5. Lower belt (Hezam Tahtani): This is wider than the upper belt where its width is normally at similar height to the inside platform of the Rowshan as shown in figure (2.18). The wooden panel is extensively carved with geometrical forms.

6. Brackets (Khradi): These are found at the lowest part of the Rowshan and they act as beams which carry the Rowshan's weight.

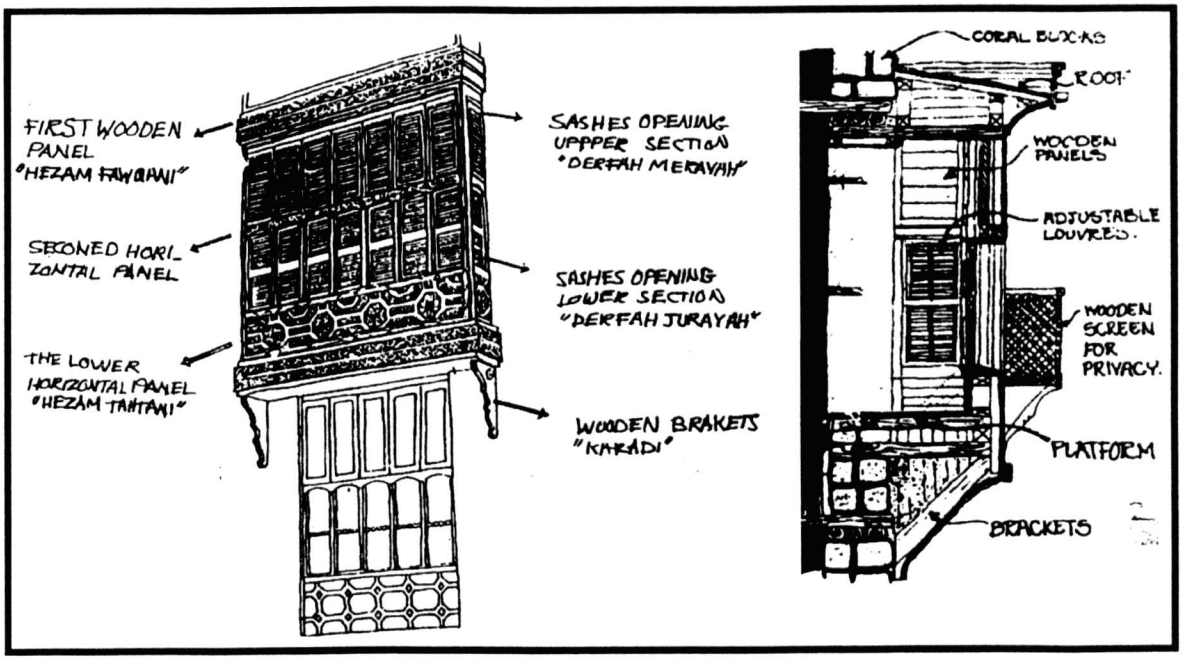

Figure (2.22): The various elements of the Rowshan. (Khan 1986 and Hariri 1991).

7. Wooden screens (Goulah): lower sashes in some Rowshans are facilitated with wooden screens placed about 0.50m away from the sash front panel, leaving a space for water jars (sharbat) to be cooled by cross ventilation. It is believed that the wooden screen also provides extra privacy for the occupants inside the house.

2.6.3. Types of Rowshans

Khan (1986) and Hariri (1992) agree that the classification of Rowshans falls under two main types including the split unit and the vertical long Rowshan (Figure 2.21). The latter extends to a number of floors to cover most of or the entire elevation. In some cases it extends from the ground level till reaching the uppermost floors or ends just under the terrace parapet located on the uppermost floor. The split units Rowshans are isolated to cover part of the room and are distributed in certain arrangements to shape the overall elevation. According to Salloum (1983), the Rowshans in Jeddah are either in the form of a simple window opening covered by wooden screens of modulated louvers, or are the extended wind bay projecting from the elevation and offering an extension to the interior spaces. Another type is on the uppermost floors, Al-Mabit, where the room is surrounded by wooden louvers on two or three sides as stated previously in this chapter (Figure2.18).

2.6.4. Rowshan Application

Through the various louver apertures, the Rowshan serves the following functions:

1. **Natural ventilation**: Cooling the occupants within the traditional dwelling through louver apertures is part of the significance of the Rowshan as it acts as a modulator to the airflow pattern, to its velocity and to the flow rate of passing air. The occupants are cooled through positioning the louver apertures at body level so that even at higher air temperature there is cooling by sweat evaporation (Al-Lyaly, 1990), (Sharma and Sharafat, 1986), (Oliveira and Bittencourt, 1998).

2. **Humidity**: The continuous cross ventilation is extremely important as it controls humidity within the space (Koenigsberger et al. 1977). Additionally, a local craftsman indicated that the Rowshans in Jeddah reduce air-moisture passing through their apertures, *"...due to the wood types used,"* (Maghrabi, 1995).
3. **Solar shading**: Generally, the direct solar radiation in Jeddah is undesirable, especially in the summer periods (Al Shareef, 1996). Shading is then desired to control the large amount of radiation, and yet, let interiors be daylit. As indicated by Khan (1986) the daylight penetrating through louvers and various screen geometries reflect an attractive play of light and shadow in the room and the patterns are altered throughout the day
4. **Privacy**: The Rowshan cantilevers from the building into the outdoor, and yet, provides a high level of visual privacy. From inside, the Rowshan platform sometimes rises from floor level and women enjoy observing the daily life in the streets while still invisible to people outdoors. Also, difference of illumination levels between indoor and outdoor favours more privacy. As explained by Al-Lyaly (1990):" *...when looking towards the Rowshan from the outside, the solid areas formed by the wooden louvers would be bright and in contrast the gaps in between would be dark prohibiting a view of the interior."*

2.7. Conclusion

This chapter has highlighted the climatic adaptation to architecture in the regional context and in particular to natural ventilation approaches seeking to adapt the micro and macroclimate environments in Jeddah.

Saudi Arabia generally falls under tropical climate zones. However, when the climate was observed it was found that the distribution of land and sea masses, added to the land topographies, have created some sub-climatic zones that may or may not refer to the general climate. This has led to various styles of traditional architecture that reveal deep responses to climatic variations. When Jeddah's climate and architecture were closely observed, the following points were concluded:

1. The climate of Jeddah is not naturally comfortable and the wind-induced natural ventilation was considered to control the excessive heat and humidity as a treatment to achieve comfort and relaxation. This is reflected on both micro and macroclimate scales.
2. Within the scale of a typical dwelling, the modulated louvered windows (MLW) found in Rowshans, Mashrabiah, Taqqat or other apertures components are believed to be the main solution to controlling the breezes needed to release climatic stresses and bring comfort within the dwelling. These types of windows answer bio-climatic necessities as well as social requirements. The MLW will be discussed in detail in the next chapter.

2.8. References

1. MS Encarta World Atlas. Anonymous (1997) 97. USA: Microsoft.

2. Al-Ansari, J., Bakhsh, H. and Madni, I. (1985) Wind energy atlas for the Kingdom of Saudi Arabia. p.56p King Abdulaziz City for Science and Technology.

3. Al-Joziah, I.A.-Q. (1997) Iqhthat Al-Lahfan Min Makaa'd Al-Shatian, 2 edn. Dar Al-Kitab Al-Arabi.

4. Al-Lyaly, S.M. (1990) The traditional house of Jeddah: A study of the interaction between climate, form, and living patterns. University of Edinburgh. Unpublished Ph.D.

5. Al-Megren, K. (1987) Wind towers for passive ventilation cooling in hot-arid regions. The University of Michigan. Unpublished Doctor of Architecture.

6. Al-Said, M. (1996) The Rowshan in the Western Province. SED-308/1416, King Abdulaziz University: School of Environmental Design.

7. Al Shareef, F.M. (1996) Natural light control in Hedjazi Architecture; An investigation of the Rowshan performance by computer simulation. University of Liverpool. Unpublished Ph.D. thesis.

8. Awbi, H.B. (1991) Ventilation of Buildings, London: E & FN Spon.

9. Bokhari, A. (1978) Jeddah, a study in urban formation. University of Pennsylvania, Philadelphia. Unpublished Ph.D.

10. Danby, M. (1980) "The Islamic architectural tradition and the house, with special reference to the Middle East". p.200-208, Dammam, Saudi Arabia: King Faisal University.

11. Edwards, F. (1987) Climate and Oceanography. In: Edwards, A. and Head, S., (Eds.) Red Sea, London: Pergamon Press.

12. Evans, B. H. (1979) "Energy conservation with natural air flow through windows". **(5)**, 2 edn. p.641-650, ASHRAE Transactions.

13. Fathy, H. (1986) Natural Energy and Vernacular Architecture, Chicago: Chicago press.

14. Fathy, H. and Sultan, A.A. (1985) "Al Malkaf: A traditional cooling and ventilation system". Sun World **9-(2),**

15. Givoni, B. (1981) Man, Climate and Architecture, 2nd edn. London: Applied Science Publishers Ltd.

16. Greenlaw, J. (1976) The Coral Buildings of Suakin, London: Oriel Press.

17. Hariri, M. (1992) "The design of the Rowshan and its importance to the dwelling". Journal of Umm Al-Qura University **(5),** p.175-237.

18. Hariri, Majdi (1993) ""Kharijah"". p.22p, Cairo: Third International Science Conference.

19. Hemeid, A.A. (1999) Desirable courtyard orientation and proportion for the Riyadh region. pp.2B-36-2B-64. King Saud University.

20. Kaizer, T. (1984) Shelter in Saudi Arabia., London: Academy Editions.

21. Khan, S. (1986) Jeddah Old Houses, Saudi Arabia: King Abdulaziz City for Science and Technology.

22. Kilical, A.A. (199) Traditional architecture in Riyadh. pp.52-57. Riyadh: King Saud University.

23. Koenigsberger, O., Ingresoll, T., Mayhew, A. and Szokolay, S. (1977) Manual of Tropical Housing. Part One: Climatic Design, London: Longman Group Ltd.

24. Konya, A. (1980) Design primer for hot climates, London: Architectural Press.

25. Kukerja, C. (1978) Tropical Architecture, New Delhi: Tata McGrow-Hill Publishing Company ltd.

26. Maghrabi, A. (1993) The revival of adobe architecture in the Arabian region. Unpublished report.

27. Maghrabi, A. (1995). Personal communication with local craftsman. Jeddah, Saudi Arabia.

28. Mani', M. (1980) The Architectural features to old Jeddah. vol.1, pp.100-108. Jeddah: Al-Salam.

29. Markus, T.A. and Morris, E.N. (1980) Buildings, Climate and Energy, London: PITMAN.

30. Mauger, T. (1996) Impressions of Arabia, Paris, France: Flammarrion

31. MEPA 1983. Meteorology & Environmental Protection Administration. Jeddah: Meteorology & Environmental Protection Administration.

32. Najib, A. (1987) *The climate in Jeddah: the Bridge of the Red Sea*, Cairo: The Arabian publishing house for Encyclopedias.

33. Olgyay, V. and Olgyay, A. (1976) Design with climate; Bio-climatic approach to Architectural regionalism, Princeton N.J.: Princeton University Press.

34. Olgyay, V. (1963) Design with climate, Princeton N.J.: Princeton University Press.

35. Oliveira, F. and Bittencourt, L. S. (1998) "Air flow through louvered windows in small rooms". PLEA ' 98. Lisbon, Portugal, p.393-396,

36. Said, S.-A. and Al-Zaharnah, E.T. (1994) "Development of comfort zone charts using the Isopleth charts technique". Building and Environment **29 (1),** p.13-20.

37. Salloum, A. (1983) "El-Rowashin of Jeddah, Saudi Arabia". p.245-252, Crete, Greece: Passive and Low Energy Architecture (PLEA).

38. Sanderson, R. (1982) Meteorology at Sea, London: Sanford Maritime.

39. Sharma, M.R. and Sharafat, A. (1986) "Tropical summer index - a study of thermal comfort of Indian subjects". Building and Environment **21 (1),** p.11-24.

40. Winterhalter, C.P. (1982) "Environmental control in the indigenous architecture of the Eastern Province of Saudi Arabia". The Arabian journal for science and Engineering. 7 **(2),** p.112-121.

CHAPTER 3: MODULATED LOUVERED WINDOWS (MLW).

3.1. Introduction

This chapter reviews the current research and contribution made to observe modulated louvered windows (MLW) as a source of natural ventilation in buildings. In addition, it sets out the approach to the theoretical thrust of this research. The first section reviews the conventional window types and highlights some of their ventilation characteristics. Then follows the discussion of the louver window systems including the horizontal, vertical and combined systems. The third section is devoted to the review of the relevant research carried out in relation to MLW and to addressing closely the evaluation and critique of each one of them.

The chapter ends up by stating the problem of the current research based on the review of the aforementioned chapters concerning the climate and architecture in Jeddah as well as on the review of modulated louvered windows as the source of natural ventilation in buildings.

3.2. Conventional window types

Back in 1951, Holleman (1951) carried out research on airflow through conventional window openings and concluded that airflow characteristics differ significantly due to these different opening types. Holleman and Evans (1979) agreed that common windows used are classified under three basic types; simple opening, vertical vane and horizontal vane as illustrated in Figure 3.1. These categories seem valid and cover most of the types commonly employed in buildings. The perforated block walls are of porous elements that are widely employed in the tropics; they discussed here along with other window types.

3.2.1. Simple openings (Holleman, 1951)

Simple openings include the single-hung, the double-hung and the horizontal-hung. The direction of passing air was not affected and continued in the same wind direction. However, a noticeable significant change of speed was evident near the window. This was referred to as the squeeze of air and Holleman recommended this type to be used directly in living zones. The maximum opening area is one-half the total window area: 50% opening. These windows are recommended directly in the occupied zone since neither the direction nor the speed of air was altered.

3.2.2. Vertical vane openings (Holleman, 1951)

Vertical vane openings include such openings as side-hinged casement, the folding casement, and the vertical pivot. These windows allow complete opening area: 100% opening. Generally they provide alteration of airflow at horizontal level and it was recommended to allocate them directly to the occupied zone.

3.2.3. Horizontal vane openings (Holleman, 1951)

Horizontal vane openings include the projected sash, the awning, the horizontal pivoted and the jalousie or modulated louvered windows. Similar to the previous type, the opening area of this one allows full opening, too. The airflow characteristics, through a variety of combinations, vary considerably in accordance with the window types. One of the sound conclusions derived from the work bore on the modulated louvered window type. MLW was preferred over other types investigated in redirecting and altering the flow to upward and downward directions indoors as illustrated in Figure 3.2. It was then recommended to use it below the level where air movement was required.

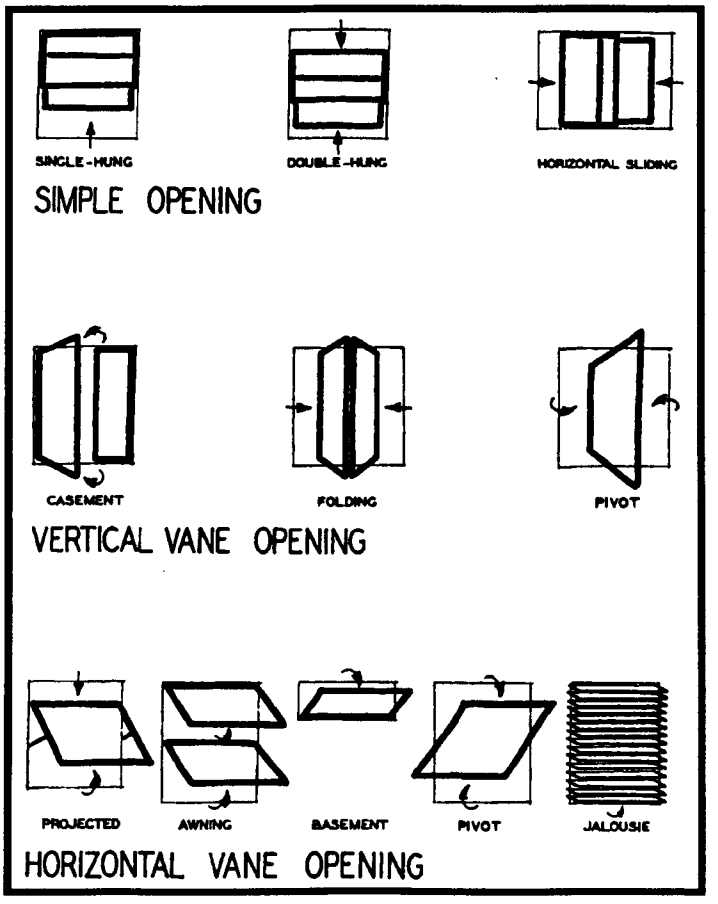

Figure (3.1): The conventional window types classified under the three main categories including simple opening, vertical vane opening and horizontal vane opening. (Holleman 1951)

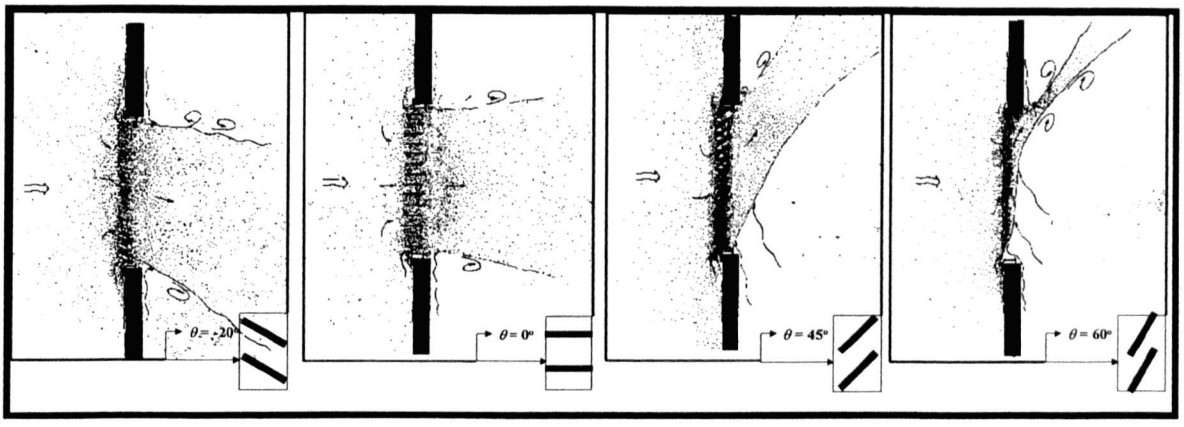

Figure (3.2): The MLW has a quality of directing air to different levels indoors. (After Holleman 1951)

3.2.4. Perforated block walls

Perforated block walls could also be enrolled under the various types of apertures discussed here. These porous elements cover either part of or the entire façade, and their geometrical configurations differ accordingly. They have been in use for a long time in Brazil, South America, Spain and other Asian countries. Bittencourt (1993) had investigated a number of perforated block walls predominately used in Brazil and had concluded that the airflow through them depends merely on their geometries. Figure 3.3 demonstrates the patterns of airflow indoors based on various block types examined under 10m/s wind speed and perpendicular wind direction: 90^{o}. Block C1 offered the maximum resistance to air velocity and hence, showed the poorest performance while C2 and C3 tend to straighten the flow indoors regardless of wind direction. It was then recommended that these apertures be best applied in warm humid climate where a continuous air motion indoors is needed.

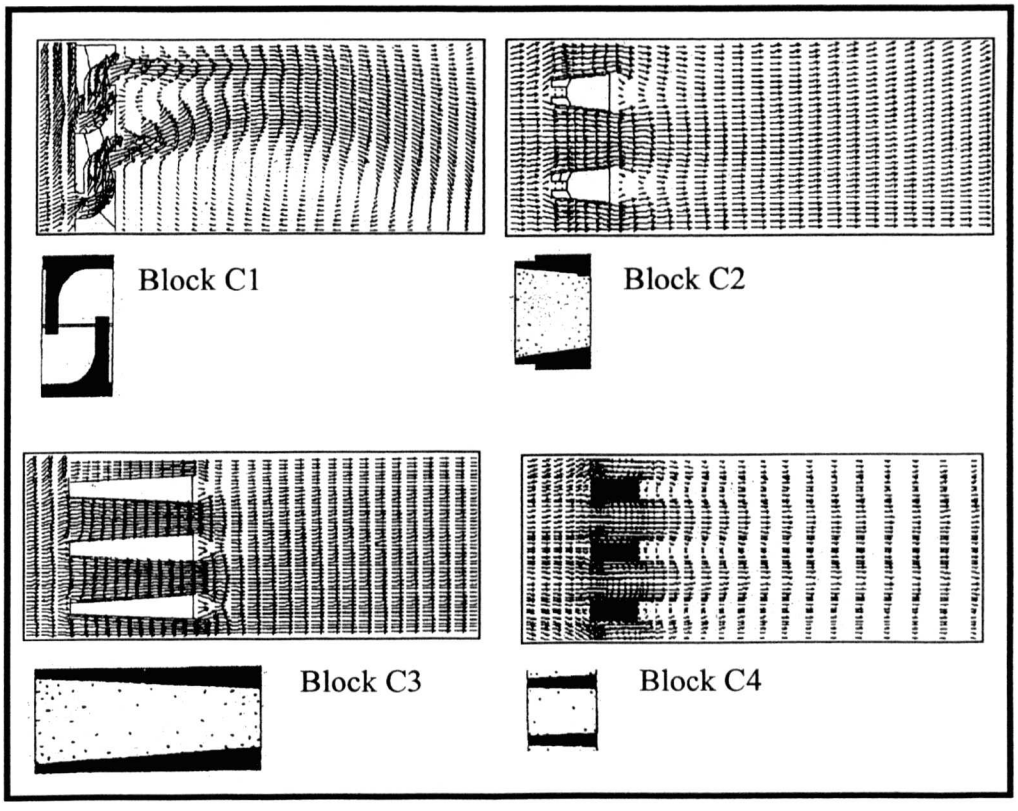

Figure (3.3): The patterns of airflow indoors based on various block types examined under wind speed=10m/s and perpendicular wind direction(90°). Block C1 offered the maximum resistance to air velocity and hence, showed the poorest performance while C2 and C3 tend to straighten the flow indoors regardless of wind direction. (Bittencourt 1993)

3.3. Louver window systems

Cross ventilation provides a good solution to releasing the overheating and excessive humidity in the tropics by natural means (Koenigsberger et al. 1977) (Givoni, 1991) (Salloum, 1983). Many techniques have been used, one of which is the louvered windows that are commonly employed in different parts of the world. The louvered window systems are categorised under three different configurations (Evans, 1980) (Muniz, 1985), (Fikry, 1981), (Al Shareef, 1996) (Figure 3.4):

1. The horizontal louvers system.
2. The vertical louvers system.
3. The egg crate system; a combined system of horizontal and vertical louvers.

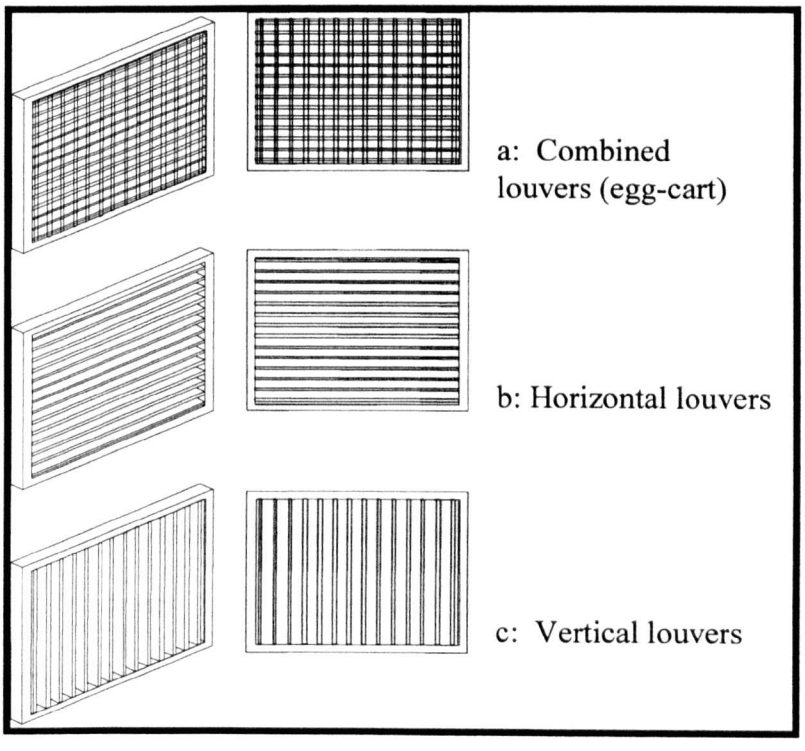

Figure (3.4): The various louver window systems.

The three systems have different shading characteristics, light reflection, view and flow patterns (Evans, 1980). Figure 3.5 demonstrates the velocity drop as a function of the three louver systems in a typical room, with best performance going to the horizontal louver system (Sobin, 1983). The setup of the egg-crate system is much similar to the perforated blocks discussed earlier and it is usually set to a certain inclination. With respect to natural ventilation, the system separates the flow passing through into cubical flow streams and offers more resistance to airflow in both dimensions than the alternatives. It was widely employed in Roman baths, in traditional Islamic and Indian architectures (Fathy, 1986). The perforated panels found in Alhambra (Granada) reveal the same principles. The construction of their perforations may vary from being egg-crate shape since their curvatures and the decoration feature also influenced their application.

One of the main features of the other types, the horizontal and the vertical, as compared to the combined system, is concerned with alteration of airstreams indoors. The vertical system alters the inflow towards lateral walls while the horizontal reflects the airstreams upwards or downwards towards the ceiling or the ground levels. Yet, when examining the presence of both systems in the architecture, it is unquestionably true that the horizontal louvers systems are more widely employed than the vertical. Their presence is even more apparent in the tropics and hot humid regions. One possible explanation for this superiority is because horizontal louver systems offer less resistance to the breeze in the room as illustrated in the previous Figure. The present study examined some characteristics of both horizontal and vertical systems and advanced some possible reasons for the widespread use of horizontal louver systems compared to vertical, as shown in Figure 3.6.

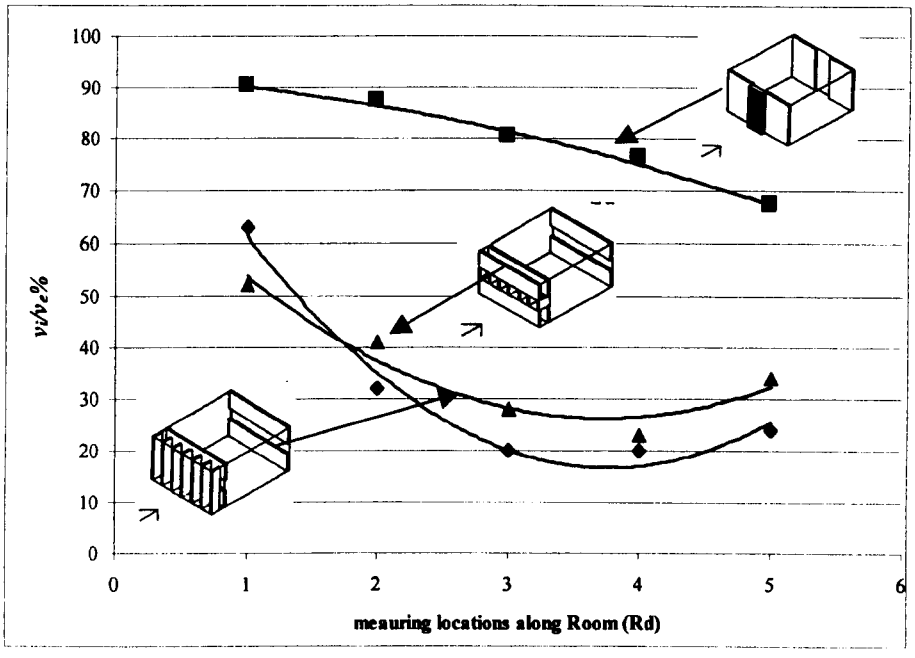

Figure (3.5): Velocity drop as function to the various louver systems including combine, vertical and horizontal. (From original data) (Sobin 1983).

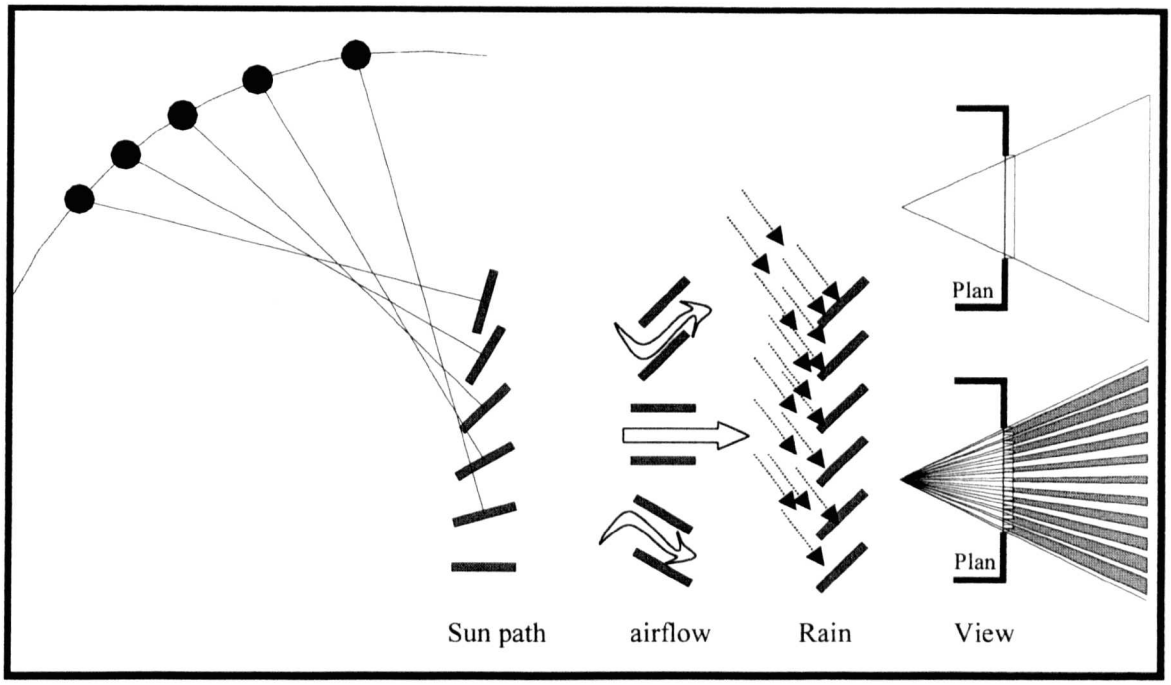

Figure (3.6): Horizontal louver systems carry preference over the vertical virtue of a number of functions. (a): the capability to alter the louvers angle to the sun altitude, (b): distribution of airflow to various level in the room, (c): protection from rain and (d): larger range of view.

3.4. Review on MLW applications in buildings

The application of porous elements reveals a level of thermal sensation in buildings. Aynsley et al. (Aynsley et al. 1977) indicated that there is a high degree of correlation between thermal comfort and porosities in building elevation. Nevertheless, flow coefficients (C_Q) representing the difference between measured and estimated airflow rates (Q) of this type of apertures is largely underestimated (Bittencourt, 1993). The work of Vickery and Karakatsania (Vickery and Karakatsania, 1987) demonstrated the flow characteristics through porous element with 46% porosity and compared it with the estimated flow coefficient expressed in the following equation:

$$C_Q = \frac{Q}{A \cdot V} \qquad (3.1)$$

where

C_Q = Flow coefficient

Q = Volumetric flow of air (m3/s)

A = Opening area (m^2)

V = Wind speed at opening level (m/s)

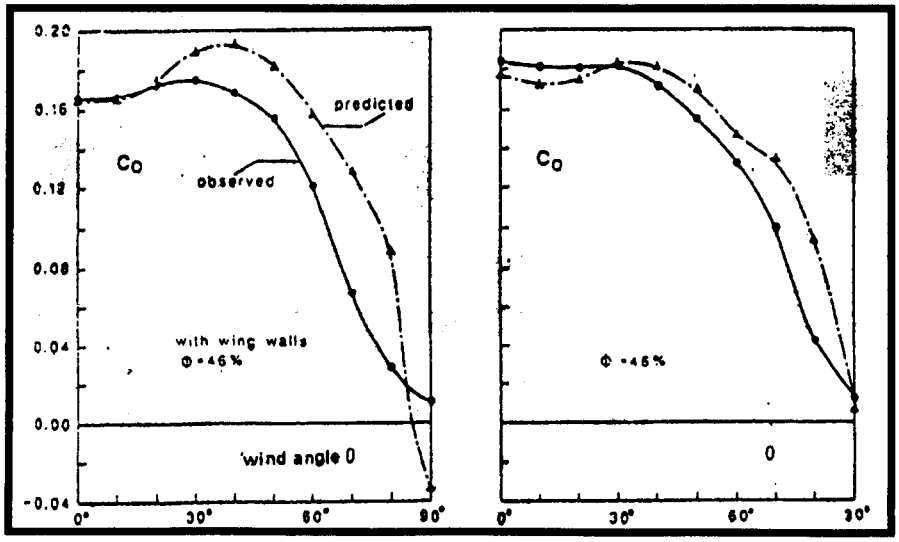

Figure (3.7): Flow coefficients for both observed and predicted curves with wall porosity of 46%. (Vickery & Karakatsania 1987).

From Figure 3.7, the observed values were obviously less than those predicted values for wind indices between 20° and 90° while in perpendicular wind (0°) both were nearly similar. Also the critical drop in both curves was present with skewed inclinations- when $\theta > 45°$- where they may then produce errors that seriously lead to mistaken readings. The

variation becomes more apparent with the presence of the wing walls as shown by the Figure.

The MLW is of those porous elements that are mostly employed in such warm climates as far east as Australia and as far west as South America. Its presence coincides with the need for protection from intense solar radiation while allowing breeze to penetrate through. The MLW is also used in cold environments, such as Europe, where the use of it is merely to protect interiors from potential overheating in summer seasons. The principle of the MLW is similar in mechanism and function, though it may be termed differently. Some of the commonly used terms are the Jalousie, adjustable, operable, blinds and movable louvers windows. The term used here, the modulated louvered window, corresponds to those terms and is also found in some literature such as (Yakubu, 1990) (Yakubu and Sharples, 1991) as well as in one of the author's recent studies (Maghrabi and Sharples, 1999)

In the traditional architecture, MLW may be found to cover most of the elevation, or even the entire elevation, as employed in Jeddah. As discussed in the previous chapter, the Rowshan is an example which is implemented in many parts of the world such as Morocco, India, Egypt and elsewhere. In certain cases, the MLW is employed in a form of separate windows. An example of this is found in Figure 3.8 where it shows the similarity in its application in a number of buildings from various regions.

MLW is used at the mouth of the tower to direct air downwards to the living spaces. As illustrated in Figure 3.9.a the downward deflection of air was obtained by using the modulated louvered panels. In large buildings with splits on floor, the application of louver sheets will help to control air patterns inside the structure. Also the splits in pitched

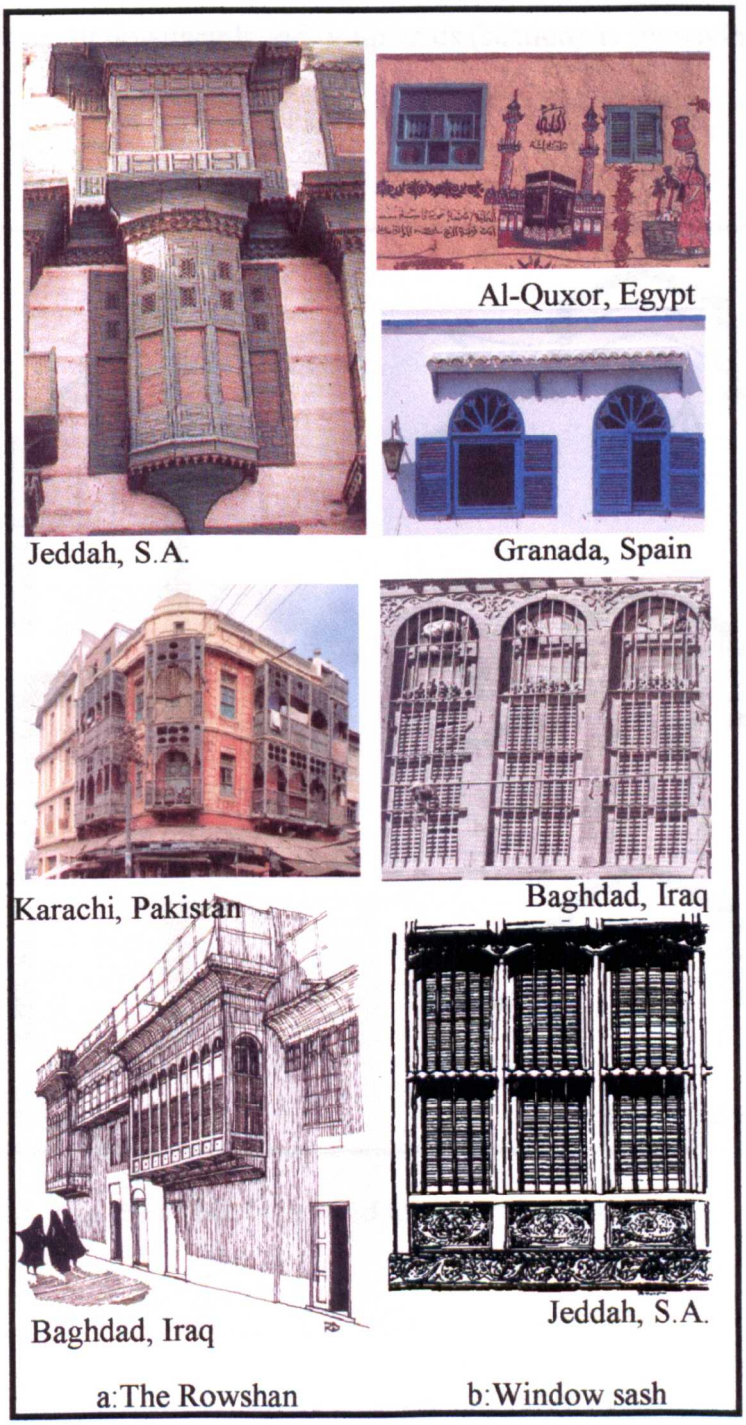

Figure (3.8): Different examples of MLW applications in apertures (Amin and Willetts 1986), (Atroshenko and Grundy1991), (Crescimbene and Balocco 1994), (Warren and Fethi 1982) .

roofs are adequately endowed with louver panels in the lateral ridges. When altered, they enable directing air downwards and or upwards (suction) as shown in Figure 3.9.b.

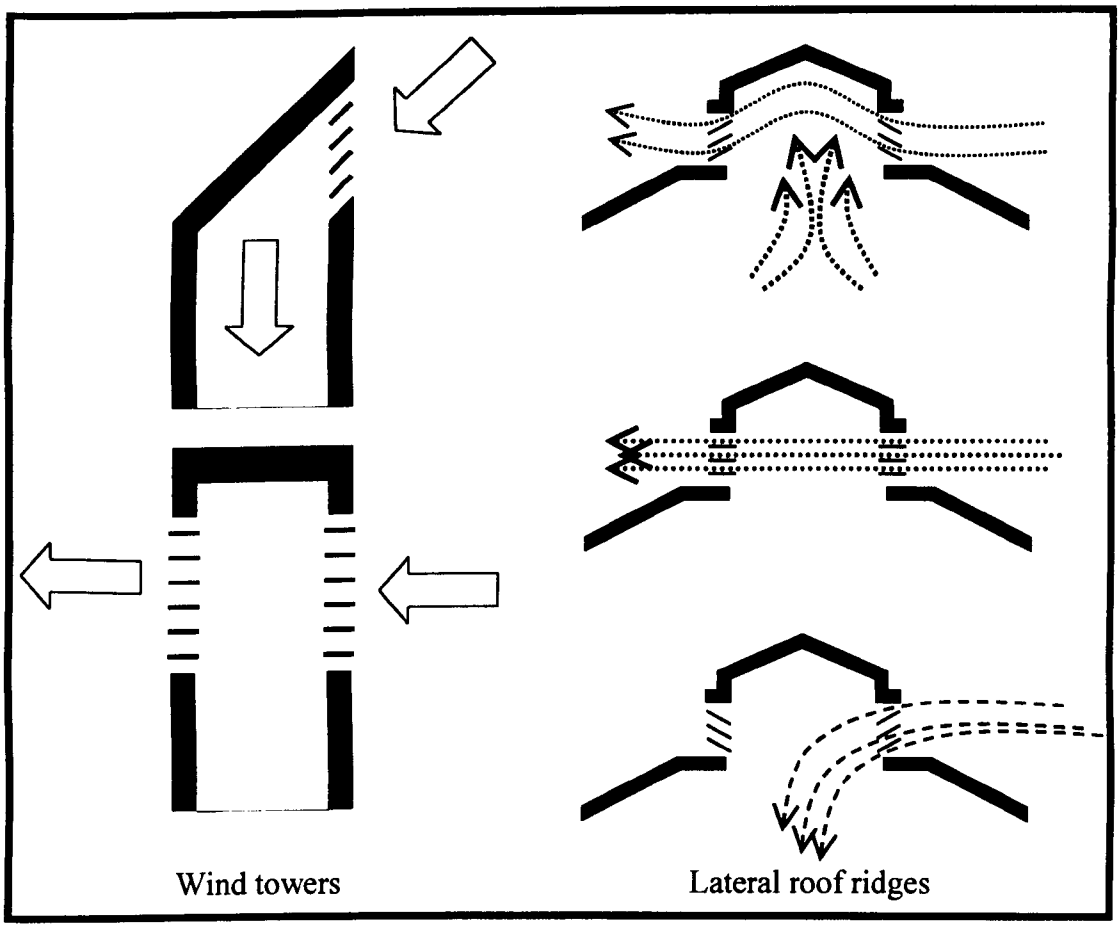

Figure (3.9): The use of MLW in wind towers and roof ridges.

The contemporary applications of MLW can be found in many buildings along the same or similar principles. For example, one of the uses of MLW is shown in Figure 3.10.a where the inclinations of louvers are replaced by movable window sashes that tilt as a function of the sash opening. Another example of that is the use of the MLW with the *ventilative sill* where both act to direct air into various levels in the room. The *ventilative*

sill (Figure 3.10.b) acts as a source of continuous ventilation for the lower level of the room where this many be useful when certain activities are practised near the ground. The other levels of the house are ventilated with the various inclinations of louvers. The technique is of usefulness in warm tropics as it provides ventilation at all lower levels within the room whilst protecting the indoors from the overheating sun.

Other applications of the MLW are found in what is called the *energy-efficient* fenestrations, some examples of which are found in Brandle and Boehm (Brandle and Boehm, 1982) and (USA Dept.of Energy, 1983). However, many designers apply the

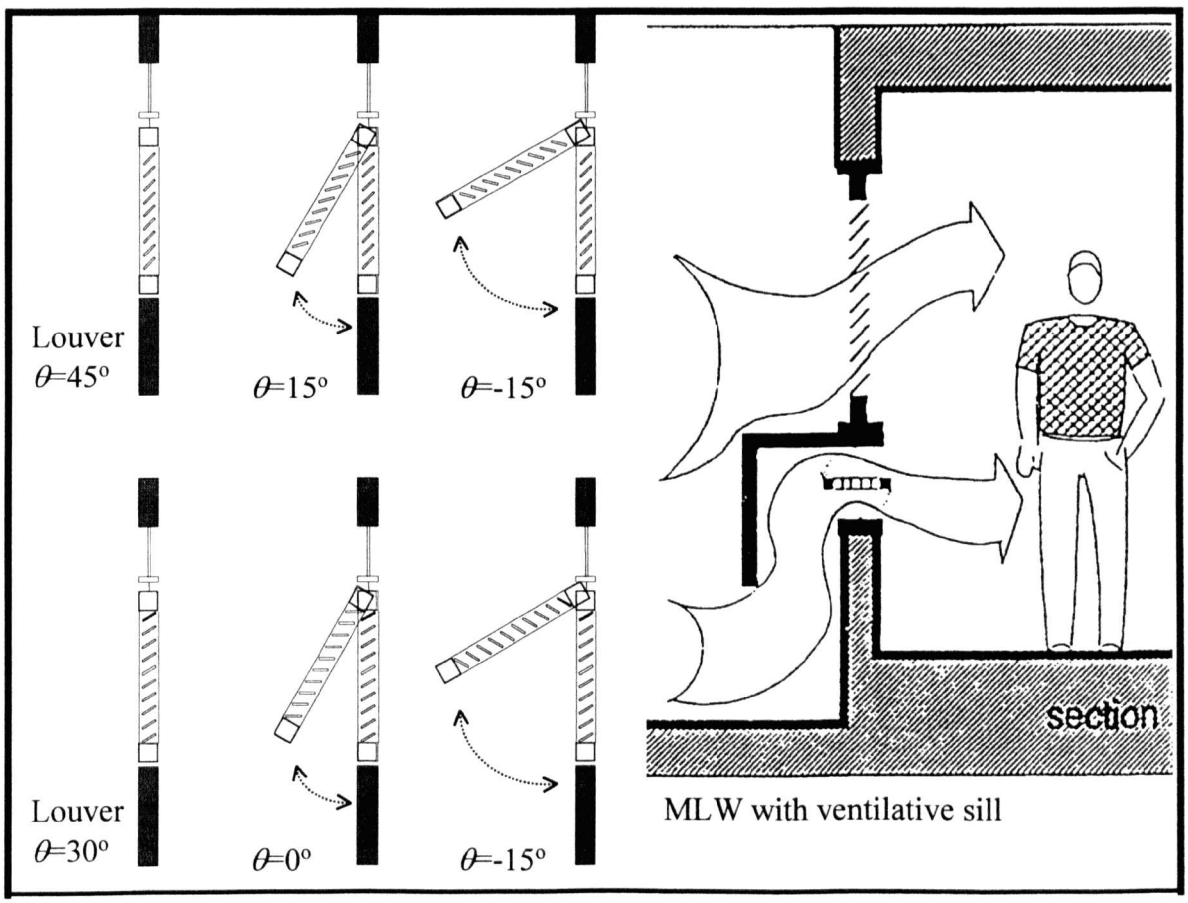

Figure (3.10): The modern application of MLW for natural ventilation. (Bittencourt 1993)

MLW to optimise the daylight and shading characteristics indoors while underestimating

its design in terms of the ventilation. This is due to many reasons amongst which the performance and design the window is given when it is closed, rather than when it is open (Evans, 1979). Another possible reason is the absence of comprehensive characteristics of ventilation performance through this type of window. The flow around a MLW is more complicated than those produced by the imagination of architects, not only on the scale of the velocity and pressure characteristics, but even on the scale of flow patterns, *"Much of this information is misleading, as it is frequently based on the limited knowledge and expansive imagination of designers, who have not thoroughly researched this topic,"* Bowen stated (1983).

3.5. Related research

Wind induced natural ventilation has been the subject of many researchers since the 1950's; yet most of them have given little consideration to the airflow indoors as a function to window treatments and accessories (Muniz, 1985). Holleman (1951) was one of the first to comprehensively underline the role of various conventional window designs with respect to natural ventilation. The study is of critical importance as it sets guidelines for designers and architects to optimize the indoor environment based on the window design. His study covered the most conventional windows implemented nowadays. Amongst these are the Jalousie windows that are preferred over other types investigated in redirecting and altering the flow in upward and downward directions indoors as discussed earlier (Figure 3.2). Further studies are found in the famous book *Design with Climate,* written in 1963 by the Olgyay brothers (1963). They gave some indications of the flow behaviour across the louvered windows. The images were useful in demonstrating the patterns indoors as function to various window parameters.

Givoni and Hoffman (Givoni et al. 1968) studied the temperature and illumination conditions in a classroom as a function of windows with fixed shading device. The work did not directly account for natural ventilation, yet it showed that the temperature variations due to open windows did not constitute a significant reduction in internal surface temperature as shown in Figure3.11. One of the explanations of this was the low wind speed under which the study was conducted as noted by the authors. In further research, Givoni (Givoni, 1968) stated that the details of the aperture would have a direct influence on ventilation conditions. The treatment involved employed wing-walls that created pressure and suction on the external wall near the window. Similar statement is found in his book, *Man, Climate and Architecture*, which was published in 1981 (Givoni, 1981).

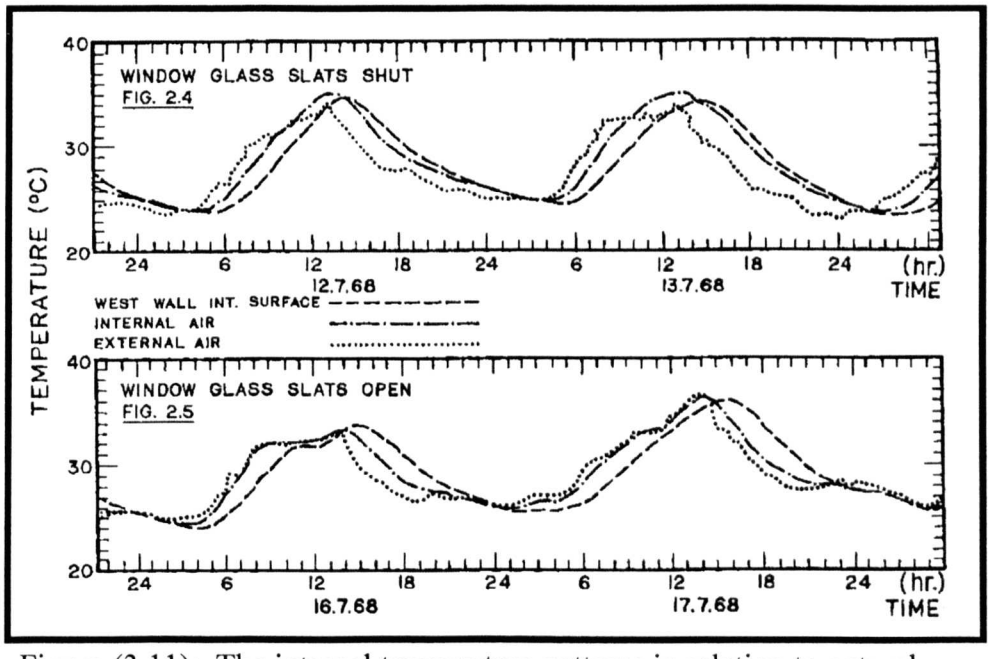

Figure (3.11): The internal temperature patterns in relation to natural ventilation when window faced north.(Givoni et al. 1968)

Some more recent research has underlined the effect of various window parameters such as size, location and orientation in improving the airflow quantity and patterns indoors. Some of this is found in Jong and Bot (Jong and Bot, 1992), Al-Jawadi (Al-

Jawadi, 1986), Chandra (Chandra, 1983) and Brandle & Boehm (Brandle and Boehm, 1982). Others have investigated the mechanism of airflow through buildings, and further, on various parameters governing air motion indoors. These are more relevant to the current review; hence they are highlighted here in more details.

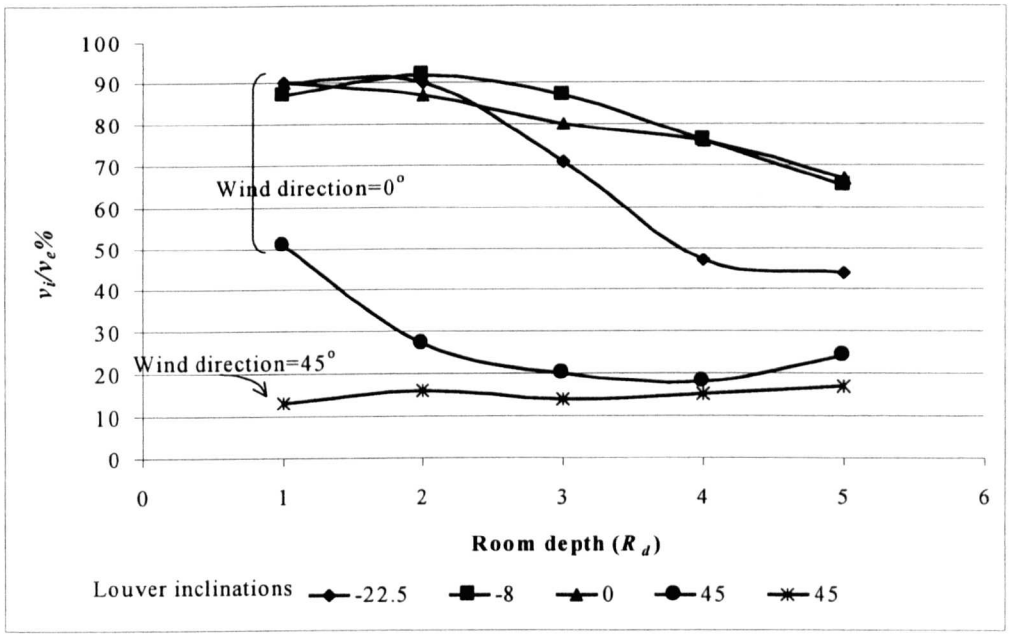

Figure (3.12): Airflow through Jalousie windows with various louver inclinations and wind directions. (Sobin 1983)

The work of Sobin (Sobin, 1963) (Sobin, 1981) (Sobin, 1983) mentioned previously has extensively studied the various parameters governing airflow indoors including the windows treatments. After more than 270 experiments that were carried out on nearly 140 aperture configurations, he demonstrated the clear contribution of the architectural features of window location orientation, treatment, outlet as well as room depth in relation to wind-induced natural ventilation. The Jalousie windows were examined amongst the other window treatments and Figure 3.12 represents the velocity drop in the centre axis along the room depth. The ratio of indoor to outdoor velocity

(v_i/v_e%) near the window was 90% for the louvers inclinations 0°, -8° and –22.5°, while a clear reduction was observed with the presence of steeper inclinations. The study also demonstrated the significance of the wind direction for the reduction of the ratio of internal velocity with respect to external (v_i/v_e%). The reduction along the room was obviously smoother with the perpendicular wind incidence. In addition, the study gave some indications of the effect of louver angle of inclination with respect to v_i/v_e% as illustrated in the Figure. Nevertheless, his work disregarded the effect of various parameters of the louvered windows on the flow indoors. Furthermore, it did not emphasise the flow rate (Q) with respect to the pressure drop (ΔP) across the window.

Muniz (Muniz, 1985) examined the effect of shading device geometries on natural ventilation, daylight and thermal comfort. The study was extensive in that it provided designers with an *analytical model* in which they could compare various shading geometries in order to optimise the indoor environment. There were three shading devices that covered horizontal, vertical and combined geometries. The velocity characteristics with respect to the former types were generally less marked in perpendicular than in oblique winds (Figure 3.13).

But when this work is examined in light of the hypothesis of the of current study, some critical limitations become apparent:

1. The study was limited to only a single wind speed.
2. The louver configurations covered, including louver depth and aperture, were too large compared with those reviewed in this investigation. The depth ranged from 0.35m to nearly 1.20m; the flow characteristics could not therefore represent those carried out here.

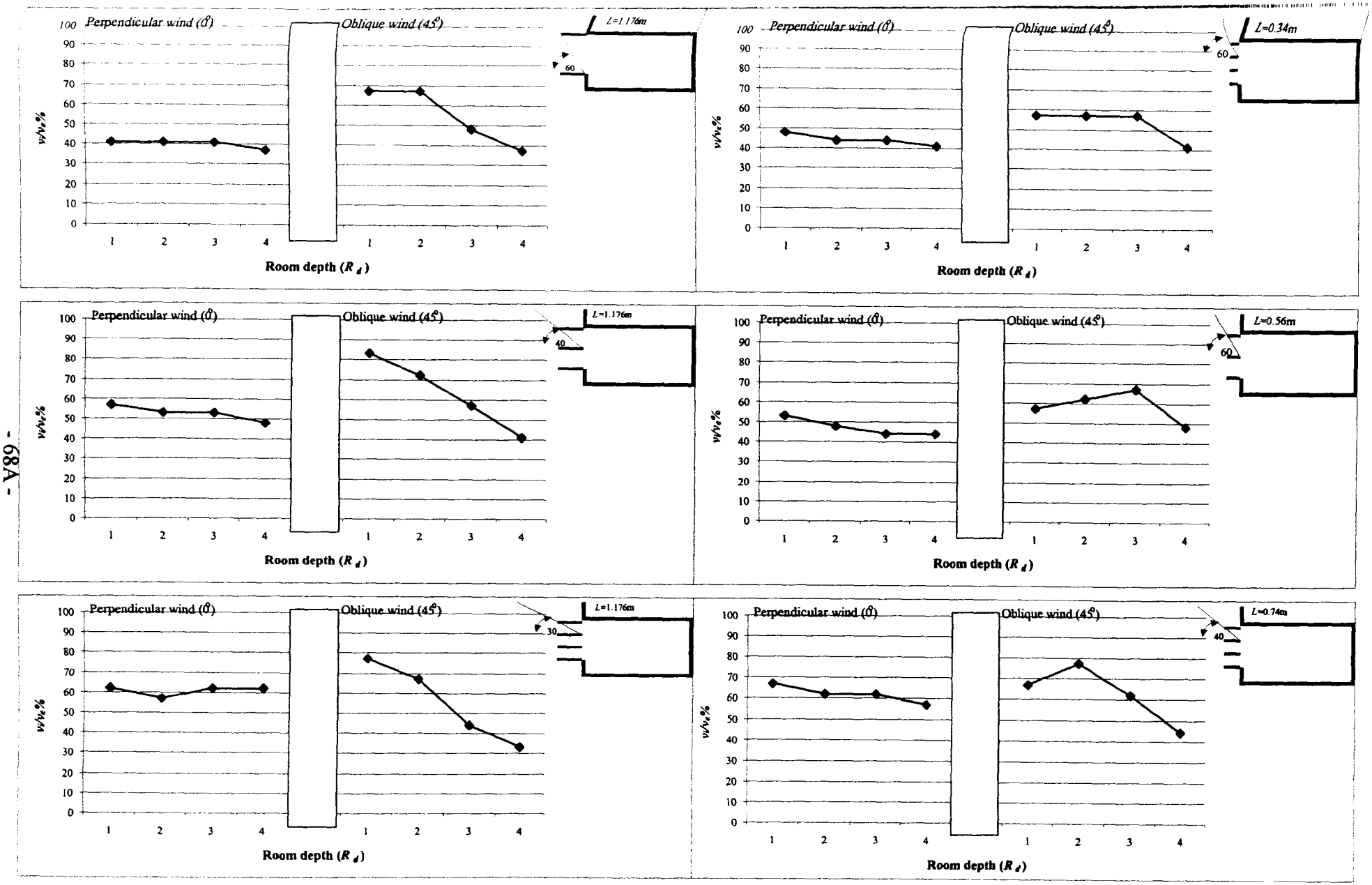

Figure (3.13): Natural ventilation performances of a number of horizontal external shading devices studied by Muniz (1985)

3. The study also disregarded the louver inclination and its contribution to the overall velocity and pressure drop inside the room.

The work of Al-Lyaly (Al-Lyaly, 1990) sheds light on the significance of the MLW to assist occupants' comfort in traditional buildings in Jeddah. Indoor temperature, air velocity and relative humidity were measured in three rooms and compared with outdoor temperature, air velocity and relative humidity, respectively. The study was conducted during the summer season with an average outdoor temperature reaching 38.5°C noontime. Although the indoor temperature was near, or even exceeded, the comfort level temperature in the three rooms examined, it did not reflect the outdoor temperature changes as shown in Figure 3.14.a. Interestingly, the air penetrating through the louvers and large apertures seemed to lower remarkably the indoor temperature by between 3°C and almost 6°C during daytime. Similarly, the relative humidity during daytime was reduced by 5% to nearly 20% before noon (Figure 3.14.b). With respect to the velocity measurements through MLW (Figure 3.14.c), the study is limited to a single louver configuration and the internal air velocity was averaged over three readings per hour. Although this is valid in long-term measurements, it does not completely reflect the velocity drop as a function to the MLW parameters, since outdoor air fluctuates and turbulences occur frequently.

Bittencourt (Bittencourt, 1993) studied the performance of typical perforated blocks employed in warm-humid climates in relation to natural ventilation. From the various wind indices and speeds examined, he concluded that the use of perforated blocks were appropriate and best used where *"openings are to remain open throughout the year"*. His study recommended the use of blocks where airflow direction is not altered within the perforation as those where this happened offered more flow resistance, and hence, were

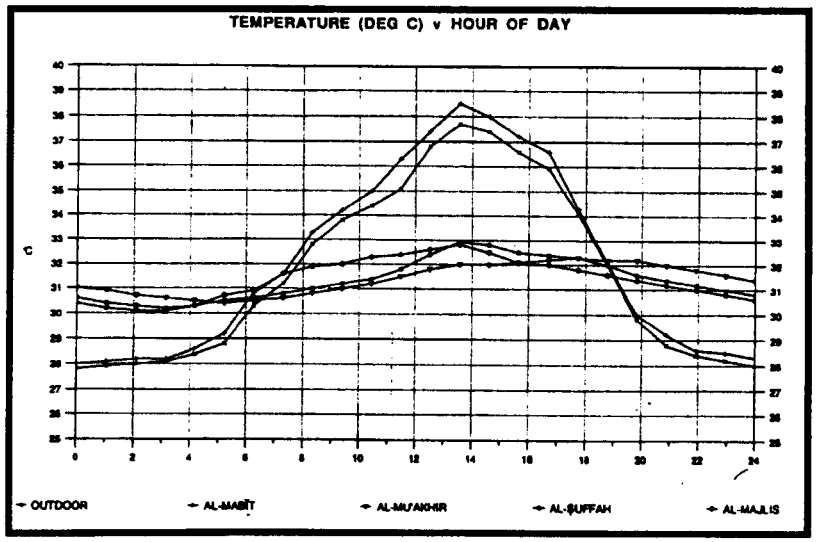

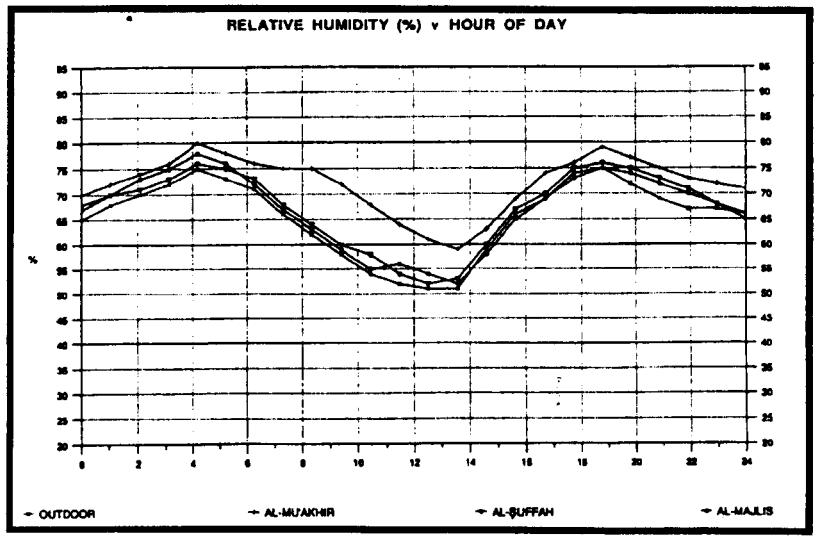

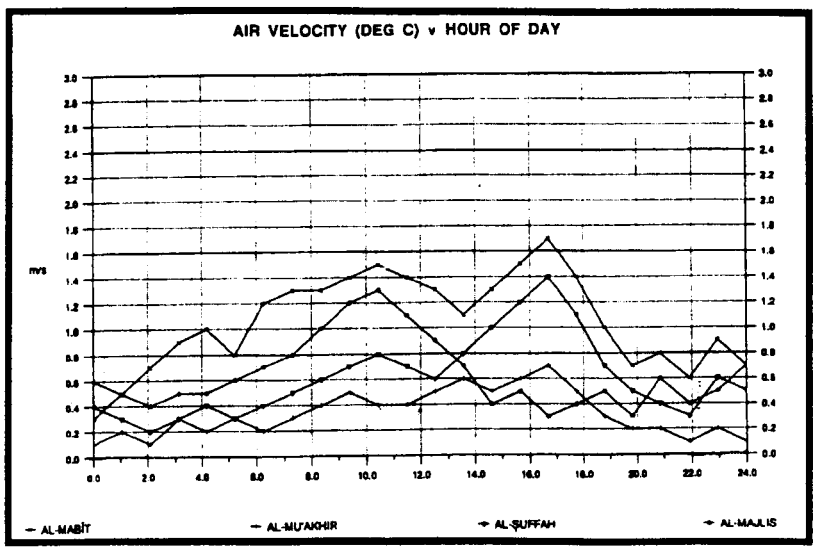

Figure (3.14): The average of three days hourly records for temperature, relative humidity and airspeed for a number of rooms and compared against the outdoor records. (Al-Lyaly 1990)

unable to produce the minimum ventilation required for comfort in that climatic region (Figure 3.15). Essentially, the previous statement reflects the importance of MLW in warm and humid climates where it offers flexibility in adjusting airflow entering the room.

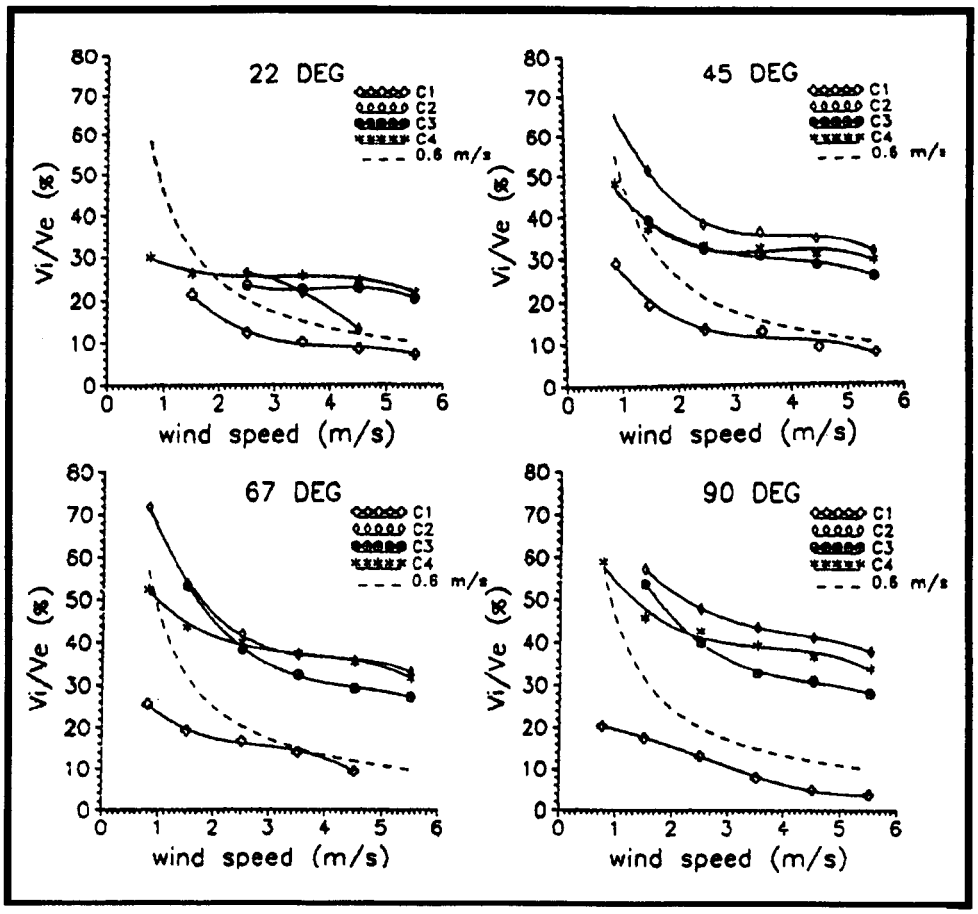

Figure (3.15): Natural ventilation through perforated blocks as function to various wind incidences. (Bittencourt 1993)

Perhaps the most relevant studies in the review are found in (Yakubu, 1990), (Yakubu and Sharples, 1991), (Pitts and Georgiadis, 1994), (Oliveira and Bittencourt, 1998) and (White, 1999). The work of Yakubu (Yakubu, 1990) and (Yakubu and Sharples, 1991) was conducted under similar louver configurations and measurements setup. Like the current study, the work investigated the performance of louver window systems under a series of air extractions. Figure 3.16 illustrates the pressure drop (ΔP) across the MLW as function to volumetric flow of air (Q). The inclination angles selected for this work ranged

from 0° to +75° at intervals of 15°. The volumetric flow of air through the MLW was independent of the resulting pressure for all louver inclinations less than 60°. One limitation of Yakubu's study was that *"The measurements are restricted to smooth wooden louvers with dimensions of 100mm in breadth and 5mm in thickness with a gap of 95mm between the louvers when they are perfectly horizontal (i.e. 0°)"* (Yakubu, 1990). In other words, his work does not take into consideration when louver breadth (L) and gap thickness (d) are changed.

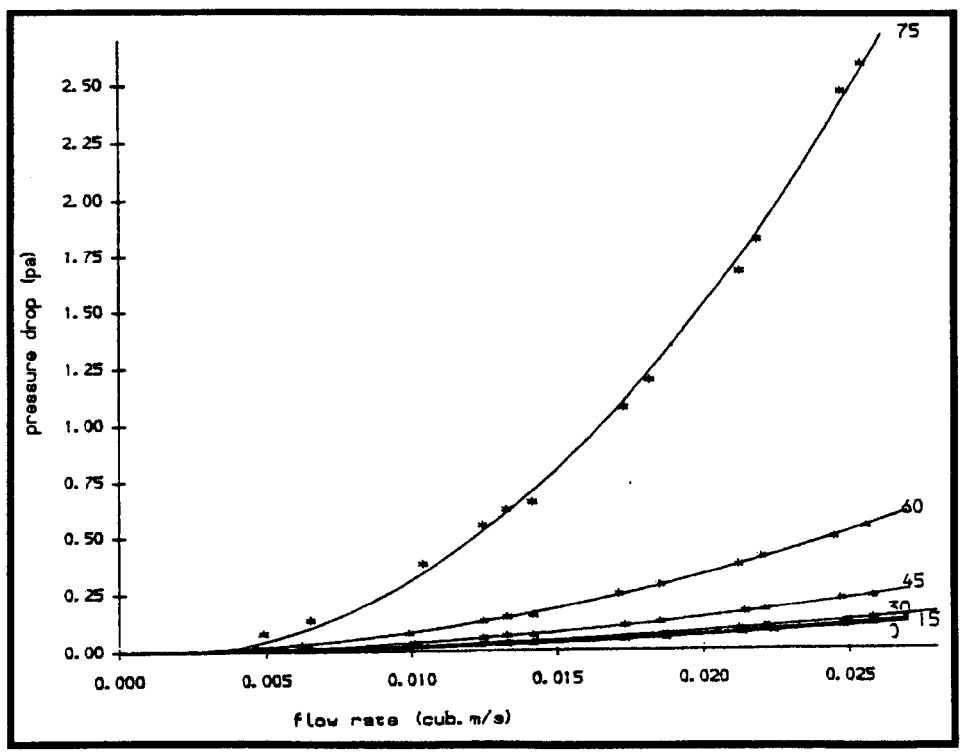

Figure (3.16): Pressure drop (DP) in relation to the flow rate of various louver inclinations. (Yakubu and Sharples 1991)

Pitts and Georgiadis (Pitts and Georgiadis, 1994) carried out a wind tunnel investigation to measure pressure drop across the opening associated with a Venetian blind with three inclinations, 0°, 45° and 85°. Similar to the former, the study showed that Q was independent of the louver inclinations until 45° (Figure 3.17). Essentially, the study made

a noticeable contribution; *"Indeed there is some evidence to suggest that the use of suitably angled blinds may actually enhance air flow through partially opened windows"*. The number of cases examined was more than the former; nevertheless, the louver configurations were limited since, *"The fins each measured 910mm wide, 50mm depth, 0.25mm thick with a spacing when horizontal of a 40mm"*. Pitts and Georgiadis suggested that further investigations to optimise the use of this type of window treatment from natural ventilation point of view were indeed essential.

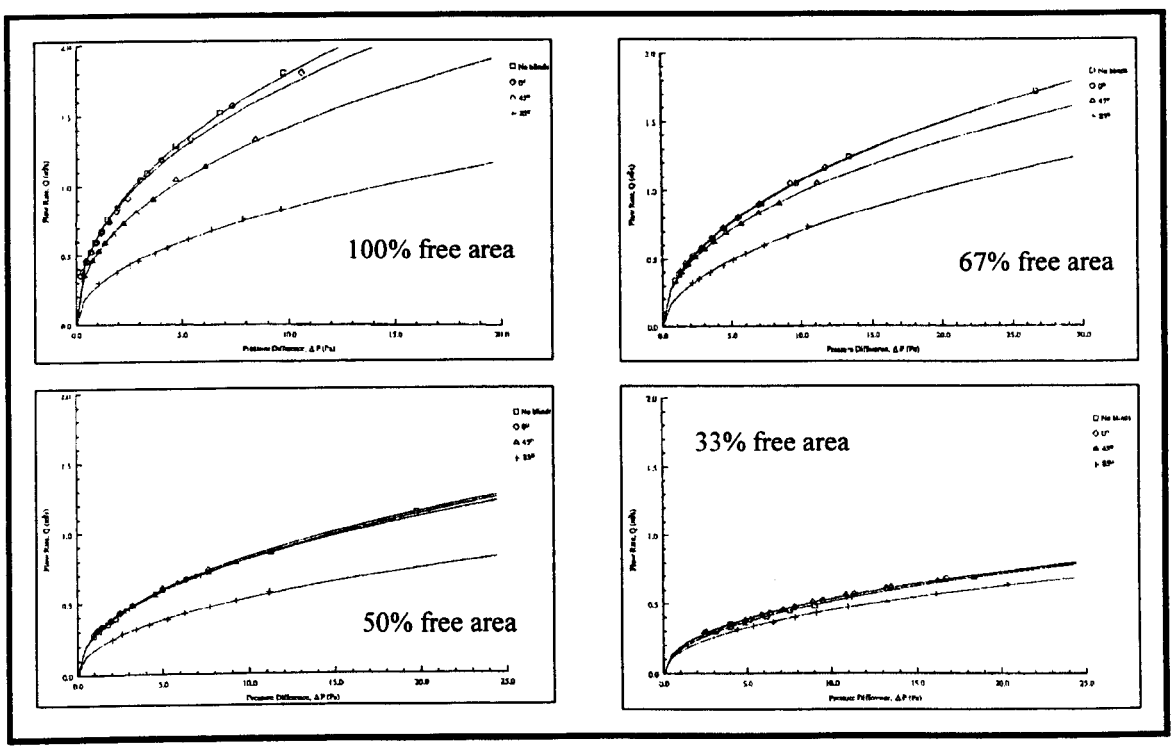

Figure (3.17): The volumetric flow of air (Q) through shading devices v the pressure drops (ΔP) for a number of opening free areas. (Pitts and Georgiadis 1994)

Another study was conducted on various ventilators and wall-vent systems, some of which contained fixed louvers (White, 1999). While the study is not directly relevant, it suggested that the airflow passage though ventilators seems more efficient than when compared with a sharp-edged hole having the same free area.

Similarly, Oliveira & Bittencourt (Oliveira and Bittencourt, 1998) carried out some recent work comparing the velocity drop with respect to both open windows and louvered windows, with and without mosquito screens. Similar louver dimensions were examined. The result demonstrated the significant variations of flow resistance as a function of wind speed and direction (Figure 3.18). However, as in the case of former studies, the study did not take into account the various louver configurations and their input to the flow characteristic, and the authors indicated the need for more comprehensive research to optimise the ventilation performance of this window type.

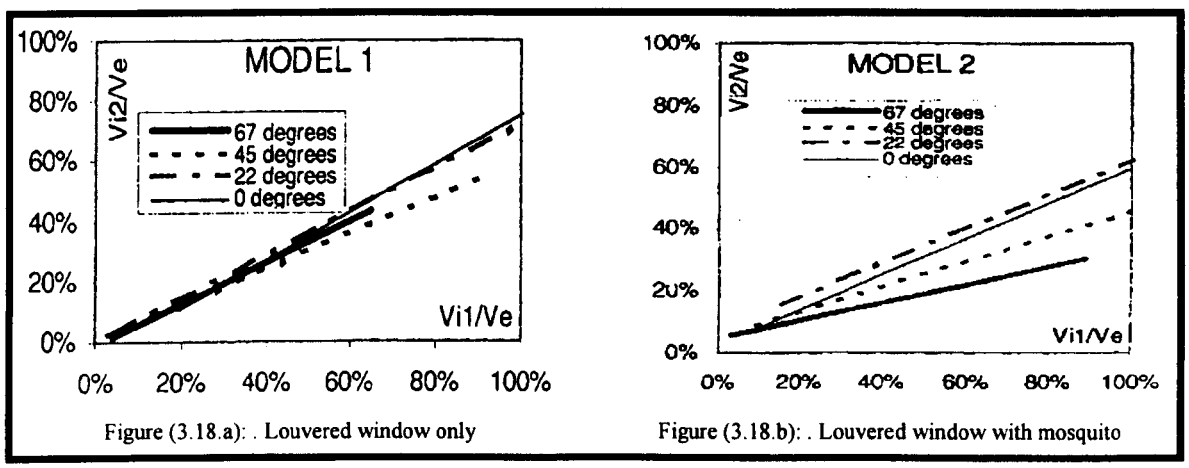

Figure (3.18.a): . Louvered window only

Figure (3.18.b): . Louvered window with mosquito

Figure (3.18): Comparison of airflow resistance for both window types. (Oliveira and Bittencourt 1998)

Most of the above studies stressed the hypothesis of this thesis that more research is needed to investigate effect of MLW various parameters with respect to pressure drop (ΔP) as well as velocity drop (v_i/v_e%) along the room depth (R_d), since they are rarely known. The body of literature analysed and the issues of ventilation with respect to MLW did not cover the complete configurations, and hence, work remains to be done.

3.6. Statement of problem

This section is devoted to setting the hypothetical statement of the current research based on the review in the aforementioned chapters concerning the climate and architecture in Jeddah as well as the review on the modulated louvered windows as the source of natural ventilation in building.

From the literature review it was found that Jeddah is located in a hot-humid climatic zone and wind-induced ventilation is a main source of human comfort by natural means. Various ventilation strategies to improve the indoor climate were employed, amongst which the MLW, as part of Rowshan, was given the most attention. The application of MLW systems is also found elsewhere. The body of literature pertaining to this window accessory dealt with its solar control performance and the optimization of its various dimensions and configurations in relation to natural ventilation is far from being satisfactory. A number of studies have addressed the need for a comprehensive analysis of this issue.

In this context, the design of MLW acquires special importance as air mainly flows inside buildings through its (MLW) apertures. There is a need to move a step forward to trace more carefully the significance of various MLW components with respect to natural ventilation. Entire parametric studies are still needed to investigate pressure and velocity characteristics as function of MLW various components. Therefore the present study will, through its various appraisal stages, enable the researcher to elaborate on the pressure and velocity characteristics as functions of the MLW parameters. These are highlighted as the following:

- The role of the modulated louvered windows parameters, such as louver depth (L), aperture (d), angle of inclination (θ), free area (A_f), $d/L\%$ and others.
- The thorough investigation of the overall performance in relation to integrating all variables.
- The external prevailing wind conditions represented in wind speed and direction.
- The critical MLW configuration when the flow characteristics would experience major alteration and resistance.
- The room configuration and its contribution to this effect.
- The airflow patterns in relation to the common Rowshan configurations employed Jeddah.

3.7. References

1. Al-Jawadi, M.H. (1986) Window optimisation for Iraqi houses. Department of Architecture and building science, University of Strathclyde. Unpublished Ph.D. Thesis.

2. Al-Lyaly, S.M. (1990) The traditional house of Jeddah: A study of the interaction between climate, form, and living patterns. University of Edinburgh. Unpublished Ph.D.

3. Al Shareef, F.M. (1996) Natural light control in Hedjazi Architecture; An investigation of the Rowshan performance by computer simulation. University of Liverpool. Unpublished Ph.D. thesis.

4. Aynsley, R.M., Melbourne, W. and Vickery, B.J. (1977) *Architectural Aerodynamics*, London: Applied Science Publishers Ltd.

5. Bittencourt, L.S. (1993) Ventilation as a cooling resource for warm -humid climates: An investigation on perforated block wall geometry to improve ventilation inside low-rise buildings. Architectural Association Graduate School. Unpublished Ph.D. thesis.

6. Bowen, A (1983) "Design guidelines on lateral through and around buildings". p.517-533, Crete, Greece: 2nd International PLEA Conference.

7. Brandle, K. and Boehm, P. E. (1982) "Airflow windows: Performance and application". p.361-379, ASHRAE Trans.

8. Chandra, Subrato (1983) "A Design procedure to size windows for naturally ventilated rooms". p.105-110, USA: American Solar Energy Society, Inc.

9. Evans, B. H. (1979) "Energy conservation with natural air flow through windows". (**5**), 2 edn. p.641-650, ASHRAE Transactions.

10. Evans, M. (1980) *Housing, Climate, and comfort*, London: Architectural press.

11. Fathy, H. (1986) *Natural energy and vernacular architecture*, Chicago: Chicago press.

12. Fikry, A.A. (1981) An Investigation into window shading devices to optimize the control of the internal environment. University of Sheffield. Unpublished Ph.D.

13. Givoni, B. (1968) Ventilation problems in hot countries. Haifa: Research report of Ford foundation, Building research station, technion.

14. Givoni, B. (1981) *Man, Climate and Architecture*, 2nd edn. London: Applied Science Publishers Ltd.

15. Givoni, B. (1991) "Performance and Applicability of Passive and Low Energy Cooling Systems". *Energy and Buildings* **(17)**-

16. Givoni, B., Neeman, E., Hoffman, M.E. and Becker, M. (1968) Effect of orientation and details of windows and fixed shading devices upon indoor temperature and illumination conditions of classroom. Haifa, Israel: Building research station.

17. Holleman, T.R. (1951) Air flow through conventional window openings. 33, p.45 Texas: Texas Engineering Experiment Station, College Station.

18. Jong, T. and Bot, G.P.A. (1992) "Flow characteristics of one-side mounted windows". *Energy and Buildings* **(19)**-p.105-112.

19. Koenigsberger, O., Ingresoll, T., Mayhew, A. and Szokolay, S. (1977) *Manual of Tropical Housing. Part One: Climatic Design*, London: Longman Group Ltd.

20. Maghrabi, Amjed and Sharples, S. (1999) "Air flow characteristics through Modulated Louvered Windows". **(1)**, p.507-514, Brisbane, Australia: PLEA.

21. Muniz, P.A. (1985) The geometry of external shading devices as related to natural ventilation, daylighting and thermal comfort, with particular reference to tropical hot-humid climates. Unpublished Ph.D.

22. Olgyay, V. (1963) *Design with climate*, Princeton N.J.: Princeton University Press.

23. Oliveira, F. and Bittencourt, L. S. (1998) "Air flow through louvered windows in small rooms". p.393-396, Lisbon, Portugal: PLEA ' 98.

24. Pitts, A. C. and Georgiadis, S. (1994) "Ventilation air flow through window openings in combination with shading devices". 15th AIVC Conference edn. p.432-439, AIVC.

25. Salloum, A. (1983) "El-Rowashin of Jeddah, Saudi Arabia". p.245-252, Crete, Greece: Passive and Low Energy Architecture.

26. Sobin, H. (1963) "Post-Graduate Research: Air movement study". *Architectural Association Journal* **(78)-871,** p.310-311.

27. Sobin, Harris (1981) "window design for passive ventilative cooling: An experimental model-scale study". p.191-195, Miami Beach, Florida, USA:

28. Sobin, H. (1983) Analysis of wind tunnel data on naturally ventilated models. p.287 Tucson, Arizona, USA: Harris Sobin & Associates.

29. USA Dept.of Energy (1983) Energy efficient windows. A key to energy performance. 8p USA: Us Department of Energy.

30. Vickery, B. J. and Karakatsania, C. (1987) "External wind pressure distribution and induced ventilation flow in low rise industrial and domestic structures". **(2),** USA: ASHRAE Trans.

31. White, M. (1999) "Ventilators: Ventilation and acoustic Effectiveness". *BRE* **(IP4/99)**-p.1-8.

32. Yakubu, G.S. (1990) Modulated solar shielding of buildings: A study of a solar radiation control strategy for low energy buildings in hot dry and semi-arid climates. University of Sheffield. Unpublished PhD.

33. Yakubu, G.S. and Sharples, S. (1991) "Airflow through modulated louver systems". *Building Services Engineering Research and Technology* **(12)**-p.151-155.

CHAPTER 4: NATURAL VENTILATION IN ARCHITECTURE

4.1. Introduction

This chapter reviews ventilation and airflow research within buildings with an emphasis on wind induced natural ventilation. Besides the introduction, it contains four sections including airflow dynamics in buildings, airflow around buildings, ventilation within buildings and ends up by highlighting some common techniques employed in ventilation research.

The first section underlines the basic principles in architectural aerodynamics including the common mathematical representations of wind induced natural ventilation around and within buildings. This establishes the ground for the laboratory appraisal of airflow characteristics across the modulated louvered windows (MLW) that is carried out in Chapters 6 and 7. The pressure characteristics around the structure as a function of wind are also covered here. Then comes the wind movement around buildings with respect to a number of determinants including the urban fabric, the topography, building surroundings, and building geometry in altering the characteristics of airstreams.

The discussion in respect to natural ventilation within buildings is of importance to comprehend the various building components and their contribution to natural ventilation indoors. More emphasis in this section is given to the window as a main source of natural ventilation in buildings. Window treatments and controls as well as indoor and outdoor modifications, such as wing-walls and partitions, are also considered. The last section reviews some of the most common techniques employed in ventilation research and sheds light on the features and drawbacks of each technique.

4.2. Airflow dynamics in buildings

Architectural aerodynamics in buildings involve a number of complications in the real environment. As a result a number of mathematical representations of airflow characteristics within the building are established to assist an understanding of the dynamics of airflow in buildings. It is worth mentioning that most of the researchers agree those theoretical representations of flow components are treated with some simplicity and assumptions (Etheridge and Sandberg, 1996) (Awbi, 1991) (Koenigsberger et al. 1977) (Aynsley et al. 1977) (Massey, 1989) (Maghrabi and Sharples, 1999) (Bittencourt, 1993) . Despite the fact that in practice they may differ, the assumptions made in the mathematical models considers that airflow is in steady state and is isothermal. Nevertheless, most of the equations discussed in the following subsections are considered accurate enough to examine the airflow around and within the buildings.

4.2.1. Airflow in buildings

The dynamics of airflow within and around buildings is basically caused by the following variables:

- Wind induced natural ventilation.
- Buoyancy forces caused by temperature difference (stack effect).

The phenomenon of wind induced natural ventilation is simply understood when an obstacle, such as a building, obstructs the wind causing pressure difference (ΔP) across the windward and leeward sides. When apertures are provided on both walls, cross ventilation through the building occurs. This depends on many variables discussed in this chapter. The temperature difference between outside (T_o) and inside (T_i) the building will also

contribute to ventilation rates as a function of ΔT. In low-rise buildings a 10°C temperature difference could result in an indoor air speed of 0.5m/s (Bittencourt, 1993). The vertical magnitude of temperature differences between different levels within a building could result in significant ventilation. The phenomenon is known as the stack effect whereby air ascends to higher floors, and low-pressure zones in lower levels cause air suction. However, *"Stack effect ventilation is not a powerful ventilation mechanism and has several limitations that reduce its applicability"* (Abrams, 1986). In addition, in warm and hot humid climates the effect of temperature is not significant since external temperature almost nears or even exceeds limits of comfort zones all year-round. So T_i and T_o do not suffer much variation. The typical temperature difference ranges from 2°C to 5°C depending on the thermal mass of building and other variables (Aynsley et al. 1977), (Fleury, 1990), (Bittencourt, 1993) and (Van Straatan et al. 1965). Wind-induced natural ventilation is therefore the main factor in assessing thermal comfort in building by natural means while the stack effect is negligible with the presence of even a slight breeze. Thus, the effect of stack effect is excluded and not examined in the following discussion. Evans (1979) has indicated that thermal comfort in buildings relies, to a high extent, on the *energy-free* source; i.e. natural ventilation.

4.2.2. Wind induced natural ventilation

The blowing of wind on a structure creates positive and negative pressure zones on windward and leeward sides, respectively. Low-pressure zones are also created along the sides of the building and above the roof with the presence of higher wind velocities (Abrams, 1986). It is important to indicate at this stage that in a hot humid climate, it is the airflow which should be taken into consideration when assessing human comfort, not the air changes (Muniz, 1985). Although models identifying air changes per hour (ACH) are

important in ventilation research they are not addressed here for the above-mentioned reason.

The highest-pressure drop arises when wind is perpendicular to the building (Evans, 1979). The American Society of Heating, Refrigerating, and Air-conditioning Engineers (ASHRAE) Handbook of Fundamentals (1985) states that wind pressure (P_w) is a function of the square of wind velocity (V) and expressed as follows:

$$P_w = 0.5C_p.\rho.v^2 \qquad (4.1)$$

where

P_w = wind pressure (Pa)

C_p = static pressure coefficient

ρ = air density (Kg/m3)

v = wind speed at datum level (m/s)

The magnitude of pressure on windward side for a square or a rectangular structure varies from 0.5 to 0.9 times the velocity pressure (P_w). On the downwind side, the pressure is negative from –0.3 to –0.9 the velocity pressure (Abrams, 1986). The ASHRAE Handbook of Fundamentals (1985) and the Chartered Institution of Building Services Engineers (CIBSE) (1976) have similar values for these figures. The magnitude of pressure is usually described as the pressure coefficient (C_p) and is the ratio of the total wind pressure acting on the building. It is dependent mainly on the type of flow, whether turbulent or laminar, and building geometry as will be mentioned later here (Etheridge and

Sandberg, 1996). The surroundings such as topography and terrain type, may also have some effects on the pressure (BRE, 1978) and (Awbi, 1991). Pressure coefficient represents only a single point on building surface and is obtained through direct measurements or through wind tunnel models. Values of C_p on a number of buildings geometries are found in (BS, 1980) and in (Liddament, 1986) and others.

4.2.3. Equations of airflow mechanisms

The mathematical models to calculate the volumetric fluid flow (Q) across an orifice are related to a large extent to the pressure difference (ΔP) across the orifice. These models are represented in a form of flow network consisting of a number of nodes where each node is then represented by a number of equations. Some of these models are mentioned in the following subsections.

4.2.3.1. Common orifice flow equation

In buildings with large apertures, the airflow (Q) seems turbulent under normal pressure (Awbi, 1991). The common orifice flow equation represents the turbulent airflow with large openings in the building as being proportional to the square root of the pressure difference across the aperture. It is expressed as follows:

$$Q = C_d . A \sqrt{\frac{2\Delta P}{\rho}} \qquad (4.2)$$

where

C_d= discharge coefficient of an opening.

A = openings area (m^2)

ΔP = pressure drop across the opening (Pa)

ρ = air density (Kg/m^3)

The discharge coefficient (C_d) for a sharp-edged orifice flow is 0.61 and is independent of the Reynolds number (R_e) (see section 4.2.7). Etheridge (1977) noted that C_d is not observed in most buildings due to the configuration of the openings and the variations in pressure difference depending on inside and outside building conditions determining the effective leakage areas, C_d A, either through pressurisation and depressurisation tests or directly from the ASHRAE Handbook of Fundamentals (1985).

4.2.3.2. Power law and quadratic airflow model equations

The validity of the power law and quadratic airflow model equations have been investigated by many researchers in ventilation studies to set standards for building envelopes, ventilation requirements and many other infiltration models. Both calculation methods have been broadly accepted and the discussion as which is the most suitable one to apply is still ongoing. In general the power law equation has been widely used to describe the relationship between differential pressure (ΔP) and the volumetric flow rate (Q) through various ranges of apertures in buildings such as gaps around doors and windows, cracks, slits, etc, (Sherman et al. 1979), (Liddament, 1987), (ASTM Standard E779, 1982), (CGSB Standard 149.10-M86, 1986), (ISO Standard, 1995), (Awbi, 1991) and (Etheridge and Sandberg, 1996). (Liddament, 1987) considers the power law function as best to fit measurements of air infiltration within buildings. The power law function is expressed as:

$$\Delta P = a' \cdot Q^n \qquad (4.3)$$

where:

ΔP = pressure drop across orifice (Pa)

a' = is a constant proportional to the effective leakage area of the crack (m^3/s Pa),

Q = is the volume flow rate (m^3/s) n = is the exponent.

But equations of this type, however, are not dimensionally homogeneous because they do not obey Reynolds law of similitude (Etheridge, 1987). Equation 4.3 gives the function of pressure drop for a known Q. Alternatively, the flow rate can be expressed in another form:

$$Q = a \cdot (\Delta P)^n \qquad (4.4)$$

where $a = \sqrt{\frac{1}{a'}}$

The flow exponent n was determined to be the square root of pressure as the flow rate is almost proportional to the square root of ΔP (Sherman et al. 1979), (Dick, 1950). On the other hand, Walker et al. (1998) suggested that n has a value of 0.5 for fully developed turbulent flows and 1 for laminar flow. This formulation is called the square law. But this relationship does not fit in practice for a number of reasons(Hopkins and Hansford 1974):

- Due to distortion of the crack, the increase in ΔP would be accompanied by an increase in aperture area.
- The value of the C_d of the orifice plate equation that is used to estimate the leakage area was assumed constant. Hence, any change in the discharge coefficient would result in deviation from the theory.
- The approximation in square law equation could not be applied for all types of cracks and their various configurations and differential pressures.

Alternatively, other researchers in the field applied the quadratic model equation. Etheridge (1987) (1997) (Etheridge and Sandberg, 1996) prefer the quadratic equation method to determine the air infiltration. Baker et al. (1987) stated, *"Although the quadratic disregards the existence of a critical velocity of transition between streamline and turbulence flow, it has the practical advantage that at both extremes, i.e.* $Q \to 0$ *and* $Q \to \infty$, *it gives the correct forms corresponding respectively to laminar flow and to complete turbulence. The coefficients A and B remain independent to the rate of flow"*. This formulation is expressed as follows:

$$\Delta P = AQ + BQ^2 \qquad (4.5)$$

where

A = the flow coefficient for fully developed laminar friction losses [(Pa s)/m^3].

B = the coefficient of entry, exit and turbulent flow losses [(Pa s^2)/m^6].

Practitioners have also found that the quadratic is better in estimating leakage areas through cracks and that it gives a better fit to the data obtained from their pressurisation and depressurisation experimental results as found in (Thomas and Evans, 1951), (Baker et al. 1987), (Yakubu, 1990), (Yakubu and Sharples, 1991) and recently in Maghrabi and Sharples (1999). The quadratic equation had some theoretical validity by using the basic flow equation for laminar flow through infinite parallel plates and it is dimensionally homogenous (Fox and MacDonald, 1978).

Coefficients A and B are determined by the standard fluid mechanics principles:

$$A = \frac{12\mu z}{Ld^3} \qquad (4.6)$$

$$B = \frac{\rho Y}{2d^2 L^2} \qquad (4.7)$$

where

μ = the dynamic viscosity (kg/ms)

z = the plate length (m)

L= the breadth of the plate (m)

d = the gap thickness(m)

ρ = the fluid density (kg/m^3)

Y = a factor depending on crack geometry.

Substituting coefficients A and B in Eq. (4.5):

$$\Delta P = \left(\frac{12\mu z}{Ld^3}\right)Q + \left(\frac{\rho Y}{2d^2 L^2}\right)Q^2 \qquad (4.8)$$

The factor of loss coefficient as a function of crack geometry is assumed to be 1.5, 2.5 and 3.5 for straight crack, L-shaped crack and double crack respectively (Baker et al. 1987). Hence, loss coefficient is increasing with a value of 1 for each sharp bend (Baker et al. 1987). Awbi (1991) pointed out that some researchers had compared these models equations at higher pressures and they found that both equations in the form of quadratic and power-law models were identical. He added, *"However, this study was by no means conclusive and*

more test cases are needed before a true assessment of the two equations can be achieved at low pressure ranges". The latter quotation establishes a solid base for the further comparison between these models with respect to the type of window in hand: the modulated louvered windows.

4.2.4. Airflow calculation models

A number of calculation models are reported here with several references. As it was indicated previously, these model equations are developed with some simplifications.

4.2.4.1. ASHRAE model

The ASHRAE model (1985) of the volumetric flow of air is expressed as follows:

$$Q = C_d \cdot A \cdot V \qquad (4.9)$$

where

Q = volumetric air flow (m^3/s)

C_d = effectiveness of the opening (discharge coefficient), 0.5 to 0.6 for perpendicular wind and 0.25 to 0.35 for diagonal wind.

A= free area of inlet opening (m^2)

V= wind velocity (m/s)

One advantage of this model is that only two variables are involved; wind velocity and area of the opening. However, the simplicity of this equation may have some drawbacks when applied in prediction. The equation does not take into account cases

when inlet and outlet areas are not equal in dimensions. In architecture the areas of inlet and outlet may vary depending on many factors. Moreover, as indicated by Aynsley (1982), the model does not account for surroundings such as topographic features, vegetations or other obstructions. On the scale of a window, no consideration is given to the location and size of the inlet or any treatments.

4.2.4.2. The discharge method

The algorithm produced by Aynsley (Aynsley et al. 1977), (1979) (1982) takes into account the C_d for each opening along with the pressure coefficient (P_c) for both windward and leeward openings. The model represents a higher degree of efficiency in predicting airflow rates since a balance between simplicity and accuracy is obtained (Bittencourt, 1993). The model covers a number of openings in series and is presented as follows:

$$Q = \left[\frac{(C_{pw} - C_{pl}) Vz^2}{\frac{1}{C_{d1}^2 A_1^2} + \frac{1}{C_{d2}^2 A_2^2} + \ldots + \frac{1}{C_{dn}^2 A_n^2}} \right]^{0.5} \qquad (4.10)$$

where

Q = airflow rate (m^3/s)

C_{pw} = windward pressure coefficient

C_{pl} = leeward pressure coefficient

Vz = mean wind velocity at z height above the ground (roof level) (m/s)

A_1 = inlet area (m^2)

A_2 = internal opening area (m^2)

A_n = outlet area (m^2)

n = number of openings in series

C_d = discharge coefficient of an opening

The wind incidence would have an effect on the inlet area (A_1). The A_1 is then corrected with respect to the projection of the opening area that is perpendicular to wind speed. But when wind incidence is greater than 60° then the representation of A_1 becomes more complicated (Aynsley, 1988). In addition, wind pressure characteristics could be estimated directly for a solid building or with a wall opening less than 10% of wall area (Lee et al. 1980). However, in cases where the opening area exceeds 20% of wall area C_p could not be estimated except from real measurements or wind tunnel tests. The difficulty of obtaining C_p inside the building when the flow is divided into a number of branches adds another disadvantage to the model equation (Al-Megren, 1987).

4.2.4.3. British Standards (BS)

The formula of airflow rate due to wind developed by the British Standards (BS 5925) (1980) for single sided ventilation is represented as:

$$Q = 0.025AV \qquad (4.11)$$

where

Q = airflow rate (m^3/s)

A = inlet area (m^2)

V= wind velocity (m/s)

However, in tropical areas more concern is given to cross ventilation that requires openings at windward and downwind sides. The BS 5925 (BS, 1980) algorithm for the cross ventilation due to wind only assumes the two-dimensional flow through a building with openings on opposite walls, and ignoring internal partition, to be as follows (see Figure 4.1):

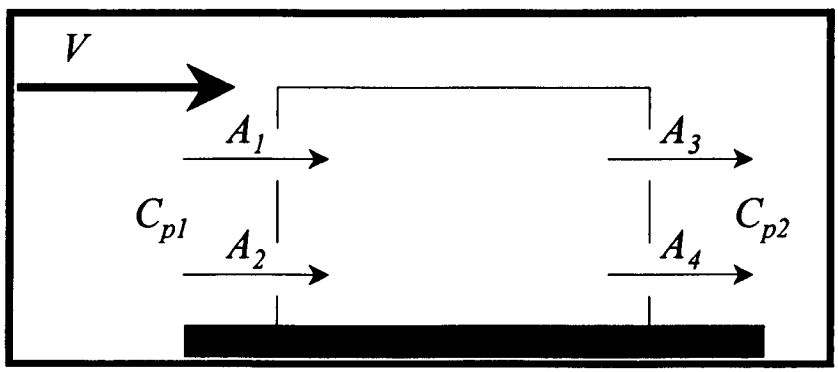

Figure (4.1): BS 5925 for cross ventilation due to wind only. (After Awbi 1990)

$$Q = C_d A V (C_p)^{1/2} \qquad (4.12)$$

where

Q = airflow rate (m^3/s)

A = inlet area (m^2)

C_d= discharge coefficient of an opening

V = wind velocity (m/s)

C_p = Pressure Coefficient

And the total equivalent area when openings are in series is:

$$\frac{1}{A^2} = \frac{1}{(A_1 + A_2)^2} + \frac{1}{(A_3 + A_4)^2} \qquad (4.13)$$

Where A_1 and A_2 are inlet area for openings in parallel on windward side and A_3 and A_4 are the outlet area in parallel on leeward side as shown from the Figure. The equivalent area employed here could be from the actual opening area for large windows. But in the case where window treatments are applied, such as MLW, the equivalent area has to be taken empirically. For parallel openings, the overall equivalent area is calculated by arithmetically adding the openings. But when openings are in series the equivalent area is obtained by the addition of the inverse square root of the total areas (Awbi, 1991).

4.2.4.4. CIBSE method

The estimation of flow rates covered by the Chartered Institution of Building Services Engineers (CIBSE) is known as the CIBSE-method (1976). The discharge coefficient (C_p=0.65) is considered constant for all openings and it is expressed as:

$$Q = 0.827 A(\Delta P)^{0.5} \qquad (4.14)$$

where

Q = airflow rate (m^3/s)

A = Total area (m^2)

ΔP = the pressure drop across the orifice (Pa)

When a number of openings in parallel are involved then the equivalent area represents the summation of the total areas of the openings:

$$\sum A = A_1 + A_2 + \ldots + A_n \qquad (4.15)$$

where

A_1 = inlet area on windward side (m^2)

A_n = inlet area on downwind side (m^2)

With openings in series the effective equivalent area is obtained graphically for a number of A_2/A_1 % as in Figure 4.2. Alternatively, it is mathematically obtained using the following equation:

$$\sum A = \left(\frac{A_1 A_2 \ldots + A_n}{(A_1^{\,2} + A_2^{\,2} + \ldots + A_n)^{0.5}} \right) \qquad (4.16)$$

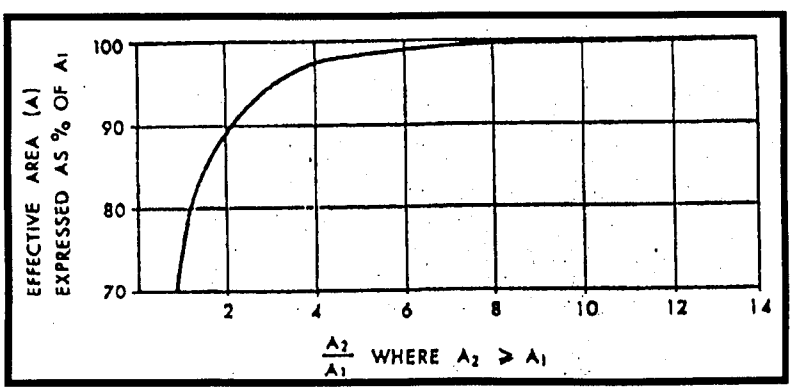

Figure (4.2): The effective equivalent area of two openings in series. (CIBSE 1976) (Bittencourt 1993)

A quantitative comparison between some of the models mentioned earlier along with other models was carried out by Al-Megren (1987). The comparison was based on a single square room with two windows in series. The window area was 15% of the wall area and

was located at approximately 2.2m heights from the ground level. Al-Megren indicated that various models examined had quite different results although the study was conducted on a single room. He added, *"Significant differences are therefore expected when computations are performed for larger buildings"*. The variations were referred to a number of factors one of which of concern here being the window treatments *"Some models do not account for some of the variables that extremely affect the flow, such as window screens"*.

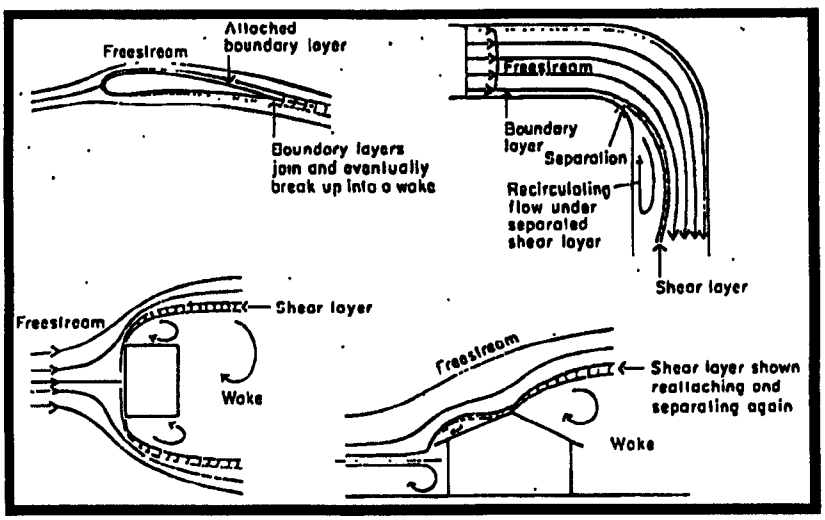

Figure (4.3): The flow regimes around various shapes.
(Aynsley et al 1977)

4.2.5. Pressure characteristics around buildings

When airstreams hit an object, they create flow regions depending on the characteristics of that object. The three regions that are mainly found around the object include freestream, wake and shear layer. In architectural aerodynamics these are known as flow fields (Aynsley et al. 1977). As shown in Figure 4.3, the freestream is a continuation of the flow airstreams of wind. Roughly speaking, when representing these

airstreams of wind into graphical parallel lines, they become more condense as function of building shape. The shear-layer is formed as a separation between the freestream and the wake zone where re-circulation and vortex form behind the shear layer. Around a streamed-lined body (see Appendix A.1), the free stream moves adjacent to the body and the pressure increases depending on the curvature of the body. The wake region is minimized and the pressure around it contributes to lift and drag forces (Aynsley et al. 1977). The forces are components of the wind velocity force over the body. Lift-forces tend to deflect airstreams in perpendicular to wind direction, and drag-forces are dragged parallel to the airstreams direction. The developments of the three regions are more obvious with bluff bodies and sharp-edged elements (Appendix A.1). In architecture, the bluff bodies represented in square or rectangular building shapes are employed more than the streamlined building forms. Therefore, some detailed description of the pressure fields around bluff bodies is mentioned, bearing in mind that the presence of more than 20% of aperture to wall area will have different pressures characteristics (Lee et al. 1980).

The pressure fields are formed as function of flow separations as well as of the building shape. As shown in Appendix A.1, "*The algebraic sum of the pressure, kinetic energy per unit volume, potential energy per unit volume has the same value of any two points on a streamline*" (Bittencourt, 1993). The equation is expressed as follows:

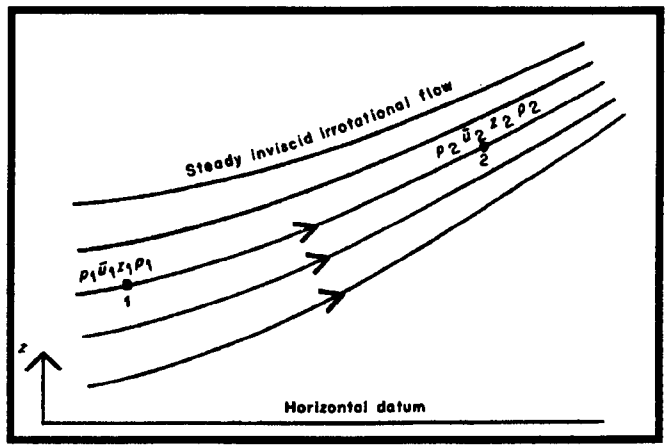

Figure (4.4): The flow field where the Bernoulli's equation could be valid. (Aynsley et al. 1977)

$$P_1 + \frac{\rho.Vm_1^2}{2} + \rho.g.z_1 = P_2 + \frac{\rho.Vm_2^2}{2} + \rho.g.z_2 \qquad (4.17)$$

where:

P = static pressure (Pa)

ρ = density of fluid (Kg/m^3)

Vm = mean velocity

g = gravitational acceleration (m/s^2)

z = height above a horizontal reference datum (m)

The above equation is known as Bernoulli equation (Figure 4.4) (Aynsley et al. 1977) and is valid with steady flow. In low-rise buildings, gravity is negligible and air density constant, hence the third term of the equation, $\rho\, g\, z$, could be omitted:

$$P + \frac{\rho.Vm^2}{2} = \text{Constant} \qquad (4.18)$$

showing that the pressure decreases with the enhancement of the wind speed and vice versa. On the other hand, *Vm* is significantly reduced as it reaches the centre of the windward side of the bluff body, say at point *a*, and the pressure is expressed as follows:

$$P_a = P + \frac{\rho.Vm^2}{2} \qquad (4.19)$$

It is also called stagnation pressure (see Appendix A.1). But at any other point far from the centre on the windward wall, say point *b*, the acting pressure is significantly more than that recorded at free stream $P_b > P$ and $Vm_b < Vm$ and lift-forces occur. The developments and separations of the flow regions occur at far edges of the windward wall, say point c, and $Vm_c \geq Vm$ and $P_c \leq P$. However, within the shear layer, say at point d, it is evident that $Vm_d > Vm$ and $P_d < P$. The suction zone where wake region occurs turbulent vortex and eddies are developed and the pressure at point, say *e*, is the average $P_c \rightarrow P_d$ (Aynsley et al. 1977). At certain distance from the leeward side the flow regions may join and redevelop in a form of a fresh freestream dependent on a number of factors amongst which the urban tissue and building configuration are of interest to the current study. In such phenomenon, Bernoulli equation is valid at the freestream region and could not be employed at the other regions of flow, i.e. shear layer and wake zone (Aynsley et al. 1977) and (Massey, 1989).

The behaviour of the wind pressure when blocked by the building is also dependent on the shape and orientation of the structure (Aynsley et al. 1977), (Markus and Morris, 1980) and (Sawachi et al. 1999). The peak wind pressure (positive pressure) is near the

centre on the windward side of the building and the suction (negative pressure) peaks at corners and edges as seen in Figure 4.5 (Markus and Morris, 1980).

4.2.6. Laminar and turbulent flows

The flow is known as laminar when a streamline is in steady state and where pressure and velocity are independent of time. But when the velocity profile is affected by the presence of aperture, for instance, this would cause instability to the flow due to velocity disturbances. This represents one way of flow turbulence due to velocity disturbances. The turbulence in flow is dependent, to a high extent, on the frequencies of

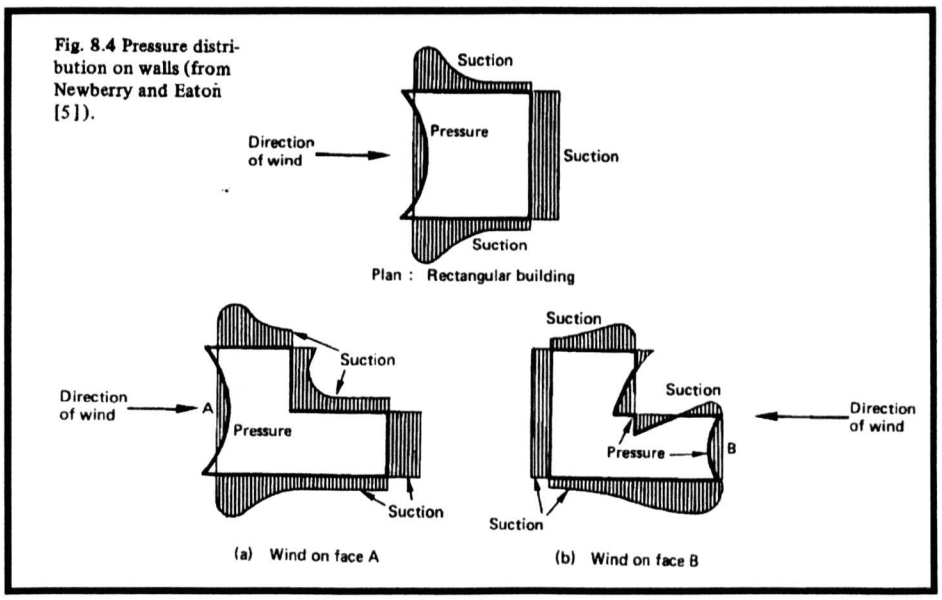

Figure (4.5): The pressure distribution on the walls of various buildings shapes. (Markus & Morris 1980)

the disturbances, velocity profile and the Reynolds number at which flow is considered turbulent. Etheridge and Sandberg (1996) stated, *"These factors determine whether or not transition to turbulence takes place, and the length of the so-called transition region which separates the completely laminar and fully turbulent parts of the flow"*. High Reynolds numbers are usually considered turbulent in architecture aerodynamics.

4.2.7. The Reynolds number

Reynolds number is the ratio measure of two different forces acting on the elements of air where these forces are the inertial force and the viscous force (Etheridge and Sandberg, 1996), (Al-Jawadi, 1986) and (Aynsley et al. 1977). In physical terms, the inertial force is, *"The blocking force generated by the frontal impact of the streamline against a barrier"* and the latter is, *"The force made up to the viscous actions between air strata"* (Bittencourt, 1993). The inertial forces around streamlined bodies are small and increases with blunt structures. On the other hand, the viscous force is reduced at the latter type of structures and is high with aerodynamic shapes (Bittencourt, 1993). The Reynolds number is given by:

$$Re = \frac{\rho.U^2.L^2}{\mu.U.L} = \frac{\rho.U.L}{\mu} \qquad (4.20)$$

where

ρ = air density (Kg/m^3)

U = wind velocity (m/s)

L = Length of the structure (m)

μ = Dynamic viscosity (Kg/ms)

The above equation clearly shows that high Reynolds number indicates low dynamic viscosity and vice versa. In natural ventilation in warm climates both ρ and μ could be considered constant (Aynsley et al. 1977). Then this leaves us with the only two variables U and L which are the representatives of the two forces involved. The physical

interpretation of this in architecture aerodynamics is that the blockage caused by L dimension could, to a high extent, determine the behaviour of the flow from laminar to fully turbulent.

The value under which the *Re* is considered laminar or turbulent is not fixed. Depending on the frictional forces, it is ranged from 10^5 to 3.6×10^6 and is called the *critical Re* (Melaragno, 1982) (Etheridge and Sandberg, 1996). Above this, the range of transition indicates that boundary layer is turbulent as the functional increase of frictional forces. In the opposite, low *critical Re* indicates reduction in the frictional forces and the boundary layer is more likely laminar.

The *Re* of the structure differs from that across an aperture or those smaller components. The flow through MLW is more likely a piped flow and the *critical* value of *Re* to consider laminar or turbulent flow is also not fixed. In most cases if *Re* value exceeds 2000 then the jet flow is considered turbulent. Etheridge and Sandberg (1996) mention that some studies showed that fully turbulent flow could be of about 4000. Similarly, Massey (1989) indicated that the *critical Re* for the later flow regime ranged from 2000 to 4000.

4.2.8. Flow regime through bounded flow

Amongst the flow regimes through an aperture, the regime of flow through the reviewed MLW seemed to fall under the piped flow regime or bounded flow regime. A number of factors affect the flow regime through piped object. Frictional losses are the most important in causing resistance to the fluid flow as a function of pipe roughness, kinematics' viscosity and pipe shape (Etheridge and Sandberg, 1996), (Awbi, 1991). Entry and exit diameters of an inlet added to any diversion of flow within the pipe, such as elbow

shaped pipe or louvers tilted to various inclinations, would share head losses (Massey, 1989). Figure 4.6 shows the graphical representations of flow separation and reattachment on the entry of the bounded shape such as the MLW. It is obvious that eddies and turbulent bubbles occur just at the entry edge as functions to the sharpness of the edge. With sharp-edged inlets, the reattachment occurs some distance away from separation while with more smooth-edged inlets, the reattachment distance is reduced and the flow of turbulent bubbles is diminished. The head losses vary with the P_w and are represented as follows:

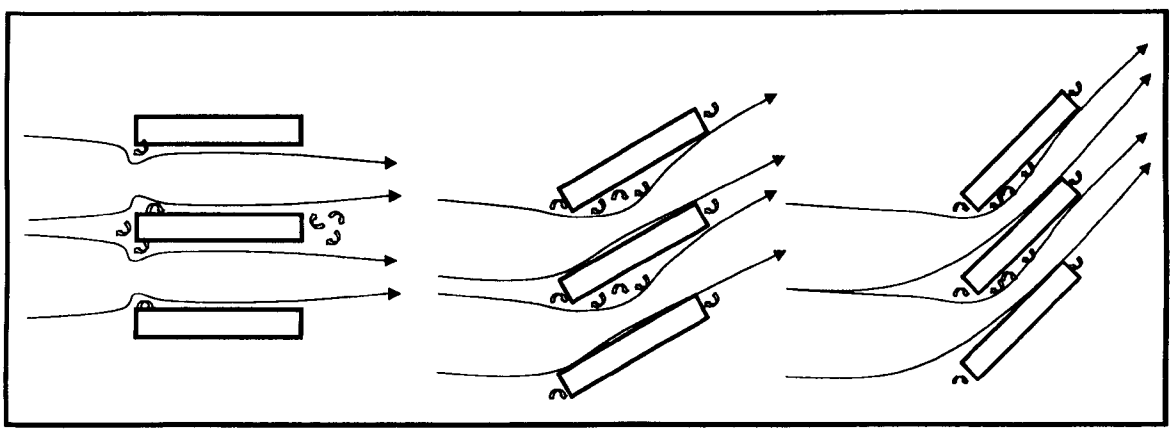

Figure (4.6): The flow separation and reattachment on the entry through louvers.

$$K = C.P_w \qquad (4.21)$$

where

K = the head loss

C = coefficient obtained from experimental measurements

P_w = velocity pressure (Pa)

The value of C differs from the entry and exit of an inlet. Baker et al. (1986) investigated the airflow through perforated screens at small-scale pressure difference and recommended that the value of C at entry side of an inlet be 0.5 and at exit side of the inlet 1. The latter value of C is correspondent to exit losses when the airstreams within the pipe leave it into the freestream inside the room or the enclosure. The governing principles of the flow regime at exiting side of an inlet are discussed in the following section.

4.2.9. Air Jets

The principles of air jets are mainly encountered with the mechanical ventilation systems where, *"Air jets are used to mix the processed air from the plant with the room air"* (Awbi, 1991). Similar principles of air jets are encountered with cross ventilation. Roughly there are two types of jets, namely the free air jet and the wall jet. Both phenomena are discussed here since they are directly relevant to the flow regime encountered through the reviewed modulated louvered windows.

4.2.9.1. Free air Jet

The free air jet occurs when air leaves an aperture or a nozzle and travels into the space where no solid boundaries affect the flow patterns. *"The static pressure within the jet is the same as the static pressure of the surrounding space"* (Awbi, 1991). The velocity magnitude increases at the jet centerline and a free shear layer is developed around the edges of the regime. The shear layers from both sides shape jet boundaries as an indication of the velocity discontinuity and they expand as function of distance from the opening. The downstream flow becomes more turbulent as function of the distance from the opening due to the velocity reduction in air jet. Four zones of free jets are developed depending on the variation of velocity centerline caused by distance from the opening; potential core

region, characteristic decay region, asymmetric decay region and terminal decay region (Appendix A.2).

4.2.9.2. Wall Jet

The Wall jet effect occurs when the fluid inside the space flow is adjacent to a flat surface and the velocity magnitude moves parallel to that surface. This phenomenon is widely know as *Coanda effect* (Awbi, 1991), (Etheridge and Sandberg, 1996), where the jet keeps attached to the surface recording the highest velocity near it till reaching the opposite wall where it then deflects downward in the room. The shear layer here is developed only from the other side of the surface and expands in a proportional and similar fashion to the free air jet. In architectural aerodynamics, the wall jet could produce some sort of draught within the living room specifically when the re-circulation of air, such as cross ventilation, is not present. In this case, two zones of wall jets are developed including potential core and the characteristics decay (see Appendix A.3).

4.3. Natural ventilation around buildings

There are a number of parameters affecting airflow around buildings. Some are referred to the environment and surroundings while others are related to the building geometry. Of the first determinant, the type of terrain, topography, streets and alleys, and landscape are of most significance. On the other hand, building determinants include array and distribution of buildings, building shape and orientation. These are discussed here in brief as they are not directly relevant to the current study.

The global wind circulation in the atmosphere follows two dominant directions of circulation, horizontal and vertical, and each circulation dimension is dependent on the

other (Koenigsberger et al. 1977), (Markus and Morris, 1980). Wind flow across the earth's landscape is subjected to frictional effects depending on the type of terrain. Appendices A.4 and A.5 shows the various types of terrain and their characteristic roughness. The mean velocity at the surface is zero and velocity ingredient increases exponentially until reaching the gradient height where wind velocity becomes free from the terrain effect (Koenigsberger et al. 1977), (Markus and Morris, 1980), (Aynsley et al. 1977) and (Al-Jawadi, 1986). The hilly and mountainous sites have an effect on wind patterns, directions and velocities that differ from that of valleys, sea level or open country.

As far as the building concerned, wind velocity and pattern profiles are distorted in the three dimensional airstreams when hitting buildings' external walls and roofs causing various positive and negative pressure zones as discussed earlier. These zones occur due to blockage of airflow added to the roughness of the urban fabric. Roughly speaking, the

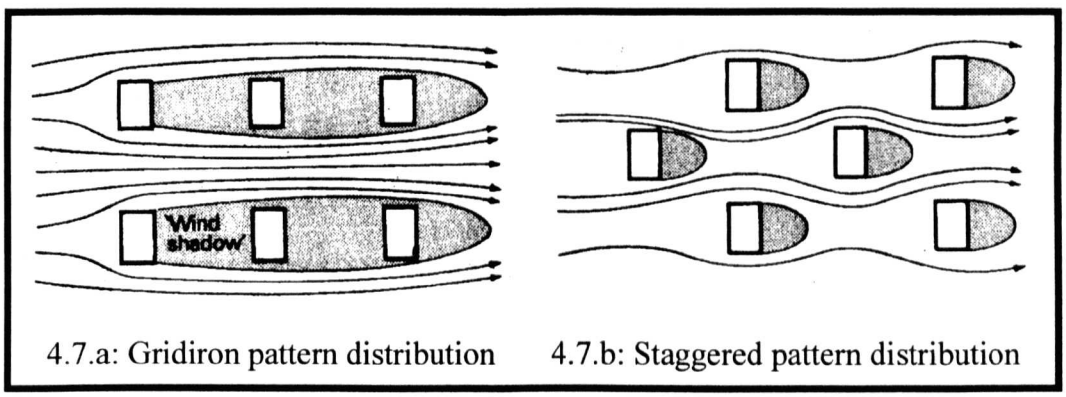

4.7.a: Gridiron pattern distribution 4.7.b: Staggered pattern distribution

Figure (4.7): The flow patterns around buildings as a function to the building arrays and distributions. (Koenigsberger et al. 1977)

staggered buildings distribution has some preference over the gridiron distribution since it eliminates the stagnant air zones and the wind-shadow zones (Figure 4.7). A correction is therefore needed: the spaces between both buildings in the downwind should be six times the building height (Koenigsberger et al. 1977). These guidelines are of extreme

importance in respect to the warm climate where cross ventilation is needed for almost every single building within the settlement.

Building shape and orientation also have an effect on the acting wind force. Similarly, the magnitudes of alleys and streets between scattered or uniform building distributions will affect directly the inertia of air. Wind between buildings is weakened and even fades in sheltered streets with irregularities in direction. On the other hand, wind speed is recovered with wider streets parallel to breeze. This provides a sound solution in humid climates (Koenigsberger et al. 1977), (Kaizer, 1984), (Konya, 1980) and (Al-Lyaly, 1990). Recalling this in conjunction with the streets and alleys layout in Jeddah mentioned previously (section 2.5.4) we would acknowledge the presence of wider streets radiating from the waterfronts that channelled air into the settlement.

4.4. Natural ventilation within building

As discussed in the previous Chapter (section 3.2), the type of window has a direct effect on the ventilation characteristics within the room. Additionally, there are a number of other parameters governing natural ventilation inside buildings. These are underlined here in details.

4.4.1. Inlet/outlet ratio (A_i/A_o%)

The airflow characteristic around the structure is a function of the ratio of aperture to wall area in both sides of the structure (Lee et al. 1980). Based on a given outdoor velocity, the ratio of inlet/outlet (A_i/A_o%) has a sound contribution to the average indoor air velocity. This was concluded when the effect of window size on indoor air motion was examined. Givoni (1965) concluded that the dimension of the smaller opening, i.e. inlet or

outlet, would determine the indoor air velocity. Chandra (1983) supported this conclusion where airflow within a room was affected by the smaller area A_i *or* A_o. Consequently, an equation was developed:

$$A = \frac{A_o \cdot A_i}{\sqrt{A_o^2 + A_i^2}} \qquad (4.22)$$

For a given inlet opening, a considerable increase in the airflow is found proportional to the increase in outlet area (A_o). This was indicated by both Holleman (1951) and Chand (1970) when the impact of the relative sizes of windows on the magnitude of indoor ventilation was examined over a number of outlet areas for a given windward opening (A_i). As shown in Figure 4.8, Chand (Chand, 1970) found that the

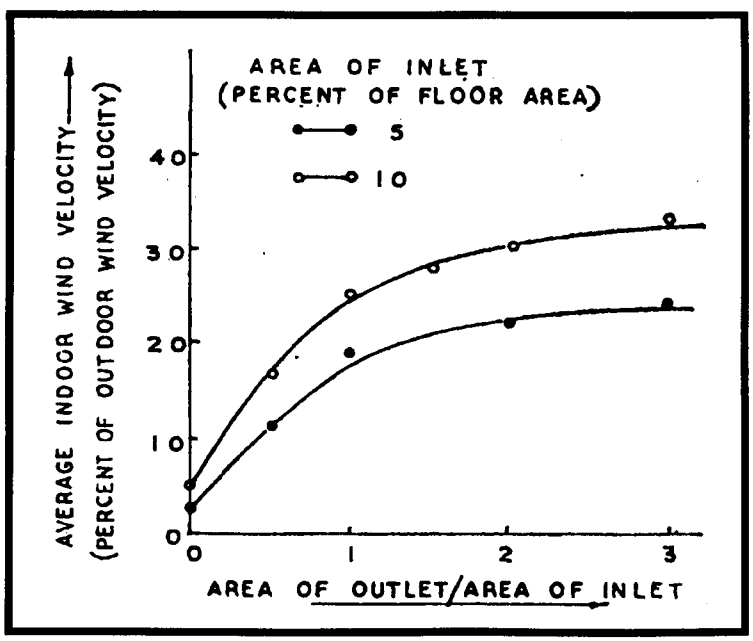

Figure (4.8): The effect of *Ao/Ai%* to average indoor air velocity (*vi/ve%*). Highest average of velocity indoors was found when *Ao/Ai*=2.5. (Chand 1970)

maximum air velocity inside the room was obtained when A_o/A_i=2.5 and when no further value had much significance. Similarly, Sobin (1983) indicated that any reduction in the

inlet area to the outlet area would have major contribution to average indoor speed. Sobin found that the highest average values of velocity indoors were for A_o/A_i ranges from 1.0-2.25. In contrast, when the size of the inlet is larger than the outlet, a more uniform pattern of air distribution was found (see Figure 4.9) and the speed increased as it approached the outlet (Chand, 1970).

In general, larger outlets favour air speed to increase near the inlet and vice versa (Abrams, 1986). Yet, larger windward openings are preferred with the presence of wind incidences or when the flow through the entire room was required (Koenigsberger et al. 1977). The latter provides an optimum alternative for the warm and humid climates where cross ventilation is needed for almost every single space within the structure.

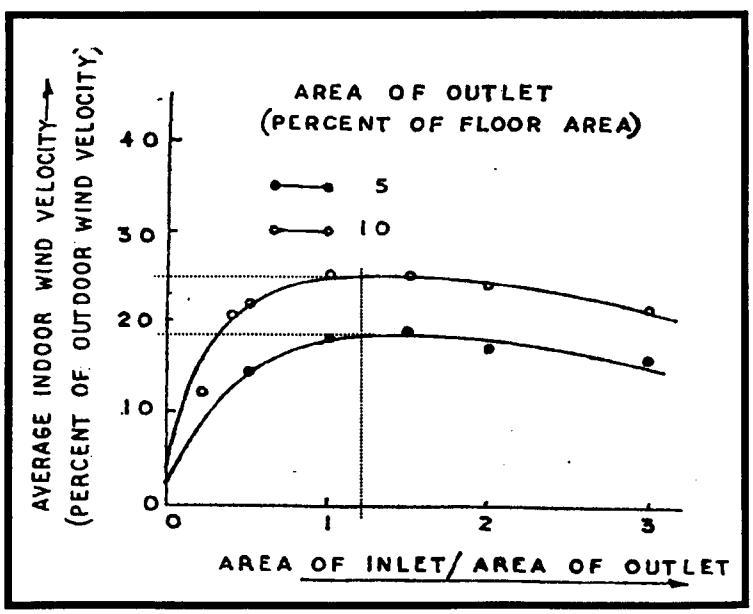

Figure (4.9): The effect of $Ai/Ao\%$ to average indoor air velocity ($vi/ve\%$) showing that the increase in $Ai/Ao>1$did not improve the average indoor air velocity. (Chand 1970)

The aperture width has also some influence on the ratio indoor air velocity to outdoor (v_i/v_e%). The work of Givoni (1965) compared various window widths against the wall width and found an increase of 5-20% in the averaged v_i/v_e%. Further, Kukreja (1978) noted that this increase could extend to nearly 35% when window width/wall width is nearly 75%. The optimum fenestration to wall ratio on the windward side is 30-50% (Chand, 1970).

The increase in aperture width also has a substantial effect on air motion inside the room, more than its increase in height. The work of Sobin (1981) mentioned earlier

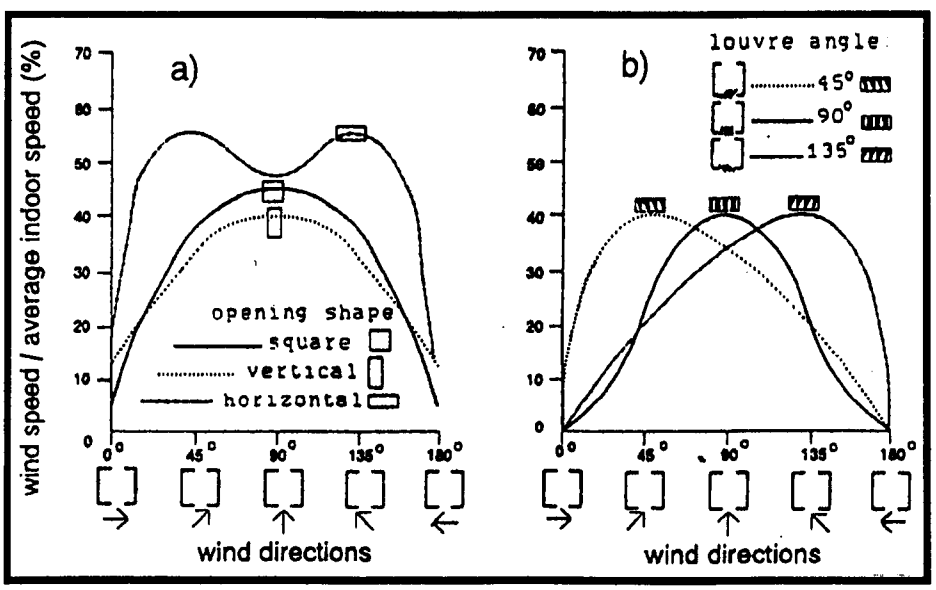

Figure (4.10): The three opening shapes examined under various wind directions and showing the preference of the horizontally-shaped inlets compare to other shapes. (Sobin, 1981)

compared the horizontal and vertical openings against the simple square opening. The three shapes were investigated under five different wind directions ranging from 0° to 180° at intervals of 45°. The study concluded that the horizontal opening shape was superior to both vertical and simple square ones at wind incidences examined as shown in Figure 4.10.

4.4.2. Window location

Location of the window could share in the flow within the room, especially when considering wind incidences. The location of aperture within the wall creates pressure zones on and velocity components around it. These pressure zones and velocity magnitudes have an effect on the flow of air inside the room. Relatively speaking, the flow is either straight or skewed with respect to window location. Evans (1979) indicated that the flow within the room follows a similar direction if the window is located in the centre of the wall. However, patterns would deviate towards the wall if the window was located off-centre. The flow could also be directed upwards or downwards within a room if the window was located off-centre as illustrated in Figure 4.11. Flow passing through the window in the upper floors is forced upwards while in the case of the window in ground floor the flow is directed downwards. Similarly, the flow entering a building is skewed by the horizontal location of the window. An example of this is shown in the previous Figure where the pressure build-up in front of the elevation governs the direction of indoor airstreams independently from leeward opening location.

The arrangement of both windward and leeward apertures contributes directly to flow variations and therefore to velocity magnitudes occurring. Basically, a leeward aperture in respect to the inlet is either located in series or adjacent on a sidewall. For a given inlet and outlet sizes, airstreams flowed unchanged with some eddies occurring on the corner of the room and slight flow along sidewalls (Givoni, 1981). The latter finding was with perpendicular wind, 90°, and when oblique wind was present, 45°, better circulation on sidewalls and around corners was obtained. Additionally, the latter wind direction to the inlet openings has some preference over the perpendicular wind from the velocity magnitude. As shown in Figure 4.12 the oblique winds produced better

ventilation efficiencies than perpendicular wind in all cases examined. Nevertheless perpendicular wind was more effective when the two apertures were adjacent. Other researchers, as stated by Bittencourt (1993), may not support the latter statements, *"The lateral apertures can only partially compensate for the reduction in the airflow rates if they have predominantly horizontal shapes"*.

The inlet height is also effective in directing air within the room. Air movement is regularly directed to the living zone up to 2m high. Koenigsberger et al (1977) indicated

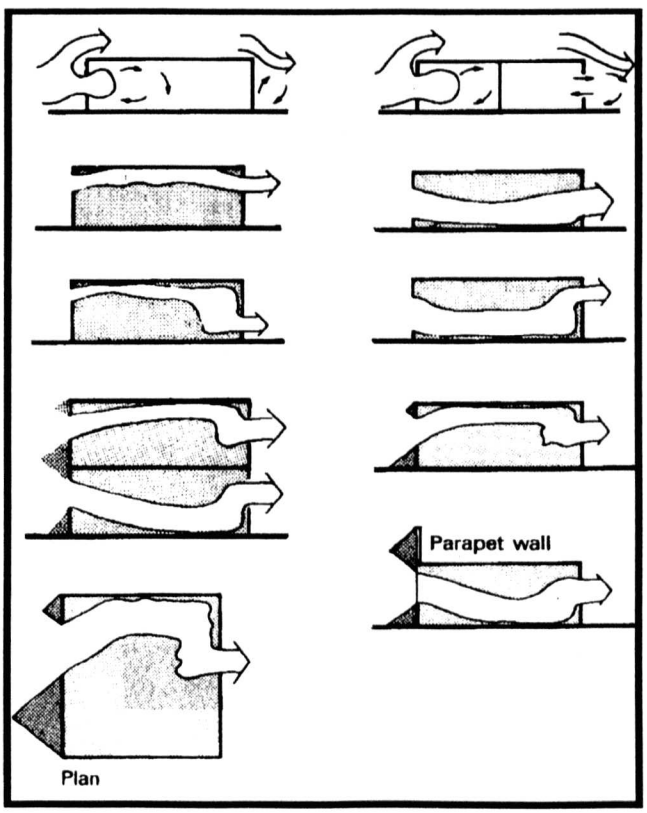

Figure (4.11): The flow pattern indoors as a function of window location. (Koenigsberger et al.1977)

that the location of the inlet is a more determinant factor than that related to the outlet. Melaragno (1982) noted the importance of the relative heights of both inlet and outlet. Interestingly, locating inlet higher than outlet or vice versa would provide better flow

regimes in all vertical layers in the space including flow around body level or living zone. On the other hand, positioning the outlet in various heights affected neither the incoming air nor the pattern of the flow (Holleman, 1951), (Givoni, 1981), (Olgyay and Olgyay, 1976).

The vertical location and type are the main controls of indoor flow patterns (Muniz, 1985). Bowen (Bowen, 1983) demonstrated a number of sketches of flow patterns within the room as a function of various parameters mentioned in the section.

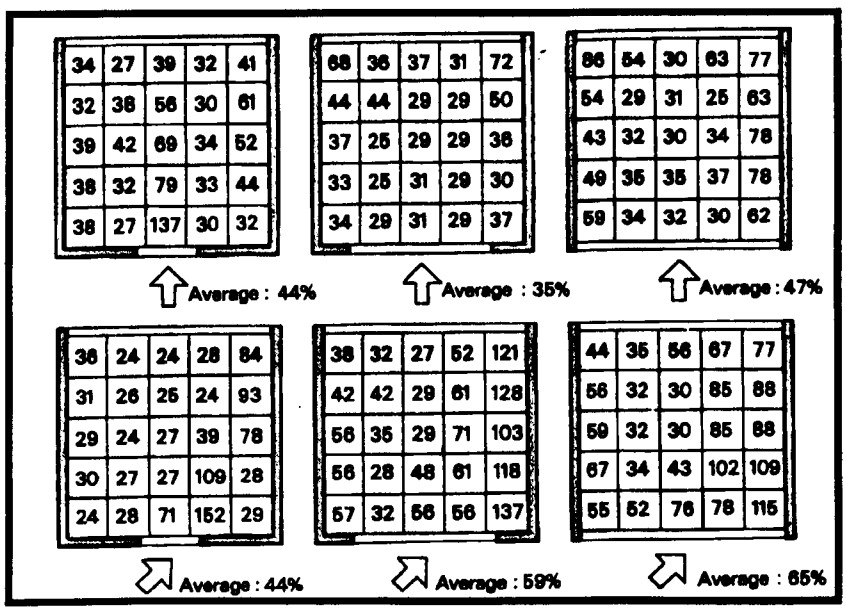

Figure (4.12): The effect of wind direction and the windward opening size on the average air velocity indoors. (Koenigsberger et al.1977), (Givoni 1981)

4.4.3. Window orientation

Building orientation is a significant task for designers when considering the environmental variables. Similarly the window design, on the scale of an aperture, is of appreciable importance. The orientation of a window in relation to the wind angle of

incidence was found to be much more important than the size. But when using window controls (such as a solar shading device or a MLW) the case may differ; *"In ventilated buildings with effectively shaded windows the internal temperatures are virtually independent of orientation"*(Givoni, 1981).

4.4.4. Controls

The discussion of the window design in tropics is related, to a high extent, to window control systems (Koenigsberger et al. 1977), (Givoni, 1981), (Muniz, 1985), (Olgyay and Olgyay, 1976), (Bittencourt, 1993), (Yannas, 1990) (Kukerja, 1978) (Oliveira and Bittencourt, 1998) and (Sharples and Maghrabi, 2000). In other words, the need to control the environmental aspects, including sun radiation, glare, rain and ventilation through the window, are borne in mind with the control systems. The protection from direct solar radiations as well as controlling the airflow patterns indoors have been the major consideration behind using the shading devices. As stated previously, window controls in tropics should have the utmost attention (Muniz 1985).

Two controls such as horizontal louvers, vertical louvers, combination of both louvers (known as egg-crates) and perforated block were discussed in details in section 3.3. The overhangs incorporate slotted hood, solid hood, louvered hood and projected ceiling. They may be found under different names though their concept is still the same. Various studies have been carried out to study the effect of each type over natural ventilation performances. Vertical louvers tend to reduce the effect of ventilation efficiencies with oblique winds. But with oblique louver angles this louver favours wind incidence similar to the angles and produces better performances (Figure 4.10). Bowen (1983) and Caudill and Reeds (1952) studied the effect of some typical overhangs over the flow pattern inside

the room and found that both louvered hood and slotted hood controls cause a downwards flow pattern while the solid hood tends to cause an upward flow in the room.

Window screens (mosquito-screens) also have some effect on the velocity drop based on the porosity percentage as well as their material. Abrams (1986) indicated that the frequently used screens reduce air velocity by 50%. More precisely, other researchers studied the effect of screen materials on that drop and found that cotton, nylon, bronze-wire and plastic screens reduce velocity by 70%, 35%, 21% and 29% respectively, depending on the sheet perforations (Koenigsberger et al. 1977), (Chandra, 1982). A recent work (Oliveira and Bittencourt, 1998) highlighted the significance of velocity reduction as a function of mosquito-screens. When indoor velocity through two windows, louvered window and louvered window supplied with a mosquito-screen, was observed against an open window, the reduction as a function of the latter setup was more evident than the former under all wind indices observed, as illustrated in Figure 3.18. This is an important issue in the tropics where windows should be opened most of the day, for cross ventilation is needed while mosquitoes and other insects must be kept out of living area.

4.4.5. Wing-walls and projections

In certain circumstances where the window location does not experience much wind or is facing downwind, the use of vertical projections that are stepped out of the elevation surface may assist natural ventilation. Wing-walls are outdoor vertical projections made either from a solid or porous wall, such as perforated blocks (Bittencourt, 1993). The design and location are particularly significant since they create sub-zonal locations around windows with different pressure, and hence, cause ventilation as illustrated in 4.13. For a simple room, the inadequacy in positioning the wing-walls

around both windows could obstruct the airflow through and hence cause draught as seen from the previous figure (Fleury, 1990) (Boutet, 1987). In the case of single sided ventilation, wing-walls could also be a solution to enhance natural ventilation, specifically when accompanied with oblique winds. In this situation, the wing-walls would act as wind

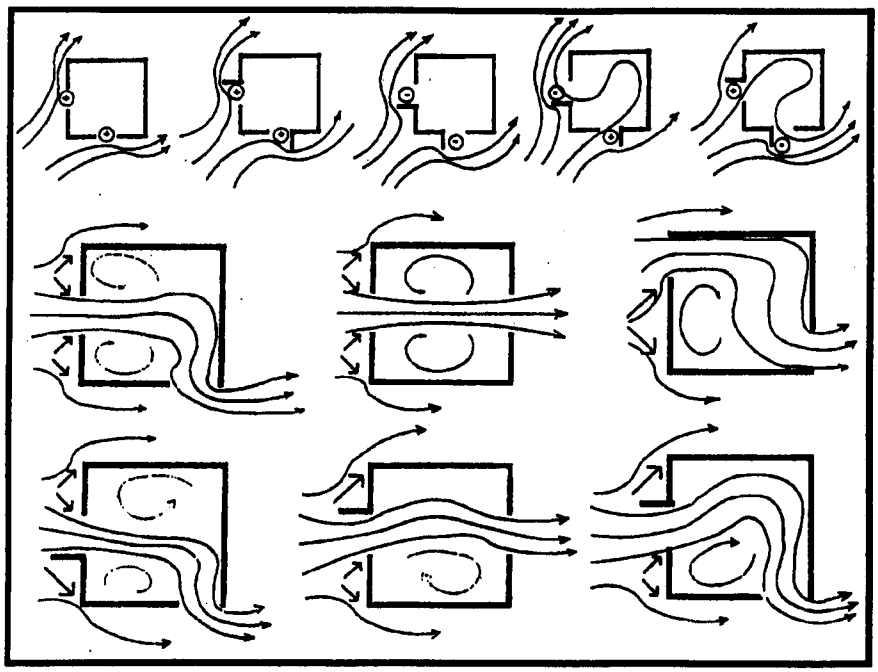

Figure (4.13): The effect of wing-walls in modifying and enhancing indoor flow patterns. (Fleury, 1990), (Koenigsberger, 1977) and (Boutet 1987)

catchers (Figure 4.14). The application of perforated blocks could reduce the pressure build up around windows, which reduces inference and flow turbulence near the window occurring at higher wind velocities.

The effect of wing-walls with eaves on the velocity inside three adjacent rooms is shown in Appendix (A.6) (Aynsley et al. 1977). The velocity coefficient for the three rooms (C_v), which is the ratio of average indoor speed against free wind speed at 10m of elevation in an open field, was plotted against various wind angles ranged from 0^o to 75^o at 15^o intervals. The effect of wing-wall was clear on the downwind room, especially with

diagonal winds. In contrast, the introduction of a wing-wall had a reverse effect on the other rooms. C_v was reduced in proportion to more skewed winds. Evans (1980) indicated that the technique was useful in many critical situations when the freestream was parallel to window panel (w_i=90^0) where cross ventilation was achieved by controlling the external walls with various lengths.

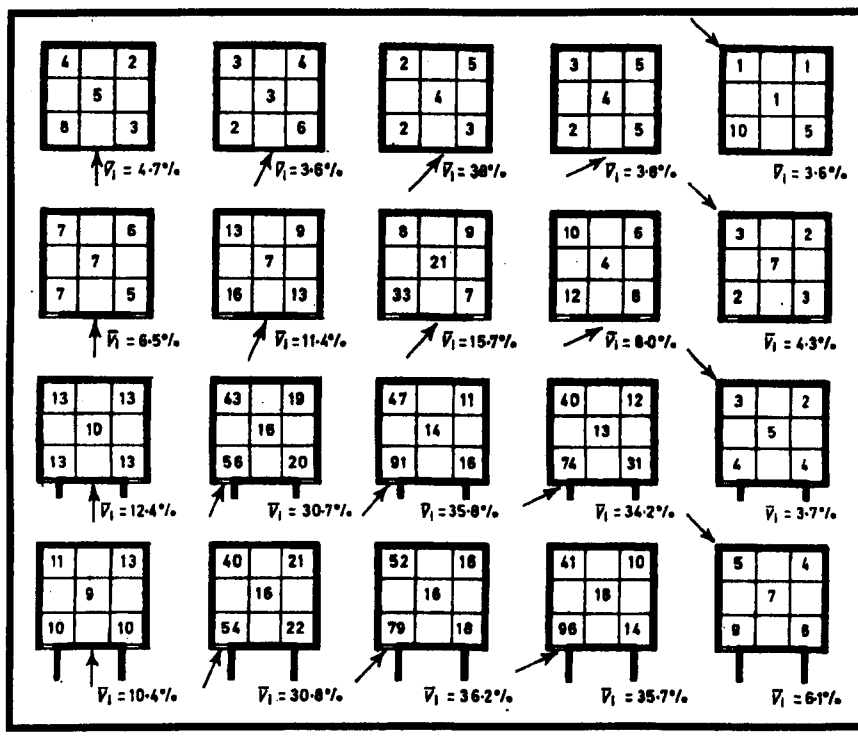

Figure (4.14): The mean indoor air velocity for a single sided ventilation was improved with the presence of wing-walls. (Givoni, 1981)

4.4.6. Room configuration

In hot humid climates, cross ventilation efficiency is the means by which human comfort is achieved, unlike other climates where the hourly air changes (ACH) are the sources of comfort (Muniz, 1985). The distribution of airflow within the building should vary with respect to the functions of the rooms. Such rooms where occupants' activities

occur at set locations should have concentrated flow regimes (Bittencourt, 1993). An example of this is the bedroom or bathroom where concentrated airflow with higher velocities is required. Other enclosures such as the living room require a uniform distribution of air. Thus the design of such a space should provide adequate and uniform distribution of air and avoid wind-shadowed or still-air areas within the room (Caudill and Reed, 1952), (Bittencourt, 1993).

When endowing the room with appropriate openings, then the room depth, length and height would have little effect on the airflow as was quoted by both Caudill and Reed (1952) and Muniz (1985). The effect on the length may have some significance for diagonal winds as indicated by Caudill and Reeds (1952). This, however, is not supported by other research findings. For example, Givoni's (1981) showed that the velocity reduction is dependent on the room depth as shown in Figure (4.12). Additionally another study has shown the influence of ceiling height and depth on the flow pattern indoors (Sharples and Maghrabi, 2000). When using controls that deflect air towards the ceiling, the stack effect will be negligible due to the breeze speed. Evans (1979) noted that flow near the ceiling helps remove the hot air build-up but may not necessarily cause a cooling sensation to occupants. As discussed before in section (4.2.9.2) this is due to the *Coanda effect* when air flows adjacently to the ceiling until reaching the outlet and is not diverted into the living zone.

4.4.7. Internal partitioning and sub-divisions

Most airflow studies are conducted using a single room with windward and leeward openings. However, airflow within a building normally passes by a number of zones before reaching the outlet. These zones are usually divided by walls or partitions which

sub-divide the building, and hence, would have a major effect on branching and channelling the flow indoors. Internal partitions have a great effect on flow pattern, direction and speed of air before leaving through the outlet. Givoni (1981) studied the effect of sub-divisions on the distribution of average internal speed (V_i) and found that the reduction ranged from 44.5% to 30.5%. He concluded that higher average V_i was obtained when the partitions were placed near the outlet as compared to the inlet. One solution suggested to reduce flow resistance caused by partitions was the application of porous partitions (Koenigsberger et al. 1977), (Al-Lyaly, 1990), (Bittencourt, 1993). This recommendation is not new but rather was employed in traditional architectures in the tropics such as in Jeddah, Yemen, Brazil, etc. However, the application of porous partitions may interfere with other aspects such as privacy and noise controls as noted by Bittencourt (1993).

4.4.8. Roofs and eaves

A number of studies have investigated the criterion of roof and eaves design in regards to flow patterns within building. Bahadori & Haghighat (1985) studied the doomed roof design in respect to reduced air temperature in buildings. They concluded that doomed roof with a crown opening on its crest is a sound alternative to asses natural ventilation in arid regions (Bahadori and Haghighat, 1985). A more recent study was conducted on the effect of roof shape on cross ventilation in a room using numerical simulation: Computational Fluid Dynamics (CFD) (Kindangen et al. 1997). The roof shape examined covered a number of possible roof shapes in tropical architecture including pitched, pyramidal, prism-shaped and semi-cylindrical roofs and was measured with reference to flat roof, with and without overhangs (eaves) (Appendix A.7.a). The significance of eaves on the flat roof depended, to a high function, on the wind inclination

angle. An amplification of 39%, 10% and 7% was found with the presence of respectively 0^{o}, 30^{o}, 45^{o} of wind incidence. Any increase beyond that was negligible (Appendix A.7.b). However, eaves on outdoors flow pattern and specifically on the percentage of wind shadow (wake depth) was minor (Evans, 1973) (Boutet, 1987). The roof height was also significant with steeper wind indices, *" For large wind angles ($60 \leq \theta \leq 90$) at the inlet, act to increase the exposed projected area on the windward side, followed by the positive pressure of the windward side"* (Kindangen et al. 1997). Interestingly, in all cases examined, the measured cell on outlet surface experienced higher speed than the adjacent cell inside the room. Similarly, wake depth as function of pitched roof height was increasingly proportional and obviously increases pressure difference between building enclosures (Boutet, 1987).

4.4.9. Landscape and vegetation

The proper positioning of plants around a building or an opening will appreciably enhance and correct flow patterns inside the room. Where window orientation does not appreciate wind currents or is not facing the freestream then hedges and trees could solve the problem (Evans, 1979). The hedges act as wing-walls and create sub-zonal locations with difference in pressures between inlet and outlet, and thus, ventilation occurs. However, Bittencourt (1993) and Chandra (1989) argued that most literature on the influence of plants on the airflow within buildings was based on a model study carried out by White in 1957 and the model does not realistically represent the plants' *"porosity"* or *"bending and alignment of leaves due to wind"*.

The influence of hedges on flow inside the room will be more effective than trees. The height and location of the hedges in relation to the building are important for *" The*

reduction in air motion reaches its peak when the hedges are located about 7 times its height from the building, but decreases sharply when the hedges are planted near the building or away from it" (Bittencourt, 1993), (Van Straatan et al. 1965).

4.5. Measuring techniques

Ventilation contribution through an opening encounters a number of complications in the real environment. Some of these are related to the physics of the fluid and others are related to the aperture and surroundings as discussed previously in this chapter. The calculation method or measuring technique selected is considerably important to decide the optimum technique for a specific task. The principle of airflow measurement would determine to a large extent the appropriateness of the technique selected. The various techniques and calculation methods implemented in ventilation research are discussed here. Table (4.1) sheds light on the advantages and disadvantages of each technique.

4.5.1. Site Observation

Perhaps the most pragmatic and most primitive technique is the site observation where the investigation procedure is conducted on a full-scale building or on an enclosure in the real environment. It may not necessarily be named site observations since it has been used on the basis of *trail-and-error experience* to treat the built environment. Aynsley (1999) indicated that the empirical knowledge obtained from observations to utilise natural ventilation in buildings goes some thousands years back; "*Ancient records from Egyptian times refer to orientation of buildings to prevailing winds as do Greek, Romans, and Chinese records*". He added, *"It was not until the development of instruments to measure atmospheric pressure and wind speed that there was an*

opportunity for a theoretical approach". In ventilation studies, however, site observations may encounter some difficulties that could not lead to optimisations and standardisations since the variables involved, such as wind speed, direction, temperature, etc., are beyond control. The technique is also a time consuming due to the fact that the work required for analysis could take a number of months of preparations. Adding these to the economic factor, such as the capital running costs and the need to analyse proposed solutions at early design stages, has led to the utilisation of other techniques.

Table (4.1): The common weaknesses and strengths of various measuring techniques. (Etheridge & Sandberg 1996)

Property	CFD	Full scale	Model scale	Simple methods
Continuum	No	Yes	Yes	No
Geometric similarity	Approx.	Yes	Approx.	Approx.
Size limitations	No	Yes	Some	No
Scale effects	Some	None	Yes	Yes
Instantaneous turbulence	Indirectly	Yes	Yes	No
Hazardous events	Yes	Limited	Limited	Yes
Modeling of moving people	Limited	Yes	Limited	Limited
Empirical content	Some	None	Little	High
Potential accuracy	High	High	Moderate	Low
Tuning required for highest accuracy	Yes	No	No	No
Capital cost	Moderate	High	Moderate	Low
Running cost	High	High	High	Low
Experienced user desirable	Yes	No	No	Yes
Usable at design stage	Yes	No	Yes	Yes

4.5.2. Wind Tunnel

The wind tunnel is an empirical scale-model approach that is widely established in ventilation research. This technique, along with others, has some preference over site observation in regards to its usefulness at an early design stage before finalising the scheme and further developing various solutions. It allows examination of different alternatives. Carey and Etheridge (1999) indicated that direct wind tunnel approach has more potential for the examination of wind effects on buildings than the theoretical approaches. The boundary layer in the wind tunnels, depending on the surface roughness, presents a good representation of wind characteristics in the real environment before reaching the proposed building; and also of how the building will influence other buildings in the downwind direction as found in Lee et al (1980), Abdulrahman et al. (1998) and Olwi et al (1988). The wind tunnel is also used to examine airflow through a particular space or a number of spaces within the building as found in (Gadi and Ward, 1989), (Warren and Parkins, 1984) and more recently in (Carey and Etheridge, 1999). Pressure and velocity drops and airflow visualisation are obtained with the use of appropriate instrumentations and equipments. In 1950's, the wind tunnels were the only available tool for testing complex cases in ventilation (Koenigsberger et al. 1977).

4.5.3. The test chamber

Another laboratorial approach is the test chamber. This is widely employed in testing building components such as a window, a door or some of their particular components, like infiltration due to cracks. The technique is widely used in measuring the volumetric flow of fluid (Q) through a component, and therefore the differential pressure (ΔP) occurring (Etheridge and Sandberg, 1996). The approach has also a history in

ventilation research that goes back to 1920's. Houghton and O'Connell (1928) carried out air leakage measurements in metal windows in 1928 using the latter approach. Some recent research applied this technique to determine airflow characteristics through cracks (Baker et al. 1987) or flow characteristics through louvered windows as found in Maghrabi and Sharples (1999), Yakubu and Sharples (1991), Sharples and Maghrabi (2000). In this study, velocity and pressure drops as functions of various MLW configurations will be carried out using the latter technique; i.e. full-scale test chamber approach.

4.5.4. Theoretical approaches

Theoretical approaches to calculate airflow within and around buildings were discussed in more details in section (4.2) and subsequent sub-sections. The assumptions are employed to answer some of the complexities accruing in practice since the full understanding of these complexities is not yet complete: *"In this approach the better models are the ones which make the more justifiable assumptions and which employ the experimental in the more appropriate manner"* (Etheridge and Sandberg, 1996). The assumptions corrections are more evident with the presence of empirical studies. In 1950, Dick (1950), when investigating air infiltration while using both techniques, reported that theoretical estimations shared a good agreement with site observation. Since then, more efforts have been made to validate the theoretical approaches with other empirical studies. Some of the most recent ones are found in (Said et al. 1995), (Wang, 1995), (Kindangen and Krauss, 1996), (Alexander et al. 1997), (Chung and Dunn-Rankin, 1998), (Sharples and Maghrabi, 2000) and others. However, theoretical techniques usually require a highly sophisticated knowledge of fluid mechanics principles and user expertise.

4.5.5. Computational Fluid Dynamics (CFD)

Computational fluid dynamics (CFD) is one of the theoretical approaches that have been widely accepted in recent years. The advancement in computational power has influenced the developments in wind engineering. In the 1970's, CFD software was feasible and was accompanied with research in the field of ventilation. CFD models are governed by the principles of fluid dynamics including conversion of mass, momentum and thermal energy represented in set of equations to solve some more complicated situations than any other measuring technique. CFD will be discussed in more details in Chapter 8 of this thesis.

4.6. Conclusion

Wind-induced natural ventilation is the main natural and free source of human comfort in hot humid climates. Its potential to cool the indoor environment as well as the occupants ensures research interest. In this chapter the airflow characteristics as a function of various elements around and within buildings were reviewed. Also, the mathematical representations of the airflow characteristics with respect to natural ventilation in buildings were highlighted. Some conclusions are derived from this review:

- The varieties of mathematical models related to airflow characteristics within buildings are treated with some simplicity and assumptions; yet they are widely accepted in ventilation research since the entire representations of flow complexities are agreed to be unfeasible. Nevertheless, the validity of most of them is based on a complete open aperture. When any treatment is involved, such as the reviewed MLW, their appropriateness is questioned,

and thus, the need for direct measurements will be more reliable than the theoretical models.

- Window accessories and controls, such as MLW, are very essential in tropical climate as they serve more than one function. Nevertheless, the relevant research conducted with respect to their contribution in the overall ventilation effectiveness and flow patterns indoors is far from being satisfactory. Also, the values for pressure and velocity magnitudes are rare in the literature. The previous statement was argued in both Chapters 3 and 4 and therefore, further research is needed to identify the coefficients of pressure and velocity magnitudes as functions to these treatments and their configurations.
- The observed measuring techniques to solve ventilation problems in buildings are widely acceptable and the selection of the appropriate technique depends on the scale and the problem, and the degree of accuracy required. From this perspective the standardisation of characterising airflow around MLW is believed to be better conducted through wind tunnels or test chambers as compared with the site observation technique. Both techniques have also preference over the theoretical models, specifically when related to MLW as discussed before. The work in Chapters 6 and 7 will be then carried out using the test chamber at the University of Sheffield Campus.

4.7. References

1. Abdulrahman, S., Kannan, K. S., and Ramli, A. H. (1998) "Prediction of indoor air movement of naturally ventilated classrooms in schools in Malaysia". **(3)**, p.1411-1414, Florence (Italy): Proc. World Renewable Energy Congress V.

2. Abrams, D. (1986) *Low-Energy Cooling*, New York, USA: Van Nostrand Reinhold Company.

3. Al-Jawadi, M.H. (1986) Window optimisation for Iraqi houses. Department of Architecture and Building Science, University of Strathclyde. Unpublished PhD thesis.

4. Al-Lyaly, S.M. (1990) The traditional house of Jeddah: A study of the interaction between climate, form, and living patterns. University of Edinburgh. Unpublished Ph.D thesis.

5. Al-Megren, K. (1987) Wind towers for passive ventilation cooling in hot-arid regions. The University of Michigan. Unpublished Doctor of Architecture thesis.

6. Alexander, D. K., Jenkins, H G, and Jones, P. J. (1997) "A comparison of wind tunnel and CFD methods applied to natural ventilation design.". p.321-326, Prague, Czech Republic: Proc. International Building Performance Simulation Association.

7. ASHRAE (1985) *ASHRAE Handbook of Fundamentals*, Georgia, Atlanta: American Society of Heating, Refrigerating, and Air-Conditioning Engineers.

8. ASTM Standard E779 (1982) *Measuring air leakage by fan infiltration pressurisation method*,

9. Awbi, H.B. (1991) *Ventilation of Buildings*, London: E & FN Spon.

10. Aynsley, R. M. (1979) "Wind-generated natural ventilation of housing for thermal comfort in hot humid climates". **(1)**, p.243-254, Proc. 5th International Conference Fort Collins.

11. Aynsley, R. M. (1982) "Natural Ventilation model studies". Gaithersburg, USA: Proceedings of the International Workshop on Wind Tunnel Modeling Criteria and Techniques in Civil Engineering Application.

12. Aynsley, R. M. (1988) "A Resistance Approach to Estimating Airflow Through Buildings With Large Openings Due To Wind". **(94)**, 2 edn. p.1661-1668, ASHRAE transactions.

13. Aynsley, R. M. (1999) "Unresolved issues in natural ventilation for thermal comfort". p.36-44, Darlington, NSW, Australia: proceedings of Hybvent Forum '99.

14. Aynsley, R.M., Melbourne, W. and Vickery, B.J. (1977) *Architectural Aerodynamics*, London: Applied Science Publishers Ltd.

15. Bahadori, M.N. and Haghighat, F. (1985) "Passive cooling in hot, arid regions in developing countries by employing domed roofs and reducing the temperature of internal surfaces.". *Building and Environment* **20-(2),** p.103-113.

16. Baker, P.H., Heap, R.D. and Sharples, S. (1986) "Airflow through perforated screens at small pressure differences.". *Building Serv Eng Res Technol*p.96-97.

17. Baker, P.H., Sharples, S. and Ward, I.C. (1987) "Airflow through cracks". *Building and Environment* **22-(4),** p.293-304.

18. Bittencourt, L.S. (1993) Ventilation as a cooling resource for warm -humid climates: An investigation on perforated block wall geometry to improve ventilation inside low-rise buildings. Architectural Association Graduate School. Unpublished Ph.D. thesis.

19. Boutet, T.S. (1987) *Controlling air movement: A Manual for Architects and Builders*, New York: McGraw-Hill.

20. Bowen, A (1983) "Design guidelines on lateral through and around buildings". p.517-533, Proc. of 2nd International PLEA Conference.

21. BRE (1978) Principles of natural ventilation. no.210, UK: Building Research Establishment.

22. BS (1980) Code of Practice and designing of buildings: Ventilation principles and designing for natural ventilation. no. 5925, London: British Standards Institution.

23. Carey, P.S. and Etheridge, D.W. (1999) "Direct wind tunnel modelling of natural ventilation for design purposes". *Building Serv.Eng.Res.Technol.* **(20)-3,** p.131-142.

24. Caudill, W.W. and Reed, B.H. (1952) Geometry of classrooms as related to natural light and natural ventilation. 36, p.53 Texas: Texas Engineering Experiment Station; College Station.

25. CGSB Standard 149.10-M86 inventor Canadian General Standards Board, (1986) Determination of airtightness of building envelopes by fan pressurisation method. 149.10-M86. 149.10-M86.

26. Chand, I. (1970) "Effect of the distribution of fenestration area on the quantum of natural ventilation in buildings". *Architect and Science Review* **13-(4),** p.130-133.

27. Chandra, S. (1982) *A Handbook for Designing naturally ventilated buildings*, Florida, USA: Florida Solar Energy Centre.

28. Chandra, S. (1989) *Ventilative cooling*. In: Cook, J., (Ed.) *Passive Cooling*, Cabridge, Massachusetts: MIT Press.

29. Chandra, Subrato (1983) "A Design procedure to size windows for naturally ventilated rooms". p.105-110, USA: American Solar Energy Society, Inc.

30. Chung, I.-P. and Dunn-Rankin, D. (1998) "Using numerical simulation to predict ventilation efficiency in a model room". *Energy and buildings* **(28)**-p.43-50.

31. CIBSE (1976) Infiltration. Guide A4- Infiltration, London, UK: The Chartered Institute of Building Services Engineers.

32. Dick, J.B. (1950) "The Fundamentals of Natural Ventilation in Houses". *JIHVE* **(18)**-p.123-134.

33. Etheridge, D.W. (1977) "Crack Flow Equation and Scale Effect". *Building and Environment* **(12)**-p.181-189.

34. Etheridge, D.W. (1987) Air infiltration review. 4,

35. Etheridge, D.W. (1997) "A note on crack flow equations for ventilation modelling". *Building and Environment* **33-(5),** p.325-328.

36. Etheridge, D. and Sandberg, M. (1996) *Building Ventilation: Theory and Measurements*, John Willy & Sons.

37. Evans, B. (1973) Natural air flow around buildings. Lecture notes: Teaching the teachers on building climatology. Stockholm: The National Swedish Institute for Building Research.

38. Evans, B. H. (1979) "Energy conservation with natural air flow through windows". **(5)**, p.641-650, ASHRAE Transactions.

39. Evans, M. (1980) *Housing, Climate, and Comfort*, London: Architectural press.

40. Fleury, B. (1990) "Ventilative cooling". Ispra, CEC, Joint research centre: Paper presented at the workshop on passive cooling.

41. Fox, D.W. and MacDonald, A.T. (1978) *Introduction to Fluid Mechanics*, 2nd edition edn. New York: Wiley.

42. Gadi, M. and Ward, I. C. (1989) "An investigation into the ventilation and thermal performance of contemporary housing in North Africa.". p.143-146, Paris, France:

proceedings "Second European conference on architecture: science and technology at the service of architecture".

43. Givoni, B. (1965) "Laboratory study of the effect of window size and location on indoor air motion". *Architectural science review* **8-(2),** p.42-45.

44. Givoni, B. (1981) *Man, Climate and Architecture,* 2nd edn. London: Applied Science Publishers Ltd.

45. Holleman, T.R. (1951) Air flow through conventional window openings. 33, p.45 Texas: Texas engineering experiment station, College station.

46. Hopkins, M. H. and Hansford, B. (1974) "Air flow through cracks". **(42),** p.123-129, IHVE Ventilation of housing symposium.

47. Houghton, F. C. and O' Connel (1928) "Air leakage studies in metal windows in a modern office building". 34 edn. p.321-336, USA: ASHVE Trans.

48. ISO Standard inventor International organisation for standardisation, (1995) Thermal insulation-determination of building airtightness-fan pressurisation method. 9972.

49. Kaizer, T. (1984) *Shelter in Saudi Arabia.*, London: Academy Editions.

50. Kindangen, J. and Krauss, G. (1996) "Investigation of natural ventilation with computational fluid dynamics. A comparison study with wind tunnel results." . *Architectural science review* **(39)**-p.113-119.

51. Kindangen, J., Krauss, G. and Depecker, P. (1997) "Effect of roof shape on wind-induced air motion inside buildings". *Building and Environment* **32-(1),** p.1-11.

52. Koenigsberger, O., Ingresoll, T., Mayhew, A. and Szokolay, S. (1977) *Manual of Tropical Housing. Part One: Climatic Design,* London: Longman Group Ltd.

53. Konya, A. (1980) *Design Primer for Hot Climates*, London: Architectural Press.

54. Kukerja, C. (1978) *Tropical Architecture*, New Delhi: Tata McGrow-Hill Publishing Company ltd.

55. Lee, B.E., Hussain, M. and Soliman, B. (1980) Predicting natural ventilation forces upon low-rise buildings. Sheffield: Building Science Unit, University of Sheffield.

56. Liddament, M.W. (1986) Air Infiltration calculation techniques-An Application Guide. Coventry, UK: AIVC.

57. Liddament, M.W. (1987) Air infiltration review. 4,

58. Maghrabi, Amjed and Sharples, S. (1999) "Air flow characteristics through Modulated Louvered Windows". **(1)**, p.507-514, Brisbane, Australia: PLEA.

59. Markus, T.A. and Morris, E.N. (1980) *Buildings, Climate and Energy*, London: Pitman.

60. Massey, B.S. (1989) *Mechanics of Fluids*, 6th edn. London: Chapman and Hall Ltd.

61. Melaragno, M.G. (1982) *Wind in architectural and environmental design*, New York: Van Nostrand Reinhold Co.

62. Muniz, P.A. (1985) The geometry of external shading devices as related to natural ventilation, daylighting and thermal comfort, with particular reference to tropical hot-humid climates. Unpublished Ph.D. Thesis.

63. Olgyay, V. and Olgyay, A. (1976) *Design with climate; Bio-climatic approach to Architectural regionalism*, Princeton N.J.: Princeton University Press.

64. Oliveira, F. and Bittencourt, L. S. (1998) "Air flow through louvered windows in small rooms". p.393-396, Lisbon, Portugal: PLEA '98.

65. OLwi, I.A., Ghazi, M.A. and Mohsen, M.A. (1988) "Wind tunnel simulation of airflow through rows of attached buildings". *Solar & Wind Technology* **5-(4),** p.445-450.

66. Said, M. N. A., Shaw, C. Y., Zhang, J. S., and Christianson, L. L. (1995) "Computation of room air distribution". , Chicago, USA: proceedings of ASHRAE Centennial Conference p.1065-1077.

67. Sawachi, T., Kiyota, N., and Kodama, Y. (1999) "Airflow and wind pressure around a full-size cubical building model in a wind tunnel: Basic data for developing a quantitative tool for cross ventilation design". **(2),** Brisbane, Australia: PLEA.

68. Sharples, S and Maghrabi, Amjed (2000) "Airflow through louvers: an experimental and CFD study". The Hague, Netherlands: Proc. 21st. AIVC Conference (To be published).

69. Sherman, M., Grimsrud, D.T. and Sonderegger, R.C. (1979) Low pressure leakage function of a building. LBL-9162, Lawrence Berekely Lab.

70. Sobin, Harris (1981) "Window design for passive ventilative cooling: An experimental model-scale study". Miami Beach, Florida, USA: Proc. International passive and hybrid cooling conference, p.191-195.

71. Sobin, H. (1983) Analysis of wind tunnel data on naturally ventilated models. p.287 Tucson, Arizona, USA: Harris Sobin & Associates.

72. Thomas and Evans (1951) Proposed interior classroom. pp.1-57. Texas: Texas Engineering Experiment Station, College Station.

73. Van Straatan, J.F., Richards, S.J. , Lotz, F.J. and Deventer, E.N. (1965) Ventilation and thermal considerations in school building Design. Pretoria: National building research institute-CSIR.

74. Walker, I.S., Wilson, D.J. and Sherman, M. (1998) "A comparison of the power law to quadratic formulations for air infiltration calculations". *Energy and buildings* **(27)**-p.293-299.

75. Wang, Z. (1995) "Study of cross-ventilation in apartment with large openings - comparisons between wind tunnel tests and simulations". **(2),** p.449-455, Canada: Second International Conference.

76. Warren, P. R. and Parkins, L. M. (1984) "Single-sided ventilation through open windows.". p.p.487, Goteborg Sweden: Proc. "Windows in building design and maintenance".

77. Yakubu, G.S. (1990) Modulated solar shielding of buildings: A study of a solar radiation control strategy for low energy buildings in hot dry and semi-arid climates. University of Sheffield. Unpublished PhD thesis.

78. Yakubu, G.S. and Sharples, S. (1991) "Airflow through modulated louver systems". *Building Services Engineering Research and Technology* **12-(4),** p.151-155.

79. Yannas, S. (1990) "Solar control techniques". p.75-98, Proceedings of workshop on Passive Cooling. London, UK.

CHAPTER 5: THE MODULATED LOUVERED WINDOWS AND THE ROWSHAN PARAMETERS

5.1. Introduction

This chapter is the outcome of the literature review carried out in Chapters 2 and 3 as well as of a number of site measurements conducted by the author to observe the modulated louvered windows as well as the Rowshan various configurations that are commonly employed in Jeddah, Saudi Arabia. The first section reviews the MLW and the Rowshan geometries and the criterion employed for the review. Then comes the MLW configurations which will be examined later in Chapters 6,7 and 8. The potential of the various selected MLW configurations for controlling solar shading and view is then discussed in brief. The shading evaluation examines the shading masks for four months, representing the four seasons of the year followed by the privacy and view evaluation as functions of the MLW various geometries. The chapter ends up with highlighting the mathematical contribution of each variable involved in the reduction of airflow across the modulated louvered window systems.

5.2. Review of MLW and Rowshan geometries

5.2.1. The standard criterion of the review

The review of MLW as well as of the Rowshan's various components and geometries discussed in this chapter and examined in Chapters 6,7, 8 and 9 are based on the aforementioned Chapters as well as on some other sources of information. These are set out as follows:

- Onsite measurements on a number of typical houses in Jeddah carried out by the author to trace the MLW and Rowshan geometries.
- The Rowshan and MLW characteristics found in the work of Hariri (Hariri, 1992) as well as the recent work of Al-Shareef (Al Shareef, 1996).
- An interview with a local craftsman (Maghrabi, 1995) who has experience of constructing this type of windows.
- In addition, other sources in the literature that have highlighted the construction and geometry of the window system in hand. Amongst these references are Al-Lyaly, (1990), Al-Said (1996), Attieh (1990), Banajah (1995), Khan (1986), Maghrabi (1995), Mani' (1980), Salloum (1983), Al-Kahtani (1996), Greenlaw (1976), Hajj Research Centre (1994) and Zahran (1995).

5.2.2. MLW configurations

The construction of modulated louvered windows does not fall under a strict rule or specification. Therefore, an attempt was made to examine a number of MLW configurations that would cover most employed parameters.

The thickness of the louver (t) has slight variations with a mean thickness of 0.01m. Thus the thickness examined in this study was chosen to be 0.01m. As far as the values of aperture between louvers (d) and depth of louver (L) were concerned, there were no specific dimensions of these values; and yet they were set in proportion. This was concluded after the onsite measurements that was carried out in addition to those found in the literature review such as Al Shareef (Al Shareef, 1996) and Greenlaw (Greenlaw, 1976). When the MLW is completely closed, the louvers are set into three different proportions. The maximum aperture is obtained when the external edge of the louver overlaps just over the internal edge of the louver underneath when it is closed with the maximum value of d obtained. A local craftsman stated, *"The distance between the two, when the louvers are completely open at 0^o inclination, should not exceed the total depth or breadth of the louver"* (Maghrabi, 1995). This overlap could also be ¼ or ½ of the louver underneath. The proportions were examined graphically and resulted in three-overlap proportions that represent the approximate ratios of d/L which are 1, 0.75 and 0.50 respectively, as illustrated in Figure 5.1. The depth of the sash frame (S_l) has the same length as the L. The number of louvers (N) within sash frame is determined by sash height (S_h), d and L. The location of the window, the orientation and the function of the room determine the width (S_w) of the sash (Figure 5.2).

The porosity (p) of the MLW depends on the geometry and the number of louver blades in each unit. When blades are in perfect horizontal position, i.e. $\theta \cong 0$, p is considered at its maximum and diminishes according to the degree of inclination, say p_θ.

The MLW has its own significant mechanism that allows louvers to incline from 0^o angle- when the window is totally open- up to the degree, say θ^o, when the outer edge of the louver will overlap the inner edge underneath where $d \cong 0$m. The louver depth, number and gaps between louver blades in the frame also determine the angle where the sash unit is considered closed.

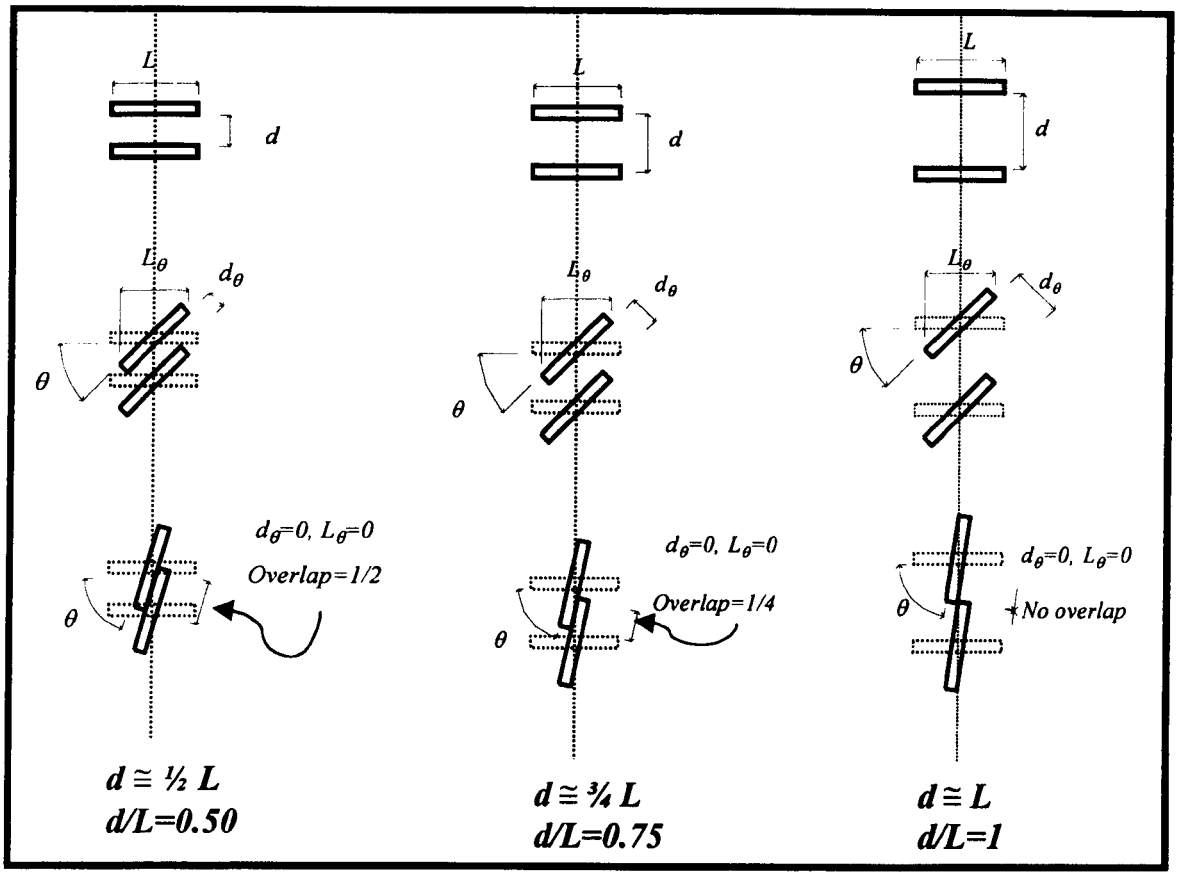

Figure (5.1): The various louver configurations that are typically employed in Jeddah, Saudi Arabia.

5.2.3. The Rowshan configurations

In Chapters 2 and 3, it was evident that the construction of the Rowshan is affected by a number of parameters. When a typical room in Jeddah is observed, one could also acknowledge the criterion of the Rowshan that is then replicated in a number of forms. Figure 5.3 shows the various forms of the Rowshan that are employed in Jeddah. The Rowshan mainly follows five different combinations that cover the most common types found in Jeddah, Saudi Arabia. The number of louvers in each combination varies accordingly. While they are either plain or projected Rowshans covering part or whole wall, they vary in louver numbers, wall configurations and dimensions. The plain Rowshan has two different forms; (Inlet-I) and (Inlet-III) and is more like the Taqqat

shown in Figure (2.16). The projected Rowshan on the other hand is much more predominant and has three different forms; (Inlet-II), (Inlet-IV) and (Inlet-V). To the other end of the room, the outlet dimensions and location that control the movement of airflow cover three various forms of outlets including a typical door (Outlet-I) or a window positioned in two locations on the outlet side: (Outlet-II) and (Outlet-III) with various dimensions (see Figure 5.3). The outlet-III is typically used over the doors connecting the various spaces to allow continuous air movement near the ceiling. This is called Al-Shakous and it is normally covered with perforated wooden screen.

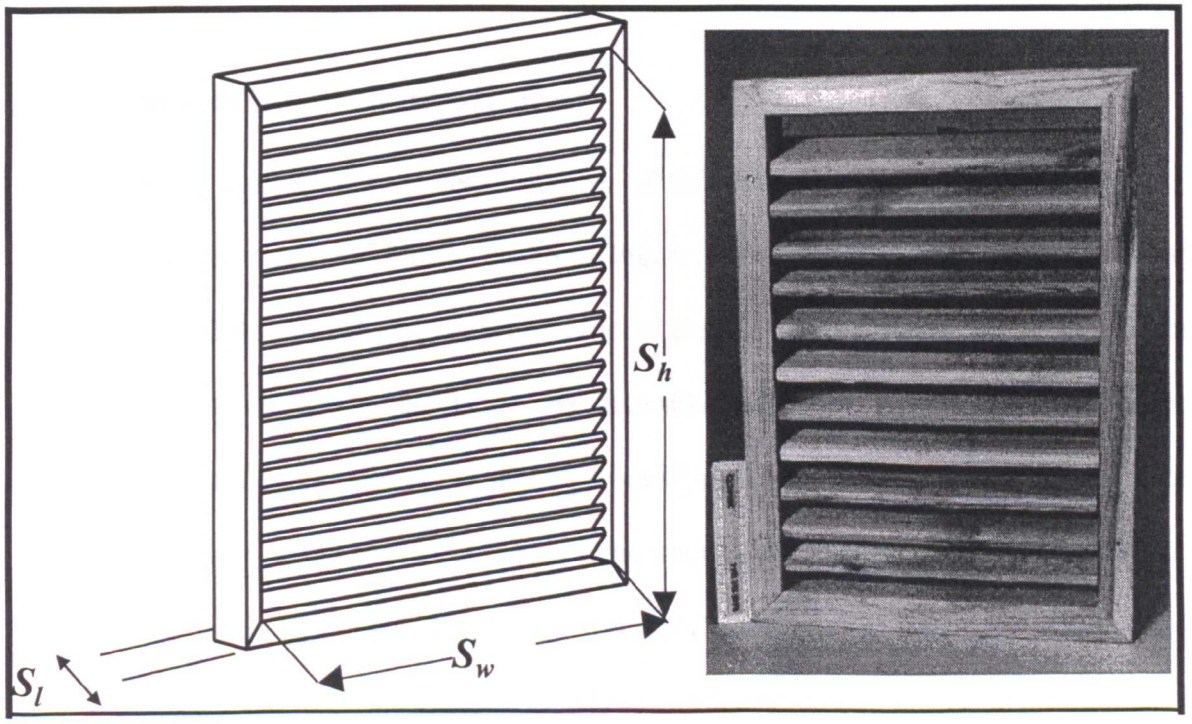

Figure (5.2): The modulated louvered window.

The MLW and Rowshan various configurations along with the various outlets involved will be recalled in the next chapters to examine the airflow characteristics inside the room as function of their configurations.

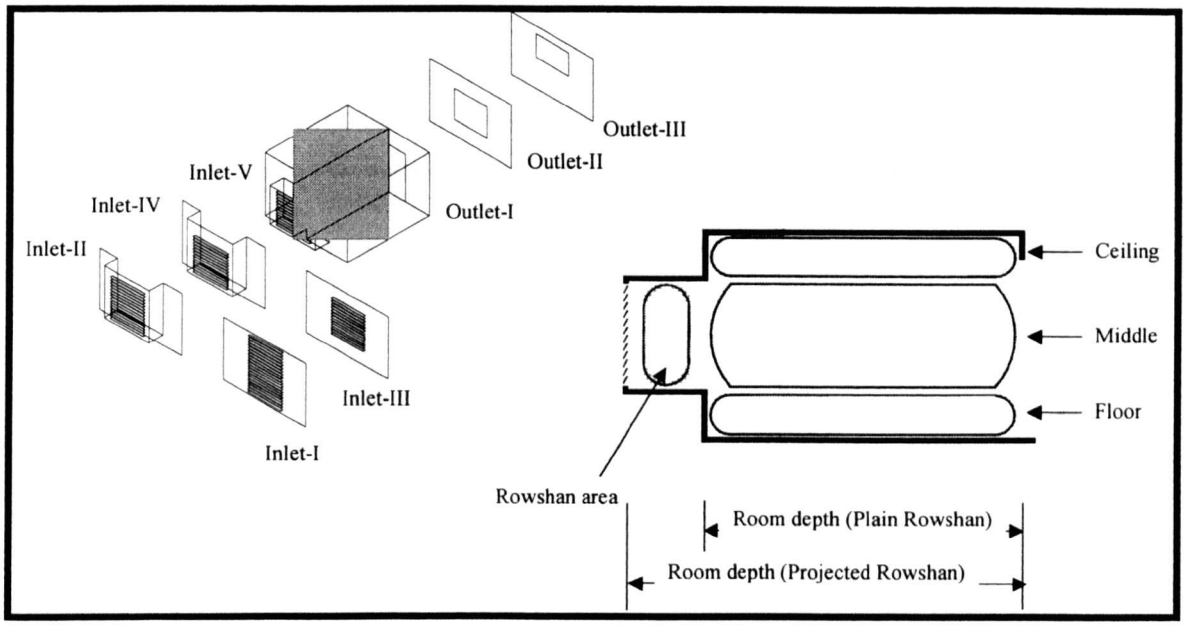

Figure (5.3): The typical combinations of inlet and outlet components in Jeddah for the projected and the plain Rowshan (Taqqat).

5.3. The examined configurations

For the evaluation purposes, a number of full-scale models of MLW fitted in sash units were constructed for further analysis (Figure 5.2). Models were made of smooth pinewood of light brown colour with various louver configurations including depths, apertures and flexibility to adjust them to the desirable inclination. Every model had its own mechanism that allowed louvers to incline from 0^{o} angle up to the degree when the outer edge of the louver would overlap the inner edge underneath. Three louver depths (L) were chosen; 0.04, 0.06 and 0.08m. The six various gap dimensions (d) chosen were 0.01, 0.02, 0.03, 0.035, 0.05 and 0.07 m (Table 5.1). These configurations included louver inclination angle (θ), depth (L), the number of louvers (N), gap between louver blades or aperture (d), the free area (A_f) and the ratio of aperture/depth ($d/L\%$). The ratio ranged from 0.5, in which half distance of the louver depth was overlapping the one underneath when MLW was considered totally closed, up to 1 where the outer edge of the louver was just overlapping the inner edge of the louver underneath as shown in Figure 5.1.

Table (5.1): The modulated louvered window (MLW) various configurations

No	Depth *L (m)*	Aperture *d (m)*	Number *N*	Ratio *d/L (%)*	The MLW configurations
1	0.04	0.01	24	0.5	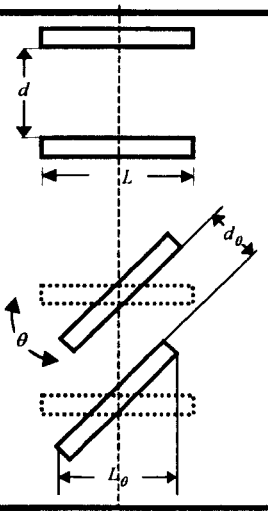
2	0.04	0.02	16	0.75	
3	0.04	0.03	12	1	
4	0.06	0.02	16	0.5	
5	0.06	0.03	12	0.67	
6	0.06	0.035	11	0.75	
7	0.06	0.05	8	1	
8	0.08	0.03	12	0.5	
9	0.08	0.05	8	0.75	
10	0.08	0.07	6	1	

5.4. Shading evaluation

This section examines, briefly, the performance of the modulated louvered windows with respect to solar shading and its contribution to daylighting effect.

5.4.1. Measures of evaluation

Shading evaluation of the MLW geometries was carried out using stereographic charts where their performance is measured based on the vertical shadow angle (ɔ) (Koenigsberger et al. 1977) (Figure 5.4). It is a simple measure for evaluating the shading performances of a window accessory which would provide designers with a threshold on the shading potential of that accessory. It may will be inaccurate to measure the *shading factor* yet it is sensible for climate regions where the sunshine is unwelcome at all times like Jeddah and to minimize risks of overheating due to sun penetration inside the building. Some research was found to support the application of the shading techniques and further readings are recommended for this purpose, (Olgyay, 1963) (Koenigsberger et al. 1977).

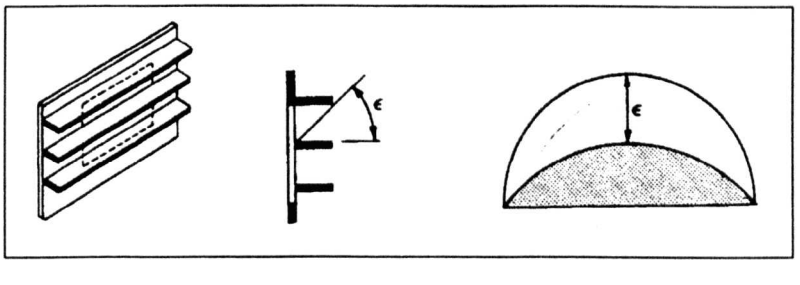

Figure (5.4): The solar shading evaluation for the horizontal shading devices. (Koenigsberger et al 1977).

In Chapter 2 (section 2.3.2) a review of bio-climatic needs concerning Jeddah was covered and Figure 2.13 showed the clear need for reducing the overheating potentials caused by the excessive outdoor temperature which rarely falls under 30°C. Although the temperature readings do not solely correspond to the overheating periods indoors, they

could give a general understanding of the potential problems inside building. The temperature is believed that to give an adequate justification to the shading needs particularly when there is no specific space or enclosure to be investigated (Bittencourt, 1993).

The sunpath chart for Jeddah, 21° N latitude, in Figure 2.12 illustrates that the summer solstice day occurs on June 21 and sunrise is at 05:18am and sunset is 6:42pm. The shortest day occurred on December 21 when daylight extends from 6:36am until 5:24pm. The criterion adopted in the evaluation was selected based on sunshine in the latter days representing both summer and winter. Also the evaluation covered the 15th September and 30th March to cover the four seasons. As it is shown from Figure 2.9, the sunpath in both latter months is identical. With regard to orientation, the study is limited to only two orientations, East and West, with an assumption of the sun being opposite to the louver systems.

5.4.2. The discussion

The protection from direct sunlight in the warm climates shapes one of the most basic ways of enhancing climatic conditions inside buildings. Based on this statement, the windows accessories should be given major attention as they shape some of the appropriate solutions to the environment stresses (Muniz, 1985). A recent study (Al Shareef, 1996) was conducted to evaluate the effectiveness of daylighting with respect to the Rowshan geometry commonly employed in Jeddah and concluded that the Rowshan contributes a sound for daylighting control to these environments.

The shading masks discussed below covered a number of MLW geometries as found from Figure 5.5 to 5.9. Various inclination angles of louvers were observed ranging from –30° to 30° at 15° intervals.

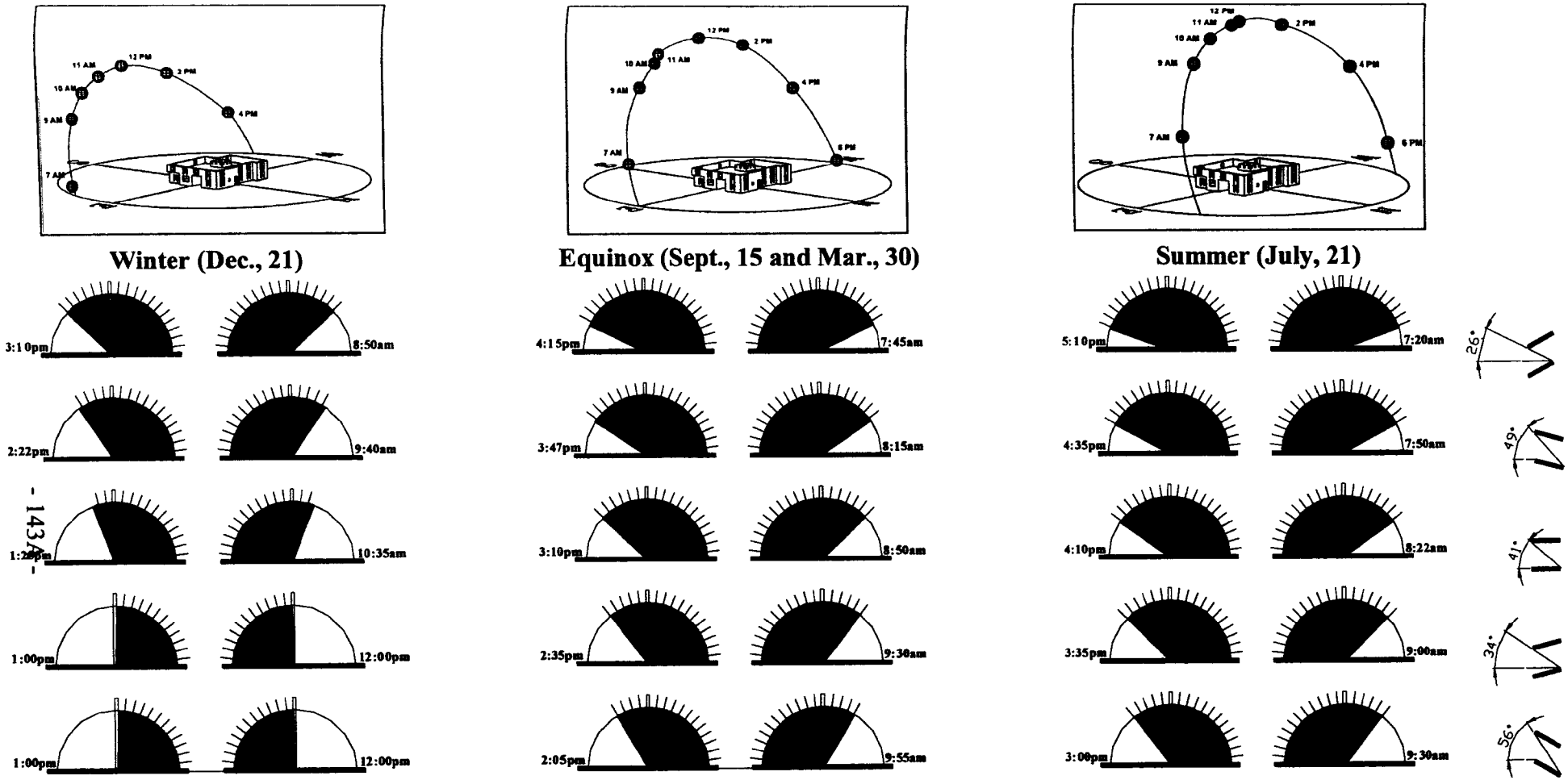

Figure (5.5): Sunshine hours for MLW configuration d=0.07m, L=0.08m.

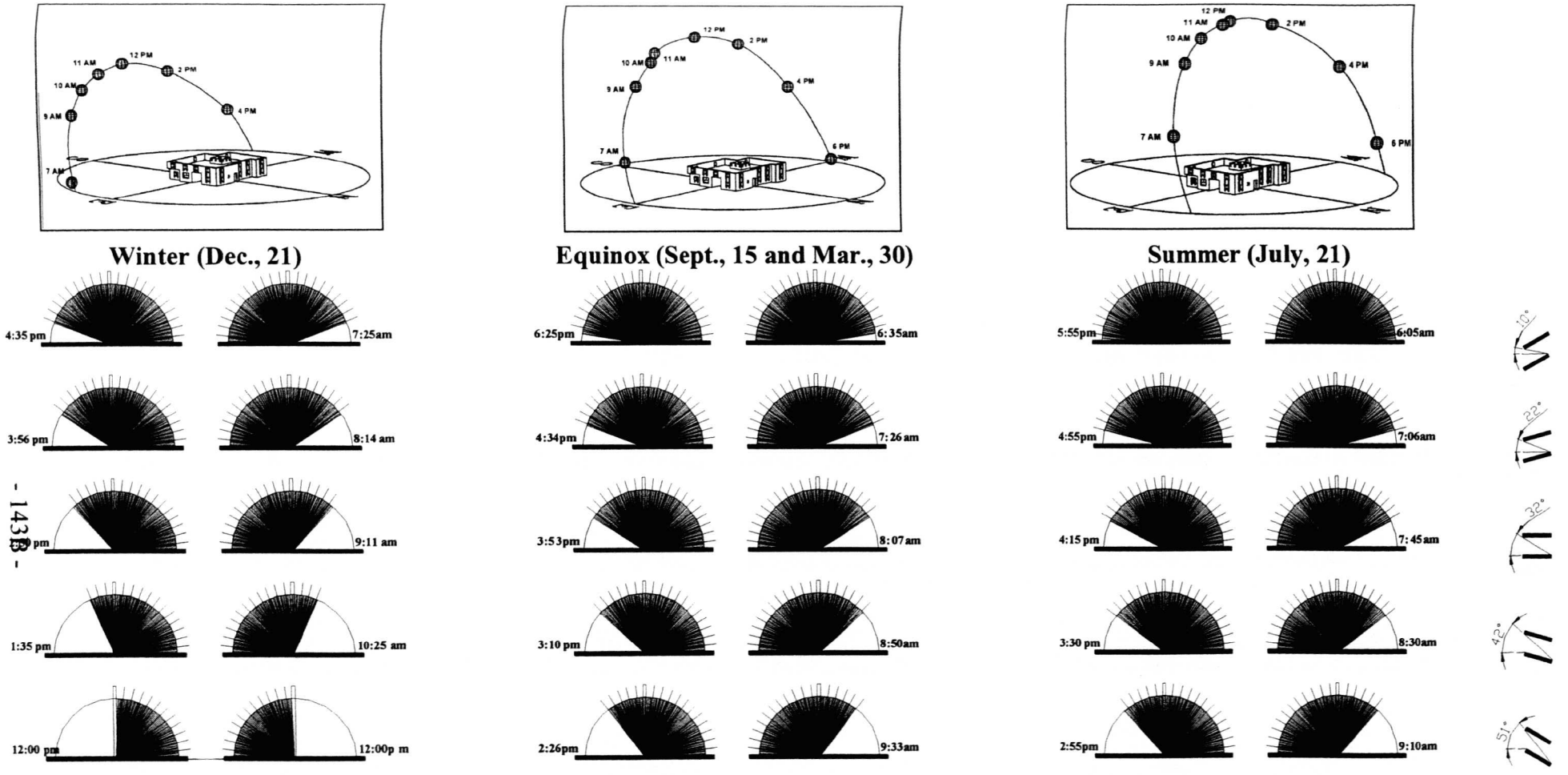

Figure (5.6): Sunshine hours for MLW configuration d=0.05m, L=0.08m.

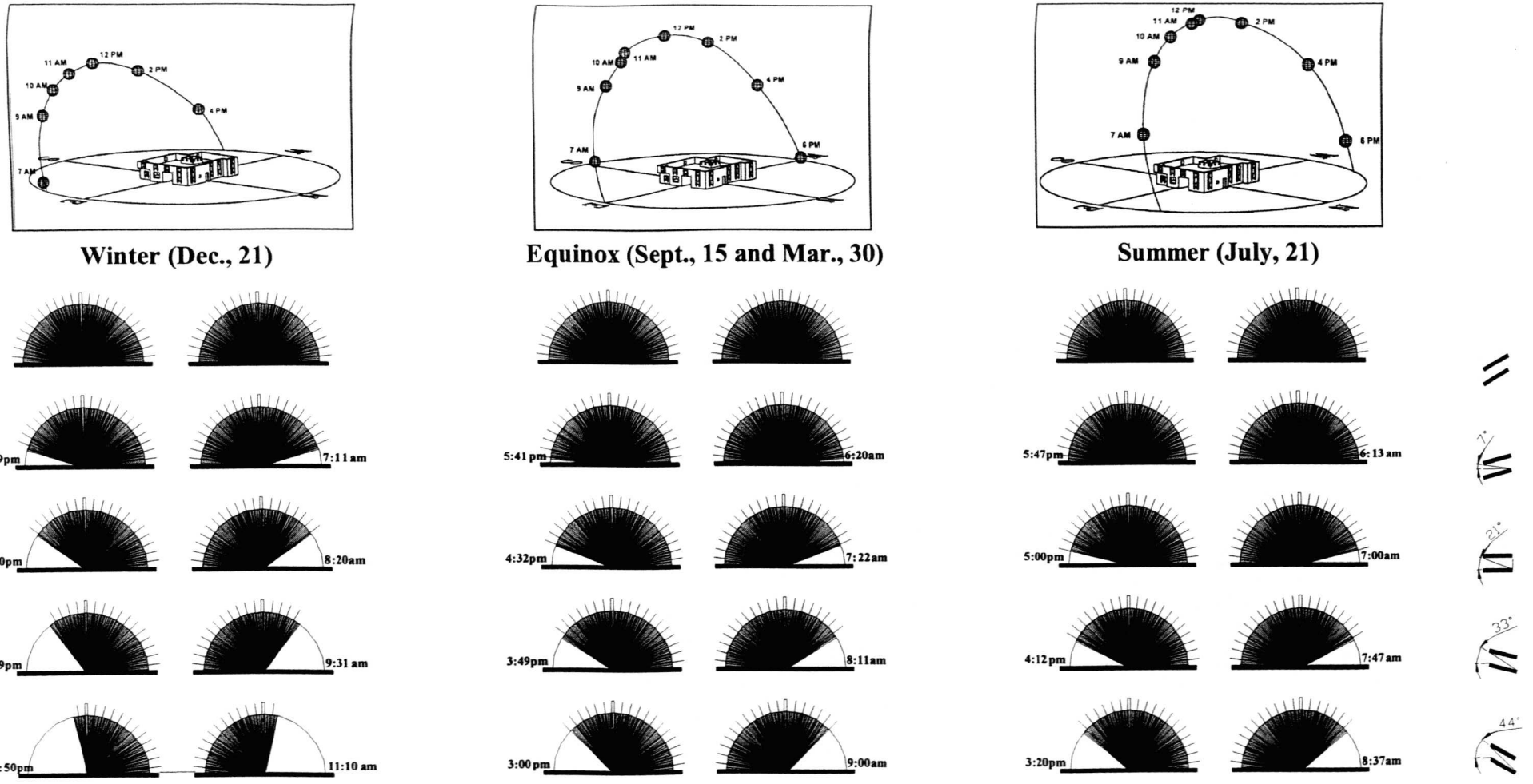

Figure (5.7): Sunshine hours for MLW configuration d=0.03m, L=0.08m.

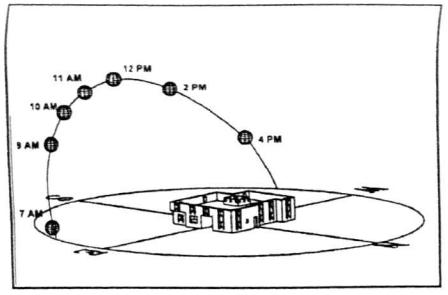

Winter (Dec., 21)

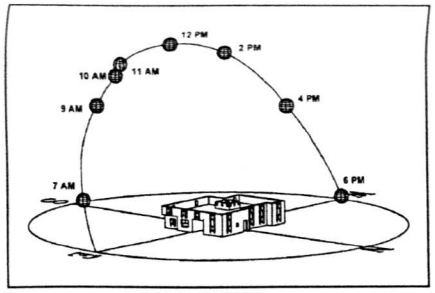

Equinox (Sept., 15 and Mar., 30)

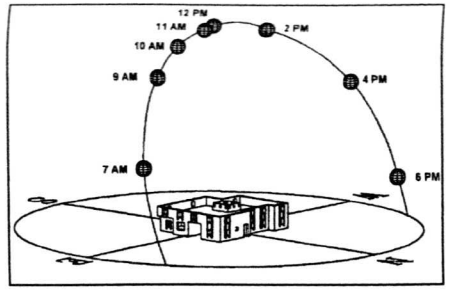

Summer (July, 21)

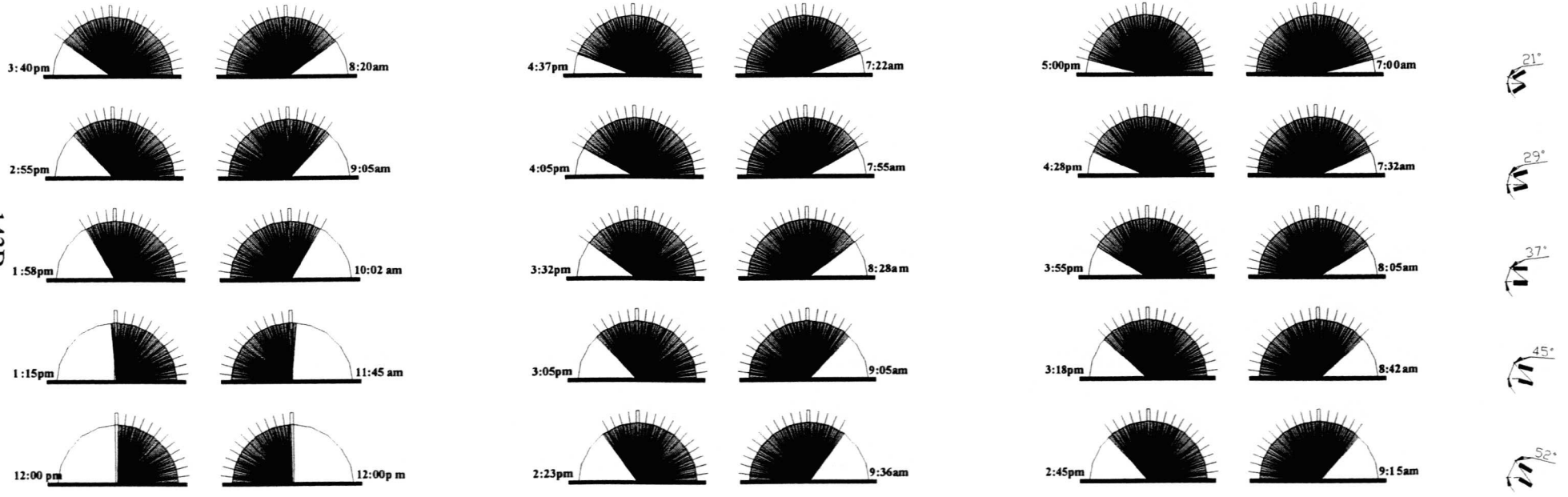

Figure (5.8): Sunshine hours for MLW configuration d=0.03m, L=0.04m.

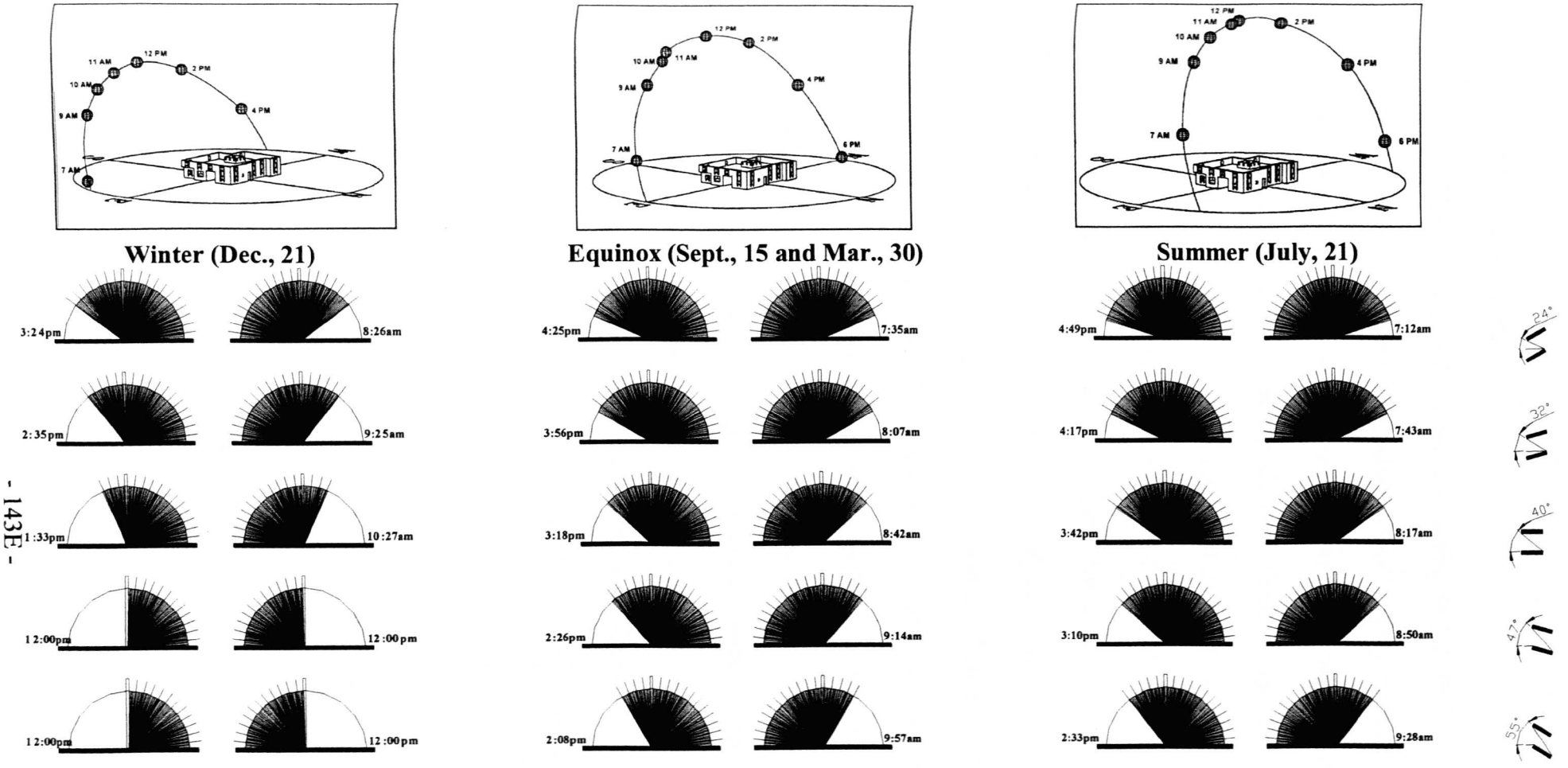

Figure (5.9): Sunshine hours for MLW configuration d=0.05m, L=0.06m.

5.4.2.1. Louver depth

The shading masks reflect the increasing potential of shading as a function to the louver depth. With the same model's geometry, the increase in depth is found appropriate to reduce the cutoff angle of the louvers which increase the masking periods. For instance, with louver depth L=0.08m, the effective shading started early morning in the summer (8:22am). This was extended to more than an hour with the presence of -30^{o}. However, this was corrected by the increase in louver depth as airflow may be directed downwards with the interior being under complete shade from early morning (around 8:30am). Similarly, in September, the shading mask started one hour earlier with L=0.03m rather than 0.07m for the same cutoff angle. In winter, when the noon solar altitude is 46^{o}, there is a big potential for over heating when the θ=-30^{o}. Both depths 0.08m and 0.06m hardly created any mask till noon since the respective cutoff angles 56" and 51" were more than the solar altitude. Meanwhile the increase in depth provided some release to the indoor environment since the cutoff angle was slightly under the sun's solar altitude; bearing in mind that in winter direct sun may be needed at day time to assist cooling the structure.

In general, it is the increase in louver depth that would assist controlling the penetration of direct solar light, which would contribute to the thermal environment indoors.

5.4.2.2. Louver aperture

The aperture also contributed to this effect since the cutoff angle was corrected according to the decrease of d. The comparison between similar MLW geometries with various apertures have shed light on the possibilities of overheating indoors. The decrease d from 0.07m to 0.05m would reduce the shading mask time from 30 minutes to more than one hour before and afternoon. While this may be acceptable during early morning, the

afternoon overheating may be increased where the sun due to the increase in cutoff angles accompanied by higher temperature (from 1:00pm till 4:00pm).

5.4.2.3. Inclination angle

The effect of louver inclination angle is clearer than the other variables. The attempt to examine the negative inclinations was to observe the possibility to determine the extent of these inclinations when altered to negative or positive angles. With louver being perfectly horizontal, the minimum summer shading period was between 8:30am and 3:30pm with the MLW with largest d and L dimensions. The shading period covers the most unwelcome sunlight that is around noon and afternoon periods. The time was even expanded with the alteration of even a small segment of louver inclination as shown in the Figures. The tilt of louver to –30 inclination is questionable since it limits the shading periods, which may cause the potential overheating indoors. In general, the other dimensions of the MLW are corrected with the presence of louver inclination even at the hottest periods of the year. Generally, to control the indoor environment, the cutoff angle should not exceed the solar altitude in the hot seasons and more specifically in the afternoons where higher temperatures are present.

The flexibility in controlling cutoff angles of the louvers is another advantage added to this window system which, on the other hand, exhibit the preference of this type of window accessories as they demonstrated a stronger potential to control the daylight in buildings.

5.5. Privacy and view

In the literature, a number of studies indicated the importance of louvers from privacy and view perspectives as the MLW design reveals some social requirements. Privacy is the main sociological factor that a Rowshan posses. This issue was thoroughly

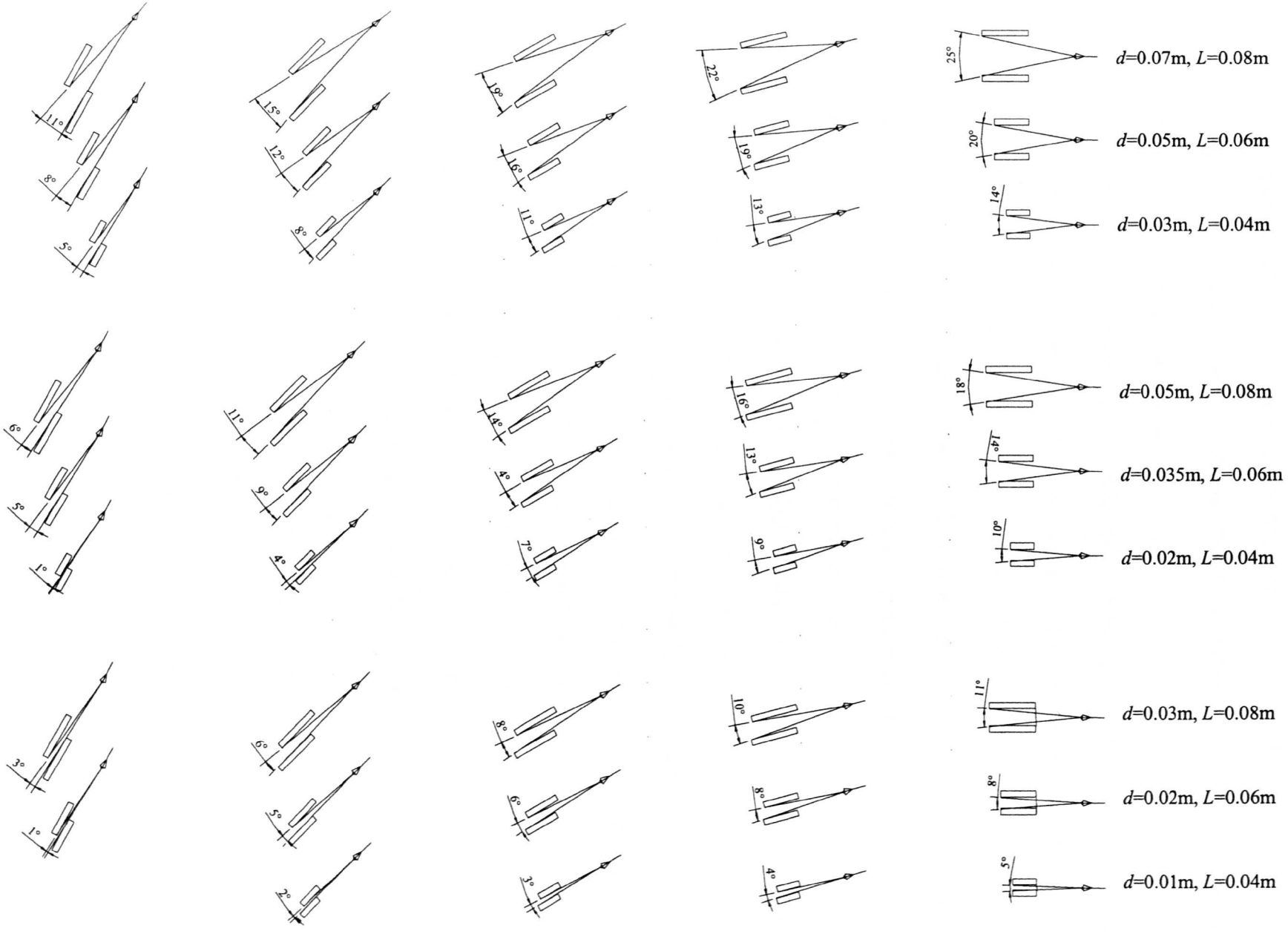

Figure (5.10): The view range across the louver blades.

investigated by other studies such as (Hariri, 1992), (Al-Lyaly, 1990), (Al-Said, 1996) (Banajah, 1995), (Khan, 1986), (Salloum, 1983) and others, and therefore will not be covered in the following discussion.

The view within the louvers blades of the Rowshan is important since at certain stage the Rowshan louvers geometry could cause conflict with the climatic requirements. The MLW setup allows different viewing angles to the outdoor environment. The reference viewpoint determines the angle of viewing. Here the point is about 0.08m away from inside louver blades. The simple diagrams that are demonstrated in Figures (5.10) gives a number of interpretations of the viewing characteristics through louver apertures.

The initial notion of the above figures demonstrates the effect of inclination of louver as a considerable factor which will diminish view angle. The view angle is diminished by almost 60% when louver is inclined to 45°. In practice this is of crucial importance since it may contradict with the solar shading requirements during noon periods in summer. Similarly, the louver aperture is also a measure to control the view through. The diminishing of louver apertures is accompanied with a reduction of view angle which ranges from 5-25% when θ=0°. The Figure also shows some effect of the louver depth where its increase is accompanied with some limitation of view angle based on the other MLW geometries.

In general, there is a significant contribution of the MLW various geometries to the view behaviour across them. Therefore, the design of MLW should give also some concern to these variables since at certain stage they may sufficiently obstruct the view through.

5.6. Reduction of volume as function of MLW parameters

The louvers' various variables including d, L and θ are factors that determine the flow patterns as well as the volume of the flow passing through a sash window. An attempt is made here to mathematically define these functions to the total reduction in volumetric flow.

Assuming a sash window with a complete open aperture and with a volume of:

$$V = S_h \cdot S_w \cdot S_l \qquad (5.1)$$

where

V = the sash volume (m^3)

S_h = the sash height (m)

S_w = the sash width (m)

S_l = the sash length (m)

when this window is facilitated with louver sheets and the total volume of louvers is:

$$V_L = S_w \cdot T \cdot L \qquad (5.2)$$

where

V_L = volume of louvers (m^3)

T = the summation of louver thickness $\sum_{n}^{1} t$. (m)

L = the louver depth (m)

then the new volume as a function of louvers' volume is expressed as follows

$$V_{new} = D \cdot S_l \cdot S_w \qquad (5.3)$$

where

D = the summation apertures between louvers $\sum_{n}^{1} d$.

$$V_{new} = V - V_L \qquad (5.4)$$

where

V_{new} = volume reduction due to louvers (m^3)

For a number of louvers (n) of V_L, the above equation is written as follows:

$$V_{new} = V - \sum_{n}^{1} V_L \qquad (5.5)$$

Substituting both equations, (5.1) and (5.2):

$$V_{new} = S_h \cdot S_w \cdot S_l - S_w \cdot T \cdot L \qquad (5.6)$$

This is when the louver at inclination $\theta = 0^o$; $L = S_l$ and L is:

$$L = \frac{S_h - T}{V_{new} \cdot S_w} \qquad (5.7)$$

Representing V_{new} in equation 5.3:

$$L = \frac{S_h - \sum_{n}^{1} t}{(\sum_{n}^{1} d \cdot L \cdot S_w{}^2)} \qquad (5.8)$$

$$L^2 = \frac{S_h - \sum_{n}^{1} t}{(\sum_{n}^{1} d \cdot S_w{}^2)} \qquad (5.9)$$

$$L = \sqrt{\frac{S_h - \sum_{n}^{1} t}{(\sum_{n}^{1} d \cdot S_w{}^2)}} \qquad (5.10)$$

$$\sum_{n}^{1} d = \frac{S_h - \sum_{n}^{1} t}{L^2 \cdot S_w{}^2} \qquad (5.11)$$

With the presence of louver inclination angle θ:

$$L_\theta = L \cdot \cos\theta \qquad (5.12)$$

$$\sum_{n}^{1} d_\theta = \sum_{n}^{1} d \cdot \cos\theta \qquad (5.13)$$

Substituting L_θ due to inclination angle θ:

$$L_\theta = \sqrt{\frac{\left(S_h - \sum_n^1 t\right) \cdot \cos\theta^2}{\left(\frac{\sum_n^1 d_\theta}{\cos\theta}\right) \cdot S_w^{\,2}}} \qquad (5.14)$$

$$L_\theta = \sqrt{\frac{\left(S_h - \sum_n^1 t\right) \cdot \cos\theta^3}{\sum_n^1 d_\theta \cdot S_w^{\,2}}} \qquad (5.15)$$

and

$$\sum_n^1 d_\theta = \sqrt{\frac{\left(S_h - \sum_n^1 t\right) \cdot \cos\theta^3}{S_w^{\,2} \cdot L_\theta^{\,2}}} \qquad (5.16)$$

Showing that d, L and θ are all functions to the total reduction in the volumetric dimension of an aperture.

5.7. Experimental setup

The elaboration of various appraisal stages involved regarding the experimental setup, calibration, measuring technique and the various equipments used are highlighted in each chapter, respectively.

5.8. Conclusion

The purpose of this chapter was to select the various parameters governing the MLW as well as the Rowshan for further evaluation. The various variables of the MLW and the Rowshan, including the inlet outlet types, are setup and will be recalled in various appraisal stages involved in this thesis. The assessment carried out in this chapter shed

light on the potentials of the reviewed MLW to control other factors that share a its function considerably. The control of sunshine hours in various seasons is easily done by the simple configurations of the MLW. Both louver depth and angle of inclination showed some level of significance to controlling shading masks indoors, and hence to managing indoor overheating during summer times. In the meantime, the aperture was less important in this respect.

With reference to view consideration, the assessment indicted the importance of various MLW parameters in affecting the view through louvers that may contradict, at certain stage, the other functions of the MLW.

These configurations of MLW and Rowshan will be recalled in the following chapters to carry out the various appraisal stages of this research.

5.9. References

1. Kahtani, A.M. (1996) Al-Khasab: The wood. SED-309/1415, King Abdulaziz University: School of Environmental Design.

2. Al-Lyaly, S.M. (1990) The traditional house of Jeddah: A study of the interaction between climate, form, and living patterns. University of Edinburgh. Unpublished Ph.D thesis.

3. Al-Said, M. (1996) The Rowshan in the western province. SED-308/1416, King Abdulaziz University: School of Environmental Design.

4. Al Shareef, F.M. (1996) Natural light control in Hedjazi Architecture; An investigation of the Rowshan performance by computer simulation. University of Liverpool. Unpublished Ph.D. thesis.

5. Attieh, A.M.A. (1990) Review and analysis of housing in Jeddah, Saudi Arabia. Dundee. Unpublished Ph.D. thesis.

6. Banajah, A. (1995) The Rowshan; Al-Mashrabiah. SED-309/1415, King Abdulaziz University: School of Environmental Design.

7. Bittencourt, L.S. (1993) Ventilation as a cooling resource for warm -humid climates: An investigation on perforated block wall geometry to improve ventilation inside low-rise buildings. Architectural Association Graduate School. Unpublished Ph.D. thesis.

8. Greenlaw, J. (1976) *The Coral Buildings of Suakin*, London: Oriel Press.

9. Hajj Research Centre (1994) *Samples of Makkan traditional houses*, Makkah: Hajj Research Centre, Umm Al-Qura University.

10. Hariri, M. (1992) " The design of the Rowshan and its importance to the dwelling". *Journal of Umm Al-Qura University* **(3rd year)-5,** p.175-237.

11. Khan, S. (1986) *Jeddah Old Houses*, Saudi Arabia: King Abdulaziz City for Science ad Technology.

12. Koenigsberger, O., Ingresoll, T., Mayhew, A. and Szokolay, S. (1977) *Manual of Tropical Housing. Part One: Climatic Design*, London: Longman Group Ltd.

13. Maghrabi, A. (1995). Personal communication with local craftsman.

14. Mani', M. (1980) The Architectural features to old Jeddah. pp.100-108. Jeddah: Al-Salam Publications.

15. Muniz, P.A. (1985) The geometry of external shading devices as related to natural ventilation, daylighting and thermal comfort, with particular reference to tropical hot-humid climates. Unpublished Ph.D. Thesis.

16. Olgyay, V. (1963) *Design with Climate*, Princeton N.J.: Princeton University Press.

17. Salloum, A. (1983) " El-Rowashin of Jeddah, Saudi Arabia". Crete, Greece: Passive and Low Energy Architecture, p.245-252.

18. Zahran, W. (1995) Al-Khasab: The wood. SED-309/1415, King Abdulaziz University: School of Environmental Design.

CHAPTER 6: PRESSURE DROP ACROSS THE MODULATED LOUVERED WINDOWS

6.1. Introduction

The first appraisal stage of this study is concerned with the pressure drop characteristics across the modulated louver windows and is discussed in this chapter. It is devoted to exploring the drop as function of the MLW various parameters reviewed in the previous chapter.

The first section sheds light on the experimental setup as well as the various instrumentation and equipment employed. The procedure followed to allocate and calibrate the equipment in addition to the measuring principles is discussed in the second section. The analysis of the observed data based on the two model equations in the form of power law and the quadratic is discussed later. At this stage, the work covers the analysis of the mathematical representations of the coefficients embedded in the equation in the quadratic form. This section also covers the mathematical representations of other variables involved in this study that are not integrated in the basic quadratic model equation.

The results discussion of this chapter is divided into three subsections including individual-variable appraisal, overall-variables appraisal and the *critical inclination* appraisal where major airflow reduction was present. Based on *critical inclination*, a statistical model is developed which represents pressure drop across the MLW as function of the other variables concerned.

6.2. Experimental Setup.

This appraisal stage of the pressure drop across the reviewed MLW was carried out at the ventilation laboratory, School of Architecture, University of Sheffield. Various tools and equipment were prepared in the laboratory prior to the experiment. The experimental setup as well as the equipment and instrumentation used are discussed in details in the following subsections.

6.2.1. The depressurising test chamber:

A test chamber was constructed to represent the environment where internal pressure would be recorded. The construction setup of the test chamber was specified in accordance with the British Standards Institution (BSI) (1998) code-prEN1314-1 concerning performance testing of components. Figures 6.1 and 6.2 show the depressurising chamber with a fixed size-mounting device opening at front. The chamber was designed with a maximum flexibility to fix any sash unit with a variety of depths. Sash models were fitted later on the opening with the four screws on borders and tilted to the desirable angle through a small door on the side elevation of the box. At the top, three small holes were equidistantly placed where internal pressure tappings were placed. The depressurising duct flow was facilitated on the opposite wall at distance of 2m away from the inlet. The distance was essential to allow uniform pressure distribution inside the chamber and to avoid the likely reading errors near duct flow where pressure reading may not reflect the actual pressure (Etheridge and Sandberg, 1996). The duct flow was equipped with a laminar volume-flow meter device, and the volume-flow air (Q) was recorded and connected to four extraction fans in series. As stated previously, similar setup was found in some recent literature such as Baker et al. (1987), Yakubu and Sharples

(1991) and Maghrabi and Sharples (1999) as well as in one famous ventilation fundamentals book, *Buildings Ventilation; Theory and Measurements* by Etheridge and Sandberg (1996).

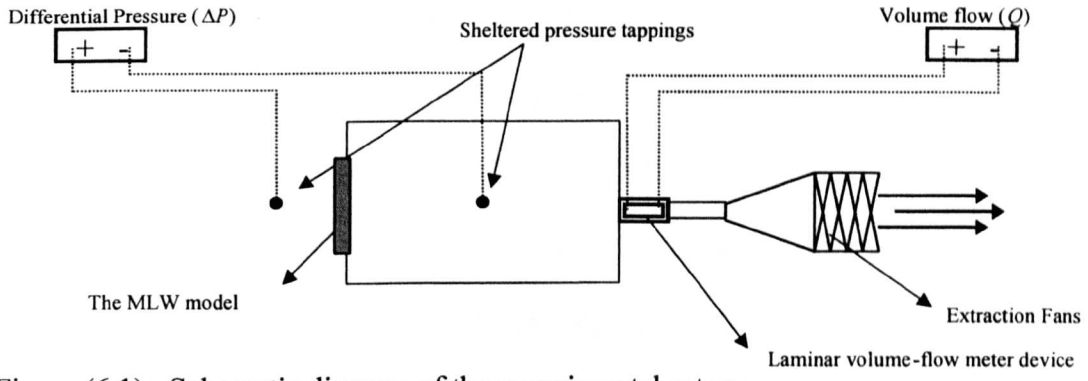

Figure (6.1): Schematic diagram of the experimental set-up

6.2.2. Micro-manometer

The two micro-manometer devices used in the experiment were manufactured by *Furness Controls Limited*, Bexhill, England. The first device *(FCO12)* was connected to the laminar volume flow-meter device to record the quantity of airflow passing through the sash unit. Through two tubes connected to the metal holes in front panel, this device records the quantity of airflow (Q) at the rate of four readings per second. Similar to that, the other device *(FCO510)* was used to record the differential pressure of inner and outer volumes of the box. Both models with ranges of 0-19.9 Pa operated with self-calibrating devices to ensure compensation for zero-drift, making them accurate enough to measure small pressure differences. The manufacturer quoted an accuracy of less $\pm$1% error for the

devices. Data from both devices were transferred to the computer through the data-logger connected.

6.2.3. The laminar volume flow-meter device

This device was used to record the quantity of airflow through the reviewed MLW (Figure 6.2). It is designed for smaller Reynolds number to preserve the laminar flow of the fluid; *Re* is less than 2000. The device is based on the linear-law correlations between Q and ΔP as in laminar flow (Awbi, 1991). While the flow is passing through the parallel flat plates, it considers the flow rate in relation to the pressure drop taken from upstream and downstream of the meter by linear relationship calibration stated by the manufacturer.

6.2.4. Fans

Four fans used for depressurisation were connected in series at the other end. The diameter of each fan was 0.48m (19 inches) and contained blades of 14° pitch capable of 1440 r.p.m. and performed under fluid temperatures of up to 40° C. Each fan was made to control the speed alteration separately from other fans. *Woods of Colchester Limited* manufactured the fans.

6.2.5. Pressure tappings

Internal and external pressure tappings were positioned away from the influence of flow through the opening. In the measurement, there was no need to make a second upstream chamber of the component such as that found in Baker et al (1987) since the laboratory pressure fluctuations, when measured, were found negligible. Shield pressure tappings were enough to measure pressure both outside and inside the test chamber.

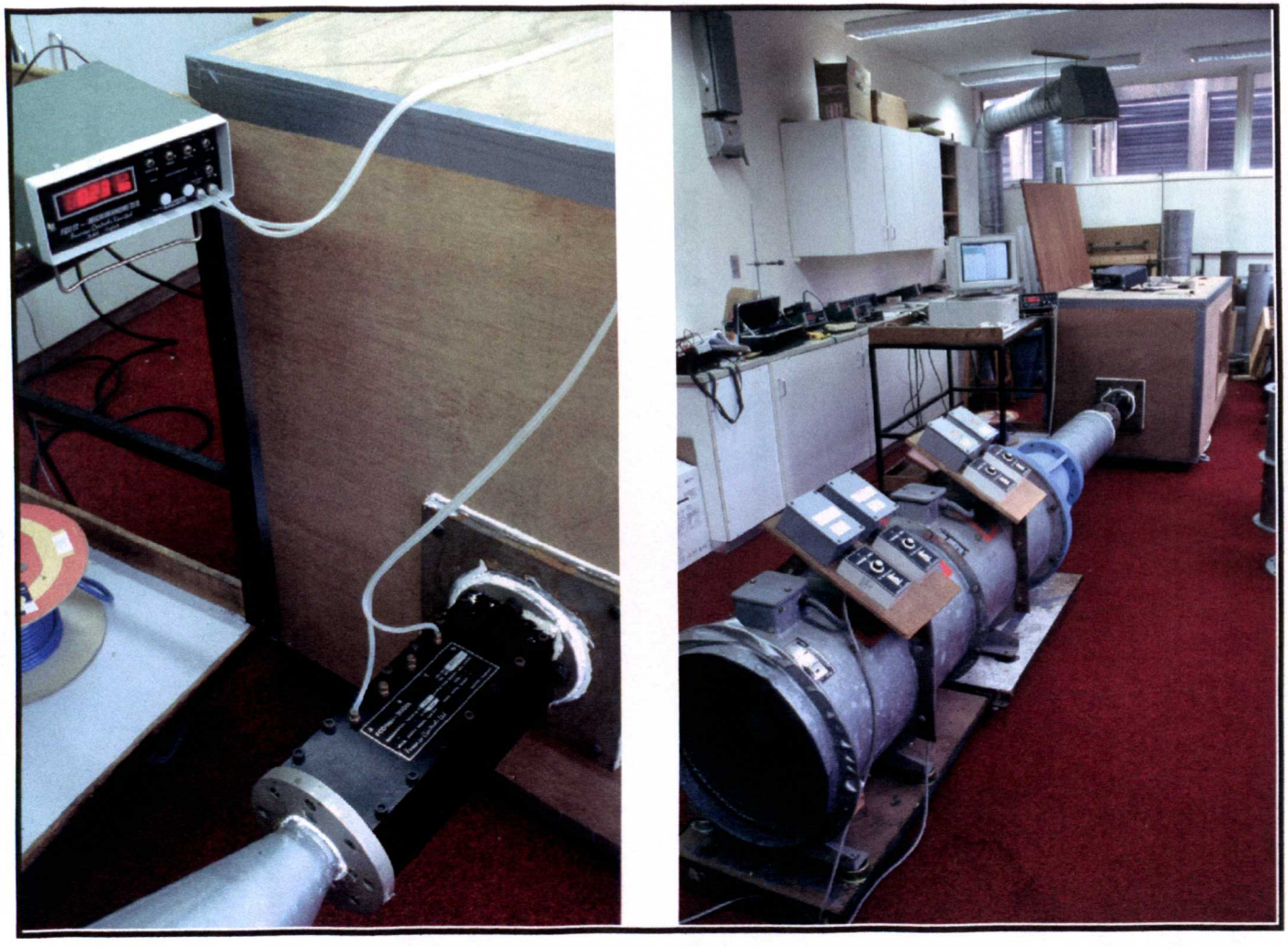

Figure (6.2): The laboratory setup with the various equipments used in the study.

6.2.6. Data-logger machine

This interface was made by *Computer Instrumentation Ltd*, England and was attached to a computer through a parallel port. Out of a series of ranges manufactured, the interface used was ***mini-POD 100***– *8 Channel high speed A-D converter* that is capable of taking up to 4 channel differential inputs or 8 single-ended channels. The ***mini-POD 100*** is supplied with soft-logger and soft-scope software for DOS & Windows, together with the Virtual Multi-meter. The data from both micro-manometers were transferred to data-logger into *millivolts (mV)* signals via wires connecting both devices.

6.2.7. Computer

The data was transferred to a computer through the Data-logger, the software that converts the data received to a CSV format for loading into a spreadsheet for further analysis.

6.3. Calibration and measuring techniques

Prior to the analysis, it was essential to start with a number of routine measurements and calibrations. These included the calibrations of various instrumentations, data conversion, selecting the appropriate location of pressure tappings, etc.

6.3.1. Air leakage through pressurisation chamber

The chamber edges were sealed with rubber silicon and tape along both its internal and external edges. Seals were also made for the three holes on top. In addition, the sash unit was firmly sealed after being fitted on the front panel of the chamber with rubber and

tape around the edges. All these precautions were made to minimise any possible infiltration that may result from air extraction. Initial measurements were carried with the box being totally sealed, including the opening in the front panel, and resulted in ΔP at extremely low flow rates, i.e Q_i=0.0038. The flow rate due to infiltration (Q_i) was measured according to testing installation conditions and uncertainty characteristics noted by BSI code-prEN 1314-1 (1998). The actual flow rate passing through the louver was then adjusted using the following equation:

$$Q = Q_t - Q_i \qquad (6.1)$$

where

Q = the actual flow rate passing through the MLW (m^3/s)

Q_t = the total flow rate (m^3/s)

Q_i = the flow rate due to infiltration (m^3/s).

6.3.2. Positioning of pressure tappings

The pressurisation chamber was designed with the flexibility to allocate the pressure tappings in many locations and, thus, achieve most accurate results. The fact that the location of the pressure tappings might influence the data reading to be analysed further (Etheridge and Sandberg, 1996) was taken into consideration. For this purpose, pressure readings were taken under two airflow rates for six different locations in the pressurisation chamber. They found that positioning pressure tappings at the centre would be the most appropriate.

6.3.3. Data-logger result conversion

The micro-manometer transferred the data to the data-logger via connecting wires. The software then received the data in its raw format, i.e. mV, and represented them into series of tables for loading into spreadsheet software. Later, this data was calibrated from mV signals into ΔP and volume-airflow Q. Series of airflow records run first and then micro-manometer transferred the data to the computer. The calibrations were made for both pressure limits of pressure bands, high and low as shown in Appendix (B.1). The results were in linear regression of raw data mV into pressure readings from the micro-manometers expressed in the following equation:

$$\Delta P = a \cdot mV + b \qquad (6.2)$$

where

a = the slope constant determined by the linear regression (Appendix B.1).

b = the intercept constant determined by the linear regression (Appendix B.1).

6.3.4. Timing of pressure

Adjusting proper timing for each average reading is an essential technique which has been taken into consideration prior to the evaluation stage. In the case of ventilation, the researcher needs to give positive timing for the flow to reach its steady state where pressure fluctuations are minimised. Too short a timing of an average reading might be less effective and does not represent the actual alteration in the pressure drop where long timing might be redundant and is time consuming. The micro-manometers and software were adjusted to give the average reading of various timings, 1, 2, 3 minutes at four

readings per second, under series of air extractions. The 2 minutes average readings were found to be the appropriate timing to carry out the rest of the analysis.

6.3.5. Pressure difference at zero airflow

For accuracy, the author aimed to examine the pressure variations due to volume variations between outside and inside of the pressurisation chamber. So the micro-manometers recorded ΔP at Q = 0m^3/s. Records were taken with respect to three time periods: 20 minutes, 1 hour and 2 hours and the ΔP were almost the same; ΔP=0.019 Pa. Though this drop was not significant it was taken into consideration in this study.

6.3.6. The work of Yakubu

The initial setup and measuring technique was similar to the work found in Yakubu and Sharples (1991). The rest of the experiment was carried out after ensuring comparable results were found in the relevant study.

6.3.7. Measuring principle

Controlling the circuit of fan systems would result in air flowing into the chamber through louvers on the other edge. As these are already pre-set at particular angles this causes differential pressure across the modulated louver window. The previous and the volume-airflow readings were both transferred when the reading had stabilised. The pervious step is repeated over a range of pressure drops obtained from the combined power of the 4 axial fans. It was ensured that the laboratory temperature was about 20°C (White, 1999), the temperature that was programmed for both micro-manometers. The procedure of the test measurement can be summarised in the following steps:

i. Various equipment to be used in the measurement were first switched on.

ii. The micro-manometers were set to zero and left some time to stabilise.

iii. A MLW unit was fitted onto the chamber and sealed. Further, an adjustment to tilt louvers to the desired angle took place. The inclination was flexibly adjusted through a vertical wood panel connecting all louver blades within the sash unit.

iv. After ensuring that only air entering the pressure chamber was flowing through the sash, adding to the room infiltration, the fan was switched on and controlled to the desired setting.

v. The data of both pressure drop and the volume-flow were taken after ensuring stability of volume flow. As stated previously, one reading is a representation of averaged two-minute records at 4 readings per second.

vi. Fan speed was set to various extraction rates to create ranges of differential pressures. Step (v) was repeated before any further readings were taken.

vii. Fans were later switched off and the louvers adjusted to the next desired angle. Step (iv) and (v) were then repeated for each setting.

viii. Nine various settings of angles, ranging from 60^{o} to -60^{o} at intervals of 15^{o}, were observed before installing other MLW unit.

ix. The software was programmed to record only the required data to be loaded later into a spreadsheet package.

6.4. Power law and Quadratic Model equations

The validity of the power law and quadratic equations has been reviewed in the previous chapter (section 4.2.4.3). Both calculation methods have been broadly accepted

and the debate about which of the two is more suitable still goes on. The results were analysed using both model equations in order to find the more appropriate model. The power law function is expressed as:

$$\Delta P = a \cdot Q^n \qquad (6.3)$$

And the quadratic model equation is expressed as:

$$\Delta P = AQ + BQ^2 \qquad (6.4)$$

For ventilation research, some correlation is needed to identify the flow rates as a function in relation to pressure difference due to wind, stack effect, .etc, which is expressed as follows (ASTM Standard E779, 1982):

$$Q = \frac{-A \pm \sqrt{A^2 + 4B\Delta P}}{2B} \qquad (6.5)$$

The values of A and B in the quadratic form could be directly measured as they refer to gap thickness between louvers (d) and the breadth of louver (L) in equations (4.6) and (4.7). However, the louver inclination θ and the ratio of d/L were not considered in the model equation. The following subsections are attempts to represent these effects in mathematical forms.

6.4.1. Pressure drop as a function to inclination angle (θ)

For modulated louvers, pressure difference could be a function to vertical inclination angles of louver assuming that two louver blades are placed at a distance d with a breadth of a blade L at initial inclination position 0°, when the two blades are perfectly

horizontal as shown in Figure (5.1). When louvers at initial setup were tilted positively or negatively to angle, say θ, this would be accompanied with a decrease in the effective gap thickness between louvers d_θ and the breadth of louver L_θ, bearing in mind that the following formulations could only be true if friction along dimension z was considered constant for all louvers' vertical inclination angles (Yakubu, 1990). The following is the interplay of the (d_θ) and (L_θ) at vertical angle θ:

$$d_\theta = d\cos\theta \qquad (6.6)$$

$$L_\theta = L\cos\theta \qquad (6.7)$$

hence, the total pressure drop for the vertical angle θ derived from Eq.(6.4):

$$\Delta P = \left(\frac{12\mu z}{L_\theta d_\theta^{\,3}}\right)Q + \left(\frac{\rho Y}{2d_\theta^{\,2}L_\theta^{\,2}}\right)Q^2 \qquad (6.8)$$

or

$$\Delta P = A_\theta Q + B_\theta Q^2 \qquad (6.9)$$

$\therefore$ the values of A_θ and B_θ

$$A_\theta = \frac{12\mu z}{L_\theta d_\theta^{\,3}} \qquad (6.10)$$

$$B_\theta = \frac{\rho Y}{2d_\theta^{\,2}L_\theta^{\,2}} \qquad (6.11)$$

Substituting the values of both d_θ (Eq 6.6) and L_θ (Eq 6.7) in the latter equations, one obtains:

$$A_\theta = \frac{12\mu z}{L\cos\theta d^3\cos\theta^4} \qquad (6.12)$$

$$= \frac{12\mu z}{Ld^3}\cdot\frac{1}{\cos\theta^4} \qquad (6.13)$$

$$B_\theta = \frac{\rho Y}{2d^2\cos\theta^2 L^2\cos\theta^2} \qquad (6.14)$$

$$= \frac{\rho Y}{2L^2d^2}\cdot\frac{1}{\cos\theta^4} \qquad (6.15)$$

By replacing both coefficients A and B for the blades when they are perfectly horizontal in latter equations (6.13) and (6.15), one gets:

$$A_\theta = A\cdot\frac{1}{\cos\theta^4} \qquad (6.16)$$

$$B_\theta = B\cdot\frac{1}{\cos\theta^4} \qquad (6.17)$$

$\therefore \Delta P_\theta$ is given as:

$$\Delta P_\theta = A\cdot\frac{1}{\cos\theta^4}Q + B\cdot\frac{1}{\cos\theta^4}Q^2 \qquad (6.18)$$

$$= \left(AQ + BQ^2\right)\cdot\frac{1}{\cos\theta^4} \qquad (6.19)$$

It is evident from the pressure difference for the parallel plate theory, and when angle $\theta = 0^{o}$ that $\Delta P = AQ + BQ^2$. Then ΔP_{θ} would be represented as follow:

$$\Delta P_{\theta} = \Delta P \cdot \frac{1}{\cos\theta^4} \qquad (6.20)$$

From the above equations it was apparent that a vertical angle θ would be a parameter to measure pressure drop function across the modulated louvers systems, in addition to other constants embodied in coefficients A and B.

6.4.2. Pressure drop as a function ratio (*d/L*)

The ratio of the gap thickness between louvers over the breadth of louver (d/L) is also another parameter considered in determining the function of measured pressure drop at any angle θ. In this study, this ratio was strictly divided into three categories from which all model configurations were selected. To simplify, these categories were represented in numerical numbers as (d/L= 0.5), (d/L = 0.75) and (d/L= 1), respectively (Figure 5.1).

So, from Eq. (6.19) it is apparent that pressure difference at any angle θ was represented as follows:

$$\Delta P_{\theta} = \frac{12\mu z}{Ld^3} \cdot \frac{1}{\cos\theta^4} Q + \frac{\rho Y}{2d^2L^2} \cdot \frac{1}{\cos\theta^4} Q^2 \qquad (6.21)$$

$$= \left(\frac{12\mu z}{Ld^3} Q + \frac{\rho Y}{2d^2L^2} Q^2 \right) \frac{1}{\cos\theta^4} \qquad (6.22)$$

Adding to the above equation a function of (Ld^3):

$$Ld^3\Delta P_\theta = \left(\frac{12\mu z}{Ld^3}\cdot Ld^3\cdot Q + \frac{\rho Y}{2d^2L^2}\cdot Ld^3\cdot Q^2\right)\frac{1}{\cos\theta^4} \qquad (6.23)$$

$$\Delta P_\theta = \left(12\mu z\cdot Q + \frac{\rho Y}{2}\cdot\frac{d}{L}\cdot Q^2\right)\frac{1}{Ld^3\cos\theta^4} \qquad (6.24)$$

$$= \Delta P\cdot\frac{1}{Ld^3\cos\theta^4} \qquad (6.25)$$

showing that the pressure drop is also a function to ratio of gap thickness between louvers over the breadth of louver (*d/L*). Although this would be theoretically consistent, it could only be true if the friction along the dimension *z* in the direction of flow was considered constant from all ratios *d/L*.

6.4.3. The comparison between both model equations

By examining the coefficient of determinations (r^2) of both model equations, it was evident that curves produced by quadratic equation were preferred particularly in models where the ratio $d/L > 0.5$. The coefficient of determination of these ratios was 0.989. The smoother curves produced by quadratic formulation fitted the scattered data at both pressure limits (i.e. higher and lower ΔP) as illustrated in Figure (6.3). On the other hand, power law curves were gradually accepted as louvers were tilted to steeper angles (θ = $\pm$60) and caused an increased pressure drop due to pressurisation with r^2 that ranged from 0.337 at $\theta = 0^\circ$ to 0.981 at $\theta = 60^\circ$ as seen from Table (6.1). This showed that power law curve fit was gradually improving from 0° to the maximum measured angle. Appendix (B.2) demonstrates the coefficient of determinations (r^2) with the standard errors of all MLW examined with both model equations. Similar conclusions of this were found in Baker et al (Baker et al. 1987), Yakubu & Sharples (Yakubu and Sharples, 1991) and (Pitts and

Georgiadis, 1994) as well as in another recent study that investigated the validity of the power law function over a range of pressure drops experienced by a naturally ventilated house using the pressurisation method (Walker et al. 1998).

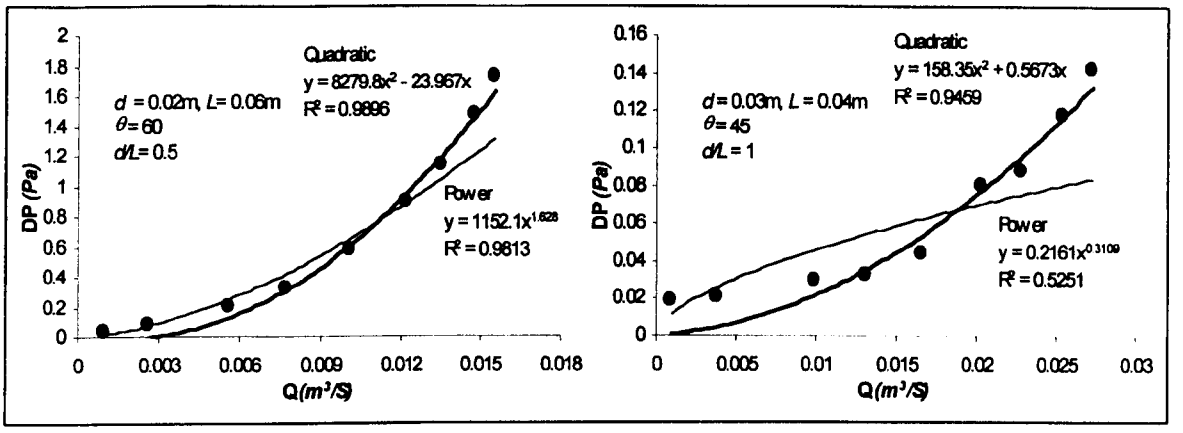

Figure (6.3): Regression curves produced by quadratic and power law model equations at both higher and lower pressure records.

Further, the representations of both coefficients evolved from the quadratic equations A (Eq. 4.6) and B (Eq. 4.7) were measured directly and calculated, based on the various parameters. It was found that the predicted values of A and B had undergone more variation than those obtained statistically. As a result, the value of ΔP presented in equation (6.4) could not be predicted. This was referred to a number of possible explanations. The first was related to physical complexities of flow characteristics passing through MLW various components. As mentioned earlier, these complexities could not be simplified theoretically. The second factor seemed more likely to relate to aperture of MLW. In 80% of models investigated, the aperture dimensions d were big enough for air to flow with not much resistance causing similar pressure drops for various d and L dimensions that are embedded in both coefficients. Similarly, the value of volume-flow of air as in equation (6.5) could not be simplified theoretically. This is merely due to the fact that the original format of equation was based on single crack theory. Thus it is assumed

that for models with series of parallel cracks, the parallel plate theory would apply (Baker et al. 1987). Here, the total flow as the sum of number of cracks evolved could not be justified due to interference to flow caused by parallel cracks. This interference would differ from that resulting from single cracks. Another possible explanation was concerned with the inclination angle. The latter equation had no relation to the inclination angle of plate. These explanations, added to others embedded in the coefficients A and B could be the possible answer for discrepancies found in theoretical representation of Q and ΔP. Such correction is beyond the scope of this investigation; so further adjustments of the quadratic model equation would be required to fit variables that might not be embedded in both Q and the coefficients A and B equation formats. Appendices (B.3 and B.4) show the measured values of a number of MLW units against the predicted values based on Eq (6.5).

6.5. The Discussion

At this stage, various variables have been taken into consideration to trace the more effective variable of pressure drop across the louvers. These variables– as mentioned earlier- included louver depth (L), inclination angle (θ), gap between louver blades (d), number of louvers (N), free area (A_f) as well as the ratio d/L. Each variable is analysed individually in relation to the statistical analysis and regression curves of each. The comparison would either be performed through analysing variations between individual models, set of models having common variables, or the general characteristics of the variable on the whole model configurations. These are highlighted in the three following subsections.

Table (6.1): The comparison of Power law and Quadratic equations for a number of MLW.

L	d	θ	Power law equation			Quadratic equation		
			a	n	r^2	A	B	r^2
0.06	0.02	60	7.4488	0.9287	0.9668	6.6358	208.85	0.999
		45	0.0701	0.4328	0.743	-0.0655	32.448	0.9942
		30	0.0239	0.3141	0.6186	0.0518	12.127	0.9901
		15	0.0128	0.2316	0.7052	0.0489	5.8264	0.956
		0	0.0102	0.2138	0.5314	0.0007	7.0921	0.9525
		-15	0.0146	0.2537	0.6386	0.0793	6.0908	0.9902
		-30	0.0248	0.316	0.6656	0.039	12.653	0.9971
		-45	0.0661	0.4358	0.6729	-0.1397	35.352	0.9964
		-60	6.0367	0.91	0.9546	3.2485	304	0.9996
	0.035	60	0.2393	0.5867	0.7293	-0.1319	72.683	0.9992
		45	0.0266	0.3239	0.6409	-0.0958	19.269	0.9882
		30	0.0266	0.3239	0.6409	-0.0931	11.005	0.9764
		15	0.0061	0.1463	0.3668	-0.1076	8.4601	0.9399
		0	0.006	0.1419	0.4298	-0.0521	5.9442	0.8738
		-15	0.008	0.1828	0.548	0.0208	4.6132	0.9522
		-30	0.0101	0.2212	0.4487	-0.0483	9.3553	0.9772
		-45	0.0404	0.3703	0.6602	-0.1809	28.482	0.992
		-60	0.1726	0.5524	0.6936	0.1519	49.023	0.9954
	0.05	60	0.1375	0.5163	0.7295	-0.0479	49.968	0.9968
		45	0.0182	0.2877	0.5285	-0.0556	14.435	0.9802
		30	0.0071	0.1763	0.3608	-0.1105	9.8711	0.967
		15	0.0041	0.1036	0.2758	-0.0288	3.8285	0.7693
		0	0.0029	0.0647	0.1351	-0.114	6.1587	0.9114
		-15	0.0063	0.1555	0.475	-0.0109	4.7459	0.9091
		-30	0.0082	0.182	0.5909	0.0537	3.2516	0.9398
		-45	0.0239	0.3176	0.586	-0.0767	17.749	0.9858
		-60	0.1726	0.5524	0.6936	0.1519	49.023	0.9954

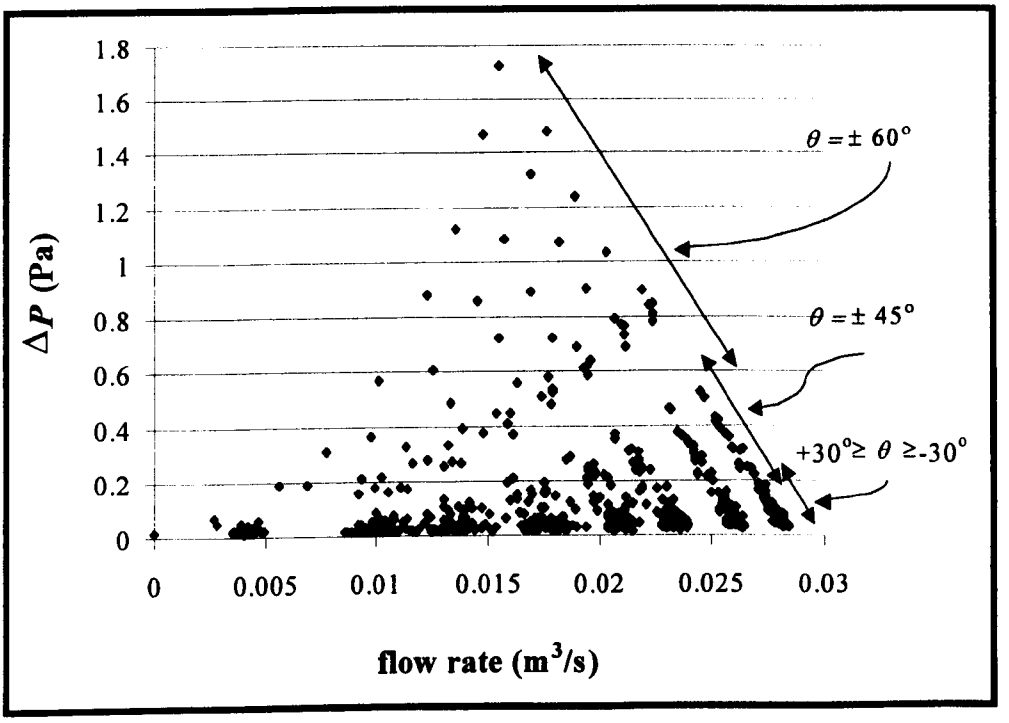

Figure (6.4): ΔP data as a function of inclination angles of MLW.

6.5.1. The individual variables

The resultant ΔP as function of louvers inclination angles (θ) was generally not significant between $-30^{\circ} \geq \theta \geq +30^{\circ}$, while a little increase was found at inclination angles -

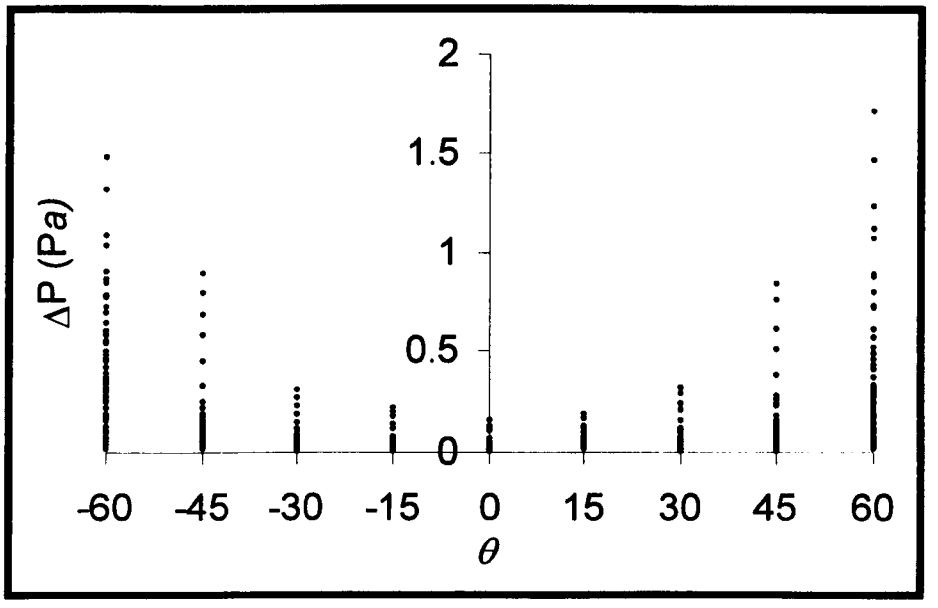

Figure (6.5): The pressure drop as function to the positive and negative inclinations.

$45^{\circ} \geq \theta \geq +45^{\circ}$. Figure (6.4) shows the various inclinations and their contribution to the overall ΔP across the MLW. The curves produced by inclination $\theta = \pm 45^{\circ}$ and those below, i.e. $+30^{\circ} \geq \theta \geq -30^{\circ}$, yielded towards lower pressure drops even at the highest volume-flow rate measured ($Q \cong 0.03\ m^3/s$). This gap was more distinguishable at inclination angle $\theta = \pm 60^{\circ}$, showing that inclinations at the last pre-set were therefore the main parameters to cause significant pressure drop as function of θ.

As far as the θ direction was concerned, variations found between positive and negative inclination angles were diminished and negligible (Figure 6.5). The reduction in pressure seemed to have had direct linear relation to angles when higher inclination angles

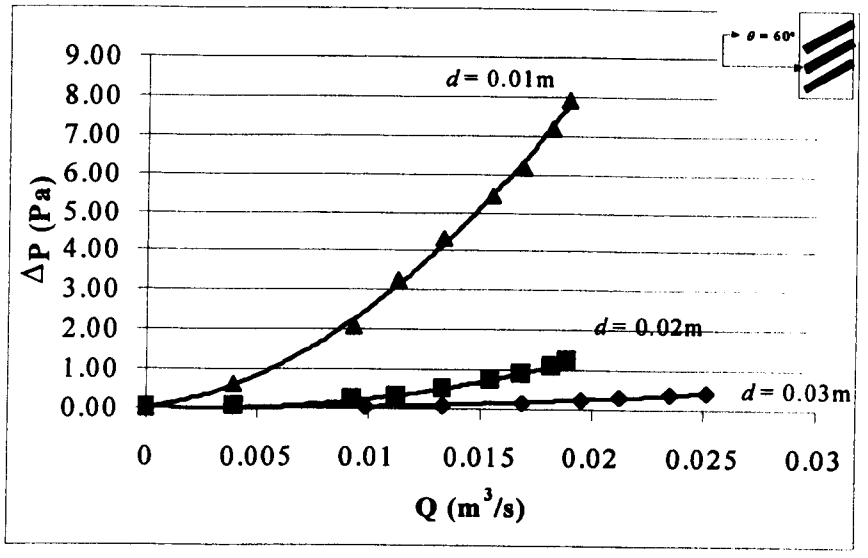

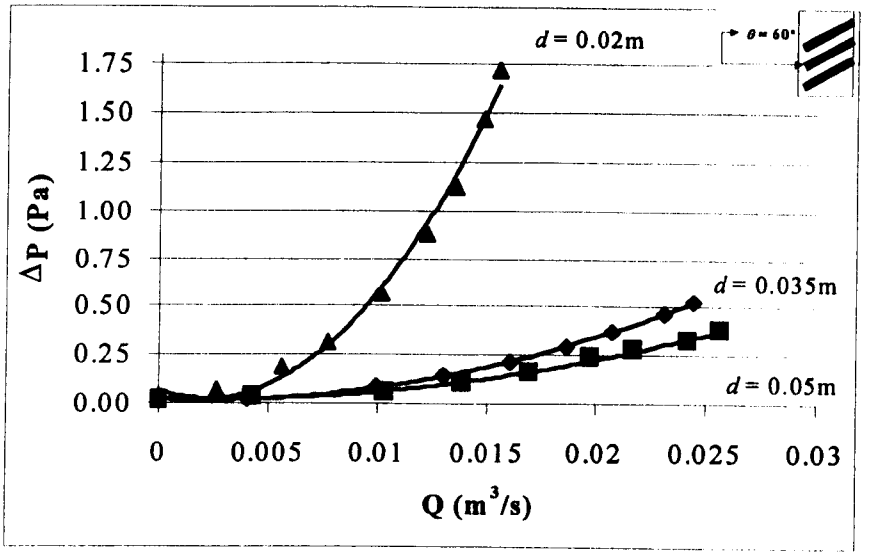

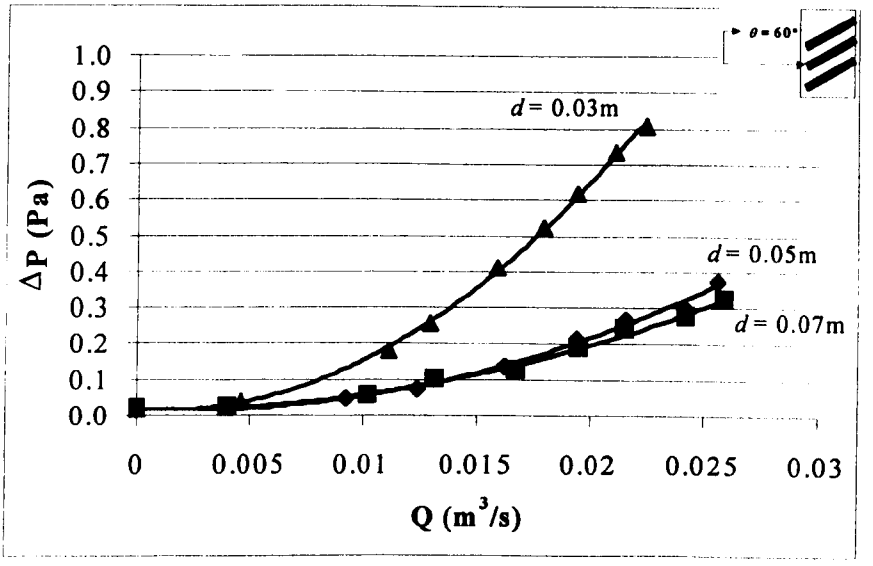

Figure (6.6): The pressure drop across the MLW as a function of various apertures examined. [a: L=0.04m, b: L=0.06m and c: L=0.08m].

occurred positively or negatively. The coefficient of determination of this variable with respect to all models examined was $r^2 = 0.135$.

The varieties of louver apertures examined, which ranged from 0.01 to 0.07m, therefore resulted in various pressure curves. In cases where aperture $d \leq 0.035m$, higher-pressure drops were achieved compared with bigger dimensions. In the latter, pressure records were diminished to lower readings (max. ΔP <0.45 Pa). Also, louver apertures played an important role when accompanied with steeper inclinations. As louvers were tilted to steeper inclinations the d_θ was lessened accordingly, causing reduction in pressure as shown from Figure (6.6). The Figure demonstrates that the maximum pressure drop across the MLW ranged from 0.35 Pa to nearly 8 Pa for the range of aperture from 0.07m to 0.01m respectively, when $\theta = 60^\circ$. It is worth mentioning here that MLW with d=0.01m

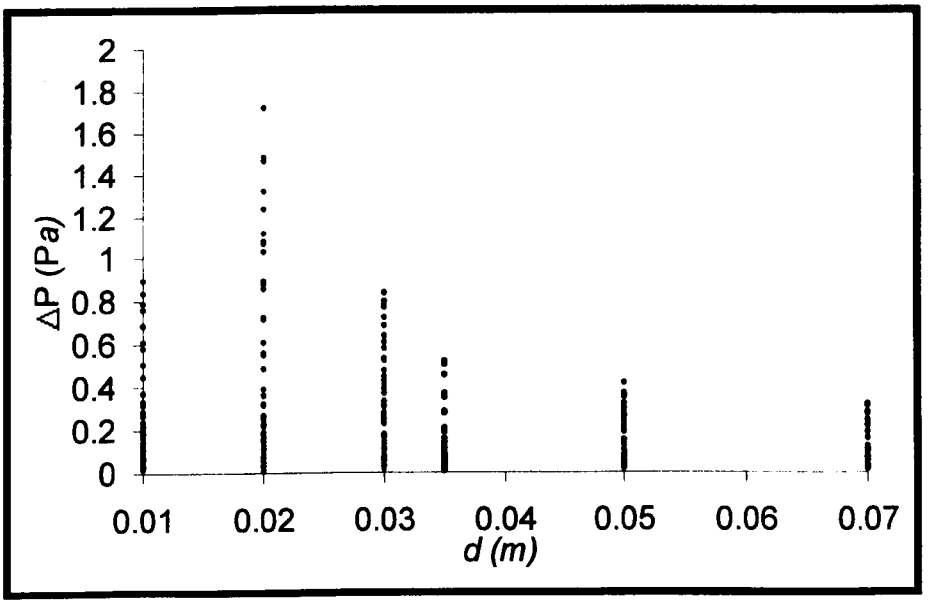

Figure (6.7): The pressure drop as function to the aperture dimensions.

was almost closed when examined under the latter inclination. In practice, the application of smaller apertures would cause more ΔP as shown in (Figure 6.7). This was the fact for all MLW models examined.

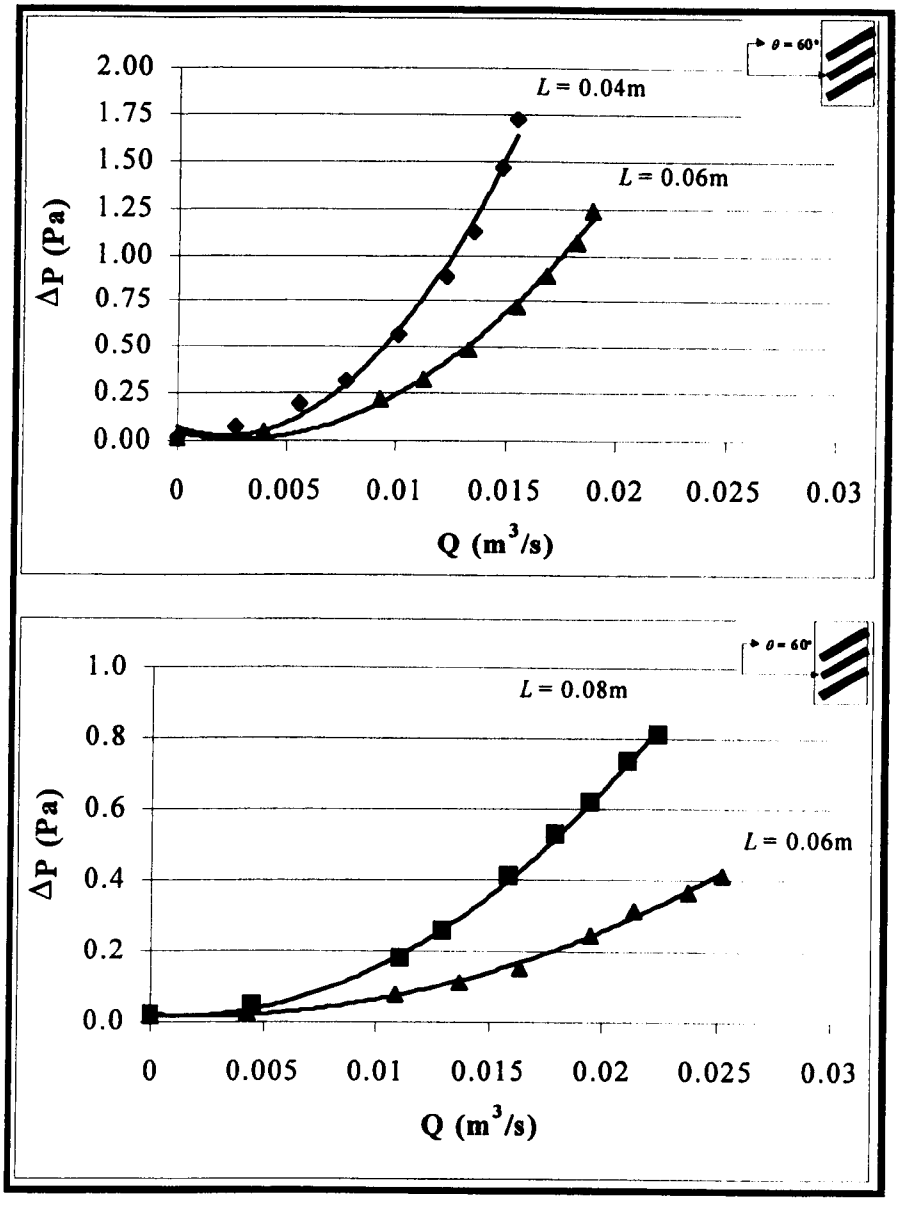

Figure (6.8): Some of the MLW where there was a significant effect of the louver depths. [a: d=0.02m and b: d=0.03m].

Generally, the reduction in aperture area due to tilting angles, say d_θ, upward or downward is one of the main answers to the drop of pressure. This was almost the common behaviour of all models selected for experiment, particularly those with deeper louver depths.

Depth of louver was the least affecting variable in the resultant differential pressures though in some cases it positively functioned as motivate barrier to airflow as illustrated in Figure (6.8). Otherwise, with various dimensions of L, MLW had minimal

pressure drops at $\theta \leq 45^{\circ}$. However, with the similar aperture models at steeper inclination the longer L caused more pressure difference than the lesser ones as demonstrated in the previous Figure. In other words, pressure drop was a function of MLW with large louver depths at d_{θ} than smaller depths. The value of r^2 of this variable was 0.25 showing that the louver depth was not a significant variable under the variety of configurations examined.

Similarly, the number of louvers *(N)* in the same MLW model caused also some considerable pressure differences of air as it reaches $N \geq 12$. As shown in Figure 6.9, there was a gradual increase of ΔP proportional to the increase in the louver number within the MLW.

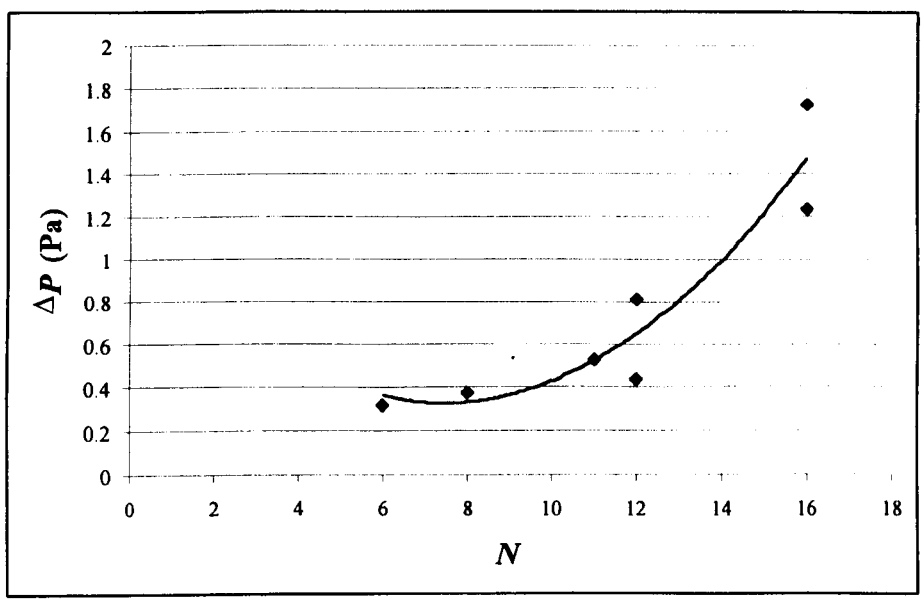

Figure (6.9): Pressure drop as function of louver number at louver inclination θ=60°.

Furthermore, the relationship between d and L dimensions was established in the form of ratio d/L. Lower ratios of d/L showed more increased pressure drops than higher ones (Figure 6.10). ΔP would be dimensionless at ratio d/L=1 no matter what other

configurations of MLW were. This dimensionless relationship could not be established at $d/L \leq 1$ since the deviation between curves produced varied with some significance (see

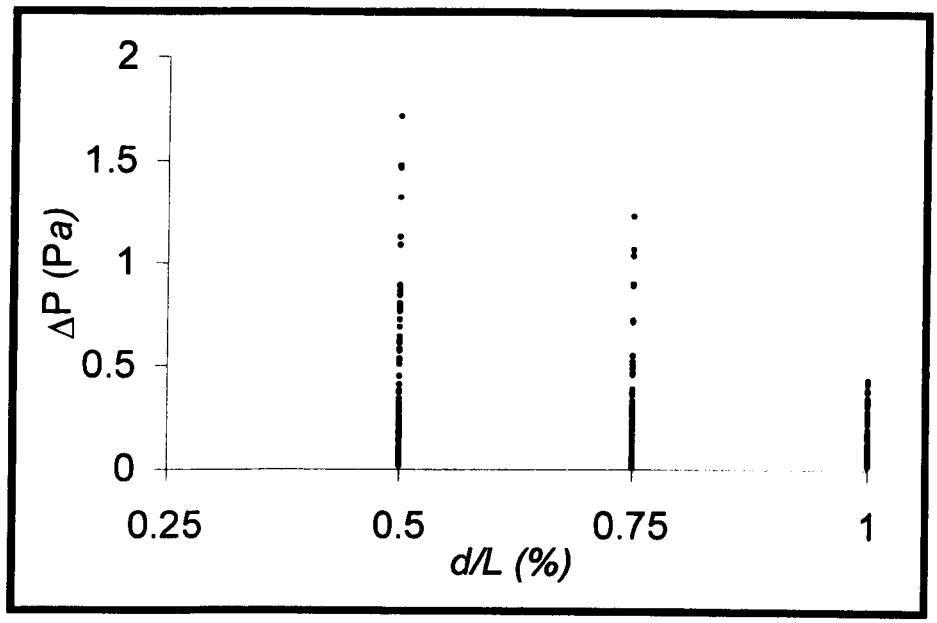

Figure (6.10): Pressure drop as function of various $d/L\%$.

Appendix B.5).

In conclusion, the individual analysis of each variable showed that the change in pressure drops could be attributed to some variables, better than others. However, the overall conclusion of the major parameter that would prove this phenomenon could not be accomplished. This is apparent from the coefficients of determinations of those variables and their descriptive analytical results as found in Appendices B.6.a to B.6.e. Yet, there was a trend of the effect of some variables when they were studied in conjunction with others. An example of this is found when analysing the effect of louver aperture on the resultant ΔP. Though pressure characteristics was not influenced by the variety of d examined, the aperture reduction as a function of various inclinations, d_θ, gave some

indication of ΔP occurring. Nevertheless, this effect of the new d_θ was only able to explain about 45% of the resulting pressure drop (see Appendix B.6.b).

The next section is devoted to analysing the integration of all variables involved in this appraisal stage and their overall contribution to ΔP.

6.5.2. The integration of all variables

The integration of all variables was observed since none of the individual variables could explain the resultant pressure drop across the reviewed MLW. Similarly, the statistical analysis of overall variables integration was not possible either. As shown in Appendix (B.7), this integration explained about only 65% with an error limit which exceeded 30%.

The discussion of the latter two sections looked more closely at the functions of individual variables as well as the integration of overall variables in resulting pressure drop across the MLW. More than 80% of MLW geometries examined were not sufficiently effective to create any pressure significance. In other words, it was discovered that louvers showed some resistance to airflow at steeper inclination, θ=60°. This was due to θ, the reduction in d as function of inclination, and the free area (A_f).

On the one hand, the above findings confirmed those reached by the two related studies conducted by Yakubu and Sharples (Yakubu and Sharples, 1991) and Pitts and Georgiadis (Pitts and Georgiadis, 1994) which were conducted in similar, limited MLW geometries. On the other hand, they clearly supported the argument concerning the validity of MLW application in buildings as a source of natural ventilation were higher airflow rates where achieved at almost minimal pressure drops. The above discussion

nevertheless gave some importance to the steeper inclination angle as a factor for initiating some considerable pressure drop across the MLW.

As a result, the following section examines the 60° louver inclination over a number of MLW units under higher flow rates (Q).

6.5.3. Pressure drop at 60° louver inclination

A number of MLW units were examined under higher flow rates aiming to establish an understanding of the MLW geometry contribution to resultant pressure drop. They were examined under 60° inclination since pressure drop was much related to this louver inclination. Table (6.2) shows the various MLW geometries examined under a series of flow rates.

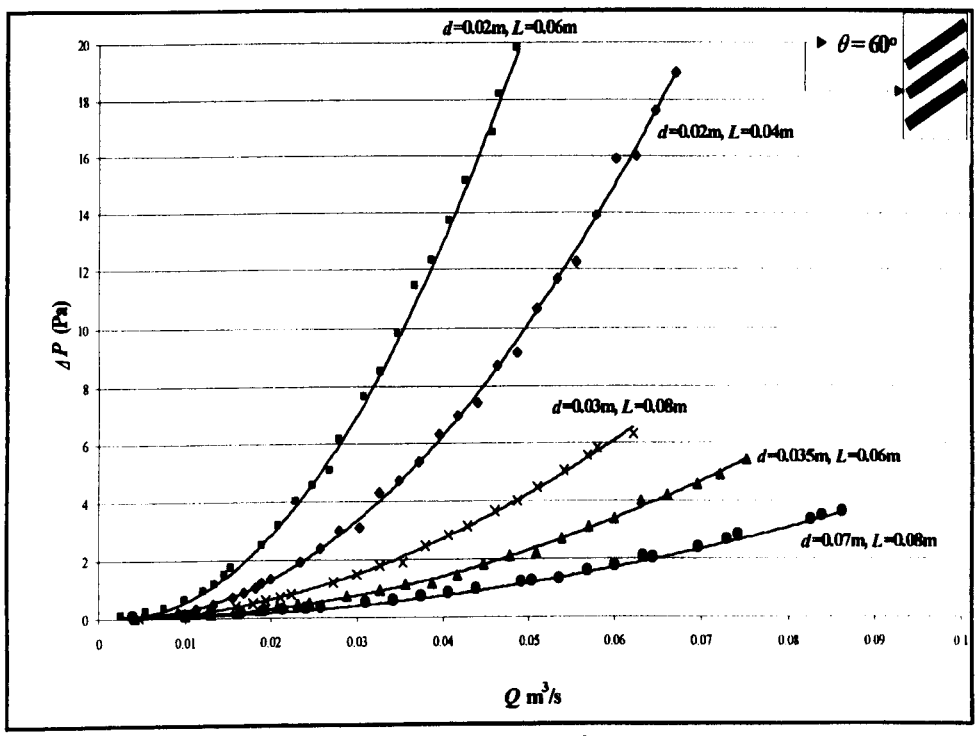

Figure (6.11): Pressure drop as a function of various MLW configurations at louver inclination 60_0.

Table (6.2): The various MLW geometries examined under a series of flow rates at inclination 60°

d=0.02m, L=0.04m, N=16, A_f=19.2m²

Q	ΔP	d_θ	L_θ
0.0039	0.050031	0.01	0.02
0.0093	0.21582	0.01	0.02
0.0113	0.326673	0.01	0.02
0.0133	0.489519	0.01	0.02
0.0155	0.723978	0.01	0.02
0.0169	0.893691	0.01	0.02
0.0182	1.072233	0.01	0.02
0.0189	1.237041	0.01	0.02
0.02	1.35668	0.01	0.02
0.023414	1.947344	0.01	0.02
0.025712	2.405201	0.01	0.02
0.028011	3	0.01	0.02
0.030309	3.1	0.01	0.02
0.032607	4.2868	0.01	0.02
0.034906	4.721094	0.01	0.02
0.037204	5.37	0.01	0.02
0.039502	6.3	0.01	0.02
0.041801	6.9667	0.01	0.02
0.044099	7.40987	0.01	0.02
0.046397	8.706003	0.01	0.02
0.048696	9.14	0.01	0.02
0.050994	10.63909	0.01	0.02
0.053292	11.67831	0.01	0.02
0.055591	12.2379	0.01	0.02
0.057889	13.90207	0.01	0.02
0.060187	15.9089	0.01	0.02
0.062486	16	0.01	0.02
0.064784	17.60107	0.01	0.02
0.067082	18.93096	0.01	0.02

d=0.02m, L=0.06m, N=16, A_f=19.2m²

Q	ΔP	d_θ	L_θ
0.00267	0.072594	0.01	0.03
0.00562	0.190314	0.01	0.03
0.00775	0.31235	0.01	0.03
0.01013	0.56898	0.01	0.03
0.01227	0.883489	0.01	0.03
0.01356	1.12246	0.01	0.03
0.0148	1.467086	0.01	0.03
0.01553	1.722636	0.01	0.03
0.019057	2.4456	0.01	0.03
0.021039	3.1508	0.01	0.03
0.023021	3.961754	0.01	0.03
0.025002	4.5	0.01	0.03
0.026984	5.024	0.01	0.03
0.02807	6.106616	0.01	0.03
0.030948	7.57908	0.01	0.03
0.03293	8.45678	0.01	0.03
0.034912	9.753975	0.01	0.03
0.036893	11.41	0.01	0.03
0.038875	12.25727	0.01	0.03
0.040857	13.659	0.01	0.03
0.042839	15.04684	0.01	0.03
0.046	16.789	0.01	0.03
0.046803	18.12268	0.01	0.03
0.048784	19.76796	0.01	0.03

d=0.035m, L=0.06m, N=11, A_f=28.6.2m²

Q	ΔP	d_θ	L_θ
0.0041	0.025506	0.02	0.03
0.01	0.085347	0.02	0.03
0.013	0.139302	0.02	0.03
0.0161	0.212877	0.02	0.03
0.0187	0.288414	0.02	0.03
0.0207	0.371799	0.02	0.03
0.0231	0.464013	0.02	0.03
0.0245	0.523854	0.02	0.03
0.02879	0.734586	0.02	0.03
0.032677	0.95761	0.02	0.03
0.035712	1.152734	0.02	0.03
0.038747	1.2045	0.02	0.03
0.041782	1.46778	0.02	0.03
0.044817	1.848451	0.02	0.03
0.047852	2.117138	0.02	0.03
0.050887	2.23	0.02	0.03
0.05392	2.709511	0.02	0.03
0.056957	3.104375	0.02	0.03
0.059992	3.375791	0.02	0.03
0.063027	3.98	0.02	0.03
0.066062	4.20894	0.02	0.03
0.06952	4.569777	0.02	0.03
0.072132	4.928693	0.02	0.03
0.075167	5.40998	0.02	0.03

d=0.03m, L=0.08m, N=12, A_f=25 m²

Q	ΔP	d_θ	L_θ
0.0046	0.040221	0.02	0.04
0.0111	0.178542	0.02	0.04
0.013	0.256041	0.02	0.04
0.0159	0.41202	0.02	0.04
0.0179	0.524835	0.02	0.04
0.0194	0.617049	0.02	0.04
0.0211	0.731826	0.02	0.04
0.0224	0.808344	0.02	0.04
0.027317	1.241631	0.02	0.04
0.029993	1.506317	0.02	0.04
0.03267	1.796848	0.02	0.04
0.035347	1.908	0.02	0.04
0.038023	2.455441	0.02	0.04
0.0407	2.823503	0.02	0.04
0.04296	3.154393	0.02	0.04
0.046053	3.637159	0.02	0.04
0.04873	4.00193	0.02	0.04
0.050993	4.479724	0.02	0.04
0.054083	5.051474	0.02	0.04
0.05676	5.5746	0.02	0.04
0.057999	5.825499	0.02	0.04
0.062113	6.3024	0.02	0.04

d=0.07m, L=0.08m, N=6, A_f=0.375m²

Q	ΔP	d_θ	L_θ
0.0041	0.021582	0.04	0.04
0.0102	0.054936	0.04	0.04
0.0132	0.097119	0.04	0.04
0.0168	0.125568	0.04	0.04
0.0195	0.191295	0.04	0.04
0.0216	0.241326	0.04	0.04
0.0243	0.25661	0.04	0.04
0.026	0.319806	0.04	0.04
0.031219	0.462525	0.04	0.04
0.034448	0.562112	0.04	0.04
0.037676	0.671732	0.04	0.04
0.040904	0.791385	0.04	0.04
0.044133	0.921071	0.04	0.04
0.049361	1.15238	0.04	0.04
0.050589	1.210541	0.04	0.04
0.053818	1.25	0.04	0.04
0.057046	1.540142	0.04	0.04
0.060274	1.719991	0.04	0.04
0.063503	2.0048	0.04	0.04
0.064731	1.984756	0.04	0.04
0.069959	2.319737	0.04	0.04
0.073188	2.601	0.04	0.04
0.074416	2.769731	0.04	0.04
0.086444	3.548221	0.04	0.04
0.082873	3.259856	0.04	0.04
0.084101	3.4	0.04	0.04

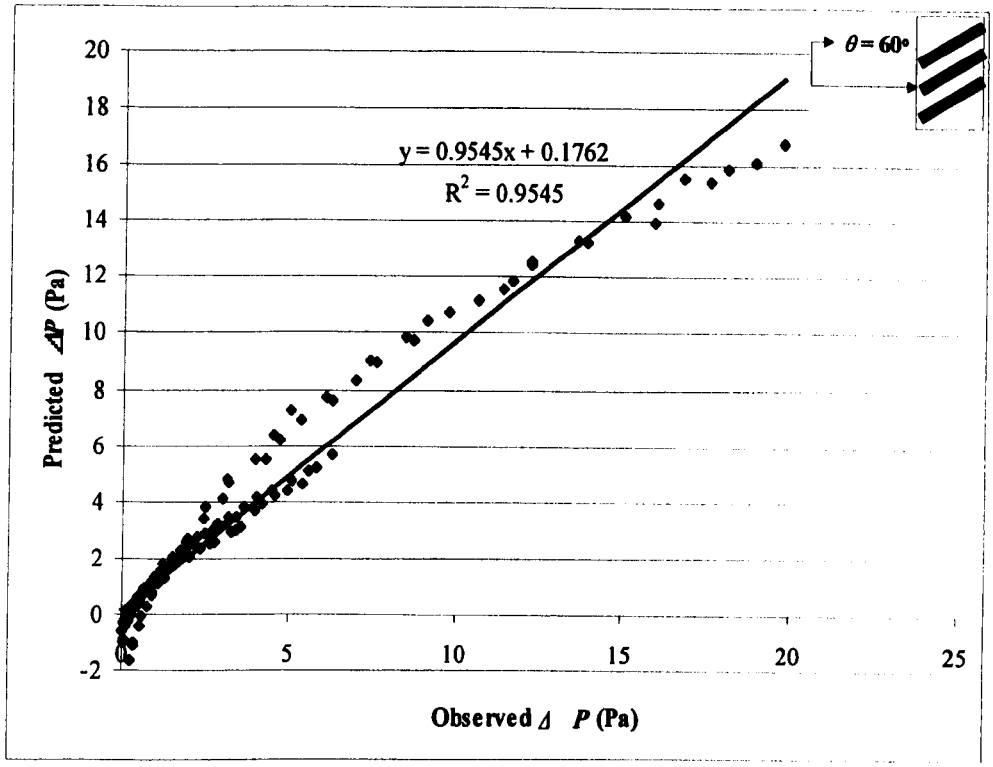

Figure (6.12): The predicted against the observed values of ΔP, based on the statistical model equation (6.26).

The various pressure drops (Figure 6.11) demonstrate more clearly the effect of each variable of MLW. This was clearly obvious as the decrease in the gaps between louvers resulted in considerable pressure drop across the MLW. ΔP showed some level of dependence on other variables examined such as the free area and aperture where the higher r^2 reported were, 0.66 and 0.61 respectively. Interestingly, the effect of the louver depth was more obvious at this stage since the r^2 of this variable reached 0.552 (see appendix B.8.a). At similar d, the louver with bigger depth encountered more resistance to airflow than the louver with a smaller one. An example of this is found in Figure 6.11 where ΔP reached nearly 20 Pa at flow rates $0.067 m^3/s$ and $0.04 m^3/s$ for depths 0.04m and 0.06m respectively.

As far as the number of louvers was concerned, ΔP showed a higher dependence on the number of louvers involved since the data observed and predicted were comparable

with r^2=0.75, with a high level of significance. Appendices B.8.a to B.8.d demonstrate the statistical analysis of each variable with respect to the observed data.

Nevertheless, the integration of all variables involved in this study was needed to establish the overall relationship of the factors mentioned earlier. The predicted value of ΔP with respect to the observed laboratorial data aimed to trace this effect. So, a statistical model equation was developed which corresponds to the integration relationship of variables involved in the latter inclination. This was essential to demonstrate the effect of various parameters of MLW at the critical inclination; i.e. 60°. The linear correlation of the observed ΔP is plotted against the predicted value in Figure 6.12 and is represented in the following equation:

$$\Delta P = c + \alpha.Q + \beta_i.d_\theta + \chi_i.A_f + \delta_i.N + \varepsilon_i.L_\theta + \left|(\alpha\beta)_{ij} \cdot Q.d_\theta + (\alpha\chi)_{ij} \cdot Q.A_f + (\alpha\delta)_{ij} \cdot Q.N + (\alpha\varepsilon)_{ij} \cdot Q.L_\theta\right| \quad (6.27)$$

where:

c = the intercept defined from the linear curve estimate in Figure 6.12 (0.1762).

α = a constant value for volume flow (141.046)

β, χ, δ, ε and ϕ are the numerical representations of the variables d_θ, A_f, N, L_θ and θ respectively.

The equation fitted the data observed with high degree of linear correlation ($r^2 \cong 0.95$) (Appendix 13.B), with standard error of less than 5%, bearing in mind that the equation is examined merely on the data obtained from Table (6.2). The aim was to highlight the critical inclination where the pressure across the reviewed MLW would encounter a

considerable drop. A further observation of this equation to fit larger number of MLW parameters was beyond the aim of this research even through it represents one of the author's future tasks. Therefore, it is not covered here.

6.6. Conclusion

This study investigated the pressure characteristics across the reviewed modulated louvered windows that are typically employed in Jeddah. The appraisal measurement showed that enhancements in pressure drops between inner and outer volumes could, at certain point, be a function to some variables involved in this analysis. Nevertheless, the major enhancement in differential pressure was not due to individual variables but rather to the combination of variables that would comprehensively describe ΔP. The considerable pressure drop could not be achieved except when reaching $\pm 60^{o}$ of inclination, where MLW offered a considerable resistance to the airflow. This was verified since more than 80% of the total cases observed have fallen under extremely low-pressure drops. The statement, in light with the hypothesis of the current study, addresses the significance of modulated louvered windows as a source on natural ventilation in buildings. Airflow across the MLW has shown independence to the MLW where $\theta < \pm 60^{o}$, regardless of the other configurations involved. In other words, this chapter has demonstrated the *critical angle* of MLW under which major airflow reduction will exist.

In addition to the above, there are a number of other conclusions derived from this chapter. They are highlighted as follow:

- The quadratic model equation suggested the best curves fits compared to those produced by power law regressions. The quadratic curves were in the

form of $\Delta P = AQ + BQ^2$. However, further adjustments of the theoretical representations of coefficients A and B that are embedded in the equation in the quadratic form would be required to fit other variables such as number of gaps between louvers, inclination angles θ, and the ratio $d/L\%$.

- The effect of louver depth showed some significance when accompanied with steeper inclinations only.
- No major variations on drops were found between louvers positive and negative inclinations.

There is some evidence to suggest that the flexibility in the design of MLW which will not encounter much reduction in airflow passing louver blades. Next chapter is the next appraisal stage to evaluate the velocity drop across the reviewed MLW.

6.7. References

1. ASTM Standard E779 (1982) Measuring air leakage by fan infiltration pressurisation method.

2. Awbi, H.B. (1991) Ventilation of Buildings, London: E & FN Spon.

3. Baker, P.H., Sharples, S. and Ward, I.C. (1987) "Airflow through cracks". Building and Environment **22-(4)**, p.293-304.

4. BSI (1998) Ventilation for buildings - Performance testing of components/products for residential ventilation - Part 1: Externally and internally mounted air transfer device. PrEN-1314-1, p.18pp London: British Standards Institution.

5. Etheridge, D. and Sandberg, M. (1996) Building Ventilation: Theory and Measurements, John Willy & Sons.

6. Maghrabi, Amjed and Sharples, S. (1999) "Air flow characteristics through Modulated Louvered Windows". **(1)**, p.507-514, Brisbane, Australia: PLEA99.

7. Pitts, A. C. and Georgiadis, S. (1994) "Ventilation air flow through window openings in combination with shading devices". 15th AIVC Conference. p.432-439, AIVC.

8. Walker, I.S., Wilson, D.J. and Sherman, M. (1998) "A comparison of the power law to quadratic formulations for air infiltration calculations". Energy and Buildings **27**-p.293-299.

9. White, M. (1999) "Ventilators: Ventilation and acoustic Effectiveness". BRE **(IP4/99)**-p.1-8.

10. Yakubu, G.S. (1990) Modulated solar shielding of buildings: A study of a solar radiation control strategy for low energy buildings in hot dry and semi-arid climates. University of Sheffield. Unpublished PhD thesis.

11. Yakubu, G.S. and Sharples, S. (1991) "Airflow through modulated louver systems". Building Services Engineering Research and Technology **12-(4),** p.151-155.

CHAPTER 7: VELOCITY DROP ACROSS THE MODULATED LOUVERED WINDOWS

7.1. Introduction

This chapter covers the experimental work carried out to investigate the velocity drop across the reviewed modulated louvered Windows. The louver depths *(L)*, inclination angles *(θ)*, apertures *(d)*, and porosity percentage *(p)* of MLW are investigated here in depth. In addition, room configurations, height *(R_h)* and depth *(R_d)*, and prevailing wind conditions including angle of incidence (w_i) and speed of wind (v_e) are also studied at this stage. The experimental setup and the calibration technique are considered first before being followed by the analysis technique selected by comparing curves produced by the power-law and quadratic statistical curve fits.

The discussion of the results is undertaken in a number of stages. First, the wind data, including wind speed and direction, are highlighted. Then follows the velocity drop as function of the room configurations. The parameters of MLW mentioned earlier are discussed in the last section of the chapter, followed by the integration of all variables in respect to the velocity drop across the MLW.

7.2. Experimental and Calibration setup

The experiment took place at Ventilation laboratory, School of Architecture, University of Sheffield. The velocity reading, which is further analysed as a function of the earlier mentioned variables, is expressed as a percentage representing the ratio between the mean indoor air velocity *(v_i)* and mean outdoor wind speed *(v_e)*. The aim of this is to establish a relationship between louvers' various configurations and that of the percentage of *(v_i/v_e)*. It is necessary to mention at this stage that the wind speeds ranged from 0.6 to 3m/s. However, for simplicity some variables were investigated under fixed wind speed of v_i=2*m/s*, unless otherwise stated. The setup and calibration of various equipments and instrumentation used in this study are discussed here in more detail.

7.2.1. The technique

The type of measurement undertaken in this chapter requires a deep analysis of the air velocity reduction as function of the MLW variables noted in chapter 5. In addition, a number of variables are also investigated here including the room configuration, wind data and external reduction of velocity near the MLW as function of porosity percentage (*p*). In here, the wind flow through the window is expressed as the fraction of wind speed near the window level. The technique is appropriate for the scale of measurement in hand. Chand et al. (Chand et al. 1988) studied the profile of wind speed on airflow rates through a cross-ventilated enclosure by identifying the wind speed near the window level and *"Without introducing practically significant errors in the results due to a variation in the type of terrain"*. In addition, a recent research is conducted by the Sharples and Maghrabi (Sharples and Maghrabi, 2000) which includes the same measuring technique.

For initial velocity measurements it was noticeable that the fans tended to generate higher velocity profile at extremes than centre axis due to turbulence produced by its blades. In the meantime, the flow has no preset direction due to the turbulence that led to discrepancies in internal and external velocities readings. Therefore, a number of measures were considered to ensure that the flow, generated by fans, represents the free wind at window level in the real environment. These measures were:

- A porous fibrous Felt-Type material, 0.01m thick, covered the fans air exiting-sides in order to enable uniform distribution of airflow on the facade of the MLW external panel.

- The v_e was measured though a shield box connecting the fans with the MLW front panel as shown. A number of measuring locations were considered before selecting the most appropriate measuring location of v_e. From velocity measurements made around the velocity device in the shield box, *Re* was calculated to be less than 2000, $Re \cong 1200$, thus a laminar flow through was assured. Consequently, the shield box controlled the wind direction.

- The size of the frontal area of the shield box was similar to the MLW area examined. This minimized the effect of the inlet/wall ratio effect on the flow pattern inside the room discussed in chapter 4.

- As far as the wind angle of incidence (*wi*) was concerned, the fans were connected to a metal bar positioned at the lower centre of the front panel. This connection was made with the flexibility to move the fans, in a semi-circle manner, to any predetermined oblique angle (experimentally represented as the external wind direction) as shown in Figure 7.2. Consequently, more precise readings were achieved (Figure7.1).

A test room chamber (Figures 7.1 and 7.2) was used to represent the indoor air movement. As stated above, the MLW units were fitted on the front panel of the chamber. The other end, the air-exiting side, was left open as an attempt to investigate the velocity drop that merely occurs due to the louver various

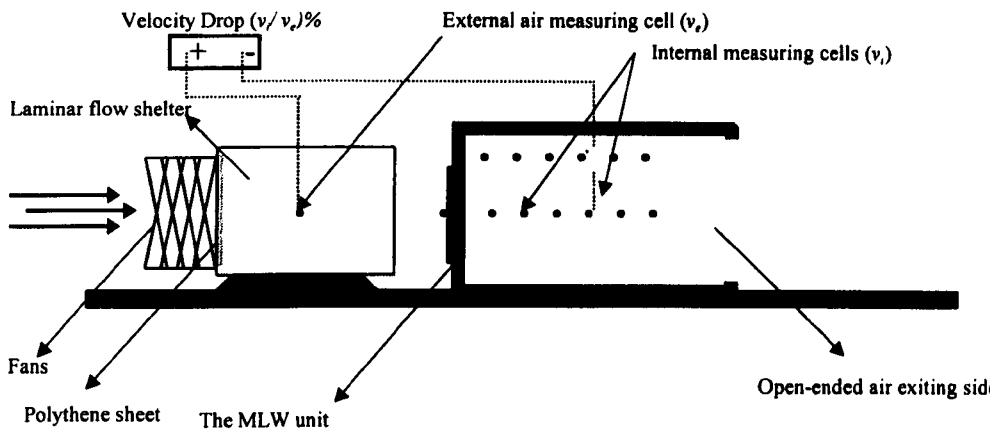

Figure (7.1): A schematic diagram of the velocity measurements experimental set-up

configurations. In other words, the outlet was about six times bigger than the inlet to minimize any effect that may occur from the outlet discussed in section 4.4.1. Pre-set holes on the floor of the room chamber were made that -precisely- represented the internal locations of velocity measurements.

7.2.2. Fans

Two fans were placed in series facing the front panel of the sash unit models. The diameter of each fan was 0.48m (19 inches), and contained blades of 14° pitch capable of 1440 r.p.m. and performed under fluid temperatures of up to 40 ^{O}C. Each fan was made to control the speed alteration separately from other fans. Woods of Colchester Limited manufactured them.

7.2.3. Velocity record instrument

The machine used to record the indoor air velocity (v_i) and the outdoor wind speed (v_e) was Model 8910 Display/Power Supply, manufactured by TSI Incorporated, USA (Figure 7.2). It was designed specifically to work with TSI air velocity transducers to provide a convenient readout of air velocity. Depending on the range selected, this machine accepts a signal of 0 to 5 volts DC and displays an output that is linearly proportional to the signal. The connected TSI air velocity transducer in the same hand is calibrated to provide a linear output of 0 to 5 volts DC. It is a precise instrument designed to measure air mass velocity in fixed installations as quoted by manufacturer. Mass velocity is a measure of air velocity with reference to standard conditions of about 20° C, the laboratory temperature under which the experiment took place. As the flow of air passes the heated sensor of the velocity transducer which is kept at a constant elevated temperature by means of electronics, more electrical power is required to maintain the sensor at the elevated temperature. Monitoring the power supplied to the sensor provides a signal that is related to the amount of air flowing past the sensor. This signal is automatically displayed in the power supply machine in terms of velocity (m/s) and transferred to the computer in voltage signals through wiring and data-logger connecting them.

The air velocity transducer was calibrated by the manufacture (refer to TSI device manual). In the laboratory, the author correlated the readings of series of air velocity (m/s) displayed from TSI machine relative to the voltage signals recorded by the data-logger. The chart developed showed linear correlation between velocity and voltages signal that ensured consistently accurate output display against that of voltage signals (see appendix C.1). The coefficient of determination of the linear regression was ($r^2 = 1$).

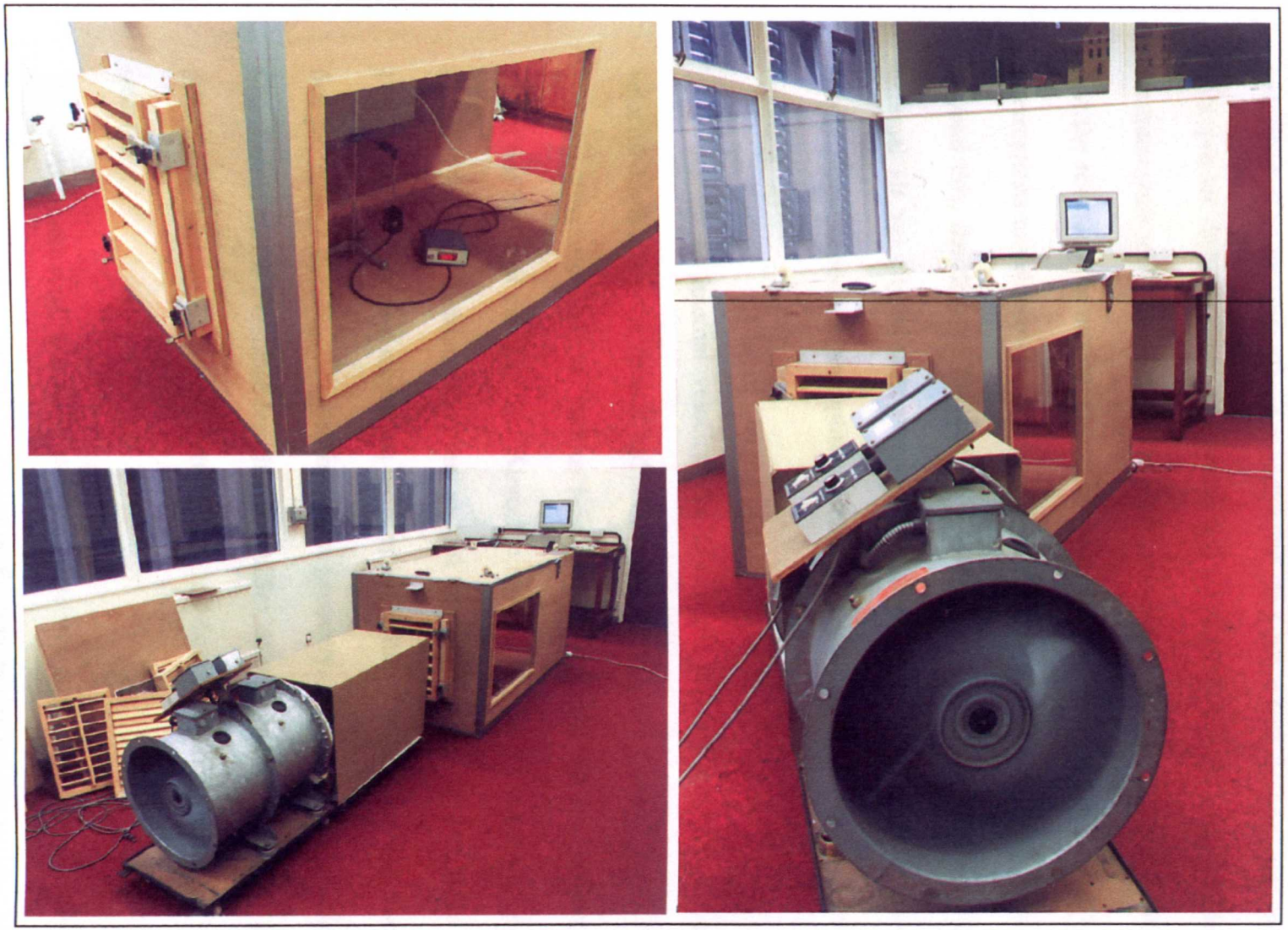

Figure (7.2): The experimental setup of velocity drop measurements showing the various equipments employed in the experiment.

7.2.4. Positioning of TSI-meter device

Two TSI-meter instruments were used to measure both external and internal air velocities. The first was placed outside room chamber at five different measuring locations at a pre-set distance from the centre axis of the MLW unit. A number of routine measurements took place before the final measuring location was chosen. It was evident that the resistance to airflow caused by both front panel and MLW units had resulted in interruptions to velocity reading and caused discrepancies in the $0.50m$ next to the panel. Beyond this, the distance towards the fans was a more appropriate location to measure external air velocity as discrepancies were diminished. The centre of shield box was finally recommended as the optimum measuring location from which wind velocity was recorded.

As far as internal velocity was concerned, detailed analysis was attempted of velocity drops along the vertical and horizontal sectional directions of flow. Therefore, six different locations with two various heights each were selected for measurements along height and depth of the chamber. Along the room depth, the six measuring locations were set at 0.25m distance from each other and the vertical location was at 0.325m (Figure 7.1). The selection of the first measuring location inside the room chamber was chosen far from free-jet flow or turbulence caused by louver geometry. The series of runs that took place first showed that at a distance less than R_d=0.25m, there were turbulences and jet flows that interrupted flow measurements being taken, and hence, the first measuring location was selected.

At a later stage, the TSI-meter instrument was positioned on the external surface of MLW for comparison with the reviewed inclination angles for the various MLW units in order to study the velocity drop as function of porosity percentage *(p)* of the MLW.

7.2.5. Timing or velocity recording

As stated in Chapter 6, there is a need to give positive time for the flow to reach its steady state and to avoid any turbulence before inscribing any reading (Etheridge and Sandberg, 1996). While too short a timing may be less effective, along timing might be redundant and is time consuming. Contrary to site measurements, wind could be adjusted at any pre-set speed and direction in laboratory measurements. This advantage could save time and therefore result in better representation of the average readings to be recorded therefore (Yousoufian, 1992). Another advantage of the latter technique is related to the time lag between internal and external readings. Time lag is the time required for measuring internal velocity to correspond with the external one (Bittencourt, 1993). Onsite observations with improper consideration of time lag could result in discrepancies found in data collected. On certain occasions, at lower air velocities and wind turbulence, the discrepancies could exceed the margin of error percentage, thus results may not be accurate, especially when $v_i/v_e\%$ is of considerable importance in the analysis. In the laboratory, errors resulting from time lag are diminished since external wind is controlled at a pre-set velocity and direction. Hence, the ratio $v_i/v_e\%$ is more likely to represent the actual drop in air velocity.

The software was adjusted to give an average reading of various timings, 30 sec, 1 min and 2 min at four readings per second under series of air velocities. The first average timing (30 sec) was chosen as no major variations resulted from the three timings examined.

7.2.6. Measuring principles

Both internal and external velocity readings from the combined power of both axial fans were transferred to the computer attached when readings had stabilised. Similar to the pressure drop appraisal stage, this step was repeated over ranges of velocity drops as well as different measuring locations involved. Steps were taken to ensure that the laboratory temperature was about 20 C (White, 1999). The procedure of the test measurement can be summarised in the following steps:

I. Various equipment used in the measurement were first switched on.

II. The TSI-meter devices were set to zero and left some time to stabilise after being fitted in the pre-set measuring locations.

III. A MLW unit is fitted onto the chamber front panel facing fan systems with adjusting louvers to the desired inclination angle.

IV. The fan is switched on and controlled to the desired setting.

V. The data of both internal and external velocities were then taken after ensuring stabilised readings.

VI. The fans were set to various wind speeds in order to create ranges of air velocities and step (v) was repeated.

VII. The TSI-meter device used to measure internal velocity was then moved to another pre-set location, vertically or horizontally, and the last two steps were then repeated.

VIII. The MLW unit was then adjusted to the next desired angle and the last three steps were then repeated for each setting.

IX. Wind speed covered from 0 to around 3 m/s.

X. External velocity was measured at the centre axis of the MLW and internal velocity was taken at the preset locations noted earlier.

7.3. The analysis

A reduced-sample of data was first analysed using the two statistical curve fits including power law and quadratic (based on the least square method). At this stage, the three curve fits were analysed based on the reduction in velocity due to external wind speed and the reduction in v_i/v_e% due to room depth and the r^2 of both model equations were examined as shown in Figure 7.3. It is important to mention at this stage that data obtained were not based on scattered data but rather on clear trend of curve fits since measurements were carried out in the laboratory.

As shown in Figure 7.3, the regression lines developed by the two curve fits corresponded to the data measured at both maximum and minimum aperture dimensions. The preference of quadratic cure fit was obvious with data representing the reduction due to room depth at both higher and lower ratios v_i/v_e, as well as with the presence of louver inclinations. Therefore, the recommendation was to carryout the discussion of results of this chapter using the curve fits in the quadratic form.

7.4. The discussion

This study investigated the velocity drop across the reviewed MLW. The louver depths *(L)*, inclination angles *(θ)*, apertures *(d)*, ratio of *(d/L)* and free area *(A_f)*, porosity percentage *(p)* of MLW are investigated here. The room configurations, height *(R_h)* and depth *(R_d)* and wind angle of incidence (w_i) were considered.

The internal velocity patterns would vary in accordance with the varieties of louver inclinations as well as other variables involved. Some measurements were taken at louver

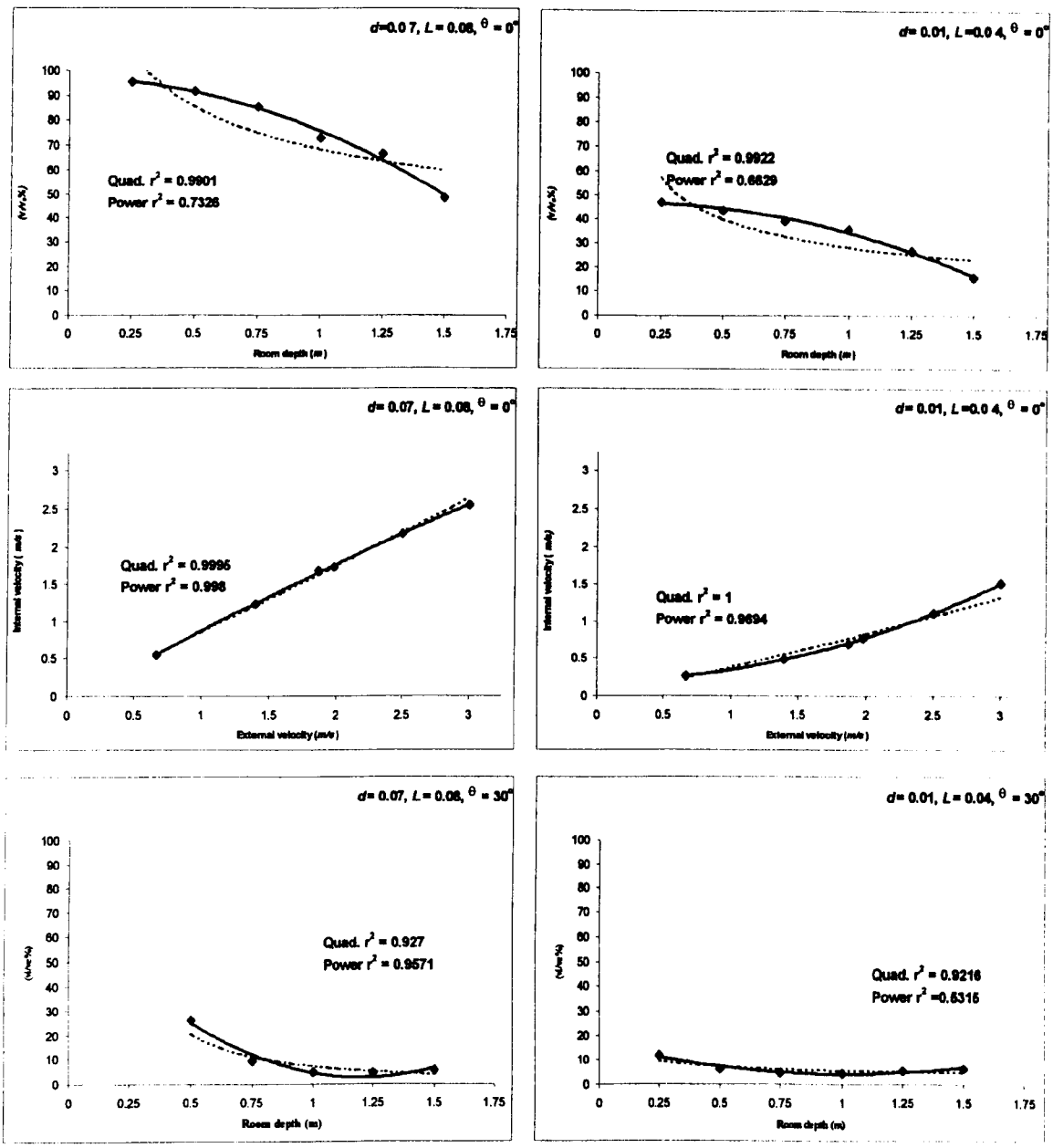

Figure 7.3: The comparison between quadratic and power law statistical curve fits.

inclination set to zero while others were evaluated with and without the presence of inclination. These are noted accordingly in each variable discussed in the following subsection.

The discussion of results was divided into sections: the velocity drop due to wind speed and the extent to which MLW would determine the reduction percentage of v_i/v_e%. The effect of wind angle of incidence will be discussed in the same section. The room geometry, including height and depth will be highlighted in another section. Subsequently, various louver configurations will be discussed and followed by the overall integration of the MLW parameters in causing significant velocity drop across.

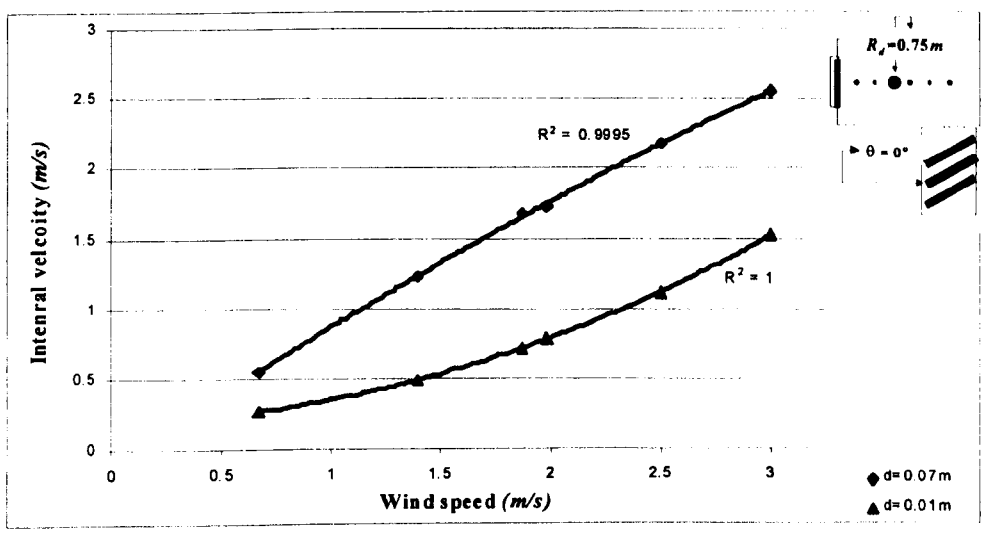

Figure (7.4): The polynomial curves for two louver apertures at R_d=0.75m

7.4.1. Velocity drop as function of wind velocity (v_e)

The MLW was examined under various wind velocity ranging from 0.6 to 3.00m/s, which corresponds to minimum indoor air velocity and to the recommended air speed indoors in humid conditions as indicated by Evans (Evans, 1980) (see Appendix C.2). Measurements of internal velocities (v_i) were taken along room and were plotted against v_e.

The polynomial curves indicating internal velocities based on wind speeds were linearly correlated. They varied significantly depending on the various louver apertures. For example, at R_d=0.75m the maximum v_i achieved for apertures 0.01m and 0.07m was 1.5m/s and 2.5m/s respectively while the minimum was 0.27m/s and 0.56m/s as shown in Figure 7.4. The practical interpretation of this showed how the selection of louver aperture dimension could determine the desired level of velocity indoors. As far as the ratio of v_i/v_e was concerned, the Figure shows the maximum aperture dimension d=0.07m tested under series of winds $v_e \cong$ 3, 2.5, 2, 1.87, 1.40 and 0.6 m/s. The v_i/v_e% corresponding to the wind speed was 85%, 87%, 87%, 89%, 87% and 82% respectively. In other words, v_i/v_e% was constant to v_i since the mean value of v_i/v_e=86% with a minimum error limit. It is worth noting at this stage that with this proportionality, the curve fit representing them started declining around v_e=2 m/s. In contrast to what was originally thought, v_i/v_e% declined rather than improve as further wind speed occurred. A sound explanation to this fact was that the MLW allowed air to penetrate through its large apertures with not much resistance or friction caused by its surface. Therefore internal velocity will be proportional to the external one. But at higher speeds of wind this proportionality would deviate as more pressure occurred on the inlet surface due to acting wind speed and resistance of MLW free area. This in fact caused the decline in flow as air loses much of its momentum force at inlet surface.

Nevertheless, this was not the general case for all apertures. The v_i/v_e% for the rest of the apertures was gradually increasing as higher winds existed even at the highest speed examined. The increase in percentage v_i/v_e% at louver apertures $d \leq$ 0.05m was less than 20% for the ranges of wind speeds examined. Table 7.1 shows the records of internal velocity and ratio v_i/v_e% as a function of wind speed for the various MLW. Readings from

Table (7.1): The reduction in indoor air velocity as function to various MLW configurations. Measured values at Rd=0.75m, θ=0°

L=0.08m

d=0.03m			d=0.05m			d=0.07m		
v_e(m/s)	v_i (m/s)	v_i/v_e%	v_e(m/s)	v_i (m/s)	v_i/v_e%	v_e(m/s)	v_i (m/s)	v_i/v_e%
3.00	2.15	71.60	3.00	2.12	70.64	3.00	2.56	85.35
2.50	1.51	60.32	2.50	1.75	69.87	2.50	2.18	87.00
1.98	1.18	59.58	1.98	1.31	66.16	1.98	1.73	87.26
1.87	1.03	55.02	1.87	1.38	73.70	1.87	1.68	89.94
1.40	0.80	56.96	1.40	0.94	67.31	1.40	1.23	87.93
0.67	0.38	57.46	0.67	0.49	73.14	0.67	0.55	82.67

L=0.06m

d=0.02m			d=0.035m			d=0.05m		
v_e(m/s)	v_i (m/s)	v_i/v_e%	v_e(m/s)	v_i (m/s)	v_i/v_e%	v_e(m/s)	v_i (m/s)	v_i/v_e%
3.00	1.90	63.21	3.00	2.09	69.79	3.00	1.98	66.09
2.50	1.55	61.98	2.50	1.57	62.70	2.50	1.73	69.33
1.98	1.08	54.53	1.98	1.20	60.43	1.98	1.47	74.39
1.87	1.03	55.02	1.87	0.91	48.94	1.87	1.32	70.48
1.40	0.80	56.96	1.40	0.75	53.81	1.40	1.07	76.76
0.67	0.35	52.96	0.67	0.38	57.00	0.67	0.51	76.37

L=0.04m

d=0.01m			d=0.02m			d=0.03m		
v_e(m/s)	v_i (m/s)	v_i/v_e%	v_e(m/s)	v_i (m/s)	v_i/v_e%	v_e(m/s)	v_i (m/s)	v_i/v_e%
3.00	1.52	50.67	3.00	2.25	74.89	3.00	2.37	79.03
2.50	1.12	44.73	2.50	1.75	70.18	2.50	1.82	72.75
1.98	0.78	39.39	1.98	1.10	55.72	1.98	1.20	60.65
1.87	0.71	38.05	1.87	1.00	53.74	1.87	1.01	54.25
1.40	0.49	35.05	1.40	0.71	50.61	1.40	0.75	53.46
0.67	0.27	39.98	0.67	0.33	50.04	0.67	0.40	59.29

the last example showed that v_i/v_e% ranged within 83-90%. As a result v_i/v_e% was found proportional regardless of wind speed range with a mean of 87% with ±5% variations of both ratio limit bands. At the same time, the ratio was 76%, 62% and 58% for apertures 0.05, 0.03m and 0.02m respectively, with less than ±15% variations of both extreme limit bands (see appendices C.3 and C.4).

The effect of louver depth was examined and found negligible. Figure 7.5, shows the insignificance effect of the louver depth under the variety of models examined, although some significance was present at the highest wind speed examined. But for the range of wind speed examined, the variation between indoor records in conjunction to the number of width examined was minor.

Table (7.2): The ratio v_i/v_e as function to various apertures.

R_d=0.25m v_i/v_e%

d	Max	Min	Mean	St.error	St. dev.
0.02	68.39516	74.9	63.0784	4.59962	3.252422
0.03	77.44133	81.486	73.23876	2.860012	2.022334
0.05	83.62352	86.098	80.98046	1.749723	1.237241
0.07	95.6	95	94.6	0.424264	0.3

R_d=0.50m v_i/v_e%

d	Max	Min	Mean	St.error	St. dev.
0.02	70.0923	54.678	63.75221	10.89956	7.70715
0.03	76.56	63.8456	70.93111	8.990438	6.3572
0.05	80.49	75.887	78.8544	3.254813	2.3015
0.07	93.09	89.69	91.7	2.404163	1.7

R_d=0.75m v_i/v_e%

d	Max	Min	Mean	St.error	St. dev.
0.02	68.45	47.678	58.41433	14.68802	10.386
0.03	73.35333	53.45507	63.4042	14.0702	9.949134
0.05	82.31667	70.27504	76.29586	8.514713	6.020811
0.07	89.93845	85.34667	87.64256	3.246883	2.295893

R_d=1m v_i/v_e%

d	Max	Min	Mean	St.error	St. dev.
0.02	63.098	44.0998	53.88594	13.43376	9.4991
0.03	62.8909	46.776	55.44158	11.39496	8.05745
0.05	69.467	54.676	61.84709	10.45882	7.3955
0.07	80.67	71.467	77.3	6.507504	4.6015

Further analysis was carried out to investigate louver apertures with respect to other measuring location within the room. As a result, it was possible to establish a relationship of the above variables at room depths R_d= 0.25, 0.50, 0.75 and 1m as the standard error variation was less than 15% in relation to the mean value of v_i/v_e%. Interestingly, the scale of error decreased as records were taken nearer to MLW unit as shown in Figure 7.6. But when the measurements exceeded R_d=1m, it was not possible to establish such correlation

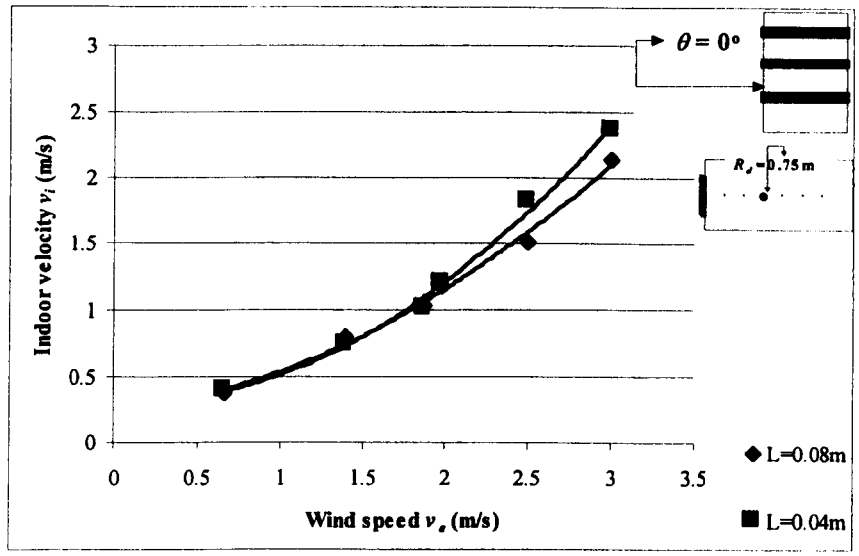

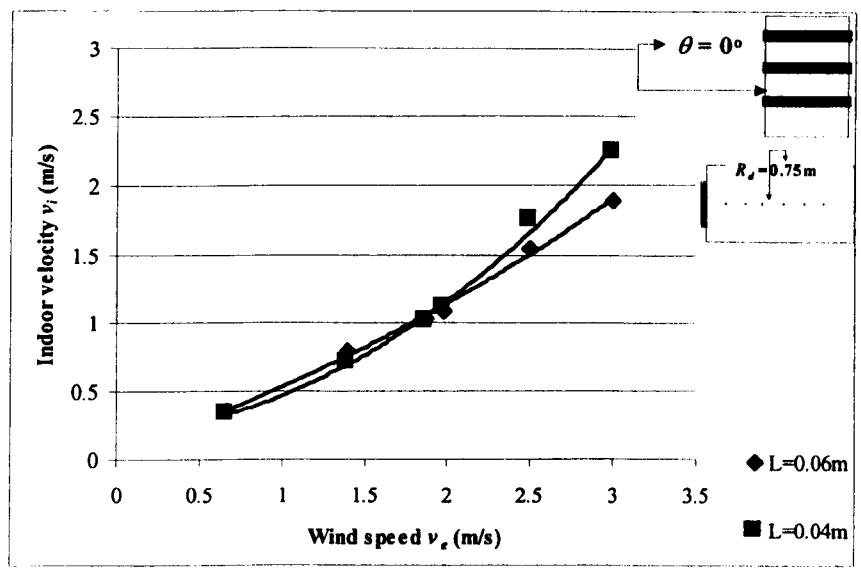

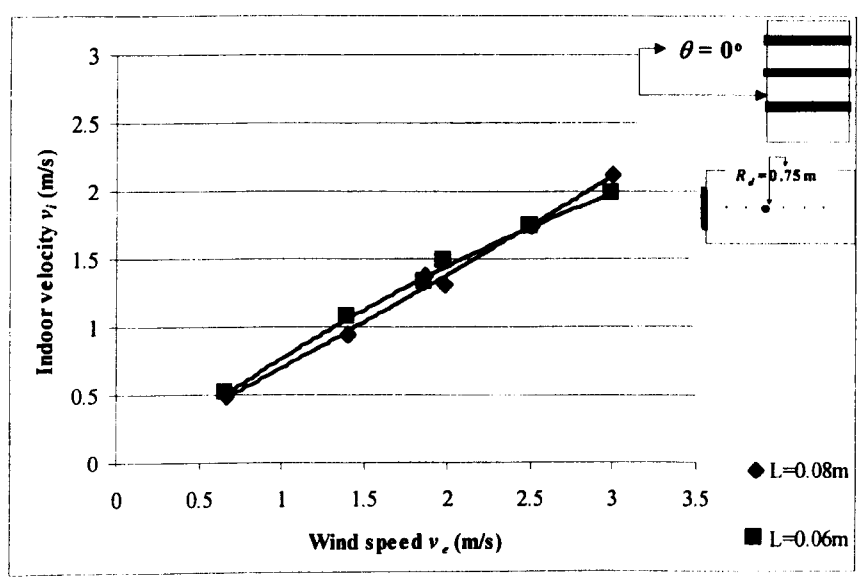

Figure (7.5): The reduction of velocity as function of louver depth.

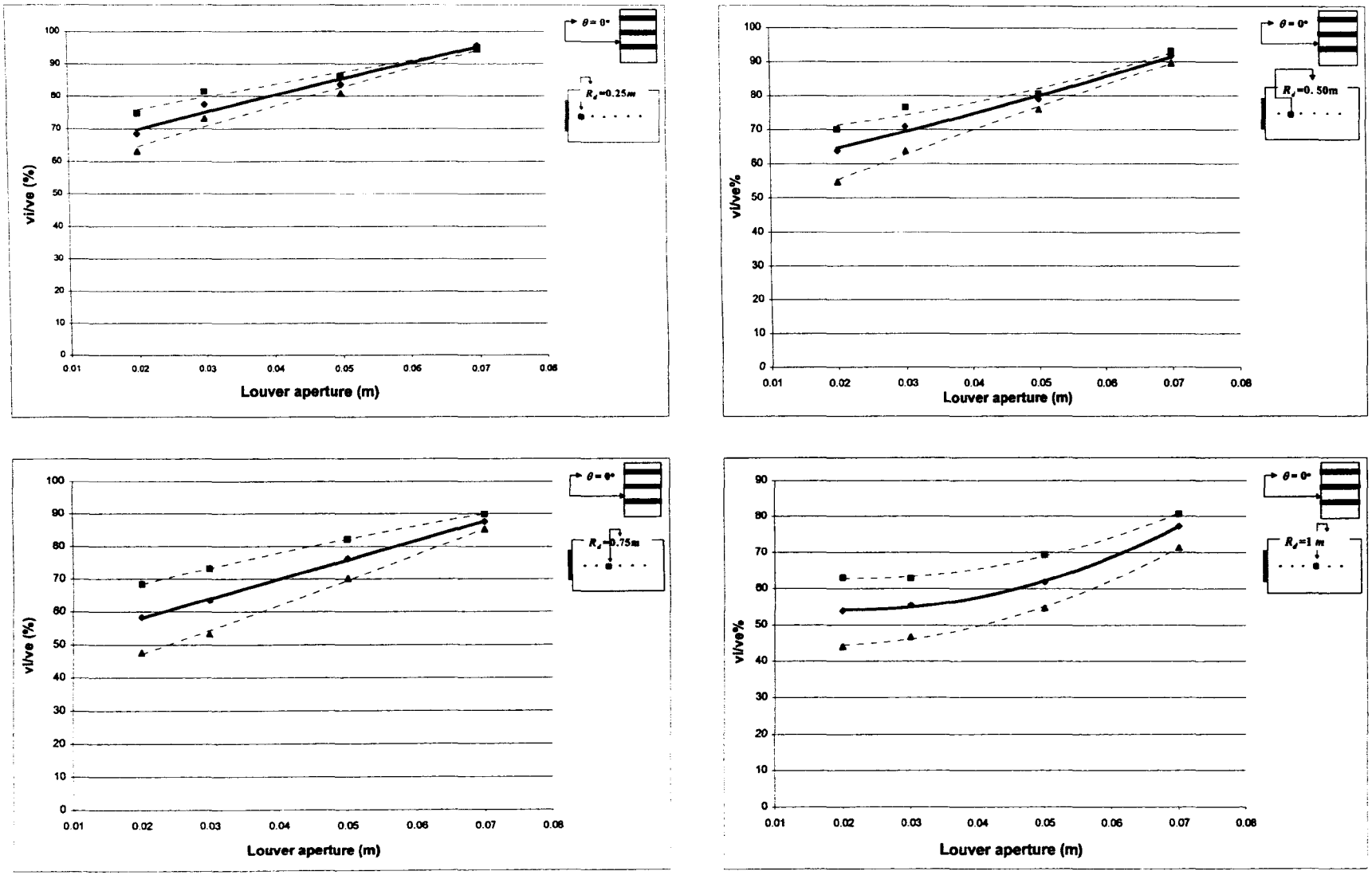

Figure (7.6): The correlation between various apertures and wind speeds at various locations inside the room

as error percentages increased beyond the acceptable limits; over 25%. Hence, polynomial regression curves were produced representing that correlation for louver apertures investigated at various room depths. Table 7.2 shows the various MLW units examined with their standard errors and standard deviations. Although louver aperture 0.01m behaved like other apertures, it was not included in the later Figure since its correlation had fallen significantly different from the rest of louver depths.

7.4.2. Velocity drop as function of wind direction *(w_i)*

Measurements covered three incidences of wind directions (w_i) 90°, 75°and 60° with blades in perfect horizontal position. The first direction is referred to as the wind perpendicular to the windward side. As mentioned earlier, the metal bar connecting both room chamber and fans made it flexible to alter fans (in a semi-circle manner) to any predetermined direction. Polynomial curves produced by the two latter directions, w_i=75° and 60° were compared with the referenced direction w_i=90° at R_d=0.25m.

The average reduction in velocity as function to wind incidence angle is illustrated in Figure 7.7 where in average it yielded nearly 21% due to tilting wind from perpendicular to incident 60°. In other words, the Figure suggested that a 30° deviation in wind angle of incident would consequently reduce 20% of initial velocity recorded at perpendicular, i.e. w_i=90°. This was the general behaviour with MLW of various aperture dimensions examined, with some reservation at d=0.01m.

The case was not proportional as measurements took place further. These percentages were further enhanced as room depth increased depending on each model configuration. Gaps between curves at wind incidences 90°, 75° and 60° were gradually increasing as velocity was measured along room depth. At 60°, the reduction reached its

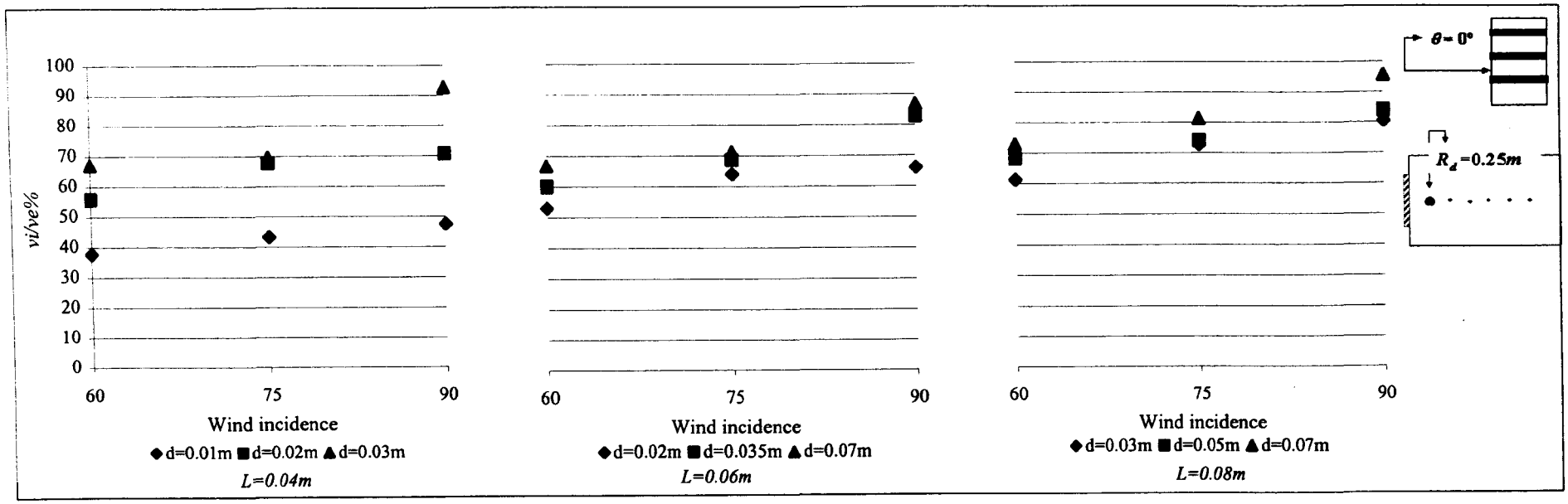

Figure (7.7): The effect on wind angles of incidence on velocity reduction near the MLW, R_d=0.25.

minimum readings in the middle of the room with some reservations at models with d=0.07m. Hence, it was thought that as further wind directions were examined, the breeze flow along room depth would be less effective for all models examined, with exception of measuring location R_d=0.25m. Generally, it was evident that velocity drop due to deviation in wind direction was significant when accompanied with room depth and varied in accordance with various d selected.

7.4.3. Velocity drop as function of room configuration

The observation mainly covered the horizontal velocity magnitude represented in the room depth. In this section, vertical velocity magnitude is also highlighted. As noted before, one of the main advantages of employing the MLW is the possibility to control the flow patterns to various sections within the room, including ceiling, living and ground zones. The following is the discussion of each of these effects.

7.4.3.1. Room Depth (R_d)

Some of the studies reviewed in the literature, such as Givoni (Givoni, 1981), Sobin (Sobin, 1983), Muniz (Muniz, 1985) and others, showed the effect of velocity drop as function of room depth. Here the six measuring locations along room (R_d) were taken at distance of 0.25m each.

The relation between R_d and v_i/v_e% contained two approaches of evaluation including the percentage of velocity reduction along room depth with reference to R_d=0.25m and the effective ventilation along room. As for the former, readings at R_d=0.25m were taken as a reference to trace the percentage of reduction at other measuring locations examined when the external wind velocity was v_e≅2m/s. In fact it was found that along room depth the flow of air had lost 30% - 50% of its momentum force at R_d=1.50m.

Figure 7.8 shows the relationship between the reduction percentages from various measuring locations along room depth.

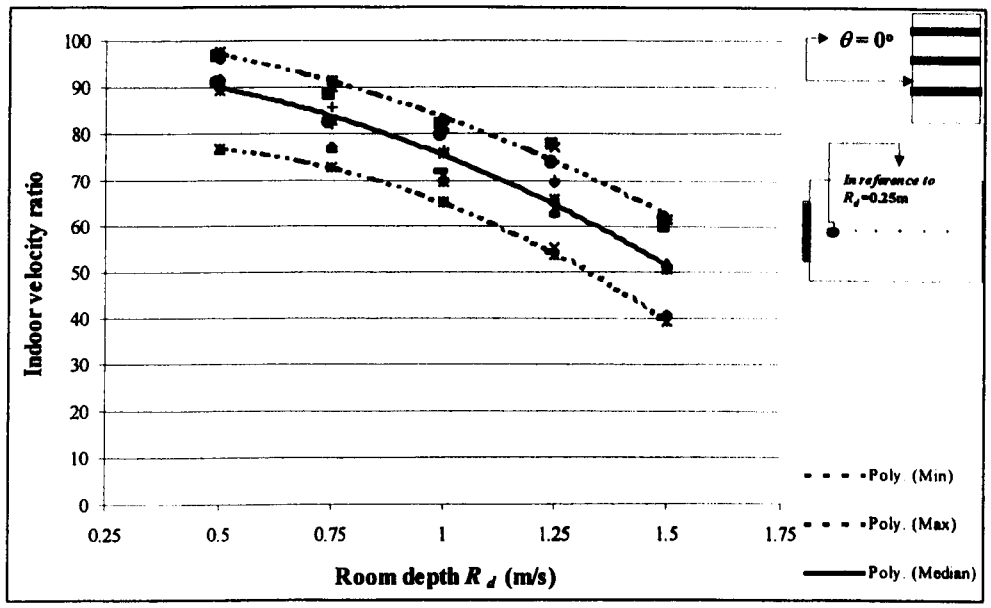

Figure (7.8): The ratio of velocity reduction along the room with reference to R_d=0.25m.

Comparable results were attained in models with same opening dimensions (d). The effect of louver depth (L) at those model configurations was from 5% in smaller depth scales up to 10% at the maximum dimension evolved showing that L effect was minor at horizontal inclinations. In contrast, when similar depths with variety of d involved, velocity drop curves varied in accordance to the size of various opening dimensions chosen (Appendixes C.5). In general, 95% of MLW units showed that curves of v_i/v_e% due to room depth were above 40%, even at the farthest measuring location, i.e. R_d=1.50m.

Also, the room depth was a sound factor when louver inclination was involved at inclinations $0° \leq \theta \leq 30°$. Steeper curve regression of R_d were produced at those inclinations due to the considerable variation occurring in v_i/v_e% between extreme ends of R_d measuring locations. These curves were smoother at inclinations $\theta \leq 45°$ as only 15% of

data were scattered above 20% of v_i/v_e at various MLW configurations examined. Thus, MLW greater than 30° of inclination would be ineffectual in producing velocity drop variations along the centre axis of room depth (Appendices C.5 to C.11).

7.4.3.2. Room Height (R_h)

Velocity measured at certain height above was taken at 0.0725m above and below MLW frame edges and at a distance of 0.185m away from ceiling to shelter against discrepancies occurring due to wall jet phenomenon (Awbi, 1991) (Etheridge and Sandberg, 1996).

The inclination $\theta = 0°$ showed the poorest performances since incoming air was not deflected upwards and continued in a similar direction. Similarly, the result found at $\theta = 60°$ was not effective, with the exception of the first measuring location, R_d=0.25m. However, other inclination angles showed higher percentages of v_i/v_e% inclinations at the specific room height. For example, the highest records of v_i/v_e were found at R_d=1.00m at inclination angle of 15°. Meanwhile, room depth at distance of 0.50m was the optimum measuring location for all models examined when louvers were tilted to 30° angle. Also, The maximum ranges of data achieved were found at distance of 0.25m for both inclinations, 45° and 60°. All these findings demonstrate that the velocity distribution patterns inside a space would vary according to MLW configurations beside other variables such as wind data and room configuration (Appendix C.5 to C.11). This is more likely the reason why curve patterns of v_i/v_e% would vary at various room heights (R_h) and depths (R_d) indoors. Finally, the v_i/v_e was found to be less than 50% at nearly 92% of data examined, showing that the maximum ratio indoors, with the presence of wind inclination will not reached more than half of the wind speed. This figure even becomes more critical with the presence of steeper louver inclinations as seen in the Appendices.

7.4.4. Velocity drop as function of MLW porosity *(p)*

The porosity (p) of the MLW depends on the geometry and the number of louver blades in each unit. When blades are in perfect horizontal position, i.e. $\theta \cong 0$, p is considered at its maximum and diminishes according to the degree of inclination, say p_θ. Thus, data measured of (v_p/v_e%) represent the ratio of velocity drop at the external front panel of MLW on the windward side (v_p) against the actual wind velocity (v_e) (Figure 7.1). The porosities ranged from 50% to 87% and were calculated on the basis of the ratio of inlet opening over the total area of the MLW unit when $\theta \cong 0$. The aim was to find out how much resistance was offered by the geometry of MLW different configurations on external reduction of airflow speed.

There was a strong relationship between porosity of MLW geometry against v_p/v_e%. The ratio $v_p/v_e \cong 62\%$ when selecting the MLW units with minimum porosity percentage, i.e. p=50%. This would in other words suggest that air stream lost approximately 40% of its momentum velocity before reaching the inlet external surface due to the resistance caused by inlet porosity percentage. However, the loss decreases as the development in porosity percentage occurs. As found at the other extreme porosity percentage, p=87%, the loss was less than 5% as the ratio v_p/v_e was found to be approximately 96%, as demonstrated in Figure (7.9).

In addition, it was interesting to underline that when measuring the velocity drop at R_d=0.25m for the same model unit both porosity percentage and the ratio v_i/v_e were almost identical, i.e. $v_p/v_e\% \cong v_i/v_e\%$. A more defined description of this phenomenon is illustrated in Figure (7.10) which shows that, as a laminar flow of air passes inlet surface of the louvers, it generates its speed along the louver depth causing a *free-jet* flow with higher speed on the outlet surface than that on the inlet. This speed along the centreline of the

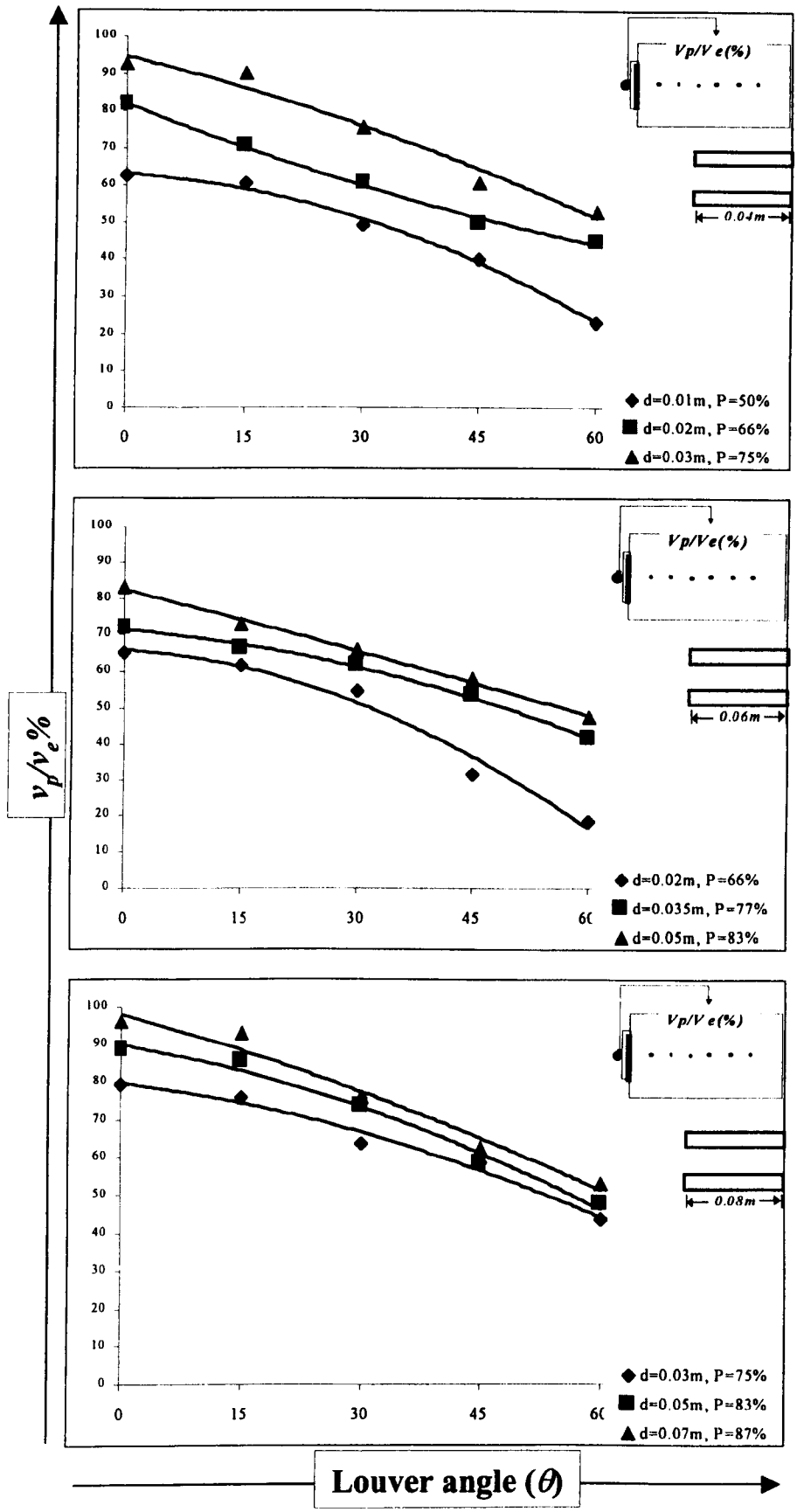

Figure (7.9): The reduction of velocity as function of porosity percentage (*p*).

free-jet eliminates and reaches its initial speed at the inlet surface at a distance that depends on a number of factors such as MLW geometry, viscosity of air, pressure drop, density, etc (Awbi, 1991). Amongst these factors is the geometry of MLW unit that is our concern at this stage. Therefore, Figure (7.11) was developed showing both v_p/v_e% and v_i/v_e% against various porosity percentages examined. It is concluded that at all MLW units with p<70% the velocity of *free-jet* laminar flow speed reached same velocity recorded at reference point before R_d=0.25m. Contrary to the rest of models both velocities were identical at that

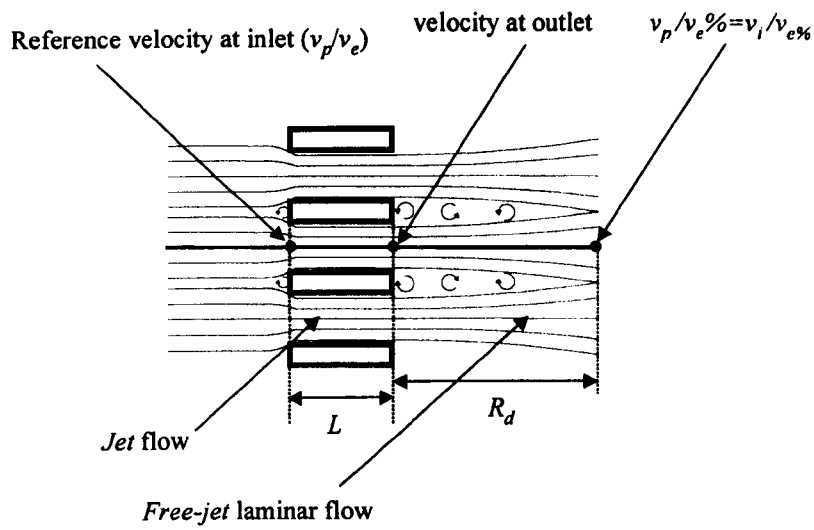

Figure (7.10): The phenomenon of relationship between v_p/v_e% and v_i/v_e%.

room depth.

In practice, data also showed that models with p≥75% were preferable when much air would be needed, to ventilate a space indoors since they provide less resistance to flow stream. Thus, designers would be able to maximize or minimize airflow within the space indoor on the basis that porosity percentages are identified.

As louvers were tilted to 15° of inclination, the reduction in v_p/v_e% due to porosity was of approximately 5%. But the correlation curves were falling apart forming a major reduction as further inclinations were selected. Figure (7.9) shows the correlation curves produced for each angle. In general, reduction in the v_p/v_e% with the presence of inclination angle of louvers ranged from 90 to 40%. This was the case in 80% of models investigated and only 20% of data were scattered above and lower limit band. It confirmed the hypothetical justification discussed in earlier chapters which states that these porous elements were made with maximum capabilities to maximize the amount of air penetrating whilst protecting indoors from direct sun radiations.

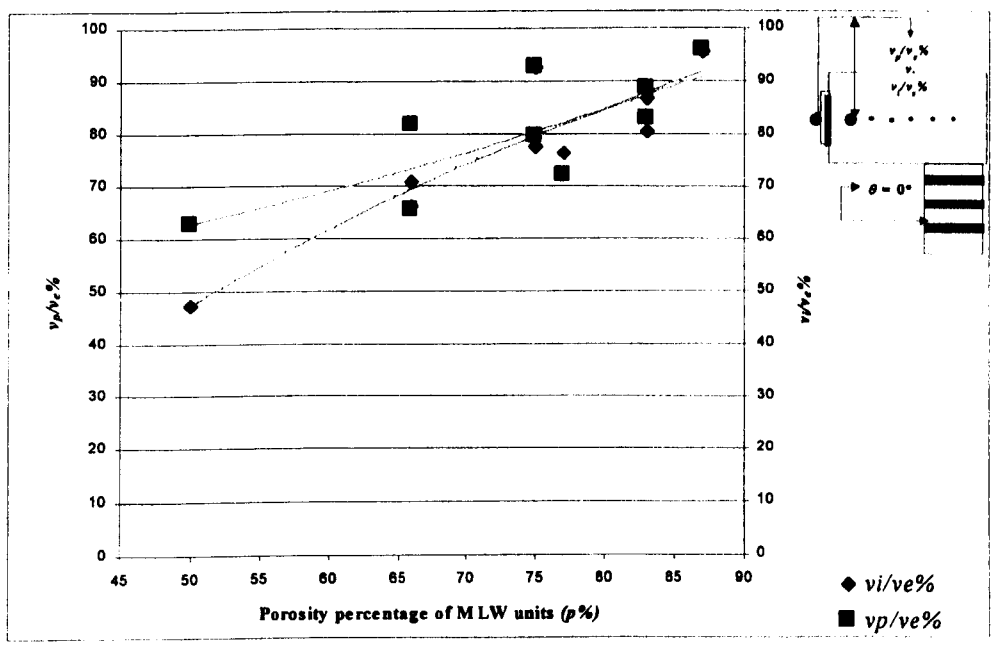

Figure (7.11): The v_p/v_e% and v_i/v_e% against various porosity percentages examined

7.4.5. Velocity drop as function of MLW configurations

The discussion of velocity drops as a function of the MLW geometry will be covered in this section. As in the previous chapter, the effect of each variable is discussed independently and is followed by the discussion of all variables integrated.

7.4.5.1. Louver depth (L)

As velocity declined with the increase of room depth no major variation was found between varieties of depths examined under similar configurations. For example, the curves representing data collected at various louver depths, 0.04m and 0.06m, were comparable and individual regression curve was then recommended to represent such relationship with standard error of less than 5% and coefficient of determination r^2=0.996. Similar results were achieved when comparing depths of 0.06m and 0.08m with similar

Table (7.3): the comparison between various louver depths and their statistical mean values along with the standard errors.

R_d	d=0.02m		Mean	St. Dev.	St. error
	L=0.04m	L=0.06m			
0.25	70.729246	66.061065	68.395155	3.3009022	2.3340903
0.5	67.827403	61.7	64.763702	4.3327286	3.0637017
0.75	61.948019	59.576079	60.762049	1.6772152	1.1859702
1	57.683573	50.088317	53.885945	5.3706571	3.7976281
1.25	54.605097	36.437043	45.52107	12.846755	9.0840273
1.5	42.038859	33.3838	37.71133	6.1200511	4.3275296

R_d	d=0.03m		Mean	St. Dev.	St. error
	L=0.06m	L=0.08m			
0.25	82.891749	77.441332	80.16654	3.8540264	2.7252082
0.5	74.236689	70.931113	72.583901	2.3373956	1.6527883
0.75	60.434015	59.853646	60.14383	0.4103824	0.2901842
1	57.683573	50.441585	54.062579	5.1208591	3.6209942
1.25	54.605097	45.1	49.852549	6.7211186	4.7525486
1.5	42.038859	29	35.51943	9.2198659	6.5194297

R_d	d=0.05m		Mean	St. Dev.	St. error
	L=0.06m	L=0.08m			
0.25	86.82816	80.418875	83.623518	4.5320495	3.2046429
0.5	84.759021	72.949786	78.854403	8.3503905	5.9046177
0.75	74.38809	66.161998	70.275044	5.816725	4.1130457
1	66.515266	57.178905	61.847086	6.6018044	4.6681807
1.25	60.98915	43.250063	52.119606	12.543428	8.8695433
1.5	53.520061	31.743629	42.631845	15.398263	10.888216

R_d	d=0.03m		Mean	St. Dev.	St. error
	L=0.04m	L=0.08m			
0.25	92.658	77.441332	85.049666	10.759809	7.6083338
0.5	71.183447	70.931113	71.05728	0.1784271	0.126167
0.75	71.5	59.853646	65.676823	8.2352157	5.8231769
1	65.2	50.441585	57.820792	10.435776	7.3792077
1.25	58.6	45.1	51.85	9.5459415	6.75
1.5	48.3	29	38.65	13.647161	9.65

level of confidence. In other words, the increase at louver depth to one half would not cause significant resistance to internal airflow measured. However, when doubling louver depth as in L=0.04m and L=0.08m, it was found that significant variations of velocity would occur at $R_d \geq$ 1m (Table 7.3). Similarly, with the larger apertures examined, there was an evidence of the significance when changing the louver depth. Nevertheless, when examining the mean values of those deviations along with there standard errors, it is believed that the variation in depth near the window, $R_d \leq$ 1m, falls within the margin of errors since the maximum error was less than 10%. In this scale of experiments, this may be acceptable to indicate the insignificance of louver depth near the window. But at

Rd>1m, this homogenous relationship was not possible since velocity drops were clearly falling apart from one depth to another. The curves would even fall apart more significantly as room depth increases as shown in Figure (7.12).

Results were homogenous with the presence of louver inclinations $15^{o} \leq \theta \leq 60^{o}$, the coefficient of determination of those curves was $r^2=0.999$ at 95% models examined with standard error of mean less than 5% (see appendices C.6 to C.9). This homogenous relationship was also found with the presence of various MLW units observed.

The general statistical value of this variable to contribute any adjustment to indoor velocity ratio was the least affecting variable since the $r^2 \cong 0.2$.

7.4.5.2. Louver inclination angle (θ)

The reduction of air velocity at $\theta=0^{o}$ was relatively smooth and the curves along the room had not shown considerable or sudden drop. Nevertheless, the curves produced for other inclinations showed some significant drops relative to the inclination selected. For instance, the effective flow at 15^{o} was present up to distance R_d =0.75m. Subsequently a major airflow velocity drop was shown for all models examined, i.e. *vi/ve*<20%. This drop was even closer to MLW unit when both inclinations of 30^{o} and 45^{o} existed as the effective flow was found only around the first measuring location near the MLW. 60^{o} Angle showed the poorest performance amongst other examined inclinations since maximum *vi/ve* < 30% regardless of the rest of MLW variables (see Appendices C.5 to C.9).

The situation was clearly different as flow above the centre axis was considered. Measurements of various inclinations carried out with the presence of room height were quite distinct from those measured at the centre. As noted before, while the flow at $\theta=0^{o}$ was found very minor and negligible, both louver inclinations of 15^{o} and 30^{o} were quite

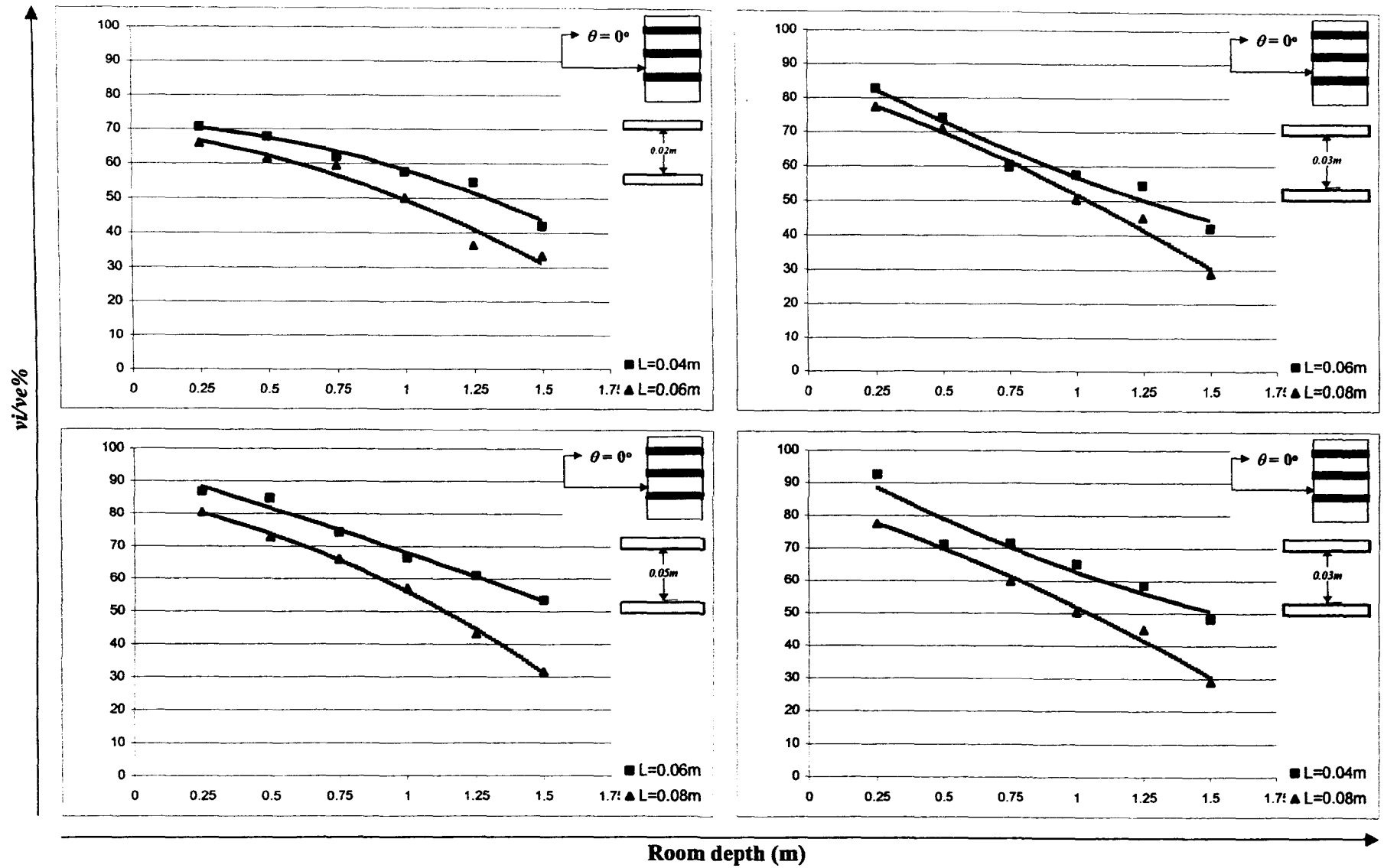

Figure (7.12): The comparison of various louver depths effect in relation to the room depth.

accepted as room depth increased. The highest records for angle of 15° was found around the measuring location R_d= 0.75m and 1m with smooth decline in flow after them. Similarly, the effective velocity at θ=30° was found around R_d = 0.50m and 0.75m away from the MLW. Finally, at the first 0.50m of room depth it was found that the optimum velocity resulted from both inclination 45° and 60° as shown in (see appendices C.8 and C.9). This was to ensure that the vertical velocity profile within a space would vary according to the change in louver inclination angle.

Interestingly, it was possible to trace the significant contribution of the louver inclination angle when examining its coefficient of determination from statistical perspective. As seen in Appendix C.12.a, the statistical behaviour of θ with respect to *vi/ve%* revealed some significance since r^2 = 0.736 for the variety of MLW geometries along the room depths examined.

7.4.5.3. Louver aperture (*d*)

Internal velocity as a function of aperture distance between louver blades shaped the major factor to the total velocity reduction indoors. It varied in accordance with the size of various opening dimensions chosen. At this stage no consideration was given to louver depth since the increase to one half would be less effective to velocity readings indoor, up to R_d=1m.

At the maximum aperture examined, air lost nearly 20% of its initial speed after reaching R_d=1m while it lost 50% at R_d=1.5m. Likewise, only 5% was lost at R_d=0.25m showing that this model configuration may be recommended where cross ventilation may be necessary. Obviously the MLW with minimum aperture showed the poorest performance since 50% of wind speed was lost at first measured location and almost 90% was lost at 1.5m of room depth as seen in Appendix (C.5). Additionally, it was found that

the decrease of 0.02m in d=0.07m would be accompanied with a decrease in v_i/v_e =10-15% near the window.

In general, curves of v_i/v_e% due to room depth were above 40% even at the farthest measuring location when d=0.01m is excluded. Figure (7.6) shows the correlation curves produced for the louver apertures measured up to R_d=1m.

However, the d_θ variable was only sufficient to explain about 38% of the total reduction in velocity drop for all models selected. As seen from the Appendix (C.12.b), this has some effect on the reduction of flow, yet its effect was less significant than the inclination angle effect.

7.4.5.4. Velocity drop as function of free area (A_f)

The free area was found to be a more appropriate variable corresponding to the velocity drop across the MLW rather than d_θ. Based on the various configurations selected, the A_f which ranged from approximately 33 to 85% were gradually accepted as the result of *vi/ve%*. The general effect showed that A_f explained nearly 65% of the air velocity characteristics inside the room as the coeffiecnt of determination exceeded 0.60 (see Appendix C.12.c). Hence, the free area was a better factor than MLW aperture.

7.4.5.5. Louver number (N)

The general behaviour of louver number was not sufficiently possible to determine the indoor velocity reduction across the MLW since the r^2=0.2 as seen in Appendix (C.12.d).

7.4.6. The integration of all variables

The above discussion shed light on the effect on each variable and its contribution to the velocity drop across the MLW. On the one hand, there was an evident effect of some variables such as the louver angle of inclination and the MLW free area. On the other hand, the statistical analysis of these variables has indicated that the louver depth has no significance near the window (see Appendix C.13). It is worth mentioning though that the coefficient of determination of each variable is enhanced when investigated only under horizontal inclination as shown from the table (for r^2 for each variable in $\theta = 0$ and the general model).

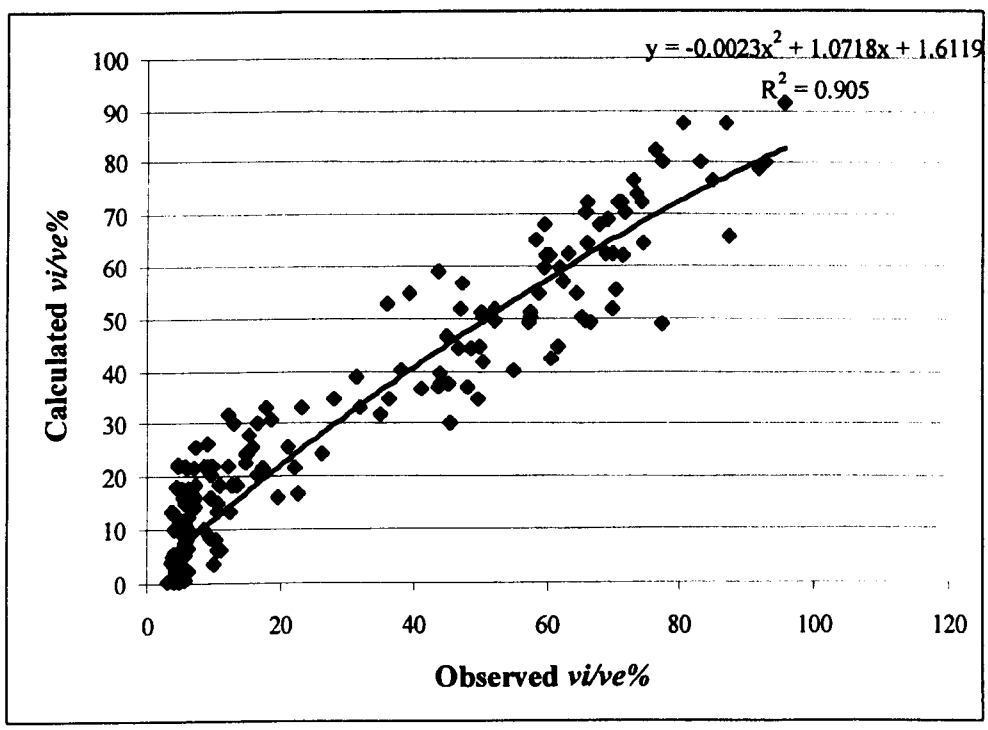

Figure (7.13): The correlation between observed and predicted values of vi/ve% based on equation (7.1).

Nevertheless, as was the case with the previous chapter, none of the variables wwas able to explain entirely the reduction in velocity drop across the reviewed MLW. Following is the integration of all variables made in an attempt to develop the statistical model that explains the total rectum in $v_i/v_e\%$.

The statistical model was developed with error percentage less than 15% and with $r^2 \cong 0.905$. Meanwhile, when including the various inclinations involved in this study, the model (Eq 7.1) was the best to sufficiently explain the velocity reductions function to various MLW geometries examined. Figure (7.13) and Appendix C.13 demonstrate the correlation between the observed values of $v_f/v_e\%$ compared with the predicted value which corresponds to the following equation:

$$\Delta P = c + \alpha.Q + \beta_i.A_f + \chi_i.\theta + \delta_i.N + \left|(\alpha\beta)_{ij} \cdot Q.A_f + (\alpha\chi)_{ij} \cdot Q.\theta + (\alpha\delta)_{ij} \cdot Q.N\right| \qquad (7.1)$$

where:

c = the intercept defined from the linear curve estimate in Figure 7.1 (1.6119).

α, β, χ and δ are the numerical representations of the variables A_f, θ *and* N, respectively.

A further observation of this equation to fit larger number of MLW parameters was beyond the aim of this research though it represents one of the author's future tasks. Therefore, it is not covered here.

As seen from the Appendix C.13, all variables selected in the model were statistically significant, bearing in mind that some variation may occur if variables not covered by this study were to be included, such as roughness or other variables noted previously.

7.5. Conclusion

This chapter has examined the velocity flow characteristics with respect to the reviewed MLW. In addition, it has highlighted the velocity drop as function to the room configurations and wind data. The conclusions derived from the investigation are as follow:

- Louver angle of inclination is found a main variable to control this while louver depth was the least affecting variables in this phenomenon except with the presence of steeper louver inclination. Nevertheless, the major indoor velocity drop was not due to individual variables but rather to combination of variables that would comprehensively describe $v_i/v_e\%$ as concluded from the various evaluation stages conducted throughout this chapter.

- The description of flow characteristics as function to the free area was found more appropriate than that related to louver aperture. While both variables showed some level of significance, the effect of the former was more practical than the latter.

- The mean indoor velocity ($v_i/v_e\%$) was increasing as a function of wind (v_e) and the maximum increase was less than 15%. This was the general behaviour of MLW under various apertures examined yet when d>0.05m the $v_i/v_e\%$ was proportional to v_e.

- Wind direction has also some significance on indoor air velocity since normally a 20% reduction in $v_i/v_e\%$ near the window was found when wind was to deviate 30° from perpendicular.

- The vertical and the horizontal velocity profiles along the room height and depth respectively are much related to the MLW configurations examined.

- The porosity percentage is a sound alternative to evaluate the performance of MLW as it gave an understanding of the flow characteristics at the windward side near the modulated louvered windows.

- Airflow velocities in a room containing an MLW result from an interaction of louver geometry, room geometry and prevailing wind conditions.
- It was possible to establish a dimensionless relationship of velocity characteristics as function to various MLW parameters involved near the window, Rd≤1m. Therefore, these results will be the base of the further evaluation stages that will be covered next chapter using the computational fluid dynamics (CFD) technique.

The appraisal stage has demonstrated the flexibility of the MLW design in relation to accomplishing similar results. In another words, similar airflow characteristics were achieved with a number of MLW configurations. There is some evidence to suggest that the flexibility in the design of MLW that will not encounter much reduction in airflow passing louver blades. These could be guidelines to be implemented in practise for further implementation in production. Some of the conclusions attained from Chapters 6 and 7 were sound and considered key elements to recall the traditional louvers geometric reviewed in earlier chapters.

7.6. References

1. Awbi, H.B. (1991) *Ventilation of Buildings*, London: E & FN Spon.

2. Bittencourt, L.S. (1993) Ventilation as a cooling resource for warm -humid climates: An investigation on perforated block wall geometry to improve ventilation inside low-rise buildings. Architectural Association Graduate School. Unpublished Ph.D. thesis.

3. Chand, I., Bhargave, P.K., Sharma, V.K. and Krishak, N.L. (1988) "Studies on the effect of mean wind speed profile on rate of air flow through cross-ventilated enclosures". *Architectural science review* **(35)**-p.83-88.

4. Etheridge, D. and Sandberg, M. (1996) *Building Ventilation: Theory and Measurements*, John Willy & Sons.

5. Evans, M. (1980) *Housing, Climate, and Comfort*, London: Architectural press.

6. Givoni, B. (1981) *Man, Climate and Architecture*, 2nd edn. London: Applied Science Publishers Ltd.

7. Muniz, P.A. (1985) The geometry of external shading devices as related to natural ventilation, daylighting and thermal comfort, with particular reference to tropical hot-humid climates. Unpublished Ph.D. Thesis.

8. Sharples, S and Maghrabi, Amjed (2000) "Airflow through louvers: an experimental and CFD study". The Hague: Proc. 21st. AIVC Conference (To be published).

9. Sobin, H. (1983) Analysis of wind tunnel data on naturally ventilated models. p.287 Tucson, Arizona, USA: Harris Sobin & Associates.

10. White, M. (1999) "Ventilators: Ventilation and acoustic Effectiveness". *BRE* **(IP4/99)**-p.1-8.

11. Yousoufian, H.H. (1992) "Correlation of residual velocity with throw terminal velocity from a louver-faced unidirectional diffuser". *ASHRAE Transactions* **(2)**-p.1-8.

CHAPTER 8: SIMULATION OF VELOCITY DROP ACROSS THE MLW: CFD APPRAISAL STAGE.

8.1. Introduction

This chapter is devoted to exploring and extending investigations carried out in the previous chapter. On the one hand it examines the CFD coding to simulate airflow around the reviewed modulated louver windows; on the other hand it highlights the airflow patterns around the MLW and the subsequent flow within the room, based on MLW and inlet configurations as well as outlet configurations that are typically found in Jeddah. It was not possible to examine them in the previous chapter due to the dimension of the physical model under which laboratory measurements were carried out. A description is first given of the historical background to the theory of numerical modelling and the application of CFD in predicting airflow in buildings. The range of CFD software packages used for simulation and justification of CFD code selection is discussed here. Basic conservation equations, turbulence modelling and other CFD requirements for simulation are also covered. The set up of MLW model configurations and the boundary conditions are discussed before the comparison of both CFD and laboratory results takes place. The chapter ends up by highlighting patterns of airflow through MLW with reference to both inlet and outlet configurations implemented in Jeddah, Saudi Arabia.

8.2. Literature Review on computational fluid dynamics

8.2.1. Historical background

In most flow regimes considerable flow complexities are commonly encountered and analytical solutions are not possible. The equations of fluid dynamics can be solved numerically with the aid of modern computers. Therefore, many computer programmes or computer codes, as they are called, have been developed specifically to solve complex flow equations. Each different code tends to have certain strength and is best suited to particular types of flow. The set of techniques and procedures to achieve this has led to the development of what is known as computational fluid dynamics (CFD). CFD is the science of developing approximate numerical solution to predict the air motion based on Navier-Stokes equations, the energy equations, the mass and concentration equations and turbulent velocity and its scale equations (Schaub et al. 1995), (Awbi, 1991), (Alamdari, 1995), (Said et al. 1995), (Jones and Whittle, 1992). The fundamental laws of the conservation of mass, momentum, thermal energy and concentration species within the microclimate, or the enclosure, describe these equations. In CFD, the conservation equations are solved numerically in order to generate field values for the static pressure, velocity components, temperature, turbulent flow and concentrations of contaminants in the enclosure (Alamdari, 1995), (Said et al. 1995). The flow is solved by a set of cells (known as control-volumes) represented by computational grid either in two or three physical dimensions. This is known by the finite-volume CFD solution. Through such a process, based on computational efficiency and level of experience of the user, the CFD model has the potential to predict the velocity, temperature variations, air cell contamination as well as the room ventilation efficiency (Awbi, 1989), (Alamdari, 1995), (Jones and Whittle, 1992). Performance of the indoor environment in relation to level of

comfort can also be predicted, and then compared with the level of discomfort or dissatisfaction of occupants in indoor environments. Although it is not possible to leave out real experiments, numerical experiments using CFD allow the determination of certain trends and give an insight into the physics of complex problems that would be impractical to study experimentally. Etheridge and Sandberg (1996) noted that CFD may or may not be the best alternative amongst other techniques applied depending on the scale and complexity of the problem to be solved. The advantages and disadvantages of each technique were reviewed in Chapter 4 and summarized in Table (4.1).

8.2.2. CFD for airflow prediction in buildings

The analysis of indoor air motion within a building has become a significant task for designers and engineers to improve indoor air quality and, in turn, to enhance the environmental conditions for occupants within buildings. A typical person spends up to 90% of his time indoors in residential and commercial environments (Chen and Jiang, 1995). Airflow principles are governed by the fundamentals of physics and are associated with variables in the environment such as temperature, pressure, obstacles, velocity, etc. Patterns of airflow in buildings, however, are related to what is mentioned above as well as other factors that control microclimate and macroclimate air motion. As stated previously, the macroclimate is defined as the flow regime around a building while microclimate relates to the regime within it. The airflow in buildings may be predicted by physical measurements including full-scale, scale mock-ups modelling and numerical techniques, i.e. computer modelling technique (Chen and Jiang, 1995), (Alamdari, 1995). The latter technique had been increasingly applied by researchers to predict room air quality, behaviour of airflow and how contaminants and pollutants are transported in the building

ventilated by natural or mechanical means. The following outline intends to highlight the CFD modelling as a tool for predicting air distribution within and around buildings.

From the increased awareness of the health problems associated with indoor air pollution emerged the interest to improve the knowledge about airflow patterns and contaminants transport in space. CFD has been used for predicting room air distribution since 1970s (Aynsley, 1999). For the past few decades engineers and scientists have been developing numerical methods and computer software to solve complex structures of partial differential equations numerically (Maghrabi and Sharples, 2000). Schaub et al. (1995) and Jones and Whittle (1992) reported that Nielsen was the first to apply CFD numerical technique to predict room air distribution in 1975, the technique that was practised by many later on. After two decades of development it is advised that CFD be an alternative tool in conjunction with experimental mock-ups and full-scale measurements techniques for room air distribution (Schaub et al. 1995), (Awbi, 1991), (Awbi, 1989), (Weathers and Spitler, 1998), (Alamdari, 1995), (Jones and Whittle, 1992).

In the building engineering field, site observations, numerical calculations and laboratory measurements have been validated using CFD. Some of those are found in (Jones and Whittle, 1992), (Murakami et al. 1995), (Weathers and Spitler, 1998), (Dascalaki et al. 1996), (Fontiane et al. 1994) and most recently in (Sharples and Maghrabi, 2000). They suggested that the CFD modelling technique has a strong potential for the validation of the results from other techniques. For example, the work carried out by Swainson (Swainson, 1997) concluded that the corresponding results obtained from CFD to investigate natural ventilation through a solar chimney were accurate to validate the experimental work. In his work concerning CFD predictions on ventilation efficiency in clean rooms, Chul (Chul, 1997) has also noted an agreement between the full-scale

experimental work and CFD technique. Interestingly, Chul concluded that CFD modelling has an economical advantage over the full-scale measuring technique. The subject has now advanced to the point where many engineers and designers rely totally on CFD results to evaluate and predict air distribution at early stages of design; some of this is found in (Chung and Dunn-Rankin, 1998), (Yaghoubi et al. 1995), (Holmberg et al. 1993), (Gan, 1995), (Kindangen et al. 1997) (Robinson et al. 1999) and others.

The scale of flow regime varies according to the approach intended. In building engineering, these approaches are either classified as macroclimate or microclimate. CFD applications in building engineering range from a small building component such as door or window up to the scale of a multi-storey building or large structure. Figure (8.1) demonstrates some scales of simulation problem solved by CFD. However, the vast majority of studies were conducted on a scale of single room size. On this scale, the model investigates the flow regime of the physical components of air such as contaminations and pollutants produced by mechanical or natural ventilation systems; it could also estimate the infiltration rates, air change per hour and trace patterns of airflow in all locations within the room (Maghrabi and Sharples, 2000). In certain cases, the air movement and thermal performances around the human body or an object could be examined (Alamdari, 1995), (Gan, 1995) (Awbi, 1989). Simulation could be extended to solve flow in large spaces or between a number of spaces within a building or an enclosure. Research conducted by Murakami et al. (1995) evaluated ventilation effectiveness and contaminant concentrations in a wholesale market structure using CFD. Also some studies investigated smoke control within buildings and in atrium spaces (Chow and Lau, 1993), (Anon., 1995a). Other research predicted natural convection between two spaces like that carried out by Williams and Baker (1994) or even in the number of flows within the same building like, that conducted by Robinson (1999). On a larger scale, the outdoor airflow simulation

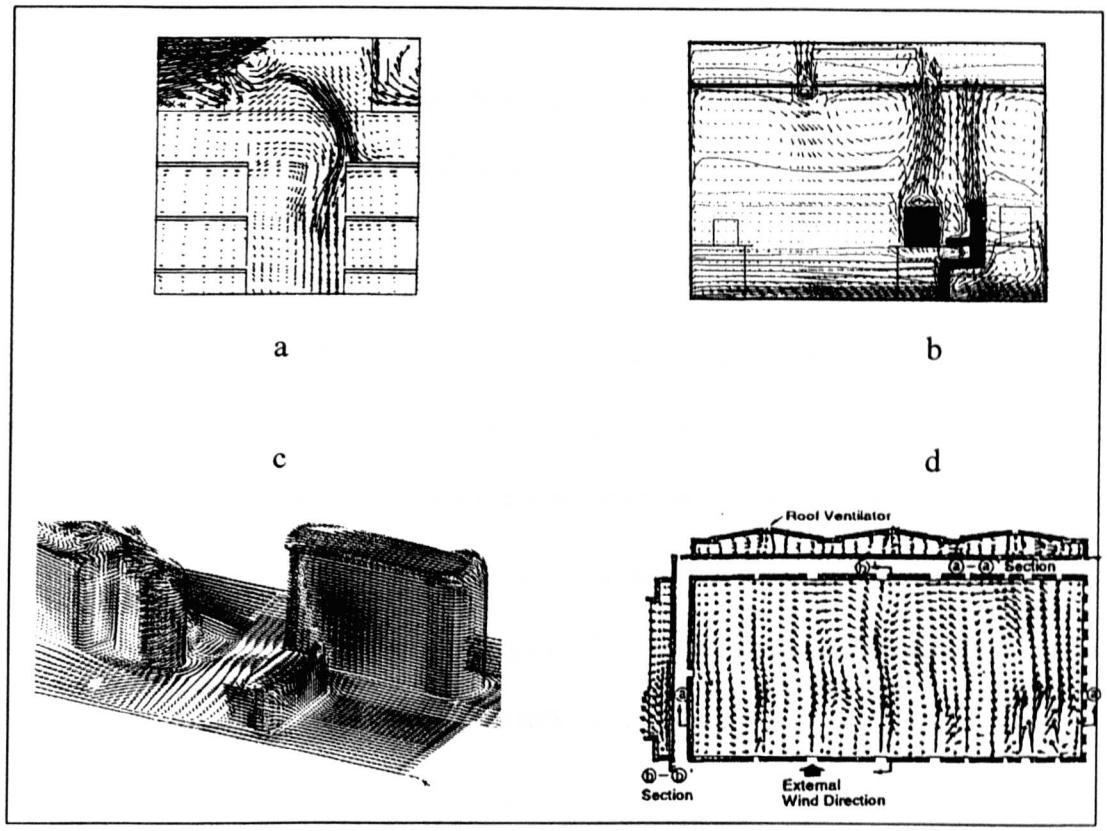

Figure (8.1): Some examples of various problem scales covered by the CFD technique. [a: A multi story building (Robinson et al. 1999)], [b: Mechanical airflow systems (Alamdari, 1995)], [c: airflow around buildings (Alamdari, 1995)] and [d: huge indoor spaces (Murakami et al. 1995)].

encounters other complications in addition to those discussed at indoor airflow simulations such as wind forces, directions and other environmental factors that could not be solved at certain stage of simulation.

In general, the application of CFD in building engineering is increasingly advancing with the enhancement in computational power. While empirical measurements should not be underestimated, CFD offers an alternative tool for building engineering problems that cannot be easily traced by other measuring techniques. A recent review work carried out by Maghrabi and Sharples (2000) indicated the challenges of using modelling technique for designers and architects in the field.

8.3. CFD applications in buildings engineering

8.3.1. CFD simulation software

There are several commercial CFD packages available at present that have the capability of modelling a wide range of fluid flow problems; amongst these packages are FLOVENT, FLUENT, FLINT, PHOENICS, STARCD and FLOW3D. They suggest similar capabilities, hence the choice of package which is most suitable for the study depends on a number of factors including the appropriateness to the fluid flow problem, the software and hardware requirements in relation to cost and user skills. Help facilities and technical user support services should also be considered.

The present work required facilities for single-phase flow and two-dimensional modelling. FLUENT software was the code chosen to perform solutions of the problem in hand. This software is used heavily in airflow simulation in buildings. Further details are available in the FLUENT user manual (1999). FLUENT was already available on site

(University network and University network remote access) with technical user support services, and the University of Sheffield network is frequently updated with the latest version of FLUENT. That is why the simulation was carried out using the FLUENT version 4.5, and hence, its description in some detail in this chapter. It is worth emphasising that not all the available options of FLUENT are mentioned here, but only those relevant to this work.

8.3.2. Basic Equations of CFD

The first step in numerical modelling is to establish the basic conservation equations based on the principles of fluid mechanics and relevant components such as heat and flow, etc. These equations constitute a system of non-linear simultaneous partial differential equations that can be solved numerically. The equations used in this numerical modelling are presented here.

The main problem of fluid dynamics is the determination of the velocity and state of the fluid subject to certain imposed conditions. Throughout this work it has been assumed that the fluids are gases at ambient pressure that behave ideally. No consideration was given of the case of chemical reactions, air contaminations or heat transfer since the aim was to investigate the air quantity rather than quality. The equations that allow the solution of the most general case of ideal gas mixture are the following:

Mass conservation:

$$\frac{\partial \rho}{\partial t} + \frac{\partial}{\partial x_i}(\rho u_i) = 0 \qquad (8.1)$$

Momentum conservation:

$$\frac{\partial}{\partial t}(\rho u_j) + \frac{\partial}{\partial x_i}(\rho u_i u_j) = \frac{\partial}{\partial x_i}\left[\mu\left(\frac{\partial u_i}{\partial x_j} + \frac{\partial u_j}{\partial x_i}\right)\right] - \frac{\partial p}{\partial x_j} + \rho g_j + F_j \qquad (8.2)$$

The left side of the equation represents the convection term, and the terms on the other side represent, in sequence, the diffusion, pressure body forces, and the momentum interaction between forces.

The continuity and momentum equations are non-linear partial differential equations and, together with appropriate boundary conditions, provide a complete description of flows for which the density is uniform.

8.3.3. Turbulence Modelling

Turbulence is one of the remaining unsolved theoretical problems in fluid mechanics (Yang, 1989). Nevertheless, there are different approaches in dealing with engineering problems. The most rigorous treatment is for predicting complex turbulent flows. As discussed in the earlier chapters, turbulence is measured based on the Reynolds number, Navier-stokes, κ–ε model equations and others. The derivation of these equations is not detailed here but some references are suggested to that effect (Etheridge and Sandberg, 1996), (Alamdari, 1995), (Chow, 1995), (Ruyssevelt et al. 1995), (Anon., 1995b), (Anon., 1995c), (Yang, 1989). It is worth mentioning that many engineers have relied on the κ–ε model equation to predict flow around the buildings (Kindangen et al. 1997), and hence, κ–ε model was used in this study.

The above equations describe the time-averaged flow when applied to a finite number of discrete control volumes. The effects of turbulence can be included by

substituting an *'effective'* viscosity in the equations consisting of the molecular viscosity augmented by its turbulent counterpart, μ_t. The differential transport equations for the kinetic energy of turbulence κ and its dissipation rate ε are:

$$\frac{\partial}{\partial t}(\rho k)+\frac{\partial}{\partial x_i}(\rho u_i k)=\frac{\partial}{\partial x_i}\frac{\mu_t}{\sigma_k}\frac{\partial k}{\partial x_i}+G_k-\rho\varepsilon \qquad (8.3)$$

and

$$\frac{\partial}{\partial t}(\rho \varepsilon)+\frac{\partial}{\partial x_i}(\rho u_i \varepsilon)=\frac{\partial}{\partial x_i}\frac{\mu_t}{\sigma_\varepsilon}\frac{\partial \varepsilon}{\partial x_i}+C_{1\varepsilon}\frac{\varepsilon}{k}G_k-C_{2\varepsilon}\rho\frac{\varepsilon^2}{k} \qquad (8.4)$$

where G_k is the generation term of k and is given by:

$$G_k = \mu_t\left(\frac{\partial u_j}{\partial x_i}+\frac{\partial u_i}{\partial x_j}\right)\frac{\partial u_j}{\partial x_i} \qquad (8.5)$$

The turbulent viscosity, μ_t, is related to κ and ε, by

$$\mu_t = \rho C_\mu \frac{k^2}{\varepsilon} \qquad (8.6)$$

where $C_{1\varepsilon}$ $C_{2\varepsilon}$ C_μ σ_k and σ_ε are empirical constants, with values 1.44, 1.92, 0.09, 1.0 and 1.3 respectively.

The equations mentioned above are transformed into a set of algebraic equations that can be solved iteratively. This transformation, also called discretisation, involves the following.

- The domain is divided into cells or control volumes.
- The governing equations are integrated over each cell.

- The algebraic equations so obtained are solved by iteration as described later. In this section consideration is given to the discretisation procedure.

8.3.4. Physical and computational domains

FLUENT requires detailed specification of flow mechanism and its boundaries in addition to the model of turbulence. The identification of physical and computational domains added to the boundary conditions shape the complicated part of the simulation procedure (Maghrabi and Sharples, 2000).

In order to perform the discretisation of the governing equations the physical space must be subdivided into a number of cells by means of a structured grid. The cells can be built using Cartesian or Body-fitted grid coordinate systems as shown in Figure (8.2). The latter is much complicated and sophisticated to make curves and cylindrical shapes while Cartesian coordinate system is widely used in the rectangular domains (Alamdari, 1995), (FLUENT, 1999). In this research, a two-dimensional Cartesian grid was generated either directly from FLUENT or FLINT (2000). FLINT code is used only to construct the models when simulating louver inclination angle since it was more complicated to use the body-fitted grids coordinate in FLUENT. Permission was given to use it by FLINT's author, as it was not yet commercialised. The node points, i.e. points where the grid lines intersect, define the cells generated. The space where the integer numbers are used is called the computational domain.

8.4. Boundary conditions

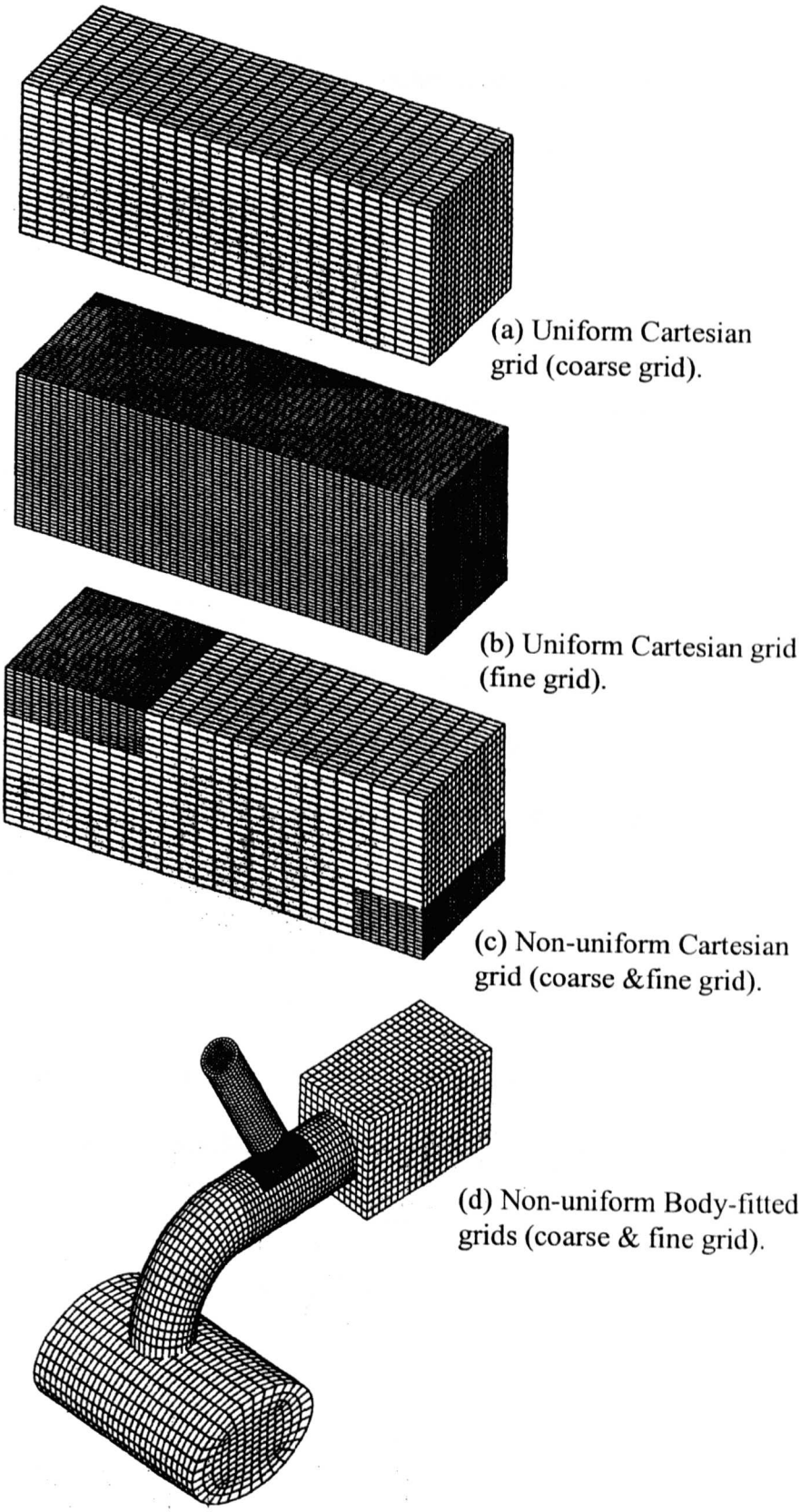

Figure (8.2): Both grid coordinates systems constructed using by FLUENT. [a, b, c: Cartesian grids coordinate system (Holmberg et al. 1993)], [d: Body-fitted grids coordinate system (Alamdari, 1995)].

FLUENT allows for a number of different types of boundary conditions. The following are the terms identified by FLUENT and various data were input to solve the problem. Data mentioned here are those related to the work in hand.

8.4.1.1. INLET

At which conditions of flow components are identified such as velocity, turbulence and composition of the flow.

8.4.1.2. OUTLET

FLUENT does not allow adjustments of the OUTLET specifications. But the normal velocities are adjusted at OUTLET boundary to satisfy an overall mass balance and no velocity gradients should exist. For precise results, it is recommended that air should be fully developed before reaching the OUTLET.

8.4.1.3. WALL

Including walls, floor and ceiling. At these boundaries, the normal velocity component vanishes. Temperature, conduction or heat fluxes were not specified as they were not of concern in the current solution. The pressure gradient is zero. If the dimensionless distance becomes less than a certain value, then a laminar expression is used instead.

8.4.2. The iterative solution procedure

The equations are not solved simultaneously at all nodes. Instead, a line-by-line solution procedure is made. The last step in the calculation is the inclusion of the interaction terms between the second phase and the fluid phase, as discussed in the chapter.

8.4.3. Uncertainties in CFD

The overall uncertainties involved in CFD modelling could be due to several sources. The CFD coding to represent complexities could be a main cause of this. Complexities occurring in a real environment could not - sometimes- be represented numerically as stated earlier. Additional uncertainties are referred to other factors:

- Modelling errors (the inaccuracy inherent in the mathematical model of certain physical phenomena), domain dependency errors, i.e. errors arising from finite representation of a domain.
- Inaccurate implementation of the boundary and initial conditions.
- Iterative convergence errors (i.e. incomplete convergence).
- Grid convergence errors (errors due to insufficient grid refinement, i.e. discretisation errors).
- Lack of user skills and experience in dealing with CFD solution.

8.4.4. Numerical errors

In 1993, the issue was raised concerning the ability of programmes to produce dependable predictions (Anon., 1995b). Different CFD models have different codes that can have significant errors when applied in prediction procedures. While the debate continues, this can be a significant issue not only for unskilled users, but embedded errors are not- sometimes- easily discovered even by highly sophisticated skilful users (Maghrabi and Sharples, 2000). Some of these errors refer to the fact that some of the complexities in the real environment cannot be simplified numerically (Etheridge and Sandberg, 1996) (Awbi, 1989). Error then must be reduced to a reasonable level before accepting solution. Cost may limit the resources that can be brought to bear on a problem. In such a case,

compromise or another approach is necessary. The distribution of grids in the domain could reduce the percentage of error. In other words, the use of finer grids near INLET, OUTLET and WALL (Figure 8.2.c and 8.2.d) would usually increase the solution accuracy and this while increasing computation power and solution timing (Awbi, 1991), (Maghrabi and Sharples, 2000).

8.4.5. Numerical setup

FLUENT necessitates definitions of parameters in order to run proper solutions. Memory allocation, dimension of computational domain (2 dimensions in this solution), size of the computational domain and number of cells must be identified first. Other parameters also must be identified to FLUENT: physical models used, fluid specifications (viscosity, density, etc,) and boundary conditions of INLET, OUTLET and WALL. As earlier stated, fluid temperature was not specified since it was not concerned in this solution.

8.4.6. Iterations of residuals

Once the set up and construction of the model took place and was ready to run, the solution parameter would then depend on the number of iterations of the solver. The residuals of iterations reflect the accuracy of obtainable results. It is applicable either to determine the number of iterations counted or by time-dependence. To activate the time-dependent option, time varying data must be carefully identified, such as flow fluctuations, before running the solution. However, in counts iteration the FLUENT is set to reach satisfactory convergence at (1×10^{-4}) of residual iterations and would stop counting, assuming that results are accurate to depend upon, and hence, save computational timing.

In some studies, the residual of iteration counts would be adjusted to converge at (1×10^{-3}), as found in (Kindangen et al. 1997), and still be acceptable.

8.5. The Models configurations and boundary setup

The general procedure employed to set up geometry, two-dimensional Cartesian grid coordinates system, specification of the boundary conditions and physical constants are discussed here. It is worth mentioning that this stage contained flaws as it is the first of trial calculations but, as always, they are used as a learning process and are improved in the subsequent specifications of the calculations.

8.5.1. Grid distribution

The consideration was taken into account to examine the CFD coding through solving and representing the airflow around the MLW. A two dimensional rectangular physical boundary was therefore constructed. FLUENT grid-based geometry was used, in which the geometry of the domain was determined by control volumes defined by the grid. This is with horizontal louvers blades evolved. As stated early, FLINT code was merely used to construct the two-dimensional domain when louver inclinations were present and the simulation process was carried out using FLUENT. Cartesian coordinates were used in which the grid lines were aligned with the Cartesian (x, y) coordinates.

The overall domain size of the room chamber and location of reference wind (v_e) were defined. A non-uniform grid aimed to enhance the accuracy of the solution. A fine non-uniform grid allowed the grid to cluster more densely in areas where the flow is complex or of interest such as louver blades, ceiling and floor locations. It also allowed the use of grid lines apart in regions that were of lesser interest. Therefore, non-uniform

grid lines were made around the louvers since the dimension is very small, being only 0.02-0.07m. The area of the louver inlet was very small compared to the area of the whole domain, and the activity in and around this entrance was important to the solution of the problem. In order to create the necessary louver inlet dimension it was necessary to alter the grid spacing so that it was concentrated at the louver inlet, in both x and y directions. A single cell around louvers was used at 0.005m far from next cell. This was necessary, as FLUENT calculates the properties of one cell and uses them as an approximation to the next cell. It would have caused great problems if adjacent cells were vastly different in size. These could be the justification that grid lines become narrower around the MLW and other locations within the domain previously stated and compared, as illustrated in Figures 8.3.a and 8.3.b.

The expansion factor (f) which was required for each segment was calculated from the equation below:

$$N_c = \frac{\ln\left[\left(\frac{L_c}{a}\right)(f-1)+1\right]}{\ln(f)} \tag{8.7}$$

where:

L_c is the segment length, α is the starting cell size and N_c is the number of cells in the segment

The grid generated was checked. A graphic examination was also carried out to observe if a good distribution of gridlines had been created as shown in Figures 8.3.a 8.3.b.

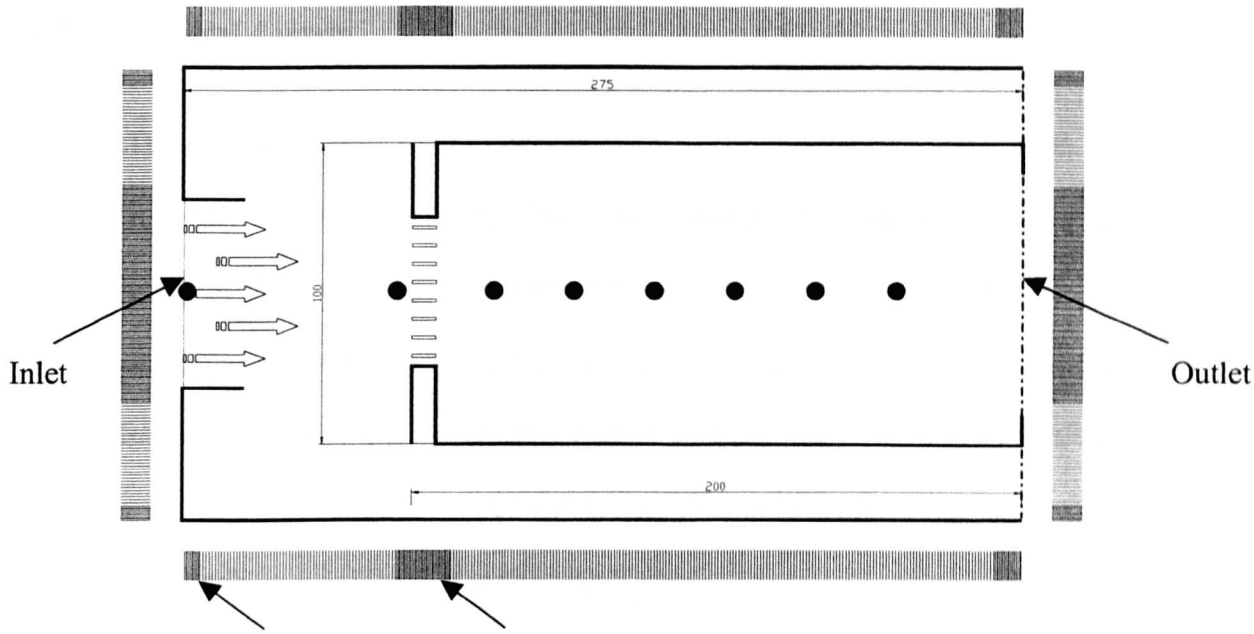

Figure (8.3.a): The model initially constructed to carry out the simulation process (case model I).

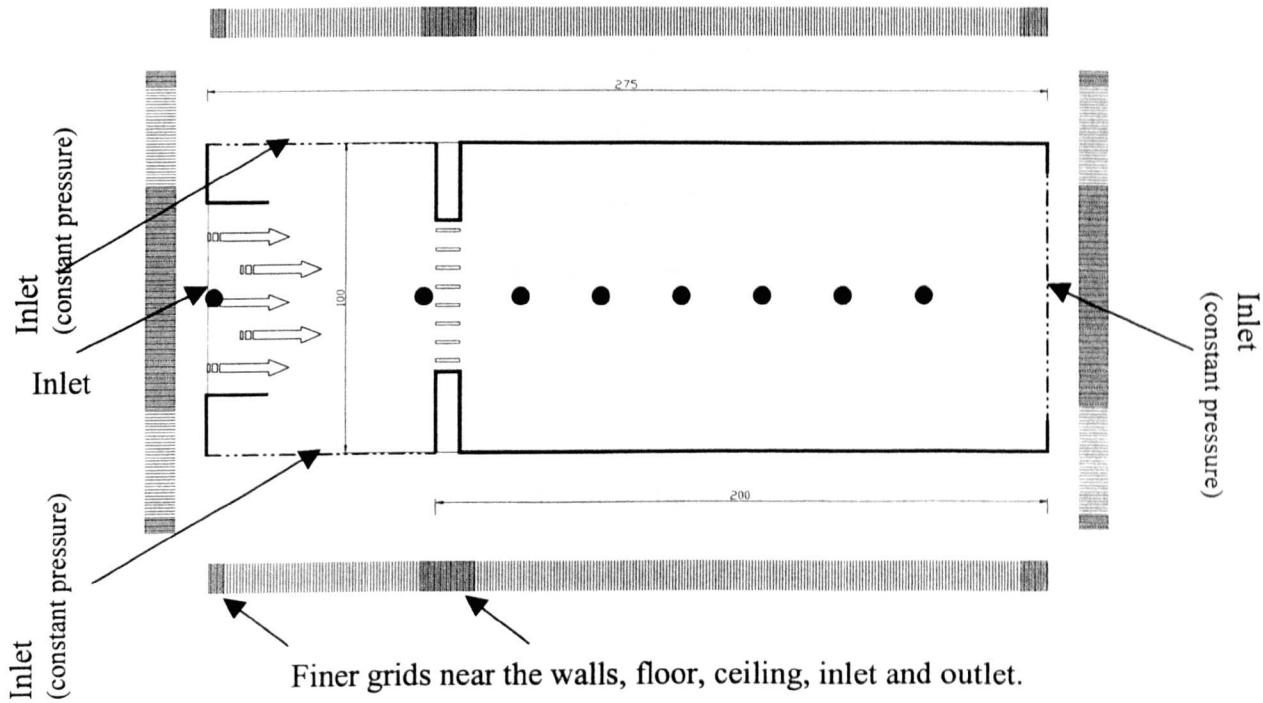

Figure (8.3.b): The modified model constructed (case model II).

8.5.2. Physical domain

The construction of the physical domain usually anticipates some flaw. So these errors were the learning process that improved subsequent specifications of calculations. Initial set up of the laboratory was simulated and both $v_p/v_e\%$ and $v_i/v_e\%$ were examined. The appropriateness of the model selected to carry out validation stage is described here taking into consideration points stated earlier in this chapter. The procedure followed to consider the appropriate model under which comparison took place was in three stages of modelling. Each case model is described next.

8.5.2.1. Simulation model (Case-I)

This case is similar to the laboratory set up (Figure 8.3.a). The test chamber was located between domains INLET and OUTLET as they shaped the vertical edges of the domain while the room chamber with the louvers was floating within them. The reference wind speed (v_e) was located at a distance similar to that noted in section 7.2.1 away from MLW models similar to the laboratory location and all characteristics of the physical domain discussed earlier were clearly specified to the model. Both $v_p/v_e\%$ and $v_i/v_e\%$ were obtained and compared to the physical measurements.

8.5.2.1.1. $v_p/v_e\%$:

The attempt was made to determine the flow resistance zone created at the windward side outside the room due to the MLW. Inevitably, CFD confirmed that MLW models had offered resistance to airflow. This zone however was depending on the MLW tested. In general, the flow resistance zone ranged from 0.35m to 0.60m on the windward side. Results of $v_p/v_e\%$ obtained from both measuring techniques were comparable as

shown by Figure (8.4) and Table (8.1). The error limit between both curves produced from a number of MLW configurations was less than 10%.

8.5.2.1.2. $v_i/v_e\%$:

The first observations of colour-filled contour and regression curve plotted for results obtained from both measuring techniques encountered major discrepancies. The indoor air ratio of mean indoor velocity $v_i/v_e\%$ obtained from CFD was undoubtedly illogical and improper, and the measured cells inside the box accompanied by higher error and discrepancies. On the one hand, the observation showed that as air passed the louver blades its kinetic momentum increased dramatically, causing a higher percentage of errors along the room chamber with a very slight decrease in the $v_i/v_e\%$. Furthermore, the regime of airflow fluctuated and was obviously illogic. Various endeavours were then performed to correct it. However, it was found that neither increasing the non-uniform computational grid cells around louvers and inside the compartment nor considering the surface roughness of the louvers corrected it. Boundary specifications on the other hand were specified correctly. Locating reference wind speeds at various positions, far from louvers, did not correct the error either. In addition, a consultation from the technical support was sought. It was then suggested that errors resulting in $v_i/v_e\%$ could be due to number of factors:

- The flow regime between various zones with dramatic change in their dimensions as found in the case in hand. The area of air gap (d) between louvers examined was much smaller when compared to the area of airflow outside (windward) or inside the room chamber simulated. In such dramatic change in flow volume the jet flow was as/if moving from free-jet condition to wall-jet, to free-jet condition again. All of this occurred through the number

of cells within louver blades and the flow encountered dramatic changes in the fluid components. Even though during the laboratory measurement this phenomenon was found only in CFD, it caused an increasing change in the kinetic force as it was based on mathematical representations of the flow. This force then affected the other adjacent cells around, which led to such error.

- Another reasonable justification of this was concerned with CFD numerical coding. In practice, the flow of air within and around porous elements such as louvers would be accompanied with dramatic complexities occurring in physical properties of air such as air viscosity, static pressure, velocity, etc. These could not be simplified theoretically, and correcting them was beyond the scope of the laboratory experiment. Therefore, the CFD equations representing them may not represent the complication in the real environment. Additionally, most available CFD packages deal with issues related to ventilation aspects in simplistic ways and may not necessarily reflect those types of complexities as noted before.

8.5.2.2. Simulation model (Case-II)

This case was similar to the latter except that the outlet was replaced by an INLET with a constant pressure (*IP*) (0 pressure difference at *IP*) that permitted air to float at inlet boundaries according to velocity and direction of a fluid (Figure 8.3.b). While this solution did not correct the problem, it gave more assurance to the accuracy of measured $v_p/v_e\%$ at laboratory (Table 8.1), (Figure 8.4).

The anticipated flaws that emerged from the two models cases discussed earlier led to the conclusion that errors emerged inside the modelled test chamber, where the $v_i/v_e\%$

Louver aperture (m)	Laboratory (v_p/v_e%)	CFD (case model I)				CFD (case model II)			
		Result (v_p/v_e%)	Resid.	Error (%)	r^2	Result (v_p/v_e%)	Resid.	Error (%)	r^2
0.03	79.43	78.24	1.19	1.50	98.50	75.76	3.68	4.63	95.37
0.05	88.49	85.92	2.57	2.91	97.09	84.85	3.64	4.11	95.89
0.07	95.79	93.39	2.40	2.50	97.50	93.43	2.35	2.46	97.54

Table (8.1): Results of (v_p/v_e%) obtained for both models built (case model-I) and (case model-II) compared with the laboratory results.

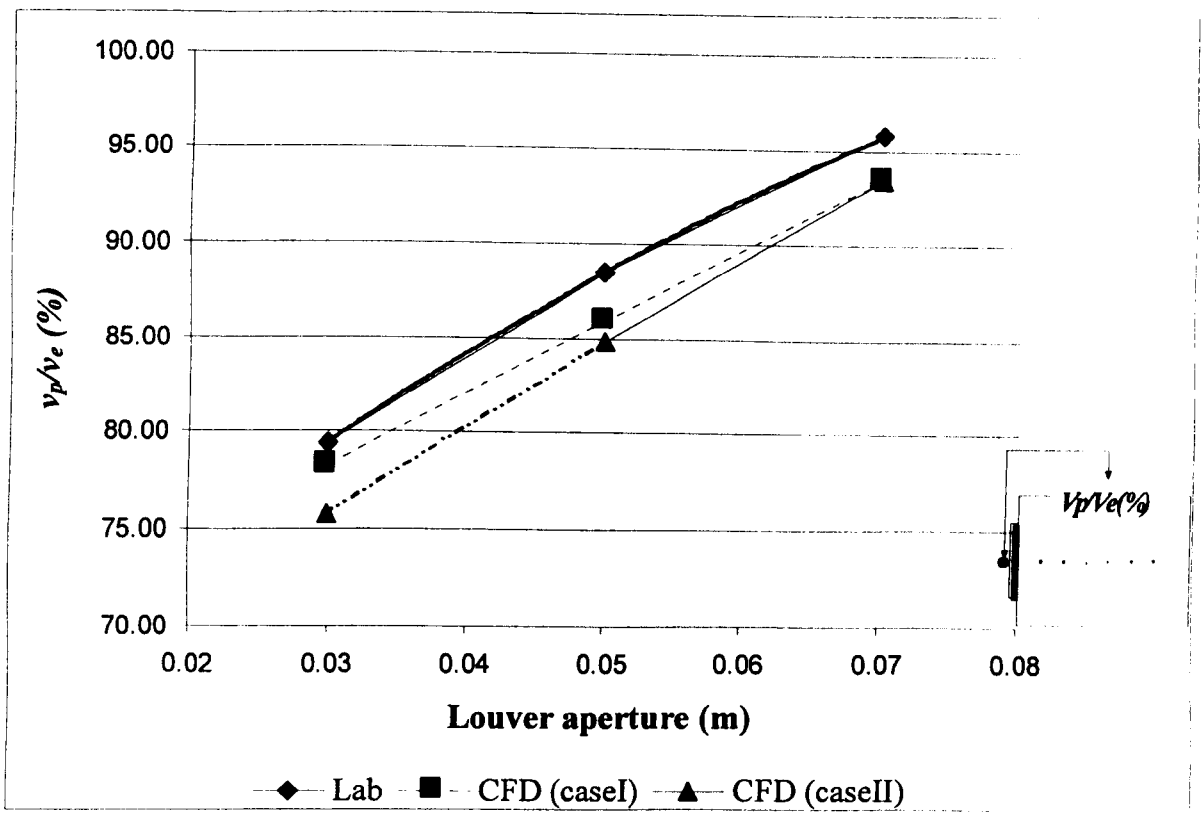

Figure (8.4): Curves of both CFD (case model-I) and CFD (case model-II) plotted against results obtained form the laboratory showing comparable curves with an acceptable margin of error, θ=0°.

examined was due to the airflow complexities occurring within the louver blades. This led to the errors found within the simulated chamber. On the other side, the flow readings outside the box, towards the windward side were less affected by that error. As shown in Figure 8.4, $v_p/v_e\%$ recorded from both model cases built have supported the findings obtained from laboratory measurements. The choice was suggested of the velocity drop due to the porosity percentages ($v_p/v_e\%$) obtained from the physical measurements as the reference velocity at the INLET. Such decision was taken into consideration because of a number of factors:

- The comparable $v_p/v_e\%$ achieved from both techniques used as mentioned earlier
- Reducing of the complications of the model which, in turn, would reduce the error percentage.
- Scaling the volume from which airflow passed through, i.e. airflow from within the louvers to the room.
- Other works in the field of CFD technique support the decision taken to consider the data of $v_p/v_e\%$ obtained from laboratory as a reference of values for inlet wind speed. For example, Murakami et. al. (1995) applied wind tunnel results obtained at the window to characterise the openings boundaries in CFD stage. Also, Weathers and Spitler (1998) conducted a comparative study between numerical predictions using CFD and full-scale measurements to study room airflow, and used the measured data to specify the boundary conditions of the inlet. Interestingly, the previous work highlighted that in ventilation research velocity distribution over the inlet area is assumed to be uniform. This is even applied with the predicting flow performance from mechanical

ventilation systems as found in Gan (1995). The work Gan conducted to evaluate room air distribution systems using CFD showed that the inlet was characterised with some simplicity rather than fully characterised. Similar justification could be found in the work carried out by Holmberg et al (1993). Nielsen (1992) carried out a much relevant research on various diffusers. In his work concerning the description of supply openings in numerical models for room air distribution, the author investigated various techniques to specify the boundary conditions at the supply openings (INLET) including direct description, box method, prescribed velocity method and computer generated supply condition method. The author stated, " *The flow profiles in the openings of the diffusers can now be used as inlet profiles for the prediction of the flow in the room*". Thus, the characterisation of INLET was represented by readings obtained form the laboratory measurements, hence the full validation stage and airflow pattern study were carried out based on this justification.

8.5.2.3. Simulation model (Case-III)

This model was constructed as a third stage of creating the proper computational domain. In this solution, velocity speed $v_p/v_e\%$ obtained from laboratory measurements was applied at the INLET reference speed because a strong potential for CFD to represent the laboratory results of $v_p/v_e\%$ was found (Figure 8.4). The model was built considering that air INLET as the first vertical grid cells between louver blades and the other side of the room chamber was the OUTLET as illustrated in Figure 8.5. The actual shape of the louver with inlets was accurately modelled under the Cartesian coordinates. This reduced the geometry complications to predict the flow regime around MLW, and in-turn, reduced error percentage and computational timing. Consequently, precise results were achieved.

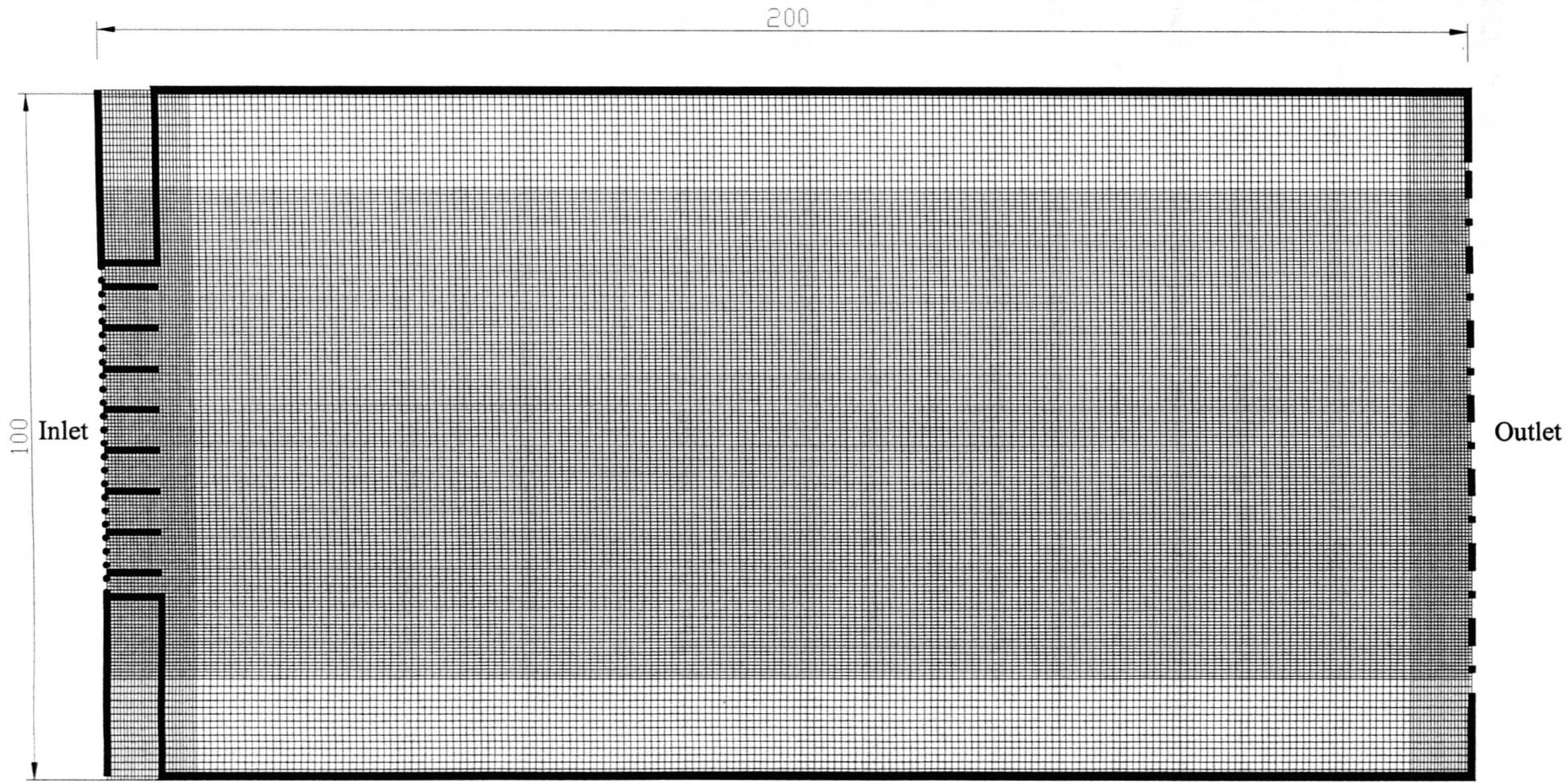

Figure (8.5): The CFD model (case model-III) built to carry on the simulation.

8.5.3. Boundary Conditions

In order to complete the numerical model, once the geometry set up was completed, initial boundary conditions needed to be specified which took into account the wind speed.

The air INLET (I1) was specified in terms of velocity and turbulence intensity. The boundary conditions specified for the input-cells were measured at a reference speed. The CFD reference speed corresponds to that achieved from the laboratory measurement when external speed at the laboratory was set to 2m/s. The Cartesian velocity components, turbulence intensity/length scale inlets were given through cell types defined at INLET boundaries. The only INLET boundary specified as (I1) presented air gaps between the louver blades, i.e. *d*. Flow exit was modelled using cells specified as OUTLET boundaries. FLUENT assumed that at the outlet boundary layer there was no change in the flow properties between the live cell upstream of the OUTLET and the exit plane. The boundary conditions at the WALL did not include wall temperature or diffusion of chemical as indicated previously.

The turbulent flow model was activated, when needed, with the relevant basic physical models and governing equations. TURBULENT FLOW in the menu defined the problem as turbulent and activated FLUENT's turbulence models. 10% turbulent intensity was used.

8.5.4. Physical Constants

Physical properties of the fluid were IDEAL GAS molecular weights, viscosity, thermal conductivity and mass diffusion coefficients. They were all given values which were appropriate for this situation to correspond to the fluid.

8.5.5. Convergence and residuals report

The process of obtaining a converged solution is of great importance in FLUENT simulations. FLUENT provided a running report of the residuals for each equation at each iteration; hence this process was monitored very carefully. The residuals demonstrated how closely each finite different equation was balanced, given the current state of the solution. The calculation was terminated when the residuals were less than 1×10^{-4} or complete convergence satisfaction was obtained. During the simulation, iteration counts normally would exceed 5000 iterations before reaching the convergence satisfaction.

8.5.6. Graphic output

Graphics of the colour-filled contours created by FLUENT which are presented in the thesis use the same colour coding range. Red represents the maximum variable plotted and blue represents the minimum for all the graphics shown in this chapter. However, the values of the plotted variables represented in the scale are not the same in the various graphs. Velocity vectors and velocity contours of the fluid flow were plotted to show the pattern of airflow based on the whole Rowshan combinations and outlet configurations.

8.6. The Discussion

The aim was to show the potential of numerical modelling, represented in the CFD technique, to compare results obtained form laboratory work for the reviewed modulated louvered windows. The comparison was performed on a small number of models covering various MLW parameters and they are noted accordingly in each variable.

8.6.1.1. Louver aperture.

The simulation observed the following apertures d=0.02m, 0.03m, 0.05m and 0.07m with various louver depths. As discussed before, notable increase of the flow within the louvers was evident. The air velocity at the exiting side of the louver panel was more than that initiated at the air entering side. This observation was common for all models examined and varies according to louver configurations. The stream of flow was apparent in models with bigger apertures than those with smaller ones as illustrated in Figures 8.6.a to 8.11.b. The comparison showed notable potential for the CFD technique to correspond with results around the louvered windows. As could be found from Figures 8.6.b, 8.7.b, 8.8.b, 8.9.b the error margin between the CFD and laboratory was less than 10% near MLW panel, i.e. $R_d \leq 1$m. Yet further measurements taken along the room showed that much velocity drop occurred in laboratory results. On the other hand, the increase in louver aperture was more likely to be accompanied with a divergence between both measuring techniques as seen from the regression curves comparing both CFD and laboratory findings. For example, results were comparable along the room depth at d=0.02m whereas the bigger the aperture involved, i.e. d=0.05m, the greater the error margin between the two curves along the room (Figure 8.12). Curves at each measuring distance near the window panel are illustrated in the latter figures. Table 8.2 shows the comparison of both measuring techniques with a statistical margin of errors.

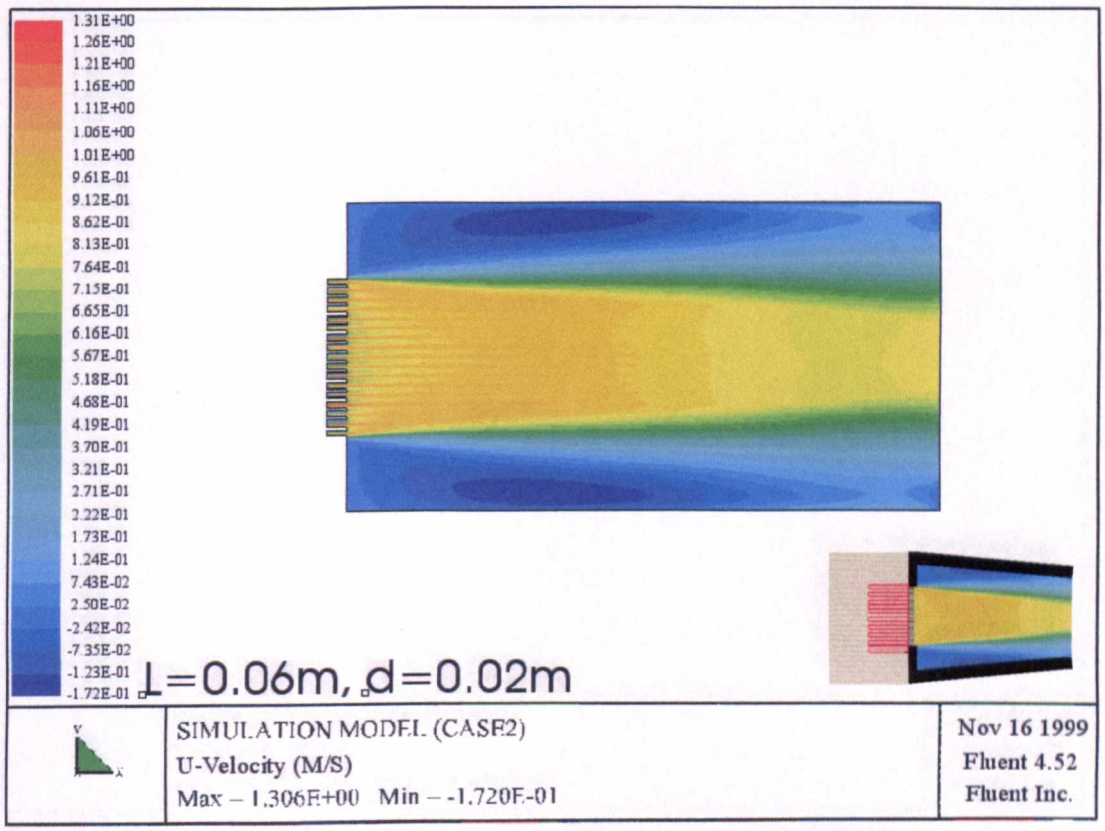

Figure (8.6.a): The colour-filled contours of airflow for the model d=0.02m and L=0.06m

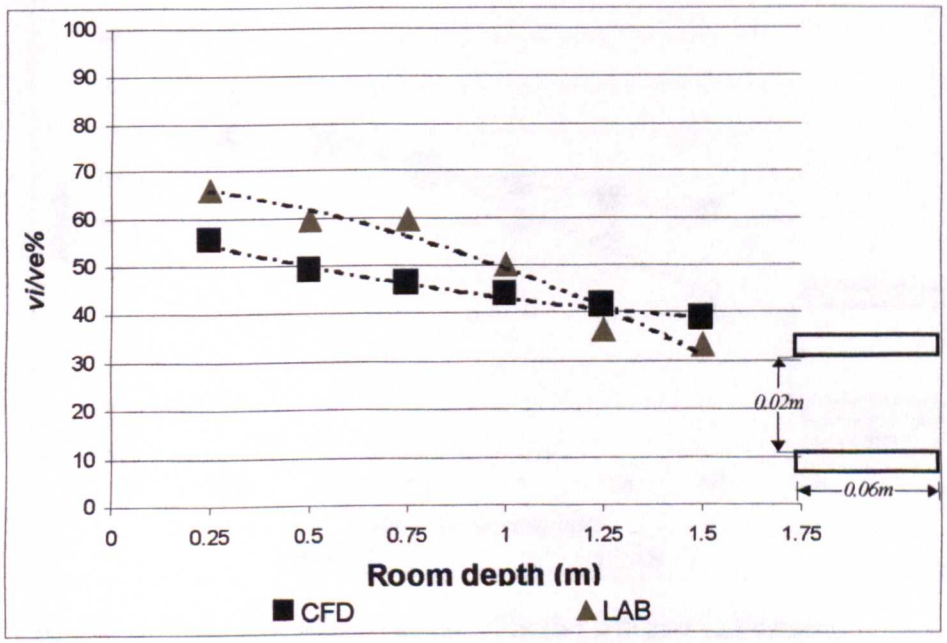

Figure (8.6.b): Regression curves of both CFD and Laboratory (LAB) along the room for the model d=0.02m and L=0.06m

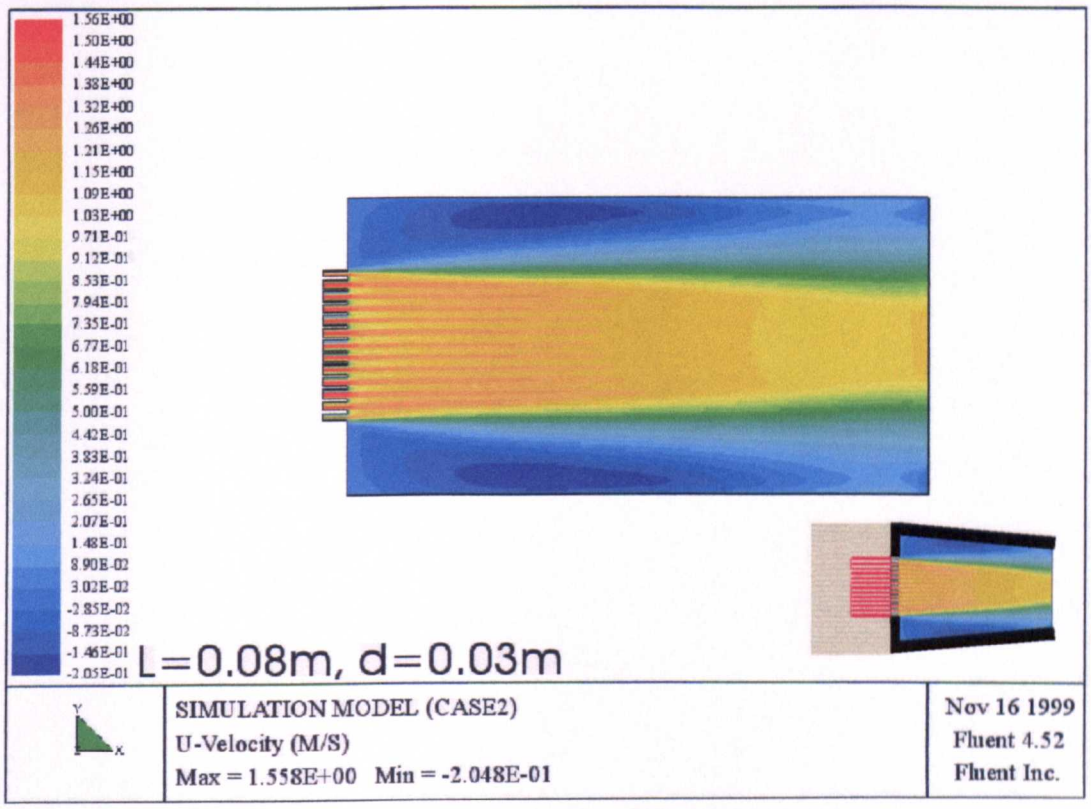

Figure (8.7.a): The colour-filled contours of airflow for the model d=0.03m and L=0.08m.

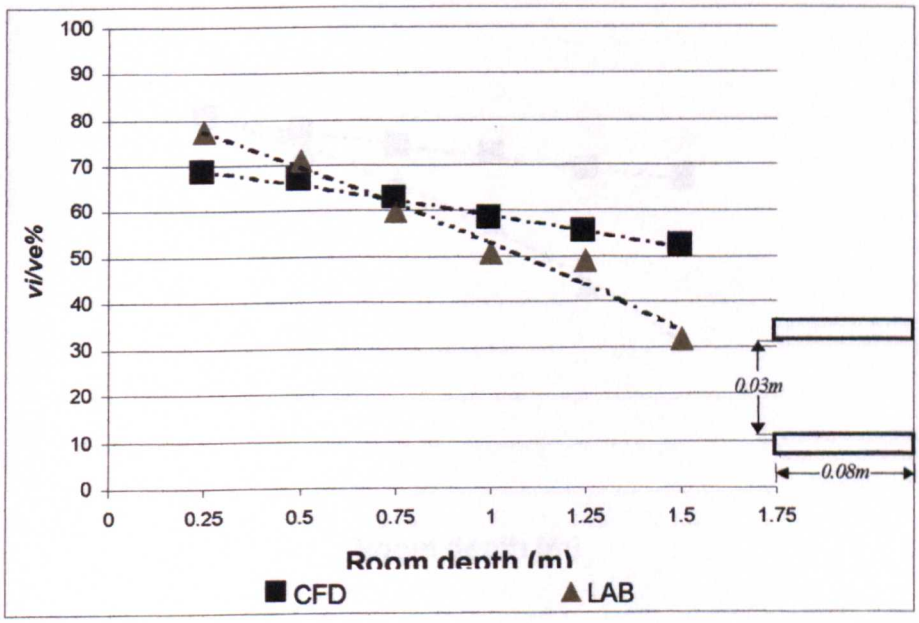

Figure (8.7.b): Regression curves of both CFD and Laboratory (LAB) along the room for the model d=0.03m and L=0.08m.

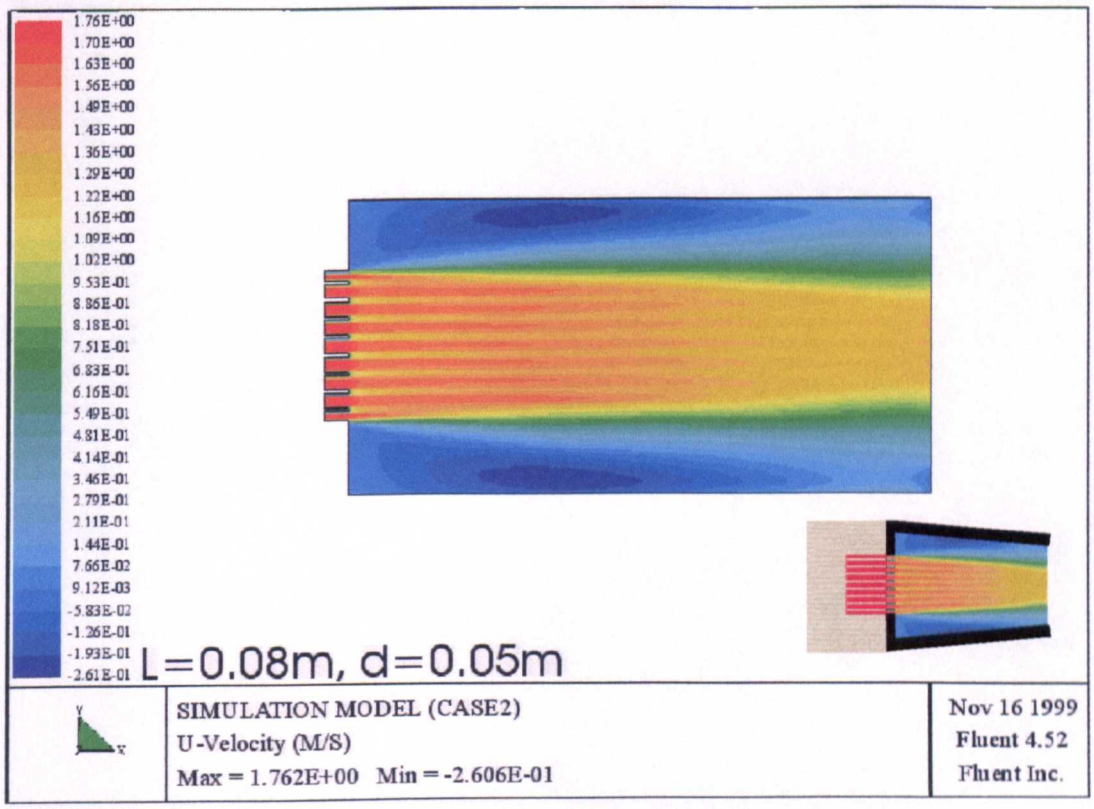

Figure (8.8.a): The colour-filled contours of airflow for the model d=0.05m and L=0.08m.

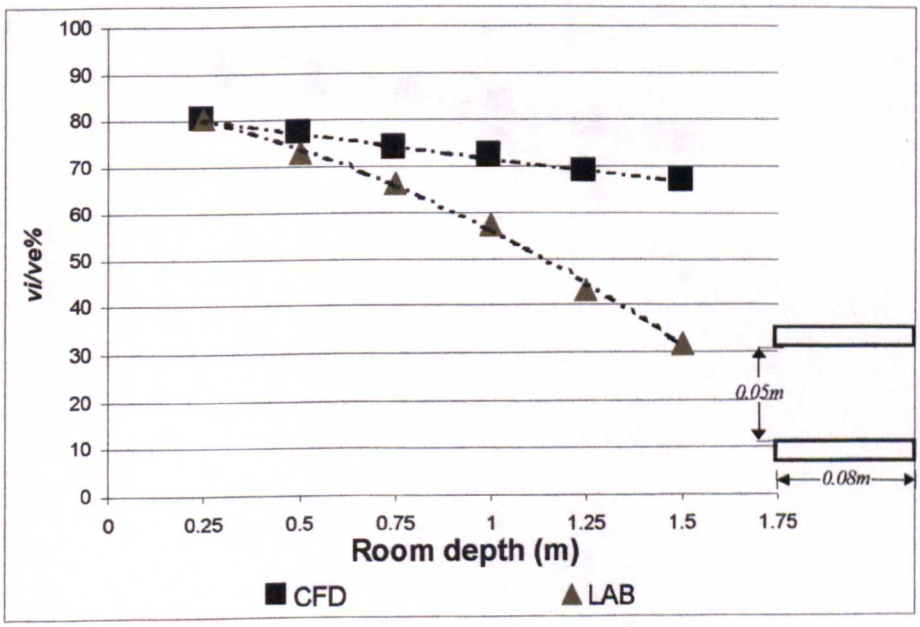

Figure (8.8.b): Regression curves of both CFD and Laboratory (LAB) along the room for the model d=0.05m and L=0.08m.

Figure (8.9.a): The colour-filled contours of airflow for the model d=0.07m and L=0.08m.

Figure (8.9.b): Regression curves of both CFD and Laboratory (LAB) along the room for the model d=0.07m and L=0.08m.

Table (8.2): The results obtained from both measuring techniques showing an acceptable margin of error within Rd=1m. (I-IV measured along the centre) and (V-VI measured above the centre).

CFD model (I) L=0.08m, d=0.07m and q=0o

Rd (m)	LAB (vi/ve%)	CFD (vi/ve%)	St. deviation	St. error
0.25	95.60	89.85	4.06	2.87
0.50	91.70	88.09	2.55	1.81
0.75	87.26	86.32	0.66	0.47
1.00	77.30	83.80	4.59	3.25
1.25	66.59	78.75	8.60	6.08
1.50	48.55	75.21	18.86	13.33

CFD model (II) L=0.08m, d=0.05m and q=0o

Rd (m)	LAB (vi/ve%)	CFD (vi/ve%)	St. deviation	St. error
0.25	80.42	80.26	0.11	0.08
0.50	72.95	76.98	2.85	2.02
0.75	66.16	73.70	5.33	3.77
1.00	57.18	72.19	10.61	7.50
1.25	43.25	68.65	17.96	12.70
1.50	31.74	66.63	24.67	17.44

CFD model (III) L=0.08m, d=0.03m and q=0o

Rd (m)	LAB (vi/ve%)	CFD (vi/ve%)	St. deviation	St. error
0.25	77.44	68.15	6.57	4.65
0.50	70.93	66.63	3.04	2.15
0.75	59.85	62.59	1.94	1.37
1.00	50.44	58.05	5.38	3.80
1.25	48.70	55.02	4.47	3.16
1.50	31.59	51.99	14.43	10.20

CFD model (IV) L=0.06m, d=0.02m and q=0o

Rd (m)	LAB (vi/ve%)	CFD (vi/ve%)	St. deviation	St. error
0.25	66.06	55.02	7.81	5.52
0.50	59.68	48.51	7.90	5.58
0.75	59.58	46.04	9.57	6.77
1.00	50.09	43.51	4.65	3.29
1.25	36.44	41.04	3.25	2.30
1.50	33.38	38.57	3.66	2.59

CFD model (V) L=0.06m, d=0.03m and q=30o

Rd (m)	LAB (vi/ve%)	CFD (vi/ve%)	St. deviation	St. error
0.25	37.17	38.57	0.99	0.70
0.50	58.62	45.89	9.00	6.37
0.75	44.81	40.99	2.70	1.91
1.00	38.30	26.25	8.52	6.03
1.25	35.30	19.34	11.29	7.98
1.50	29.93	12.00	12.68	8.96

CFD model (VI) L=0.08m, d=0.07m and q=45o

Rd (m)	LAB (vi/ve%)	CFD (vi/ve%)	St. deviation	St. error
0.25	42.59	37.05	3.92	2.77
0.50	55.89	32.26	16.71	11.82
0.75	23.49	10.60	9.12	6.45
1.00	12.79	9.99	1.98	1.40
1.25	17.13	11.05	4.30	3.04
1.50	10.72	7.57	2.23	1.58

In general, the decline of velocity due to room aperture was found comparable in both techniques. It was also notable that CFD curves produced were smoother than those produced at the laboratory. In other words, the decline of regression curves produced by CFD was generally less than that produced in the laboratory. Such variations in the regression curves were within the acceptable limit of validation when examined at smaller apertures. The same holds for bigger apertures, with some reservation found at the last two locations measured along room, i.e. Rd≥1.25m. As shown in Table 8.3 the standard error was less than 10% when examined for the smaller apertures along the room while it increased to nearly 18% with bigger apertures. The author referred this to a number of

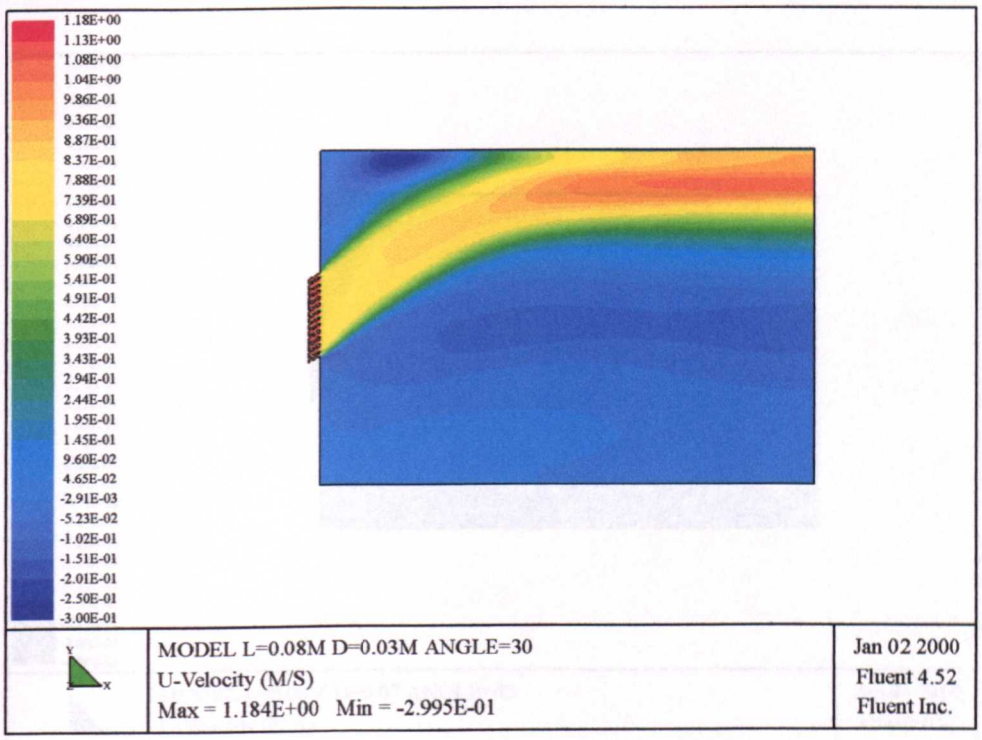

Figure (8.10.a) the colour-filled contours of airflow at angle d=0.03m L=0.08m.

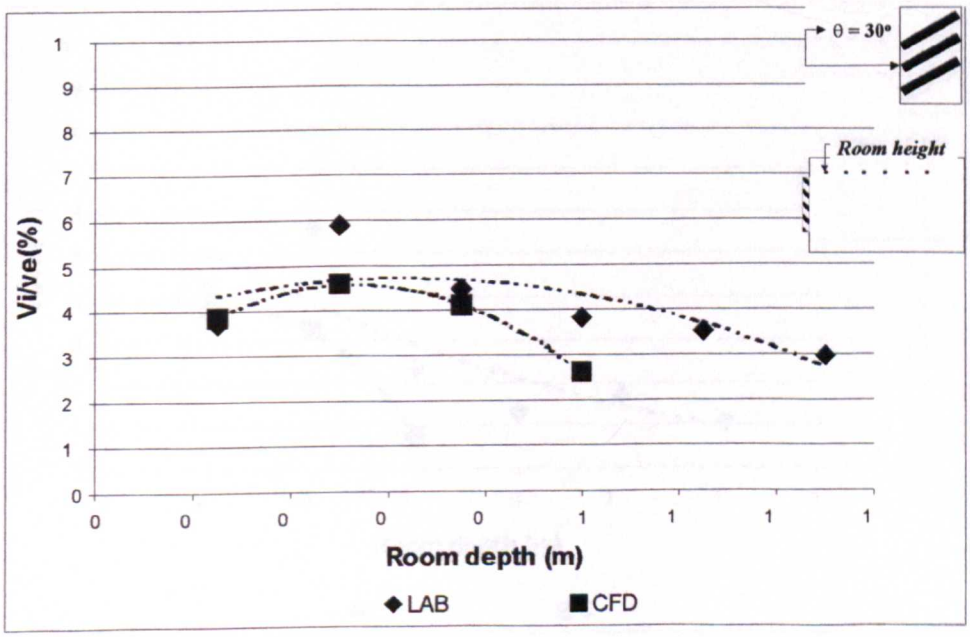

Figure (8.10.b): Regression curves of both CFD and laboratory (LAB) near the MLW models, d=0.03m, L=0.06m, θ=30°.

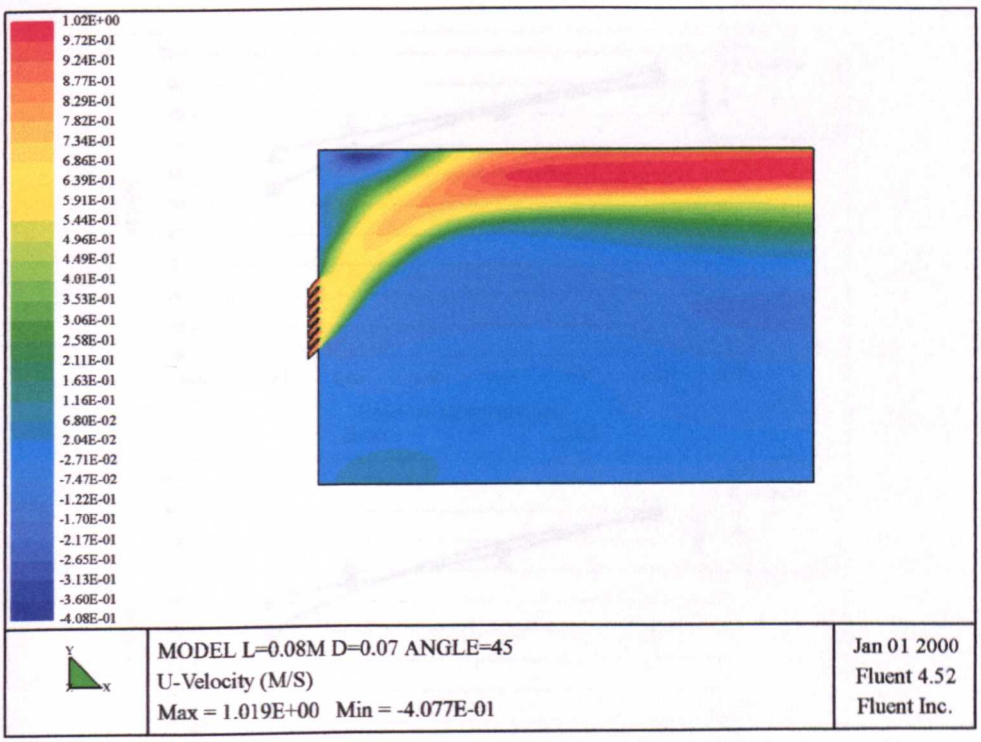

Figure (8.11.a) the colour-filled contours of airflow at angle d=0.07m, L=0.08m.

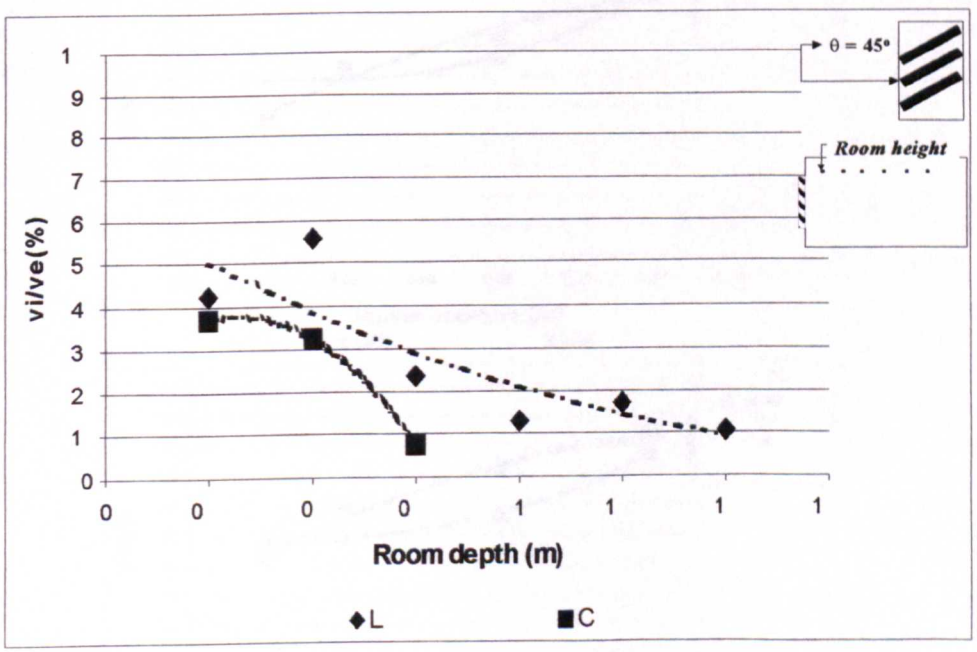

Figure (8.11.b): Regression curves of both CFD and laboratory (LAB) near the MLW models, d=0.07m, L=0.08m.

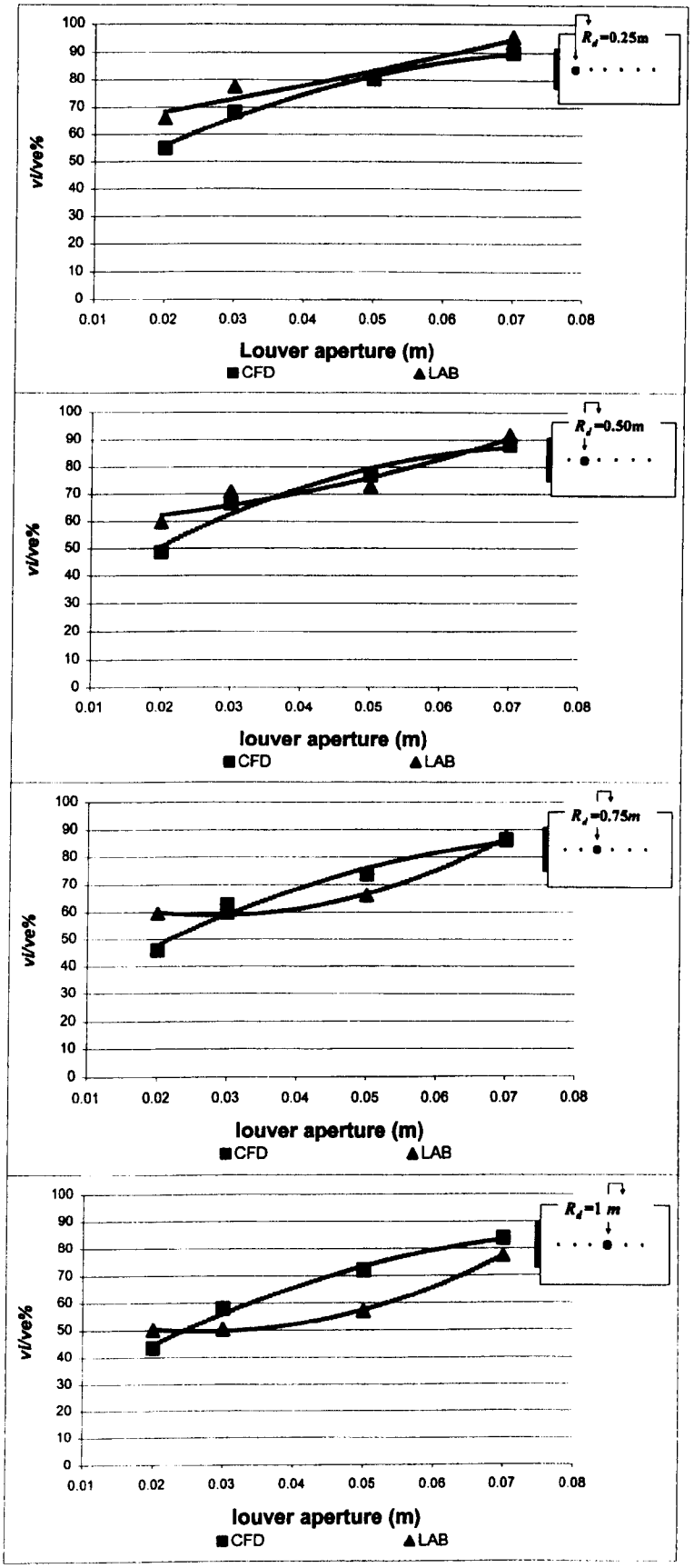

Fig (8.12): The comparison between results achieved from Laboratory and CFD. $\theta=0^{o}$

reasons, one of which was related to the laboratory. The hot-wire transducers were carefully allocated in their appropriate positions; however, the change in flow was altered in a scale of millimetres inside the box, and flow regime is so delicate that any minor alteration in the positioning of the transducer would change the readings accordingly. Although pre-set holes were made to exactly allocate the device it is agreed that this type of errors are inevitable and hence always justifiable. Another reason thought of was the neglect of louver friction. However, when this was activated the CFD results achieved were very much similar. Also the CFD algorithms and numerical equations shared this type of variations as they tended to simplify the complications occurring in actual flow mechanism in the environment.

8.6.2. Louver depth

The sample of louver depths measured confirmed what was stated in the previous chapters concerning the louver depth, i.e. L was found to be the least variable to form a considerable drop in velocity. The three depths examined were L=0.04m, 0.06m and 0.08m, with a fixed aperture, i.e. d=0.03m, and it was found that the increase in this variable would be less effective than other variables.

8.6.3. Louver inclination angle

The three louver inclinations examined included 0°, 30° and 45° and the results plotted which were investigated were those above the MLW near the ceiling (Figures 8.10a to 8.11.b. Results due to louver inclination were evidently taken with confidence, near the MLW. Higher velocities however were found near the ceiling due to the wall jet effect with the presence of steeper inclinations. The data were obtained at exact room height along the room (Figure 7.1). In the laboratory, the wall jet effect was not investigated but

the motivation of wall effect influenced by the ceiling height was discussed in some related references such as (Awbi, 1991) and (Etheridge and Sandberg, 1996). Two variable heights were examined, including the room chamber height under which laboratory measurements were taken and ceiling height of 2m. While both results obtained were comparable with what was observed with the physical measurements results within Rd≤0.75m any further measurements taken should acknowledge the fact of wall effect. Within Rd≤0.75m both measuring techniques were comparable with an acceptable margin of error, up to 15%. Additionally, the error limit was even minimised when obtained at horizontal louvers. As for further locations measured, the comparison was accompanied with a higher error margin, 20% Table 8.3. However, this error percentage would be acceptable showing that one could rely upon the results obtained from CFD near the MLW.

8.6.4. Room depth

The increase in room depth was accompanied with an increase in error percentage at horizontal and inclined louvers and variations between both techniques were examined. However, the readings obtained at the first measured location indoor showed a positive potential for the CFD technique. As shown in Figures 8.6 to 8.11, models examined were comparable and within the acceptable margin of error, i.e less than 20%, with and without the presence of a louver inclination. These harmonized results were stable and within the acceptable margin of error up to R_d=0.75m or 1m either at the centre axis measured or above MLW.

8.6.5. Velocity profile through louver blades (v_l/v_e)

The schematic patterns of the two-dimensional flow distribution within louver blades were plotted (see Appendix D.1) with an aim to study the effect of louver inclinations in causing these patterns. While this was uneasily accomplished in the laboratory measurements, simulation offers an alternative tool to deeply study these profiles within blades. The comparison was limited to one louver configuration (d=0.07m and L=0.08m) with three various inclinations, θ=0°, 30°, and 60°. It was understood that the velocity profile would differ if other MLW configurations or wind speeds were selected. However, the importance here was given to the general flow patterns occurring because of the inclination of louvers as seen in Appendix D.1. Also, in the simulation process the louver roughness was not specified, assuming smooth material with minimum friction parentage similar to what was examined at the laboratory, i.e. smooth pinewood.

At θ=0°, the flow at centre axis along L dimension seemed to be increasing as plotted deeper towards blades exiting side. The increment was nearly 5-10% more than that recorded at v_p/v_e%. On the contrary, a reduction of flow was found at adjacent cells located underneath and above louvers. It ranged from nearly $v_l/v_e \cong 25\%$ at the first measured location along L up to $v_l/v_e \cong 55\%$ near air exiting side. In other words, the flow increased at the centre of d whilst decreasing near blade surface along L dimension.

Velocity profiles across both dimensions were obviously altered when referenced to louver inclinations effect. As mentioned in earlier chapter, the tilting of louvers to 30° degrees of inclination, for instance, caused loss of about 25% in velocity near blades due to the MLW porosity, i.e $v_p/v_e \cong 76\%$. Interestingly, this reduction which continued unchanged at the centre axis of new aperture occurred due to inclination, say d_θ= 30°; however, it

decreased significantly when measured underneath louver blades, and increased above them. The decrease of MLW configuration in hand reached up to 50% (approximately $v_l/v_e \cong 1$m/s). This was the minimum cell recorded and developed proportionally across the cells towards the surface of other louver. When air reached the cell measured at the other surface of the blade $v_l/v_e \cong 105\%$ it showed that the wall effect added to the jet effect had altered the velocity profile within the louvers on both directions due to the noted inclination.

At inclination $\theta=60^\circ$, the significance in the velocity speed was also found at cells above the louver blades. However, the increase compared to other measured cells was considerable. For example, when the profile was measured at the middle of $L_\theta=60$, $v_l/v_e \cong 1.92$m/s above louver blade and $v_l/v_e \cong 0.46$m/s underneath. Meanwhile the cell measured at centre axis showed $v_l/v_e \cong 1.10$m/s showing that it was almost similar along $L_\theta=60^\circ$. At air exiting side it was noticed that facts mentioned here for both above and underneath louvers were altered.

In practice, the flow of air within louvers was very much influenced by the desired degree of inclination. While horizontal inclination provides occupants with the direct flow inside the living space, one could acknowledge the alteration of louver to maximize the flow at certain regions within the room if direct air was not desired.

8.7. Airflow Patterns through MLW

8.7.1. The case models

The simulation at this stage covered the patterns of airflow within a room based on louvers inclinations, wall inlet (windward) and outlet configurations. It is worth

mentioning that CFD simulation is well established to represent velocity directions and pattern of airflow across a room, as it is a valid alternative with the wind tunnel or smoke testing techniques in case of full-scale measurements as stated by (Kindangen et al. 1997), (Shaw, 1995), (Awbi, 1989) and others. The decision was then made to evaluate the effectiveness of MLW to produce patterns of airflow within indoors. These were traced with the influence of the five different combinations reviewed in Chapter 5 (section 5.2.3) that are typically found in the reference study, i.e. Jeddah, Saudi Arabia. The number of louvers in each combination varied accordingly. Figure 8.13 illustrates the five wall combinations at windward side. While they were either plain or projected Rowshan covering part or whole wall, they varied in louver numbers, wall configurations and dimensions. The plain Rowshan has two different forms; (Inlet-I) and (Inlet-III) and the projected Rowshan has three different forms; (Inlet-II), (Inlet-IV) and (Inlet-V). Furthermore, the outlet dimensions and location to control the movement of airflow in a room were also studied. Three various forms of outlets were considered, including a typical door (Outlet-I) or a window positioned in two locations on the outlet side; (Outlet-II) and (Outlet-III) with various dimensions.

The evaluation process of the flow patterns was made into three levels within the room. These included ceiling, middle and ground zones and were added to the Rowshan sitting zone when the projected Rowshans were examined (Inlet-II; Inlet-IV and Inlet-V). In Jeddah, it was mentioned that both middle and floor zones are considered the occupants' living zones (Al-Lyaly, 1990). A two-dimensional physical domain was made and previous procedures of setting up the model and physical domain were followed. The variety of inlet and outlet configurations were studied under three various louver inclinations; θ=0°, 30° and 60°. The following discussion is based on the results shown in Appendices D.2 to D.18.

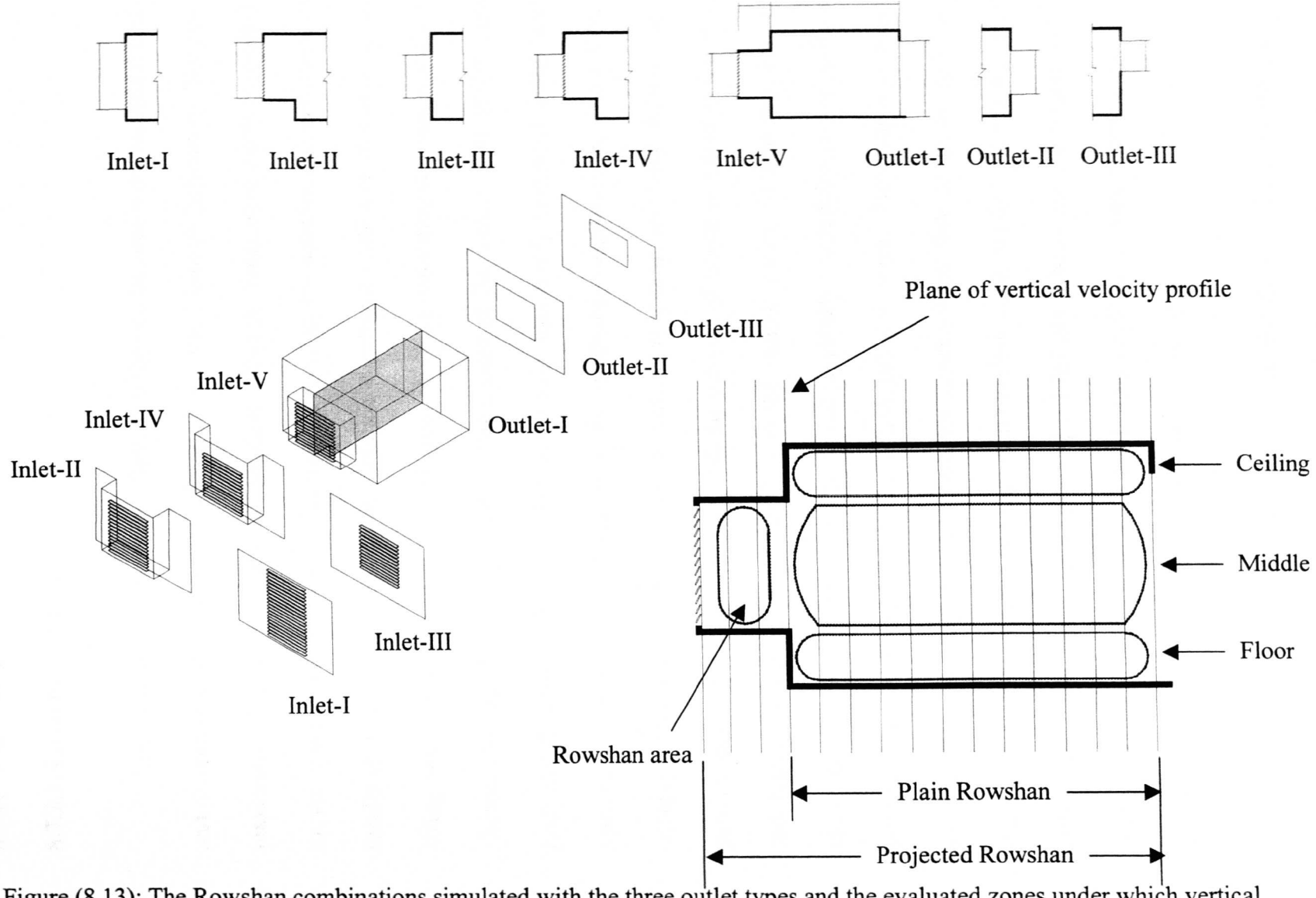

Figure (8.13): The Rowshan combinations simulated with the three outlet types and the evaluated zones under which vertical velocity profiles were examined along the room.

8.7.2. The flow patterns

8.7.2.1. Louver inclination (θ)

The flow pattern was more effective at the middle zone with horizontal inclinations and diversities of flow were shown in relation to the degree of inclination. The pattern and maximum velocities at a particular location within the room were easily controlled by the louver angle as the various inclinations involved in the solution had noticeably changed results obtained. The most rigorous solution to enhance ventilation indoor in the occupied living zone was observed at the inclination θ=0° as wind direction was not deflected or altered, shaping the most preferable flow regime at the middle zone in both plain and projected Rowshans. The Rowshan sitting zone was evenly ventilated, being next to the louvers. This solution is ideal when the maximum ventilation or direct flow to the occupant zone was desired. However, airflow at ceiling and floor showed the poorest performances. This was corrected with the increase of louver numbers as found in inlet-I and inlet-II, which enhanced the flow in the various zones. It also depends on proper selection of louver aperture *d*. As discussed previously maximizing louver aperture would minimize the percentage loss in the v_i/v_e% and vice versa. However it is important to consider that when higher wind speeds are present, direct flow in the occupied zone may not be the optimum choice and may cause feeling of discomfort. It was noted by Evans (1980), that when air exceeds certain speed indoors it becomes undesirable and leads to occupants' discomfort. Thus the control of air could be through selecting the appropriate louver aperture when the louver inclination is at θ= 0°.

The presence of louver inclination had directly altered the airflow pattern in the room. When the louver inclination was set to θ=30°, the flow near the Rowshan was maximized at ceiling and Rowshan area. Occupants' living zone was also ventilated near

the inlet, and due to the effect of inclination, the flow lessened nearly in the middle of the room. Increasing louver numbers had improved flow along the room (Inlet-I, Inlet-II). As to the far locations in the room, the flow of air increased near the ceiling while minimizing at the middle. Some flow was observed at the floor zone with opposite direction. The bi-directional flow between various zones in the room is a better solution when direct flow is not desired or when an air re-circulation is needed. The phenomenon was even more obvious at steeper louver inclinations. For example, when examining the flow pattern at θ=60° the velocity profile along the room height was much improved around the ceiling and near the floor. However, the cases examined showed that the minimum flow was around middle zone. Similarly, Rowshan sitting area was poorly ventilated. The increase in louver number did not correct that and the only Rowshan type that seemed to solve this was (inlet-V) as discussed later. The practical advantage of the latter inclination is when occupants require protection from direct airflow while the room is still ventilated or when there is a need to release the room from excessive heat and contaminants near ceiling. An example of this is demonstrated in Figure 8.14 where middle zone was not well ventilated whilst a bi-directional flow was found around other zones. In general, the greater the angle of inclination the less effective ventilation at middle zone and the more effective near the ceiling and floor.

8.7.2.2. Rowshan configurations

From the various combinations examined, the effect of Rowshan configurations was not effective to alter the flow patterns within the room when θ=0°. The only exception was found when applying different outlets. Apparently the flow at both inlet-I and inlet-II was better along the room compared with other types, and the optimum flow was near the louvers. The Rowshan configuration was a determinant factor when examined at other

inclinations. An example of that was observed when examining the vertical distribution of air for both Rowshan types mentioned here. While enhanced flow was near the ceiling, the middle zone was better ventilated when observed at the plain Rowshan than at projected Rowshan. The observation was noticeable for both inclinations. However, the simulation illustrated that sizing the projected Rowshan, as the case in inlet-V, could alter the flow to be more effective in the middles zone. Such modification of the projected Rowshan is found in Figure 8.14 where it forced air to flow more to the occupants' zone. But the flow of air was directed towards the ceiling when observed at further R_d. As far as the floor zone was concerned, the bi-directional flow was more encouraged with the presence of plain Rowshan. As shown from the appendices, this finding was for both inclinations observed.

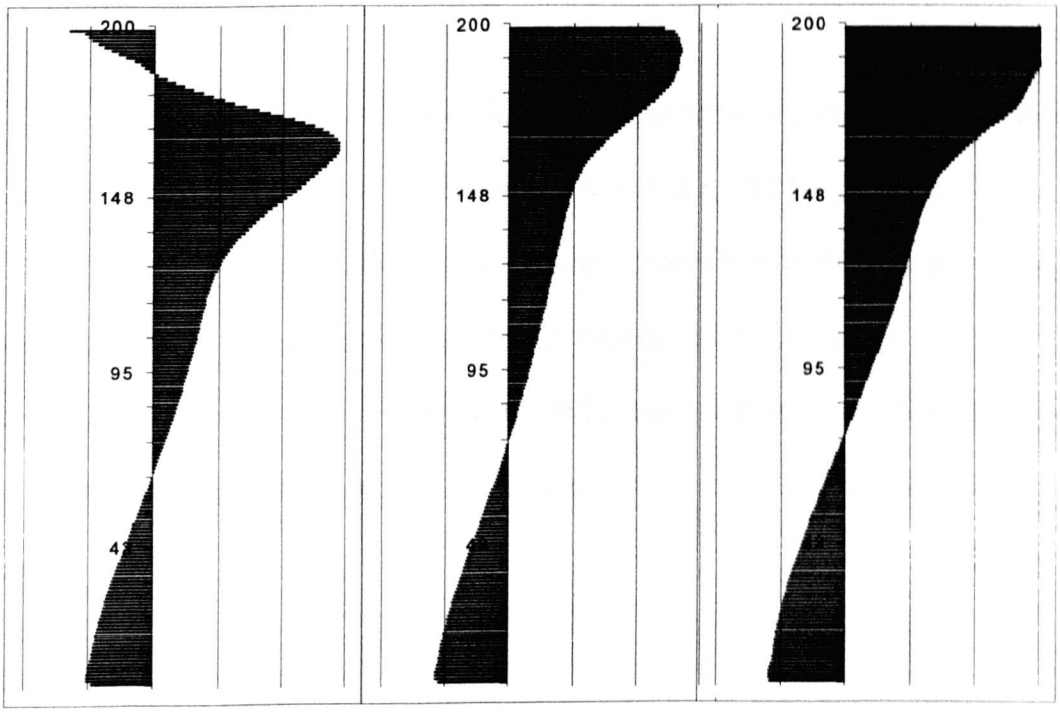

Figure (8.14): The flow pattern showing that modifying the projected Rowshan could force air flow to move in the occupants' zones rather than the ceiling, θ=60, Rd=1.5m. [a: Inlet-V][b: Inlet—IV][c: Inlet-II].

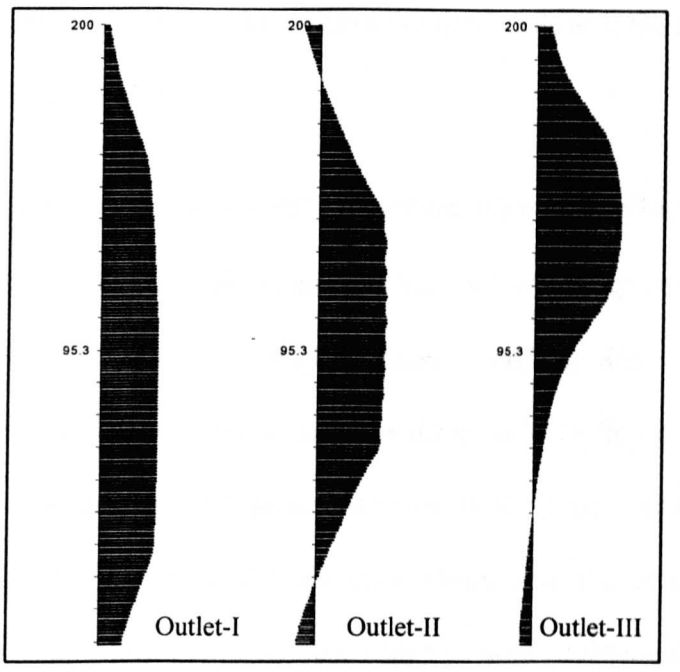

(8.15): The effect of the outlet type over the flow pattern of air near the outlet (0.25m near outlet), θ=0°

8.7.2.3. Louver number (*N*)

The flow in the middle zone was similar and has been influenced by the number of louvers with some reservations at vertical profile found at R_d=0.25m. On the other hand, a significant increase was noticeable near the ceiling especially with the presence of steeper inclinations. This is an important finding as occupants could release the room from the heat and contaminants near the ceiling whilst still protected from direct flow at the living zone. Near the ground, there was found a direct contribution of louvers number to the resultant flow.

8.7.2.4. Outlet configurations.

Outlet is typically either a door or a window and the work here covered both types. However, windows location on the leeward wall side has an importance on the flow regime inside the room and thus the window location and dimension were investigated. The

location of the room outlet was made to stress the natural flow at the ceiling zones between different spaces in the building.

When examined under horizontal inclination, no major influence of various outlets was shown near the inlet, i.e. at $R_d \leq 1$m. On the contrary, at approximately 0.25m away from outlet the flow was very much shaped to outlet configuration. An example of this is found with the vertical velocity profile near the three outlets (Figure 8.15). The similarity dwindled when traced deeper, with some exception to the door. Additionally, the vertical velocity profile for the inlet-V at Rd>1m was driven near the ceiling due to the outlet location with only minor bi-directional flow near the floor. Obviously the middle zone in all outlet types was ventilated more than other zones.

Similarly, with the presence of steeper inclinations the flow was neither changed near inlet nor changed in the middle of the room. The variation of flow regime found at the ceiling level was minor and negligible. But the previous fact was shown in the projected Rowshan (inlet-II, inlet-IV and inlet-V). On the other hand, when the vertical velocity profile was plotted for the plain Rowshan (inlet-I) the case changed. The flow near ground was induced to create more bi-directional near floor in outlet-III than that achieved from the door for example.

The valid conclusion derived from this in addition to what was mentioned earlier is the following. As the incoming air follows the same wind direction, only the middle zone would be well ventilated. An improvement to ventilate the flow near the ceiling could be achieved by adjusting the outlet configuration, for example by locating the outlet near the ceiling. The solution will in fact improve the flow at the ceiling location but with some reduction of flow in the middle zone. The utilisation of louver inclination is of importance for the designers to create various flow patterns in the room. For various louver apertures,

maximising the flow in a certain location within the room could be through the use of louver inclination. The Rowshan configuration also played a main role in the flow pattern inside the room. While plain Rowshan performed generally better than the projected Rowshan, the simulation showed that the modification in the projected Rowshan (as in inlet-V) could help direct the flow downwards towards the living space rather than the ceiling. As far as the airflow near the floor was concerned, the simulation of flow patterns had shown that tilting the louvers to steeper angles would be proportional to the percentage of bi-directional flow near the ground whilst flow in the middle zone is minimised. This provides an absolute solution for getting rid of the excessive heat and humidity near the ceiling and provides breeze of flow near the ground level. This flow near the floor is even much better when the outlet is controlled. The simulation has shown that using the window near the ceiling, as is typically used in Jeddah, is an optimum solution to improve the flow near ground, which would improve the feeling of comfort in the room. Finally at any positive inclination, the vertical flow profile was increasing as traced upwards.

8.8. Conclusions

Computational fluid dynamics has increasingly been used as a useful tool to comprehend the complications existing in the real environment. Recently, more researchers have relied on the results achieved by CFD packages, bearing in mind the limitations and restrictions embedded into them. This chapter gave a brief description to the historical background about the theory of numerical modelling and the basic equations used by CFD. Then there followed the importance of CFD in airflow predictions within buildings. In the process of evaluating the velocity results achieved from the laboratory, models were constructed using CFD to compare results from both techniques.

Additionally, the simulation covered the patterns of airflow within a room based on inlet and outlet room configurations. The following points of conclusions are obtained:

1. CFD is a reliable tool to simulate the flow near the Modulated louvered windows at the windward side, i.e. velocity drop due to porosity percentage ($v_p/v_e\%$). The correction made to the INLET boundary conditions, by replacing the reference v_e with $v_p/v_e\%$, was a good alternative to assess velocity results across the MLW. The technique has some validation in ventilation research and it reduced the model complications as well as the computational timings that, in turn, resulted in more accurate and comparable results.
2. CFD coding was a reliable tool to examine the velocity components in the room near the MLW. However, CFD results measured away from the MLW were accompanied with a level of error percentage higher than those obtained near the MLW. The errors were referred to a number of points discussed earlier in this chapter. Nevertheless within the scope of this study CFD results are acceptable since the error was less than 20% at the farthest measuring location, i.e. R_d=1.5m.
3. The simulation of vertical velocity profile within the room was the technique used to evaluate the patterns along both room dimensions and some conclusions were derived from the evaluation:

    - The presence of steeper louver inclinations angles induced a bi-directional flow within the room unlike the horizontal inclination. The latter inclination however is the optimum when direct ventilation at occupants living zone is desired.
    - The outlet type applied controls the flow behaviour and percentage of bi-directional flow.

- The plain Rowshan is generally a better choice than the projected Rowshan. Yet the flow in the living zone could be obtained be correctly sizing the projected Rowshan.

8.9. References

1. Al-Lyaly, S.M. (1990) The traditional house of Jeddah: A study of the interaction between climate, form, and living patterns. University of Edinburgh. Unpublished Ph.D thesis.

2. Alamdari, F. (1995) "Modelling airflow in buildings by computational fluid dynamics". *Building Services Engineering Research and Technology* **16-(4),** p.B44-B49

3. Anon. (1995a) Relationships for smoke control in atria. Technical Memoranda TM19, London: Chattered Institution of Building Engineers.

4. Anon. (1995b) "Simulation models: Towers of Babel or the promised land?". *Building services* **(January)**-p.23-25.

5. Anon. (1995c) "Testing time". *Building services* **(January)**-p.26-28.

6. Awbi, H.B. (1989) "Application of computational fluid dynamics in room ventilation". *Building and Environment* **24-(1),** p.73-84.

7. Awbi, H.B. (1991) *Ventilation of Buildings,* London: E & FN Spon.

8. Aynsley, R. M. (1999) "Unresolved issues in natural ventilation for thermal comfort". p.36-44, Darlington, NSW, Australia: proceedings of Hybvent Forum '99.

9. Chen, Q. and Jiang, Z. (1995) "Significant questions in predicting room air motion". **9-**(1). p.929-939, ASHRAE Transactions.

10. Chow, W.K. (1995) "Ventilation design: Use of computational fluid dynamics as a study tool". *Building Services Engineering Research and Technology* **16-(2),** p.63-76.

11. Chow, W. K. and Lau, K. W. (1993) "Field tests on atrium smoke control systems". p.461-469, USA: ASHRAE Transactions.

12. Chul, C.Y. (1997) Experimental, theoretical and computational modelling of airflow to investigate the thermalhydraulic performance and ventilation efficiency in a clean room. Bristol. Unpublished Ph.D. thesis.

13. Chung, I.-P. and Dunn-Rankin, D. (1998) "Using numerical simulation to predict ventilation efficiency in a model room". *Energy and buildings* **(28)**-p.43-50.

14. Dascalaki, E., Santamouris, M., Argiriou, A., Helmis, C., Asimakopoulos, D.N., Papadopoulos, K. and Soilemes, A. (1996) "On the combination of air velocity and flow measurements in single sided natural ventilation configuration.". *Energy and buildings***24,** p.155-165.

15. Etheridge, D. and Sandberg, M. (1996) *Building Ventilation: Theory and Measurements*, John Willy & Sons. London

16. Evans, M. (1980) *Housing, Climate, and Comfort*, London: Architectural press.

17. FLINT. FLINT (2000) version 4.1. Unpublished software.

18. FLUENT. FLUENT (1999) version 4.51. New Hampshire, USA: Fluent Inc.

19. Fontiane, J. R., Rapp, R., Serieys, J. C., and Aubertin, G. (1994) "Aerosol transport in room turbulent air flow- experimental and numerical flows". Carcow, Poland: Proceedings of Roomvent '94.

20. Gan, G. (1995) "Evaluation of room air distribution systems using computational fluid dynamics". *Energy and buildings* **(23)**-p.83-93.

21. Holmberg, Y.L., Paprocki, A. and Tang, Y.-Q. (1993) "Simulation of room flows with small ventilation openings by a local grid-refinement technique". *Building Services Engineering Research and Technology* **15-(1),** p.1-10.

22. Jones, P.J. and Whittle, G.E. (1992) "Computational Fluid Dynamics for building air flow prediction-Current status and capabilities". *Building and Environment* **27-(3),** p.321-338.

23. Kindangen, J., Krauss, G. and Depecker, P. (1997) "Effect of roof shape on wind-induced air motion inside buildings". *Building and Environment* **32-(1),** p.1-11.

24. Maghrabi, A. and Sharples, S. (2000) " Significant limitations in applying Computational Fluid Dynamics (CFD) to predict room air distribution" .(To be published).

25. Murakami, S., Kato, S., Deguchi, K., Takahashi, T., Makimura, I., and Kondo, Y (1995) "Natural ventilation of a large-scale wholesale market building". p.44-55, USA: ASHRAE Trans.

26. Neilsen, P.V. (1992) "Description of supply openings in numerical models for room air distribution". *ASHRAE Transactions* **9-(4),** p.963-971.

27. Robinson, D., Cook, M. J., Lomas, K., and Bowman, N. T. (1999) "The design and control of buildings with passive downdrought evaporative cooling". **(1),** p.453-458, Brisbane, Australia: PLEA99.

28. Ruyssevelt, P., Stankovi, S., Wilson, A., Lomas, K., Bloomfield, D. and Gouph, M. (1995) "Simulation modelling: Lessons for the future". *Building services* **(January)-** p.31-36.

29. Said, M. N. A., Shaw, C. Y., Zhang, J. S., and Christianson, L. L. (1995) "Computation of room air distribution". p.1065-1077, Chicago, USA: proceedings of ASHRAE Centennial Conference.

30. Schaub, E. G., Kelso, R. M., and Baker, A. J. (1995) "Comparing the continuity-constraint algorithm results with a full-scale laboratory test". **(2),** p.1041-1053, USA: ASHRAE Transactions.

31. Sharples, S and Maghrabi, Amjed (2000) "Airflow through louvers: an experimental and CFD study". The Hague: Proc. 21st. AIVC Conference (To be published).

32. Shaw, M. (1995) "Computer modelling as a design tool for predicting building performance: Part 1". *Building Services Engineering Research and Technology* **16-(4),** p.B41-B41

33. Swainson, M.J. (1997) Evaluation of the potential of solar chimneys to derive natural ventilation in non domestic buildings. Cranfield. Unpublished Ph.D. thesis.

34. Weathers, J. W. and Spitler, J. D. (1998) "A comparative study of room airflow: Numerical prediction using computational fluid dynamics and full-scale experimental measurements". p.144-157, USA: ASHRAE Trans.

35. Williams, P. T. and Baker, A. J. (1994) "CFD Characterization of natural convection in a two-cell enclosure with a "Door"". **(3),** p.685-696, USA: ASHRAE Trans.

36. Yaghoubi, M., Knappmiller, K. and Kirkpatrick, A. (1995) "Three-dimensional numerical simulation of air contamination dispersal in a room". *ASHRAE Transactions* **(1)**-p.1031-1040.

37. Yang, Z. (1989) Numerical simulation of incompressible and compressible flow. University of Sheffield. Unpublished Ph.D.

CHAPTER 9: CONCLUSIONS AND FURTHER RECOMMENDATIONS

9.1. Aims of the research

The research assessed the potential of the modulated louvered windows to provide ventilation as a cooling source to achieve thermal comfort inside the buildings. A number of aims and objectives were established and investigated throughout the chapters of this thesis. The main aim was to encourage the use of natural ventilation techniques by reviewing the methods of controlling natural ventilation to address the main architectural element that enhanced cross ventilation within the traditional house in Jeddah. Another aim was to present technical analysis of the potentials of the MLW in order to achieve the central aim of this thesis, i.e. to present designers with practical information concerning the airflow characteristics across this type of window accessories.

9.2. Summary of results

Dealing with the MLW geometries to achieve the acceptable air velocity indoors is quite complex. The review, analysis and discussion carried out in the earlier chapters are recalled and summarised here.

From the literature review it was noticeable that a number of strategies were considered in Jeddah on both microclimate and macroclimate scales (section 2.5). Within the microclimate scale, the MLW found in the Rowshan or any other aperture component is believed to be the main solution to control the breezes.

The review also showed that varieties of mathematical models related to airflow characteristics within buildings are treated with some simplicity and assumptions whose validity, for most of them, is based on a complete, open aperture.

When any treatment is involved, such as the reviewed MLW, their appropriateness becomes questionable; hence the need for direct measurements was recommended by a number of investigations more reliable than the theoretical models.

Dealing with the pressure and velocity drops as the main functions to control the indoor airflow characteristics was a sound choice since the temperature was found, by other research, to be less effective in controlling air movement indoors with the presence of even a slight breeze. The pressure characteristics between inner and outer volumes showed that the enhancements in pressure drops could, at certain point, be a function to some variables involved in this analysis. The adjustment of louvers to steeper blade inclination as well as the reduction of aperture and free area are main causes of poor ventilation inside the room. The considerable pressure drop could not be achieved except when reaching $\pm 60^{\circ}$ of louver inclination, the critical angle of the MLW under which major airflow reduction was found (section 6.5.3). Similarly, the control of velocity drop across the MLW was more related to the aforementioned variables. The louver angle of inclination was found to be a main variable to control this, while louver depth was the least affecting variable in this phenomenon, except with the presence of steeper louver inclination.

Interestingly, the major indoor velocity and pressure drop was not due to individual variables but rather to a combination of variables that would comprehensively describe ΔP and $v_i/v_e\%$ as concluded from the evaluation stages conducted in sections 6.5.3 and 7.4.6.

Wind direction has also some significance on indoor air velocity since normally a 20% reduction in $v_i/v_e\%$ near the window was found when wind was to

deviate 30° from perpendicular (see section 7.4.2). In addition, the vertical and the horizontal velocity profiles, along the room height and depth respectively, are much related to the MLW configurations examined as shown in sections 7.4.3.1 and 7.4.3.2. As far the room depth was concerned, it was possible to establish a dimensionless relationship of velocity characteristics as function to various MLW parameters involved near the window, $R_d \leq 1$m (see section 7.4.1 and Figure 7.6).

The reduction in air velocity near the windward side of the MLW, expressed as the porosity percentage ($v_p/v_e\%$), was a sound alternative to evaluate the performance of MLW as it gave an understanding of the flow characteristics at the windward side near the modulated louvered windows (section 7.4.4.).

The CFD appraisal stage conducted in Chapter 8 examined the viability of CFD coding to simulate airflow around the MLW and established the schematic airflow patterns based on MLW and Rowshan configurations as well as outlet configurations that are typically found in Jeddah. With or without the presence of inclination angles, CFD had successfully represented results obtained from laboratory near louvers inside the room, i.e. $R_d \leq 1$m (section 8.6.1.1). However, CFD data obtained far from the MLW could only be accepted with some reservations. On the other hand, results of the schematic airflow patterns were as follow:

- The presence of steeper louver inclination angles induced a bi-directional flow within the room unlike the horizontal inclination. The latter inclination however is the optimum when direct ventilation at occupants living zone was desired as discussed in section 8.7.2.1.

- Both types of Rowshans, the plain and the projected, showed good performances to the airflow patterns inside the room. Nevertheless, the bi-directional flow was with the presence of the plain Rowshan generally better than the projected type. Within the context of the projected Rowshan, the flow pattern enhanced with the presence of split units Rowshan, particularly with steeper louver inclinations, as the airflow pattern was directed towards living zone rather than the ceiling (section 8.7.2.2).

9.3. Design guidelines

One of the main aims of this research was to provide designers and architects with practical information concerning the airflow characteristics across this type of window accessory. A number of design guidelines are noted here.

- This window accessory has a high degree of *design flexibility* where a number of MLW geometries could be proposed to offer similar ventilation performances. This on the other hand would assist designers and architects to propose a number of MLW configurations to optimise their window treatments.
- Optimum ventilation performance inside the room is achieved when horizontal inclinations of louvers are employed.
- Inclination $\theta \geq 60^{\circ}$ was accompanied with poor ventilation performance inside the room, and thus is considered the critical MLW geometry that should be avoided. However, when this inclination is necessarily

employed, larger dimensions of louver apertures are then recommended, i.e. d/L=1.

- Steeper louver inclinations, θ>30°, will lessen ventilation performance in the living zone whilst improve it near the ceiling. In addition, airflow near the ground level is improved at those inclinations when properly sizing the outlet.
- The variation in louver depths of an MLW has no considerable effect on the ventilation performance inside the room.
- Room depth has a considerable effect on the reduction of air velocity inside the room.
- The plain Rowshan showed was generally a better performance than the projected Rowshan. In addition, sizing the projected Rowshan from top will enhance airflow in the living zone.
- Smaller outlets are recommended when bi-directional flow between various heights inside the room is required.

9.4. Conclusions

This thesis has investigated the airflow characteristics of the modulated louvered windows (MLW) with reference to the Rowshan of Jeddah, Saudi Arabia. The results obtained from the study can be implemented in other settlements in any part of the world. Throughout the various stages of the research, a number of conclusions were derived that answered the aims and objectives of the research.

1. From the literature review, the MLW was the most important element and played the major role in the provision and control of natural ventilation in the traditional architecture of Jeddah, Saudi Arabia.
2. The adjustment of louvers to steeper blade inclination as well as the reduction of aperture and free area are the main causes of poor ventilation indoors. On the other hand, the depth of louver blades does not have the same significance and is the least important variable. Nevertheless, the major pressure and velocity drops are not due to individual variables but rather to a combination of variables that would comprehensively describe ΔP and $v_i/v_e\%$ across the reviewed MLW.
3. Airflow velocities in a room containing an MLW result from an interaction of louver geometry, room geometry and prevailing wind conditions.
4. The ventilation performance of the plain Rowshan was generally better than the projected Rowshan. Yet the flow in the living zone could be enhanced by correctly sizing the projected Rowshan.
5. The quadratic model equation produced better curves fits to the data compared to those produced by power law regressions. The quadratic curve was in the form of $\Delta P = AQ + BQ^2$. However, further adjustments of the theoretical representations of equation in the quadratic form would be required to fit other variables such as number of louvers and their inclination angles.
6. CFD coding was a reliable tool to examine the velocity components in the room near the MLW. But it was less successful in predicting air velocities towards the rear of the room at some distance from the louver opening Nevertheless within the scope of this study CFD results are acceptable since the error was less than 20% at the farthest measuring location.

9.5. Further recommendations

1. The design of the modulated louvered windows must give a consideration to the variables as they play an important role in altering airflow characteristics inside the room.
2. There is no consideration allowed to the frictional factor and the roughness of the louver blades. Also, there is no barrier or medium, such as a mosquito screen or a glass, which may affect the ventilation performance across the reviewed MLW. Therefore, more research is needed to include such factors in the investigation of the MLW and Rowshan performances.
3. Further research could be conducted to investigate the effect of obstacles either inside the Rowshan in the room (such as furniture or human bodies) or around the building on the windward side (such as wing-walls or plants). These issues fall beyond the scope of the current thesis, and thus further research is needed.
4. Further work comparing the laboratory and CFD results with measurements in real rooms is needed.
5. Due to the limitations of the number and characteristics of the Rowshan structure covered in the thesis, investigations are recommended to cover cases of more complex forms of the Rowshan. This also may include the airflow through the sides of the projected Rowshan under various prevailing wind conditions.
6. Further adjustments of the theoretical representations of the equation in the quadratic form are required to fit other variables such as number of louvers and their inclination angles as noted previously.

7. Further CFD simulations are required to identify appropriate boundary conditions to improve the agreement with the experimental data for all locations within the room.
8. This study investigated the Rowshan performance in term of airflow quantity and not quality. Also, it is significant to point out at this stage that other environmental considerations such as air temperature, humidity and precipitation are not considered and the current study may establish a solid ground for further investigations concerning these issues.

This thesis has made a fundamental contribution to the study of airflow performance of the modulated louvered windows with respect to the Rowshan application in Jeddah, Saudi Arabia. As a result of this work, there is now a better understanding of the interaction between louver parameters and the characteristics of airflow through them and within the room. It is hoped that these findings will be of assistance to assess future design guidelines and building occupancy coding for this type of windows. Moreover, it is a step forward to assess the potentials of reducing energy consumptions in buildings.

Appendix A: Natural ventilation in Architecture

Appendix (A.1): The flow regimes and pressure fields around a streamed-lines and a bluff body. Aynsley 1977)

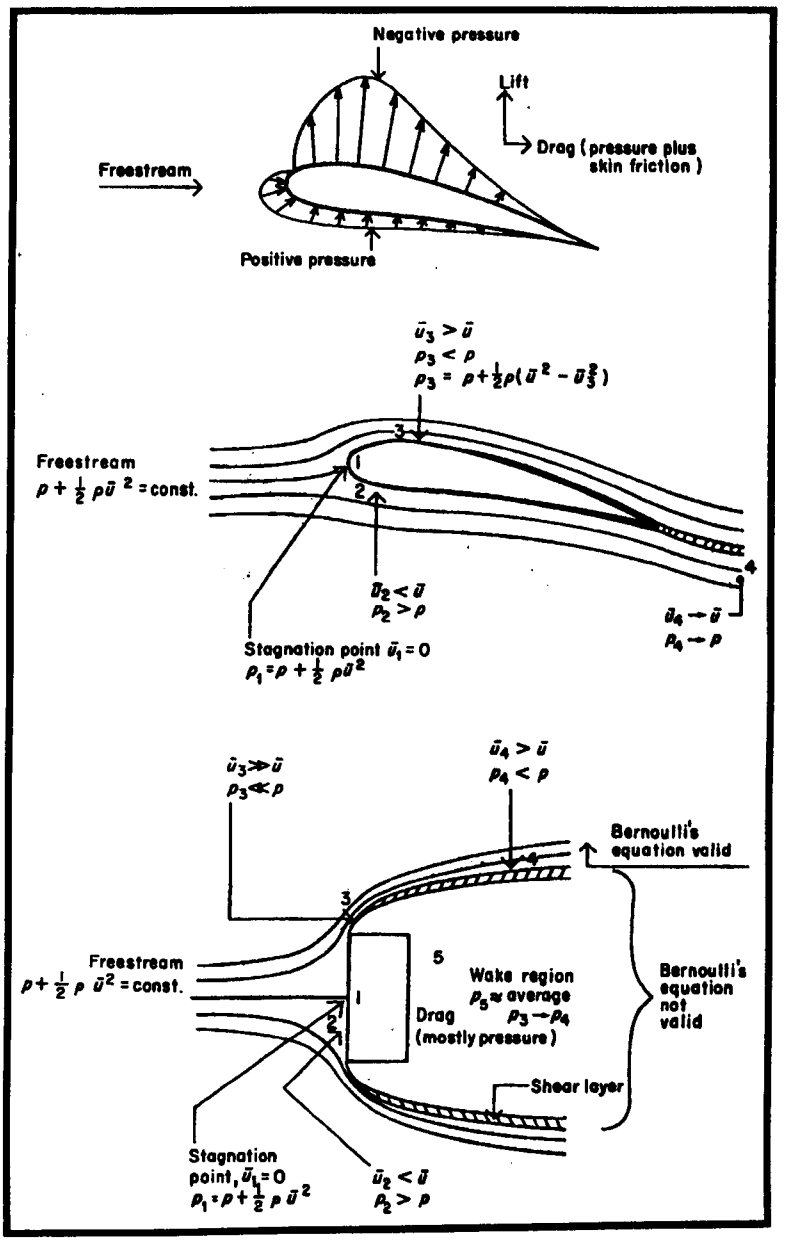

Appendix (A.2): The four regions of the free jet air. (Awbi, 1991)

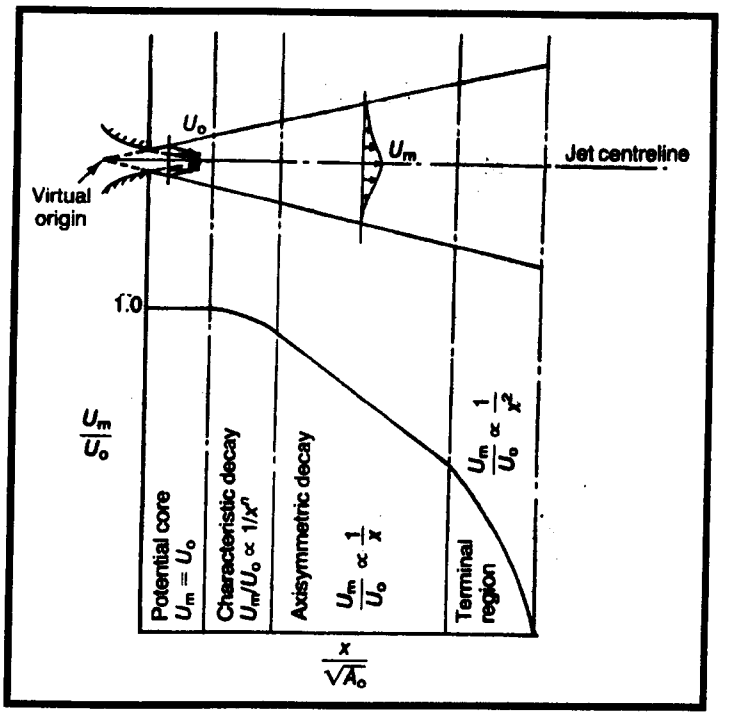

Appendix (A.3): The two regions of the wall jet effect. (Awbi, 1991)

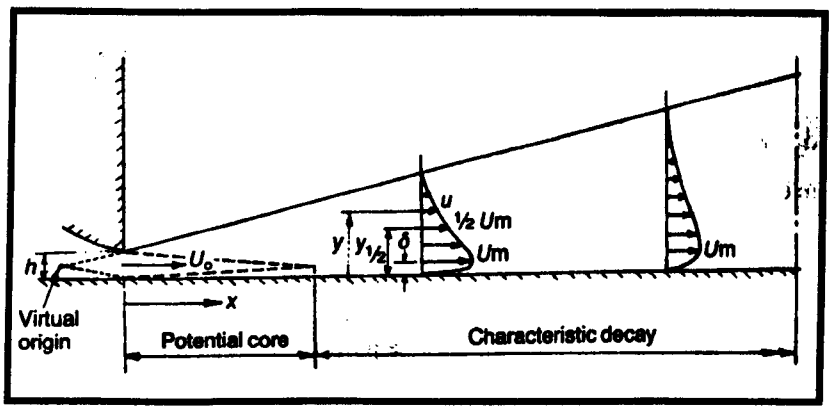

Appendix (A.4): The velocity profiles of various types of terrain. (Markus and Morris, 1980)

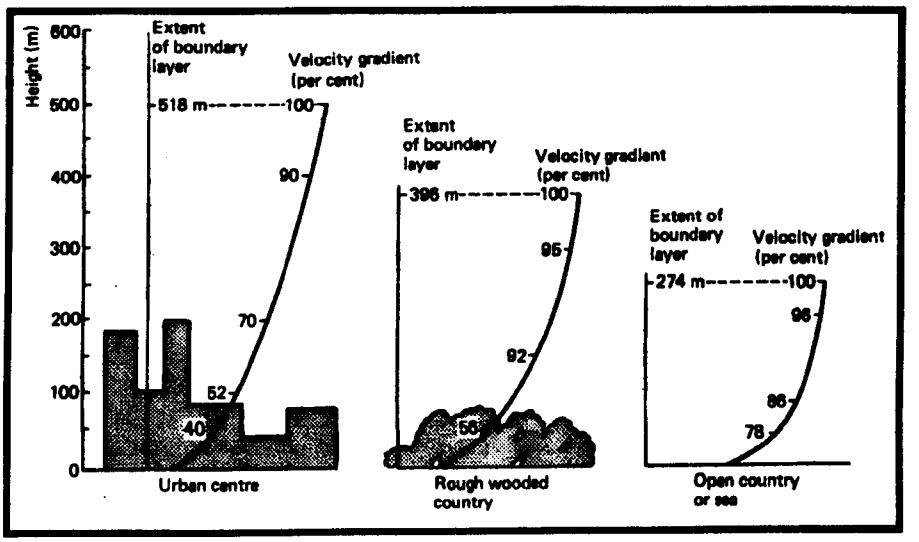

Appendix (A.5): The characteristics of terrain roughness. (Al-Ansari et al. 1985)

Terrain Type	n
Open country (sea, sand, desert)	0.10 - -.13
Moderate rough (short grass, grass crops, rural areas)	0.13 0.20
Rough (wood, Suburb)	0.20 0.27
Extremely rough (tall buildings, urban areas)	0.27 0.40

Appendix (A.6): The effect of the eaves (horizontal projection) and the wing-walls (vertical projections) on indoor air velocity. (Aynsley et al. 1977)

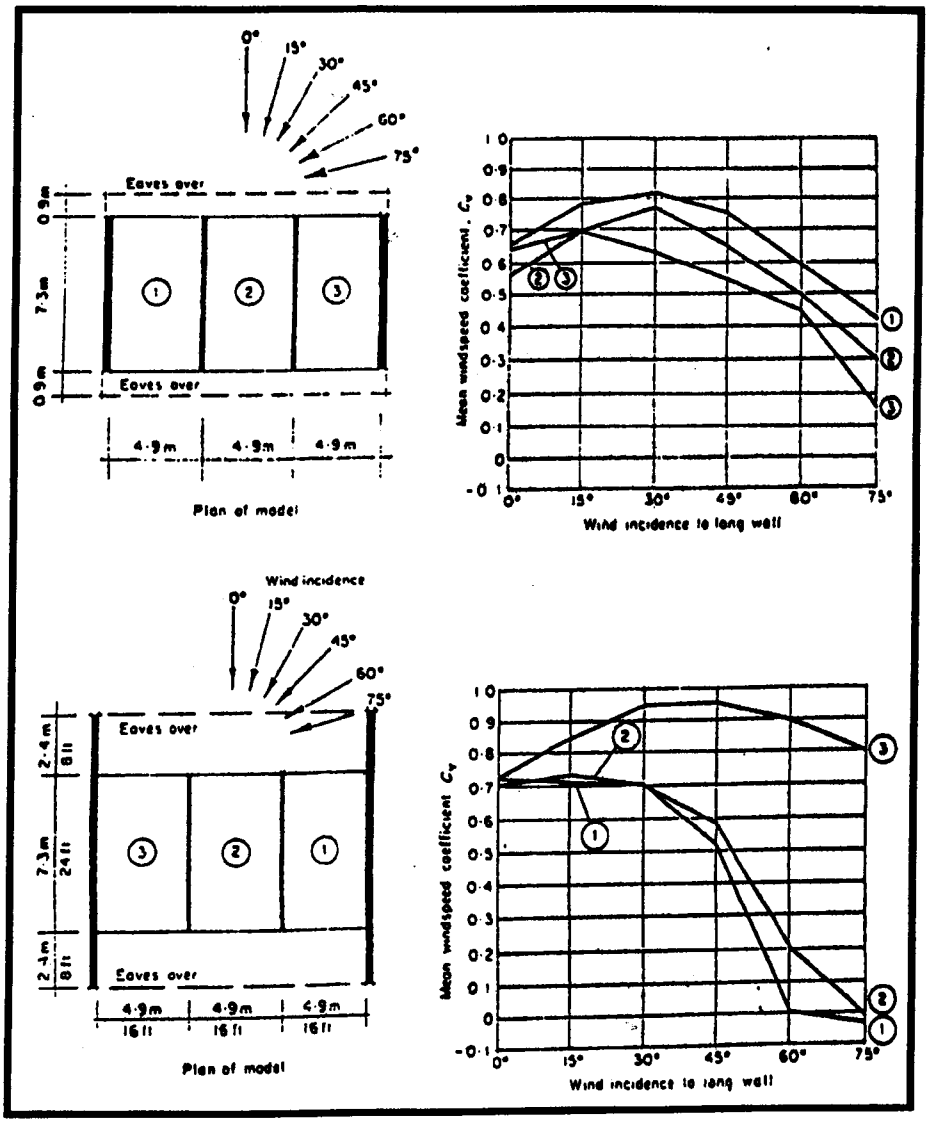

Appendix (A.7.a): The various roof configurations examined. (Kindangen et al. 1997).

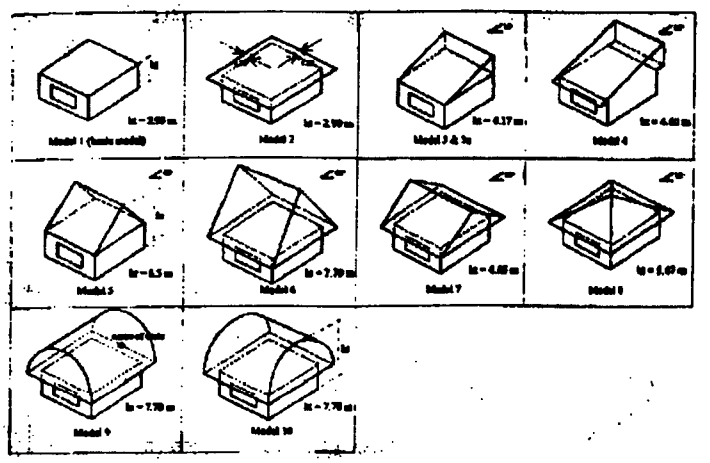

Appendix (A.7.b): Indoor air velocity as a function to various roof shapes measured at a height of 1.35m and along the centre section. The wind inclinations are (a=0°), (b=30°), (c=45°), (d=60°), (e=90°). (Kindangen et al. 1997)

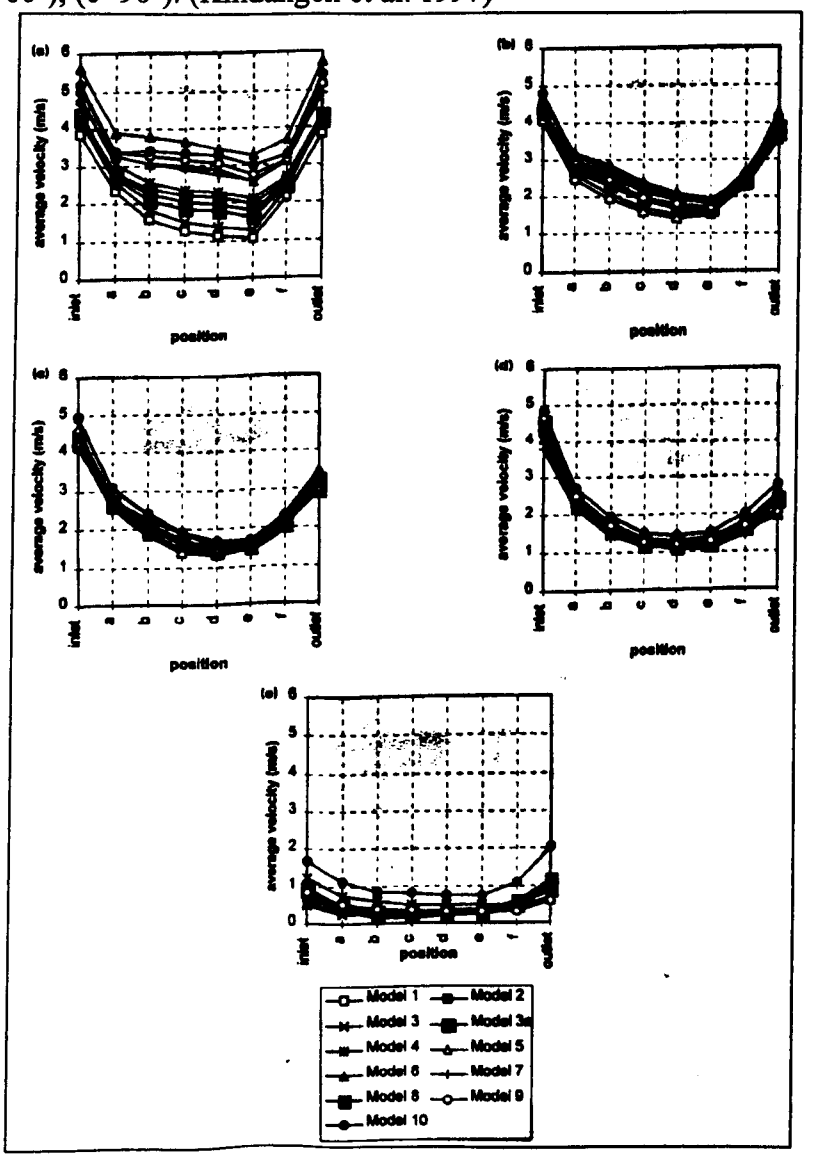

Appendix B: Pressure drop across the modulated louvered windows.

Appendix (B.1): The conversion of the data-logger results into pressure drops (DP) at both high and low pressure limits.

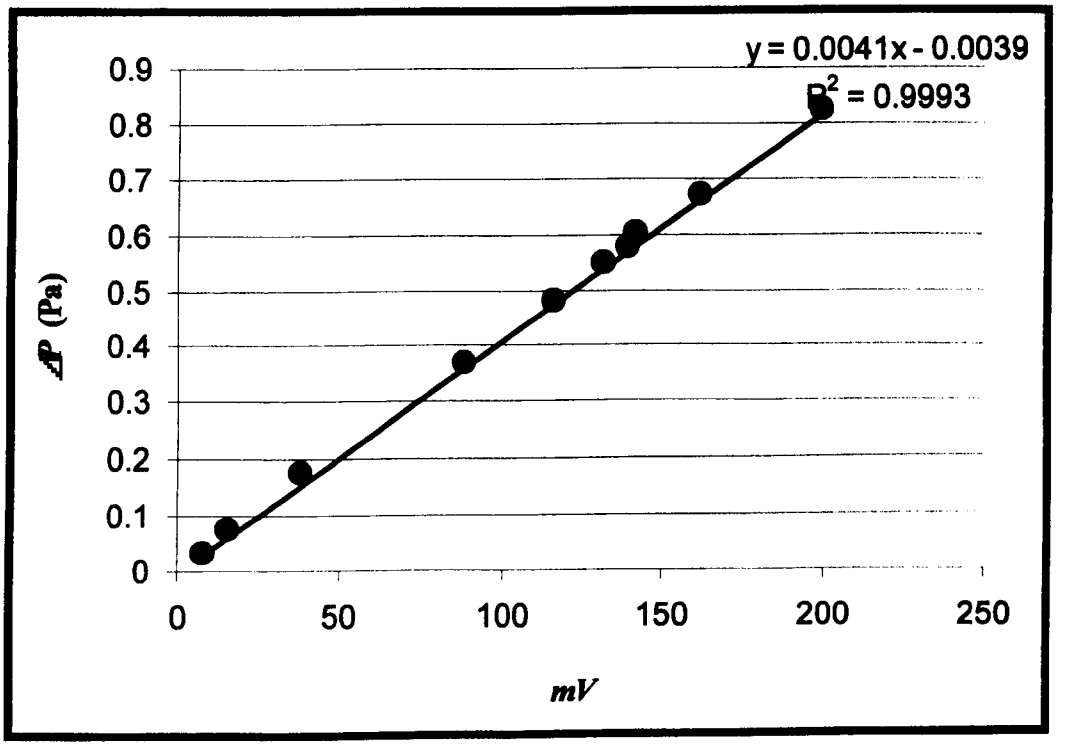

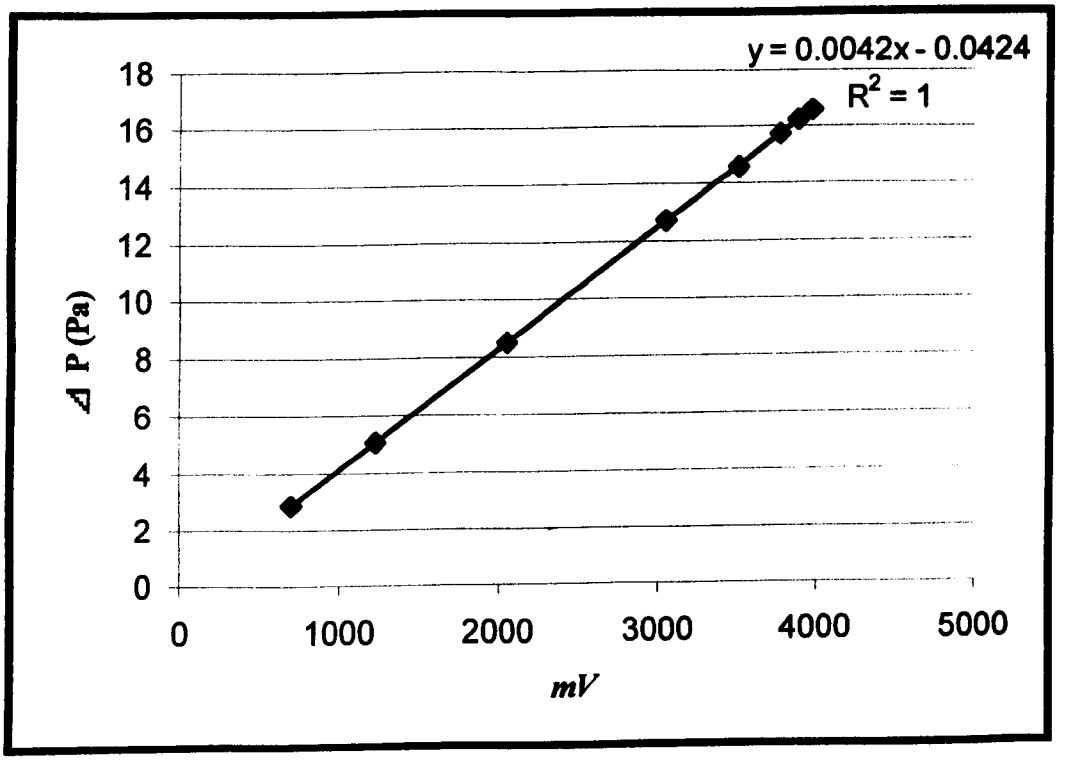

Appendix (B.2): The coefficient of determinations (r^2) with the standard errors of all MLW examined with both model equations.

L	d	θ	Quadratic reg.		Power low reg.	
			R sq.	St. err.	R sq.	St. err.
0.04	0.01	at 0°	0.939	0.003	0.543	1.288
0.04	0.01	at 15°	0.989	0.001	0.719	1.011
0.04	0.01	at 30°	0.980	0.002	0.719	1.011
0.04	0.01	at 45°	0.993	0.001	0.833	0.779
0.04	0.01	at 60°	0.9972	0.0028	0.9952	0.0048
0.04	0.01	at -15°	0.986	0.001	0.738	0.975
0.04	0.01	at -30°	0.987	0.001	0.735	0.982
0.04	0.01	at -45°	0.996	0.001	0.890	0.634
0.04	0.02	at 0°	0.689	0.006	0.267	1.633
0.04	0.02	at 15°	0.935	0.003	0.409	1.466
0.04	0.02	at 30°	0.839	0.004	0.358	1.528
0.04	0.02	at 45°	0.942	0.003	0.602	1.203
0.04	0.02	at 60°	0.985	0.001	0.837	0.769
0.04	0.02	at -15°	0.858	0.004	0.330	1.561
0.04	0.02	at -30°	0.896	0.004	0.461	1.400
0.04	0.02	at -45°	0.953	0.002	0.592	1.218
0.04	0.02	at -60°	0.983	0.001	0.796	0.862
0.04	0.03	at 0°	0.607	0.005	0.377	1.505
0.04	0.03	at 15°	0.585	0.007	0.226	1.678
0.04	0.03	at 30°	0.916	0.003	0.420	1.452
0.04	0.03	at 45°	0.921	0.003	0.517	1.326
0.04	0.03	at 60°	0.953	0.002	0.673	1.091
0.04	0.03	at -15°	0.838	0.004	0.528	1.310
0.04	0.03	at -30°	0.910	0.003	0.446	1.419
0.04	0.03	at -45°	0.966	0.002	0.587	1.226
0.04	0.03	at -60°	0.968	0.002	0.668	1.099

L	d	θ	Quadratic reg.		Power low reg.	
			R sq.	St. err.	R sq.	St. err.
0.06	0.02	at 0°	0.945	0.003	0.531	1.305
0.06	0.02	at 15°	0.987	0.001	0.705	1.035
0.06	0.02	at 30°	0.963	0.002	0.619	1.178
0.06	0.02	at 45°	0.987	0.001	0.743	0.967
0.06	0.02	at 60°	0.996	0.001	0.967	0.347
0.06	0.02	at -15°	0.979	0.002	0.639	1.146
0.06	0.02	at -30°	0.988	0.001	0.666	1.103
0.06	0.02	at -45°	0.978	0.002	0.673	1.090
0.06	0.02	at -60°	0.994	0.001	0.955	0.406
0.06	0.035	at 0°	0.774	0.005	0.430	1.440
0.06	0.035	at 15°	0.769	0.005	0.367	1.517
0.06	0.035	at 30°	0.914	0.003	0.464	1.396
0.06	0.035	at 45°	0.972	0.002	0.641	1.143
0.06	0.035	at 60°	0.981	0.002	0.729	0.992
0.06	0.035	at -15°	0.947	0.003	0.548	1.262
0.06	0.035	at -30°	0.928	0.003	0.449	1.416
0.06	0.035	at -45°	0.955	0.002	0.660	1.112
0.06	0.035	at -60°	0.968	0.002	0.704	1.038
0.06	0.05	at 0°	0.557	0.007	0.135	1.773
0.06	0.05	at 15°	0.682	0.006	0.276	1.623
0.06	0.05	at 30°	0.843	0.004	0.361	1.524
0.06	0.05	at 45°	0.944	0.003	0.528	1.309
0.06	0.05	at 60°	0.970	0.002	0.729	0.992
0.06	0.05	at -15°	0.926	0.003	0.475	1.382
0.06	0.05	at -30°	0.946	0.003	0.591	1.220
0.06	0.05	at -45°	0.957	0.002	0.586	1.227
0.06	0.05	at -60°	0.971	0.002	0.694	1.055

L	d	θ	Quadratic reg.		Power low reg.	
			R sq.	St. err.	R sq.	St. err.
0.080	0.03	at 0°	0.503	0.008	0.215	1.689
0.080	0.03	at 15°	0.812	0.005	0.350	1.537
0.080	0.03	at 30°	0.933	0.003	0.446	1.420
0.080	0.03	at 45°	0.955	0.002	0.543	1.288
0.080	0.03	at 60°	0.989	0.001	0.827	0.792
0.080	0.03	at -15°	0.958	0.002	0.592	1.218
0.080	0.03	at -30°	0.954	0.002	0.549	1.280
0.080	0.03	at -45°	0.975	0.002	0.609	1.193
0.080	0.03	at -60°	0.986	0.001	0.827	0.794
0.080	0.03	at 0°	0.527	0.008	0.125	1.783
0.080	0.05	at 15°	0.727	0.006	0.237	1.665
0.080	0.05	at 30°	0.746	0.006	0.244	1.658
0.080	0.05	at 45°	0.938	0.003	0.527	1.312
0.080	0.05	at 60°	0.946	0.003	0.624	1.170
0.080	0.05	at -15°	0.934	0.003	0.384	1.497
0.080	0.05	at -30°	0.944	0.003	0.456	1.406
0.080	0.05	at -45°	0.915	0.003	0.507	1.339
0.080	0.05	at -60°	0.949	0.003	0.630	1.159
0.080	0.07	at 0°	0.673	0.006	0.371	1.512
0.080	0.07	at 15°	0.936	0.003	0.542	1.291
0.080	0.07	at 30°	0.919	0.003	0.538	1.296
0.080	0.07	at 45°	0.954	0.002	0.523	1.317
0.080	0.07	at 60°	0.974	0.002	0.682	1.076
0.080	0.07	at -15°	0.966	0.002	0.594	1.215
0.080	0.07	at -30°	0.882	0.004	0.386	1.494
0.080	0.07	at -45°	0.976	0.002	0.579	1.237
0.080	0.07	at -60°	0.974	0.002	0.729	0.992

Appendix (B.3.a): Measured values of volume flow (Q meas) compared to calculated values (Qcalc) identified from the Eq.(6.5) for MLW L=0.06m and d=0.02m

θ	P(mmH$_2$o	Q_{meas}	Q_{calc}	Resid.
Angle 60°	0.0019	0.0001	0.0003	-0.0002
	0.0224	0.0031	0.0031	0.0001
	0.0820	0.0058	0.0095	-0.0038
	0.1291	0.0061	0.0136	-0.0075
	0.1842	0.0060	0.0178	-0.0118
	0.2224	0.0057	0.0204	-0.0147
	0.2603	0.0051	0.0228	-0.0178
	0.3046	0.0043	0.0255	-0.0212
	0.3380	0.0036	0.0274	-0.0237
Angle 45°	0.0019	0.0001	0.0087	-0.0086
	0.0031	0.0045	0.0109	-0.0065
	0.0060	0.0108	0.0146	-0.0038
	0.0074	0.0139	0.0161	-0.0022
	0.0104	0.0174	0.0190	-0.0015
	0.0146	0.0200	0.0222	-0.0022
	0.0180	0.0226	0.0246	-0.0020
	0.0232	0.0250	0.0278	-0.0028
	0.0249	0.0268	0.0287	-0.0019
Angle 30°	0.0019	0.0001	0.0105	-0.0104
	0.0022	0.0038	0.0116	-0.0078
	0.0027	0.0098	0.0131	-0.0033
	0.0052	0.0134	0.0186	-0.0052
	0.0064	0.0173	0.0209	-0.0035
	0.0081	0.0209	0.0238	-0.0029
	0.0099	0.0232	0.0265	-0.0033
	0.0109	0.0259	0.0279	-0.0020
	0.0122	0.0277	0.0296	-0.0019

θ	P(mmH$_2$o	Q_{meas}	Q_{calc}	Resid.
Angle 15°	0.0019	0.0001	0.0143	-0.0142
	0.0023	0.0039	0.0161	-0.0122
	0.0034	0.0105	0.0202	-0.0097
	0.0043	0.0133	0.0233	-0.0100
	0.0047	0.0181	0.0245	-0.0064
	0.0053	0.0215	0.0262	-0.0047
	0.0054	0.0239	0.0266	-0.0028
	0.0070	0.0264	0.0306	-0.0042
	0.0085	0.0282	0.0343	-0.0061
Angle 0°	0.0019	0.0001	0.0163	-0.0162
	0.0019	0.0038	0.0163	-0.0125
	0.0024	0.0099	0.0182	-0.0084
	0.0030	0.0138	0.0204	-0.0066
	0.0041	0.0180	0.0240	-0.0060
	0.0056	0.0213	0.0281	-0.0068
	0.0048	0.0236	0.0258	-0.0022
	0.0069	0.0262	0.0312	-0.0050
	0.0070	0.0282	0.0314	-0.0032
Angle -15°	0.0019	0.0001	0.0123	-0.0122
	0.0020	0.0043	0.0127	-0.0084
	0.0032	0.0106	0.0174	-0.0069
	0.0036	0.0141	0.0186	-0.0045
	0.0054	0.0181	0.0241	-0.0059
	0.0058	0.0212	0.0251	-0.0039
	0.0070	0.0235	0.0280	-0.0045
	0.0078	0.0261	0.0299	-0.0038
	0.0084	0.0278	0.0312	-0.0034

θ	P(mmH$_2$o	Q_{meas}	Q_{calc}	Resid.
Angle -30°	0.0019	0.0001	0.0108	-0.0107
	0.0022	0.0042	0.0118	-0.0077
	0.0035	0.0106	0.0153	-0.0047
	0.0049	0.0143	0.0182	-0.0039
	0.0066	0.0178	0.0213	-0.0035
	0.0081	0.0208	0.0238	-0.0029
	0.0091	0.0233	0.0253	-0.0020
	0.0116	0.0258	0.0288	-0.0030
	0.0125	0.0276	0.0300	-0.0024
Angle -45°	0.0019	0.0001	0.0095	-0.0094
	0.0024	0.0045	0.0104	-0.0060
	0.0047	0.0105	0.0137	-0.0032
	0.0071	0.0140	0.0163	-0.0023
	0.0108	0.0175	0.0195	-0.0020
	0.0131	0.0197	0.0214	-0.0016
	0.0180	0.0219	0.0246	-0.0028
	0.0221	0.0248	0.0270	-0.0023
	0.0254	0.0266	0.0288	-0.0023
Angle -60°	0.0019	0.0001	0.0006	-0.0005
	0.0199	0.0040	0.0044	-0.0003
	0.0635	0.0057	0.0101	-0.0044
	0.1034	0.0065	0.0139	-0.0074
	0.1553	0.0066	0.0179	-0.0113
	0.1954	0.0065	0.0206	-0.0141
	0.2392	0.0060	0.0232	-0.0172
	0.2848	0.0053	0.0257	-0.0204
	0.3219	0.0046	0.0276	-0.0230

Appendix (B.3.b): Measured values of volume flow (Q meas) compared to calculated values (Qcalc) identified from the Eq.(6.5) for MLW L=0.06m and d=0.035m

θ	P(mmH$_2$o	Q_{meas}	Q_{calc}	Resid.
Angle 60°	0.0019	0.0001	0.0061	-0.0060
	0.0026	0.0041	0.0070	-0.0029
	0.0087	0.0100	0.0119	-0.0019
	0.0142	0.0130	0.0149	-0.0019
	0.0217	0.0161	0.0182	-0.0021
	0.0294	0.0187	0.0210	-0.0024
	0.0379	0.0207	0.0238	-0.0031
	0.0473	0.0231	0.0264	-0.0034
	0.0534	0.0245	0.0280	-0.0036
Angle 45°	0.0019	0.0001	0.0127	-0.0126
	0.0024	0.0040	0.0140	-0.0100
	0.0038	0.0104	0.0168	-0.0063
	0.0043	0.0137	0.0177	-0.0040
	0.0057	0.0173	0.0199	-0.0026
	0.0088	0.0206	0.0240	-0.0035
	0.0098	0.0230	0.0252	-0.0022
	0.0132	0.0255	0.0287	-0.0033
	0.0140	0.0273	0.0295	-0.0022
Angle 30°	0.0019	0.0001	0.0180	-0.0179
	0.0020	0.0039	0.0185	-0.0146
	0.0020	0.0095	0.0183	-0.0088
	0.0028	0.0124	0.0208	-0.0084
	0.0040	0.0165	0.0238	-0.0073
	0.0041	0.0205	0.0241	-0.0035
	0.0060	0.0229	0.0280	-0.0052
	0.0072	0.0261	0.0302	-0.0041
	0.0075	0.0280	0.0307	-0.0027

θ	P(mmH$_2$o	Q_{meas}	Q_{calc}	Resid.
Angle 15°	0.0019	0.0001	0.0226	-0.0225
	0.0024	0.0039	0.0245	-0.0206
	0.0019	0.0097	0.0228	-0.0131
	0.0021	0.0132	0.0232	-0.0100
	0.0025	0.0171	0.0248	-0.0076
	0.0037	0.0204	0.0282	-0.0077
	0.0046	0.0231	0.0304	-0.0073
	0.0053	0.0262	0.0323	-0.0061
	0.0053	0.0282	0.0321	-0.0039
Angle 0°	0.0019	0.0001	0.0227	-0.0226
	0.0024	0.0038	0.0248	-0.0211
	0.0025	0.0093	0.0252	-0.0159
	0.0023	0.0127	0.0244	-0.0117
	0.0022	0.0170	0.0243	-0.0073
	0.0039	0.0204	0.0303	-0.0099
	0.0048	0.0231	0.0332	-0.0101
	0.0045	0.0263	0.0323	-0.0060
	0.0050	0.0282	0.0338	-0.0056
Angle -15°	0.0019	0.0001	0.0181	-0.0180
	0.0018	0.0039	0.0178	-0.0139
	0.0026	0.0097	0.0214	-0.0117
	0.0028	0.0137	0.0224	-0.0087
	0.0041	0.0176	0.0278	-0.0101
	0.0036	0.0210	0.0258	-0.0048
	0.0048	0.0235	0.0302	-0.0067
	0.0057	0.0262	0.0330	-0.0068
	0.0057	0.0281	0.0330	-0.0049

θ	P(mmH$_2$o	Q_{meas}	Q_{calc}	Resid.
Angle -30°	0.0019	0.0001	0.0170	-0.0169
	0.0014	0.0041	0.0152	-0.0111
	0.0022	0.0105	0.0180	-0.0076
	0.0028	0.0142	0.0200	-0.0058
	0.0045	0.0176	0.0246	-0.0070
	0.0044	0.0208	0.0245	-0.0036
	0.0053	0.0234	0.0265	-0.0031
	0.0066	0.0261	0.0292	-0.0031
	0.0077	0.0279	0.0314	-0.0035
Angle -45°	0.0019	0.0001	0.0119	-0.0118
	0.0031	0.0041	0.0141	-0.0100
	0.0039	0.0104	0.0153	-0.0049
	0.0049	0.0139	0.0166	-0.0027
	0.0074	0.0174	0.0197	-0.0023
	0.0117	0.0204	0.0237	-0.0033
	0.0132	0.0228	0.0249	-0.0021
	0.0164	0.0253	0.0274	-0.0021
	0.0194	0.0271	0.0295	-0.0024
Angle -60°	0.0019	0.0001	0.0048	-0.0047
	0.0026	0.0040	0.0059	-0.0019
	0.0073	0.0101	0.0108	-0.0006
	0.0114	0.0130	0.0138	-0.0008
	0.0199	0.0159	0.0187	-0.0028
	0.0284	0.0185	0.0226	-0.0041
	0.0362	0.0207	0.0257	-0.0050
	0.0467	0.0232	0.0294	-0.0062
	0.0514	0.0247	0.0309	-0.0062

Appendix (B.3.c): Measured values of volume flow (Q meas) compared to calculated values (Qcalc) identified from the Eq.(6.5) for MLW L=0.06m and d=0.05m

θ	$P(mmH_2O)$	Q_{meas}	Q_{calc}	Resid.
Angle 60°	0.0019	0.0001	0.0066	-0.0065
	0.0032	0.0043	0.0085	-0.0042
	0.0060	0.0104	0.0114	-0.0011
	0.0103	0.0139	0.0148	-0.0009
	0.0158	0.0170	0.0183	-0.0013
	0.0239	0.0198	0.0223	-0.0026
	0.0282	0.0217	0.0242	-0.0025
	0.0332	0.0242	0.0262	-0.0020
	0.0382	0.0257	0.0281	-0.0024
Angle 45°	0.0019	0.0001	0.0135	-0.0134
	0.0019	0.0042	0.0135	-0.0093
	0.0026	0.0106	0.0154	-0.0048
	0.0034	0.0140	0.0173	-0.0032
	0.0052	0.0179	0.0209	-0.0030
	0.0068	0.0213	0.0237	-0.0023
	0.0091	0.0234	0.0271	-0.0038
	0.0103	0.0258	0.0287	-0.0029
	0.0104	0.0277	0.0288	-0.0011
Angle 30°	0.0019	0.0001	0.0205	-0.0204
	0.0016	0.0043	0.0195	-0.0152
	0.0023	0.0103	0.0219	-0.0116
	0.0018	0.0140	0.0201	-0.0061
	0.0031	0.0183	0.0241	-0.0057
	0.0042	0.0209	0.0271	-0.0061
	0.0042	0.0235	0.0270	-0.0035
	0.0057	0.0260	0.0304	-0.0044
	0.0064	0.0280	0.0317	-0.0037

θ	$P(mmH_2O)$	Q_{meas}	Q_{calc}	Resid.
Angle 15°	0.0019	0.0001	0.0263	-0.0262
	0.0018	0.0039	0.0260	-0.0220
	0.0017	0.0104	0.0254	-0.0150
	0.0025	0.0138	0.0297	-0.0159
	0.0017	0.0185	0.0251	-0.0066
	0.0033	0.0214	0.0334	-0.0120
	0.0039	0.0240	0.0358	-0.0119
	0.0034	0.0265	0.0338	-0.0072
	0.0038	0.0284	0.0353	-0.0070
Angle 0°	0.0019	0.0001	0.0291	-0.0290
	0.0017	0.0035	0.0281	-0.0246
	0.0018	0.0089	0.0288	-0.0199
	0.0017	0.0129	0.0281	-0.0153
	0.0015	0.0172	0.0276	-0.0104
	0.0020	0.0207	0.0296	-0.0089
	0.0028	0.0233	0.0324	-0.0091
	0.0034	0.0263	0.0344	-0.0081
	0.0035	0.0284	0.0348	-0.0064
Angle -15°	0.0019	0.0001	0.0211	-0.0210
	0.0017	0.0042	0.0198	-0.0156
	0.0025	0.0110	0.0241	-0.0131
	0.0026	0.0147	0.0247	-0.0101
	0.0032	0.0186	0.0270	-0.0084
	0.0029	0.0208	0.0261	-0.0052
	0.0042	0.0231	0.0311	-0.0080
	0.0053	0.0260	0.0347	-0.0087
	0.0048	0.0280	0.0329	-0.0049

θ	$P(mmH_2O)$	Q_{meas}	Q_{calc}	Resid.
Angle -30°	0.0019	0.0001	0.0172	-0.0171
	0.0020	0.0040	0.0177	-0.0136
	0.0027	0.0119	0.0215	-0.0096
	0.0033	0.0154	0.0245	-0.0091
	0.0031	0.0190	0.0235	-0.0045
	0.0048	0.0218	0.0311	-0.0094
	0.0049	0.0239	0.0315	-0.0076
	0.0056	0.0263	0.0339	-0.0076
	0.0053	0.0280	0.0331	-0.0051
Angle -45°	0.0019	0.0001	0.0127	-0.0126
	0.0020	0.0043	0.0130	-0.0087
	0.0035	0.0105	0.0163	-0.0058
	0.0039	0.0143	0.0171	-0.0028
	0.0053	0.0179	0.0196	-0.0017
	0.0088	0.0210	0.0245	-0.0035
	0.0094	0.0231	0.0253	-0.0022
	0.0123	0.0257	0.0285	-0.0029
	0.0129	0.0274	0.0292	-0.0018
Angle -60°	0.0019	0.0001	0.0048	-0.0047
	0.0023	0.0042	0.0055	-0.0012
	0.0062	0.0107	0.0098	0.0009
	0.0126	0.0142	0.0146	-0.0004
	0.0198	0.0175	0.0186	-0.0011
	0.0265	0.0197	0.0217	-0.0021
	0.0312	0.0217	0.0237	-0.0020
	0.0359	0.0239	0.0255	-0.0017
	0.0429	0.0253	0.0281	-0.0028

Appendix (B.4): Measured values of volume flow (Q meas) compared to calculated values (Qcalc) identified from the Eq.(6.5).

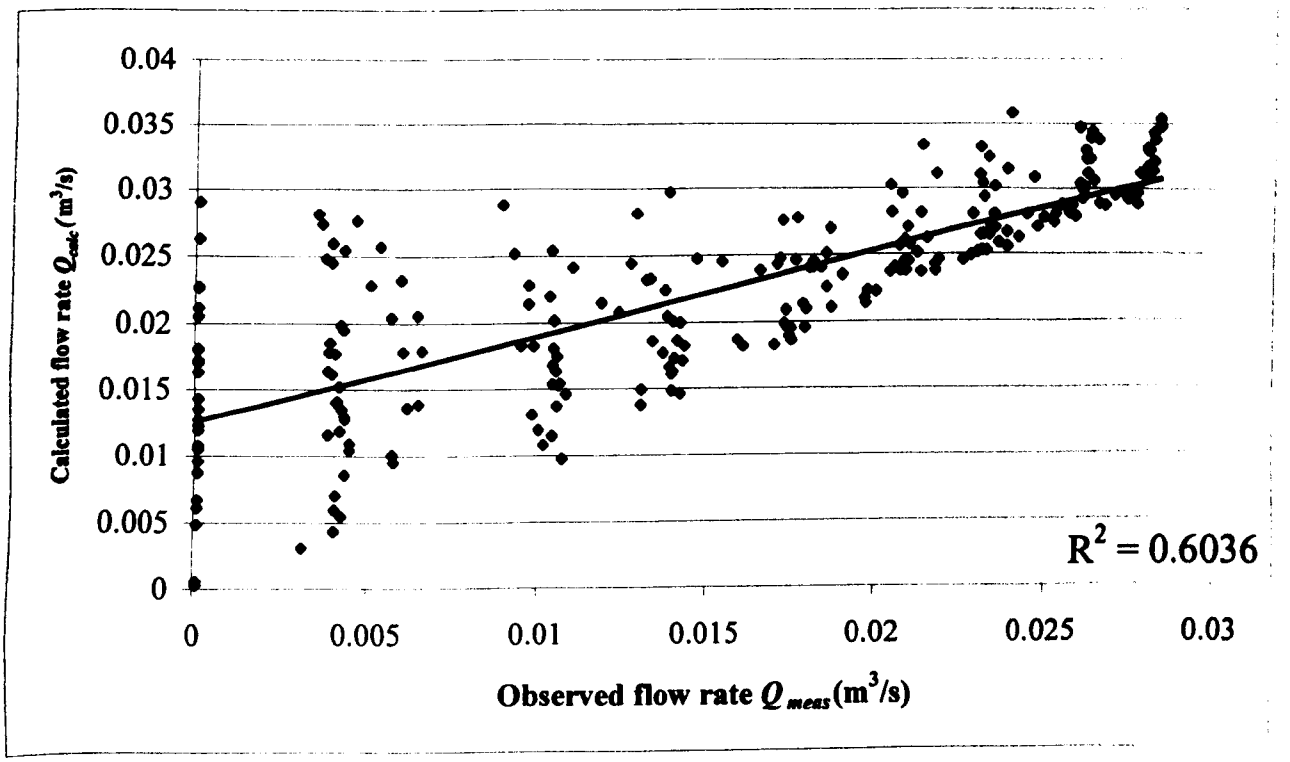

Appendix (B.5): Differential Pressures as function of various d/L ratios. [a: d/L=0.5, b:d/L= 0.75 and c: d/L=1].

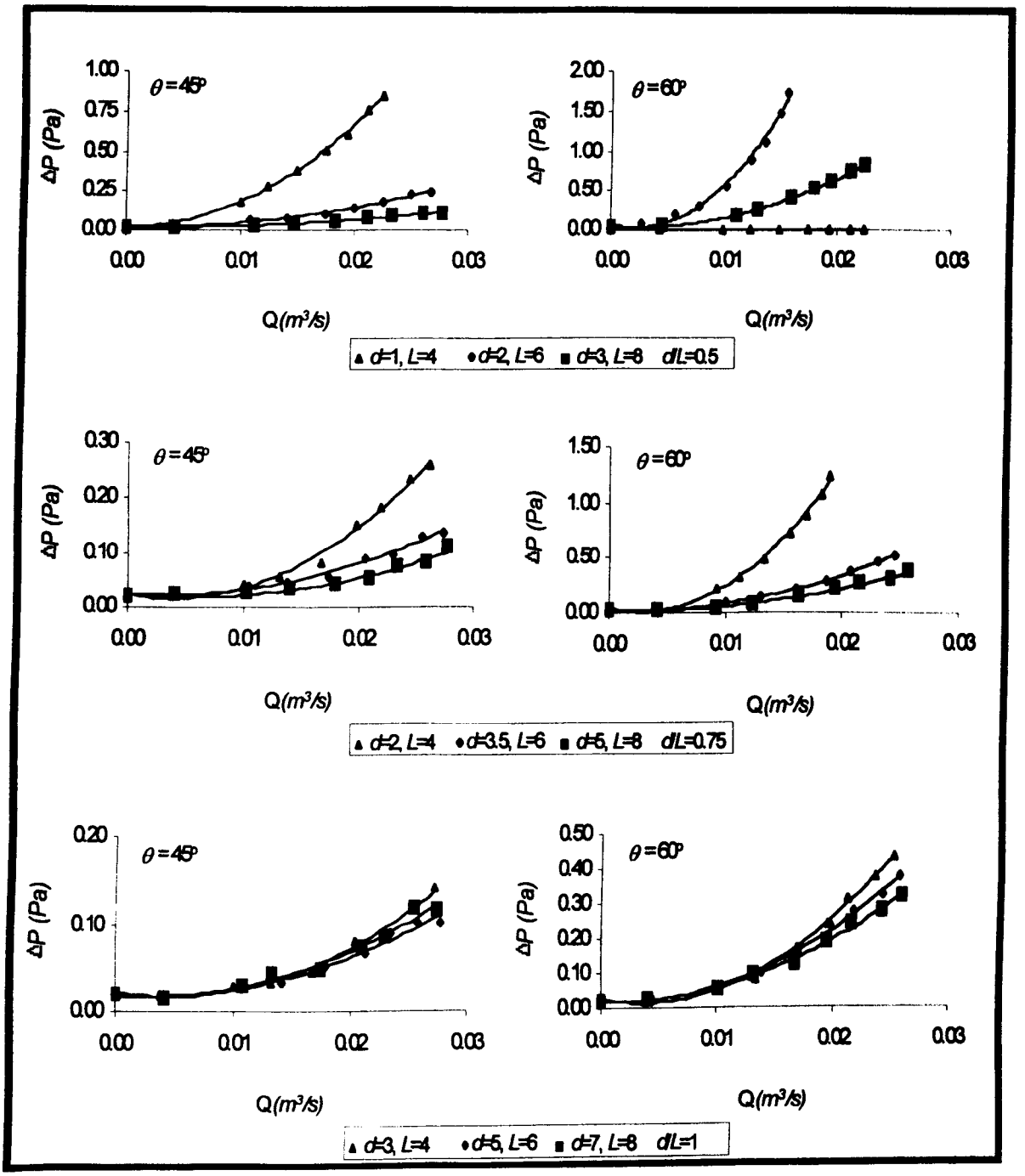

Appendix (B.6.a): The statistical analysis of the louver inclination effect

Tests of Between-Subjects Effects

Dependent Variable: PRESSURE

Source	Type II Sum of Squares	df	Mean Square	F	Sig.
Corrected Model	4.005[a]	3	1.335	38.041	.000
Intercept	9.548	1	9.548	272.080	.000
ANGLE	1.847E-02	1	1.847E-02	.526	.468
FLOW	7.045E-04	1	7.045E-04	.020	.887
FLOW * ANGLE	.477	1	.477	13.583	.000
Error	24.811	707	3.509E-02		
Total	38.364	711			
Corrected Total	28.816	710			

a. R Squared = .139 (Adjusted R Squared = .135)

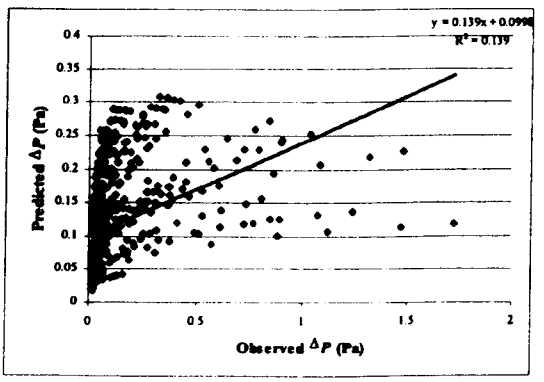

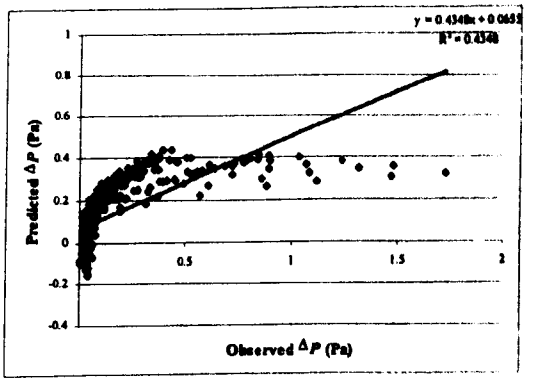

Appendix (B.6.b): The statistical analysis of the louver aperture effect

Tests of Between-Subjects Effects

Dependent Variable: PRESSURE

Source	Type II Sum of Squares	df	Mean Square	F	Sig.
Corrected Model	12.529[a]	3	4.176	181.295	.000
Intercept	9.548	1	9.548	414.482	.000
APERTURE	6.507E-02	1	6.507E-02	2.824	.093
FLOW	3.069	1	3.069	133.207	.000
FLOW * APERTURE	2.119	1	2.119	91.998	.000
Error	16.287	707	2.304E-02		
Total	38.364	711			
Corrected Total	28.816	710			

a. R Squared = .435 (Adjusted R Squared = .432)

Appendix (B.6.c): The statistical analysis of the louver depth effect

Tests of Between-Subjects Effects

Dependent Variable: PRESSURE

Source	Type II Sum of Squares	df	Mean Square	F	Sig.
Corrected Model	7.200[a]	3	2.400	78.497	.000
Intercept	9.548	1	9.548	312.296	.000
DEPTH	7.921E-02	1	7.921E-02	2.591	.108
FLOW	1.774	1	1.774	58.035	.000
FLOW * DEPTH	.922	1	.922	30.164	.000
Error	21.616	707	3.057E-02		
Total	38.364	711			
Corrected Total	28.816	710			

a. R Squared = .250 (Adjusted R Squared = .247)

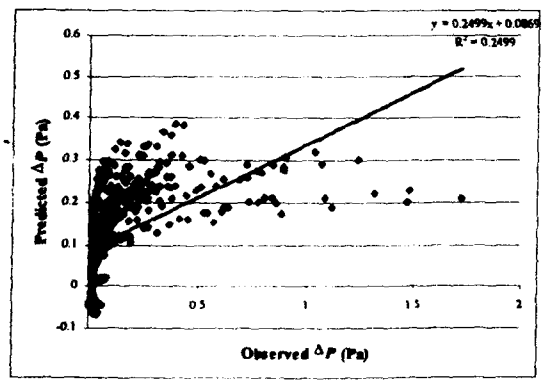

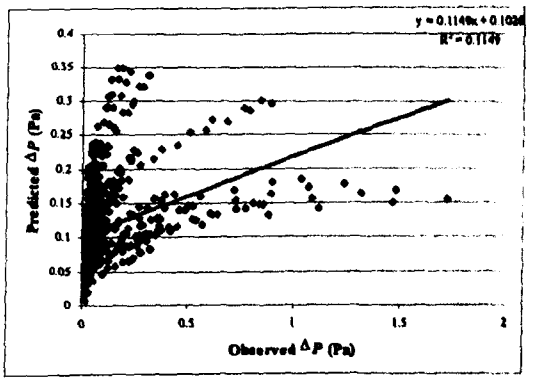

Appendix (B.6.d): The statistical analysis of the louver number effect

Tests of Between-Subjects Effects

Dependent Variable: PRESSURE

Source	Type II Sum of Squares	df	Mean Square	F	Sig.
Corrected Model	3.310[a]	3	1.103	30.586	.000
Intercept	9.548	1	9.548	264.669	.000
NUMBER	8.507E-02	1	8.507E-02	2.358	.125
FLOW	4.126E-03	1	4.126E-03	.114	.735
FLOW * NUMBER	.170	1	.170	4.723	.030
Error	25.506	707	3.608E-02		
Total	38.364	711			
Corrected Total	28.816	710			

a. R Squared = .115 (Adjusted R Squared = .111)

Appendix (B.6.e): The statistical analysis of the louver free area effect

Tests of Between-Subjects Effects

Dependent Variable: PRESSURE

Source	Type II Sum of Squares	df	Mean Square	F	Sig.
Corrected Model	14.054[a]	3	4.685	224.378	.000
Intercept	9.548	1	9.548	457.309	.000
FREEAREA	5.794E-02	1	5.794E-02	2.775	.096
FLOW	3.862	1	3.862	184.990	.000
FLOW * FREEAREA	2.510	1	2.510	120.195	.000
Error	14.762	707	2.088E-02		
Total	38.364	711			
Corrected Total	28.816	710			

a. R Squared = .488 (Adjusted R Squared = .486)

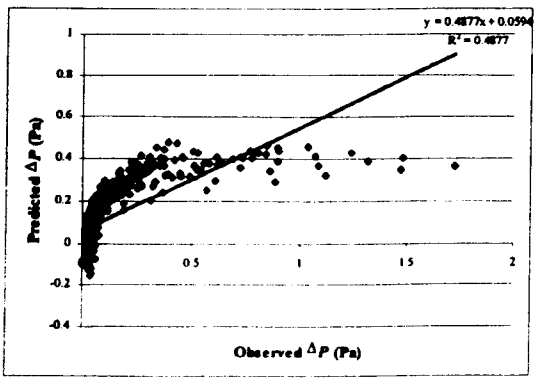

Appendix (B.7): The statistical analysis of the integration of overall variables.

Tests of Between-Subjects Effects

Dependent Variable: PRESSURE

Source	Type II Sum of Squares	df	Mean Square	F	Sig.
Corrected Model	17.996[a]	10	1.800	116.430	.000
Intercept	9.548	1	9.548	617.739	.000
ANGLE	7.453E-03	1	7.453E-03	.482	.488
NUMBER	8.180E-03	1	8.180E-03	.529	.467
DEPTH	.161	1	.161	10.429	.001
APERTURE	5.283E-02	1	5.283E-02	3.418	.065
FREEAREA	6.789E-02	1	6.789E-02	4.392	.036
FLOW	1.695E-02	1	1.695E-02	1.097	.295
FLOW * ANGLE	8.144E-03	1	8.144E-03	.527	.468
FLOW * NUMBER	5.873E-02	1	5.873E-02	3.800	.052
FLOW * APERTURE	.541	1	.541	35.023	.000
FLOW * FREEAREA	.849	1	.849	54.942	.000
Error	10.820	700	1.546E-02		
Total	38.364	711			
Corrected Total	28.816	710			

a. R Squared = .625 (Adjusted R Squared = .619)

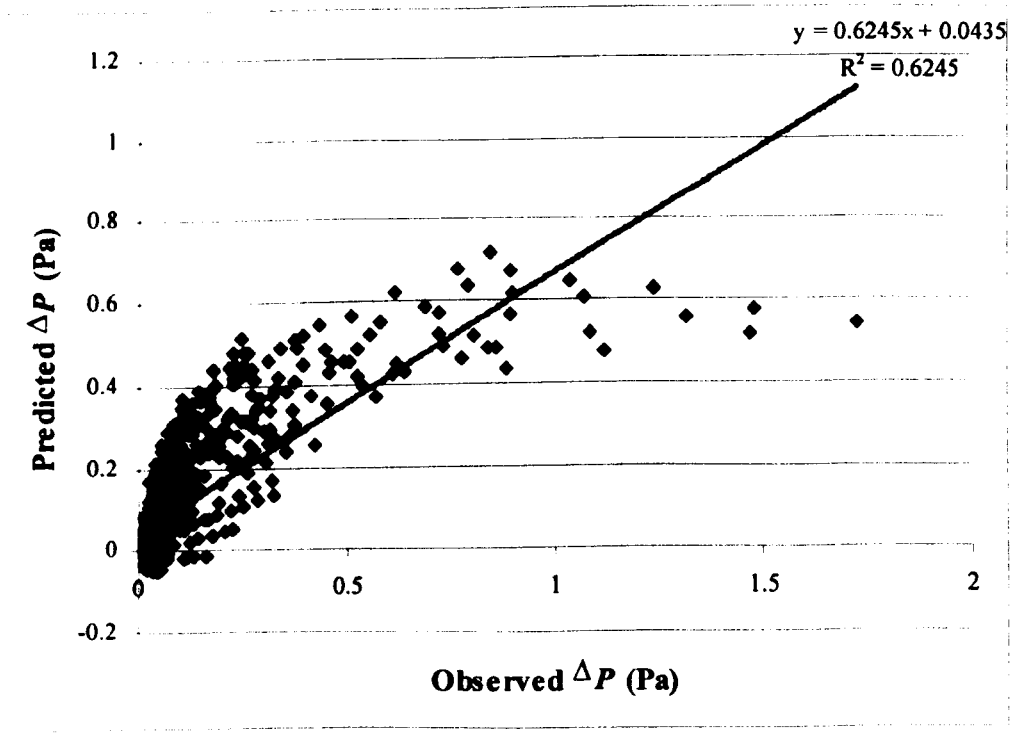

Based on the statistical model:

$$\Delta P = c + \alpha.Q + \beta_i.d_\theta + \chi_i.A_f + \delta_i.N + \varepsilon_i.L_\theta + \phi_i.\theta + \left[(\alpha\beta)_{ij} \cdot Q.d_\theta + (\alpha\chi)_{ij} \cdot Q.A_f + (\alpha\delta)_{ij} \cdot Q.N\right]$$

Appendix (B.8.a): The statistical analysis of the louver depth at θ=60°

Tests of Between-Subjects Effects

Dependent Variable: PRESSURE

Source	Type II Sum of Squares	df	Mean Square	F	Sig.
Corrected Model	1539.454[a]	3	513.151	49.601	.000
Intercept	1873.314	1	1873.314	181.075	.000
Depth	46.175	1	46.175	4.463	.037
FLOW	654.823	1	654.823	63.295	.000
FLOW * Depth	399.004	1	399.004	38.568	.000
Error	1251.805	121	10.345		
Total	4664.573	125			
Corrected Total	2791.259	124			

a. R Squared = .552 (Adjusted R Squared = .540)

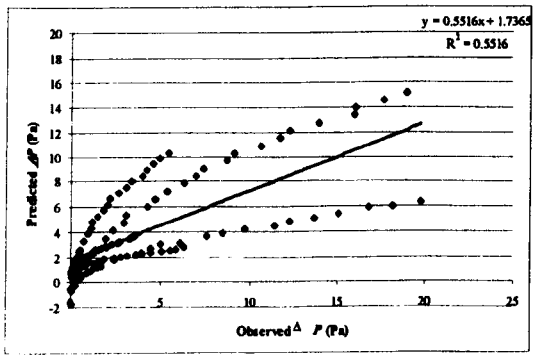

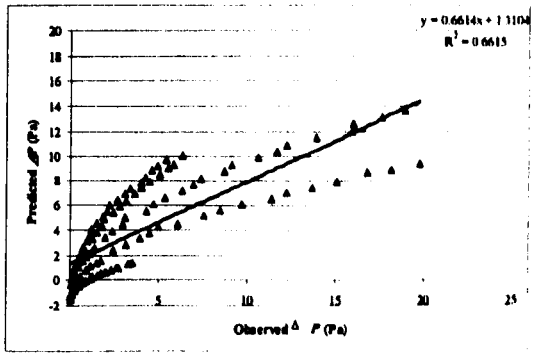

Appendix (B.8.b): The statistical analysis of the louver aperture at θ=60°

Tests of Between-Subjects Effects

Dependent Variable: PRESSURE

Source	Type II Sum of Squares	df	Mean Square	F	Sig.
Corrected Model	1846.379[a]	3	615.460	78.815	.000
Intercept	1873.314	1	1873.314	239.894	.000
FLOW	958.186	1	958.186	122.704	.000
Aperture	1.415	1	1.415	.181	.671
FLOW * Aperture	340.477	1	340.477	43.601	.000
Error	944.879	121	7.809		
Total	4664.573	125			
Corrected Total	2791.259	124			

a. R Squared = .661 (Adjusted R Squared = .653)

Appendix (B.8.c): The statistical analysis of the louver free area at θ=60°

Tests of Between-Subjects Effects

Dependent Variable: PRESSURE

Source	Type II Sum of Squares	df	Mean Square	F	Sig.
Corrected Model	1860.088[a]	3	620.029	80.569	.000
Intercept	1873.314	1	1873.314	243.426	.000
Free-area	15.477	1	15.477	2.011	.159
FLOW	617.599	1	617.599	80.253	.000
FLOW * Free-area	415.104	1	415.104	53.940	.000
Error	931.171	121	7.696		
Total	4664.573	125			
Corrected Total	2791.259	124			

a. R Squared = .666 (Adjusted R Squared = .658)

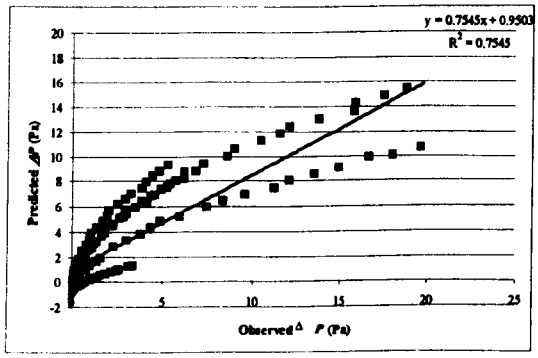

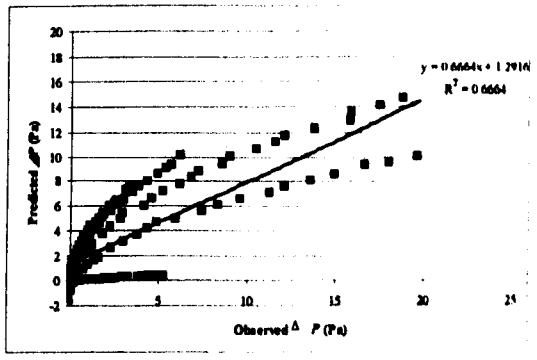

Appendix (B.8.d): The statistical analysis of the louver number at θ=60°

Tests of Between-Subjects Effects

Dependent Variable: PRESSURE

Source	Type II Sum of Squares	df	Mean Square	F	Sig.
Corrected Model	2105.871[a]	3	701.957	123.925	.000
Intercept	1873.314	1	1873.314	330.720	.000
Number	3.569	1	3.569	.630	.429
FLOW	68.965	1	68.965	12.175	.001
Number * FLOW	439.489	1	439.489	77.589	.000
Error	685.388	121	5.664		
Total	4664.573	125			
Corrected Total	2791.259	124			

a. R Squared = .754 (Adjusted R Squared = .748)

Appendix (B.9): The statistical analysis of integration of the overall variables at θ=60°

Tests of Between-Subjects Effects

Dependent Variable: PRESSURE

Source	Type II Sum of Squares	df	Mean Square	F	Sig.
Corrected Model	2664.337[a]	9	296.037	268.231	.000
Intercept	1873.314	1	1873.314	1697.356	.000
Aperture	3.559	1	3.559	3.225	.075
Depth	9.810E-04	1	9.810E-04	.001	.976
Free-area	1.002	1	1.002	.908	.343
Number	4.392	1	4.392	3.979	.048
FLOW	80.279	1	80.279	72.738	.000
Aperture * FLOW	108.166	1	108.166	98.006	.000
Depth * FLOW	51.227	1	51.227	46.415	.000
Free-area * FLOW	1.701	1	1.701	1.541	.217
Number * FLOW	128.703	1	128.703	116.614	.000
Error	126.922	115	1.104		
Total	4664.573	125			
Corrected Total	2791.259	124			

a. R Squared = .955 (Adjusted R Squared = .951)

Appendix C: Velocity drop across the modulated louvered windows.

Appendix (C.1): The calibration of the air velocity transducer.

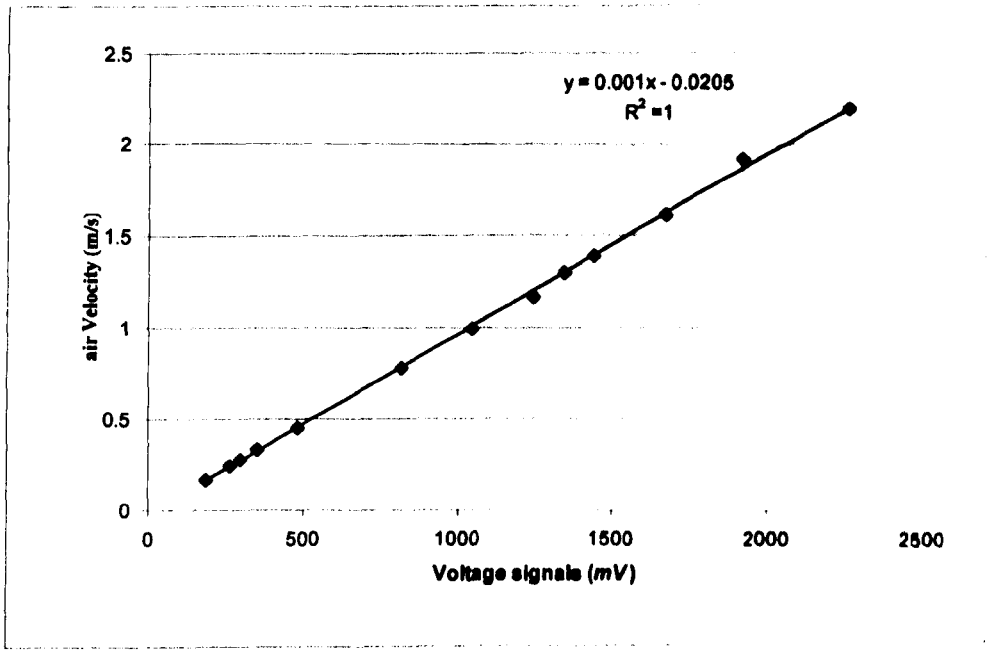

Appendix (C.2): The various wind speed required indoors. (Evans, 1980).

Speed m/sec	Mechanical effect	Effect on man	Cooling effect (deg C) Dry skin Ambient air temperature 15°C	20°C	25°C	30°C	Moist skin 30°C
0.1	Minimum likely in domestic situations	May feel stuffy	0	0	0	0	0
0.25	Smoke (from cigarette) indicates movement	Movement not noticeable except at low air temperatures	2	1.3	0.8	0.8	0.7
0.5	Flame from a candle flickers	Feels fresh at comfortable temperatures, but draughty at cool temperatures	4	2.7	1.7	1.0	1.2
1.0	Loose papers may be moved, equivalent to walking speed	Generally pleasant when comfortable or warm, but causing constant awareness of motion, maximum limit for night comfort	6.7	4.6	2.8	1.7	2.2
1.5	Too fast for desk work with loose papers	Draughty at comfortable temperatures, maximum limit for indoor activities	8.5	6.7	3.6	2.0	3.3
2.0	Equivalent to a fast walking speed	Acceptable only in very hot and humid conditions when no other relief is available	10	8.7	4.0	2.3	4.2

Note: Effect on man relates to domestic situations. In factories and other buildings higher windspeeds may be desirable, and comfortable.

Appendix (C.3): The reduction in indoor air velocity as function to various MLW configurations. Measured values at Rd=0.75m.

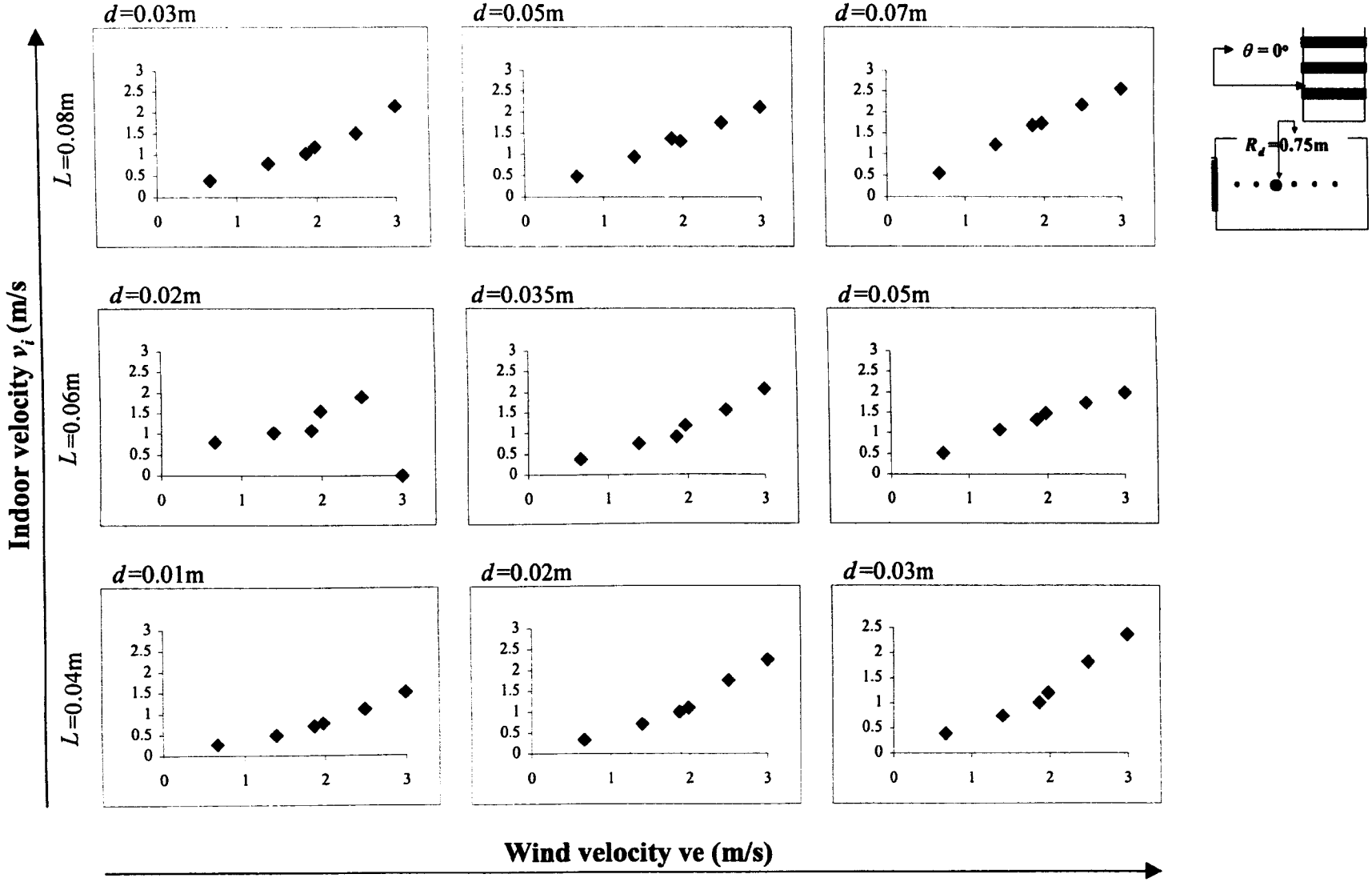

Appendix (C.4): The ratio v_e/v_i as function to various MLW configurations. Measured values at Rd=0.75m.

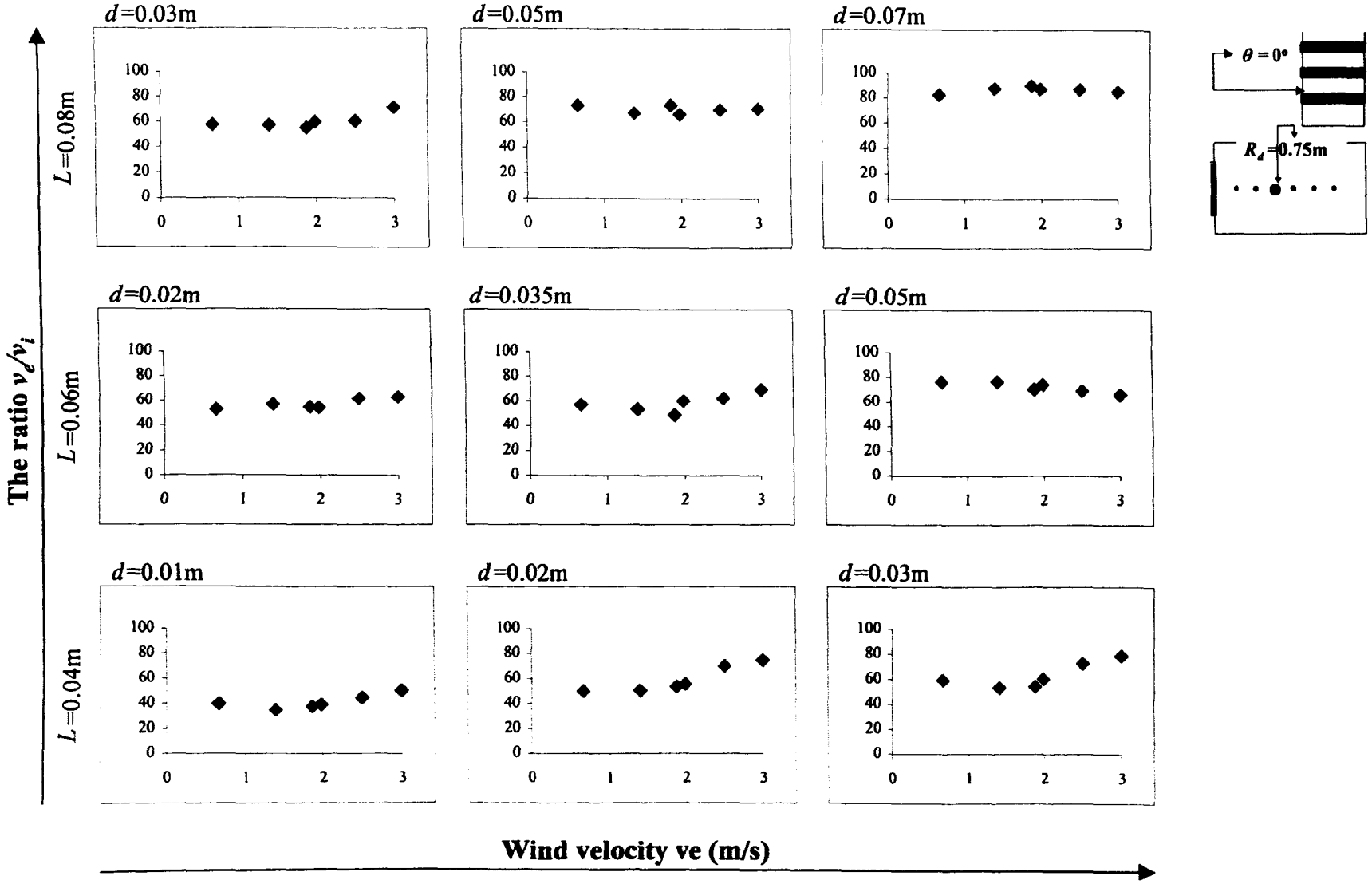

Appendix (C.5): The ratio of vi/ve as function to room depth along and above centre

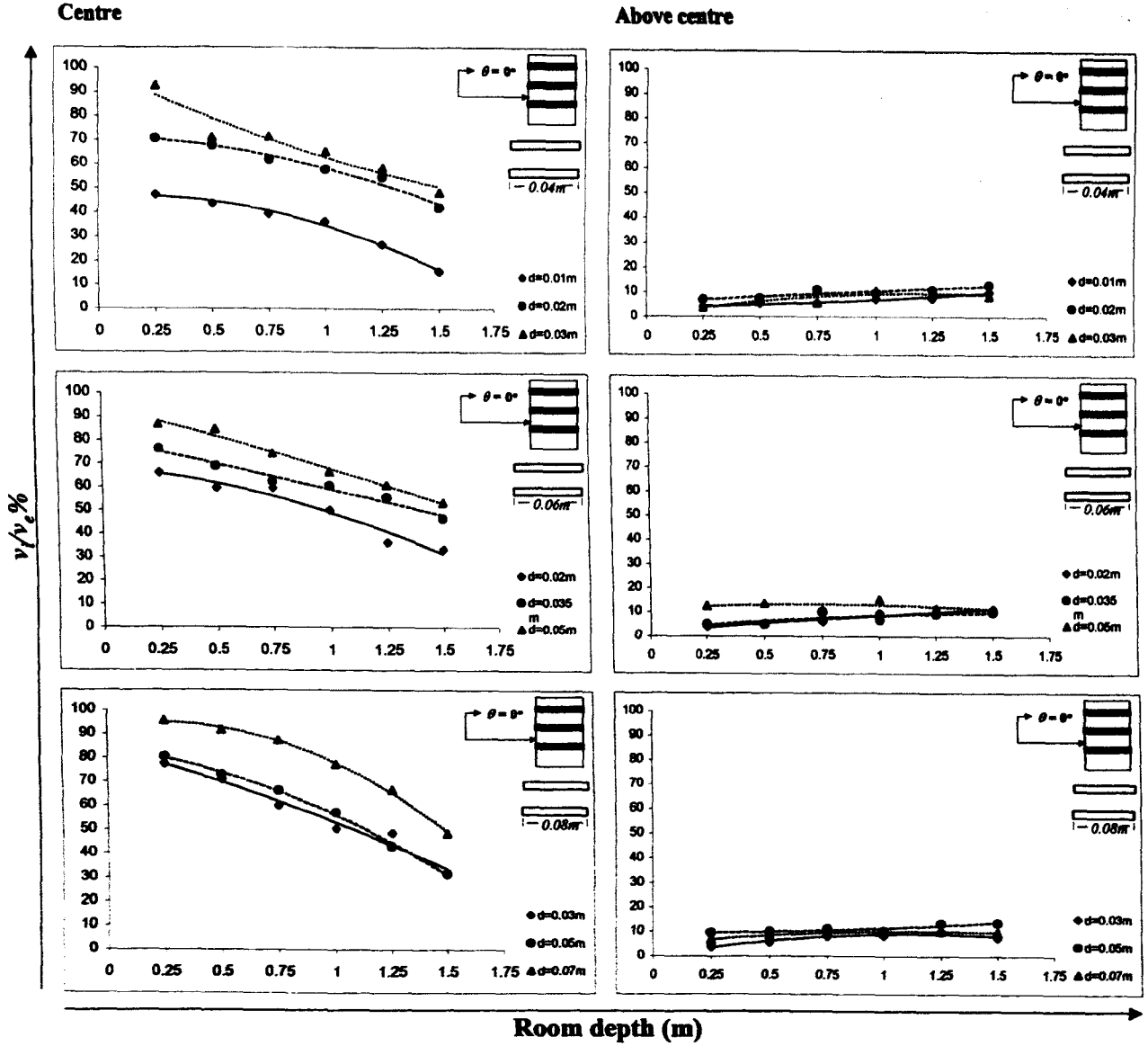

Appendix (C.6): The ratio of vi/ve as function to room depth along and above centre

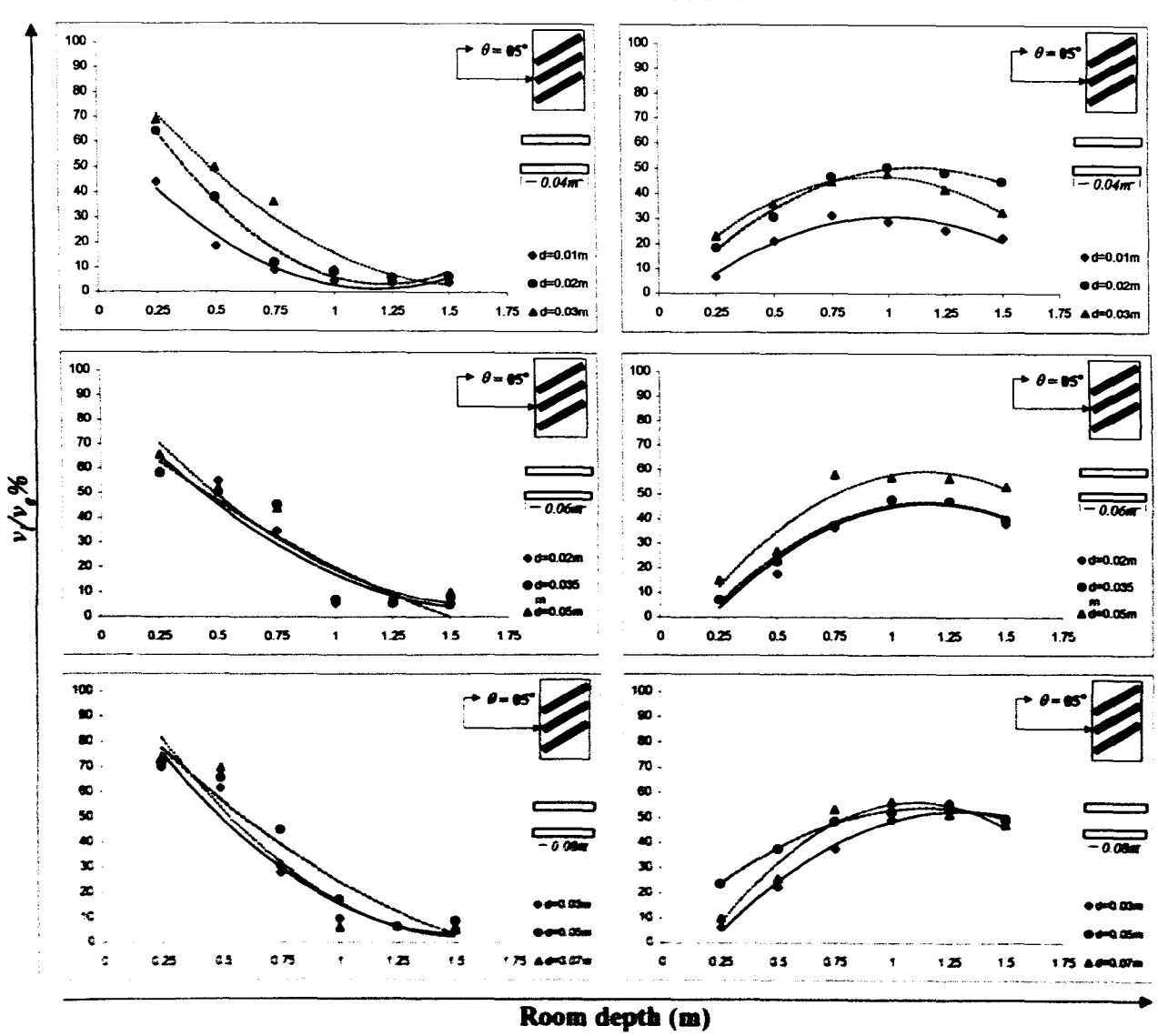

Appendix (C.7): The ratio of vi/ve as function to room depth along and above centre

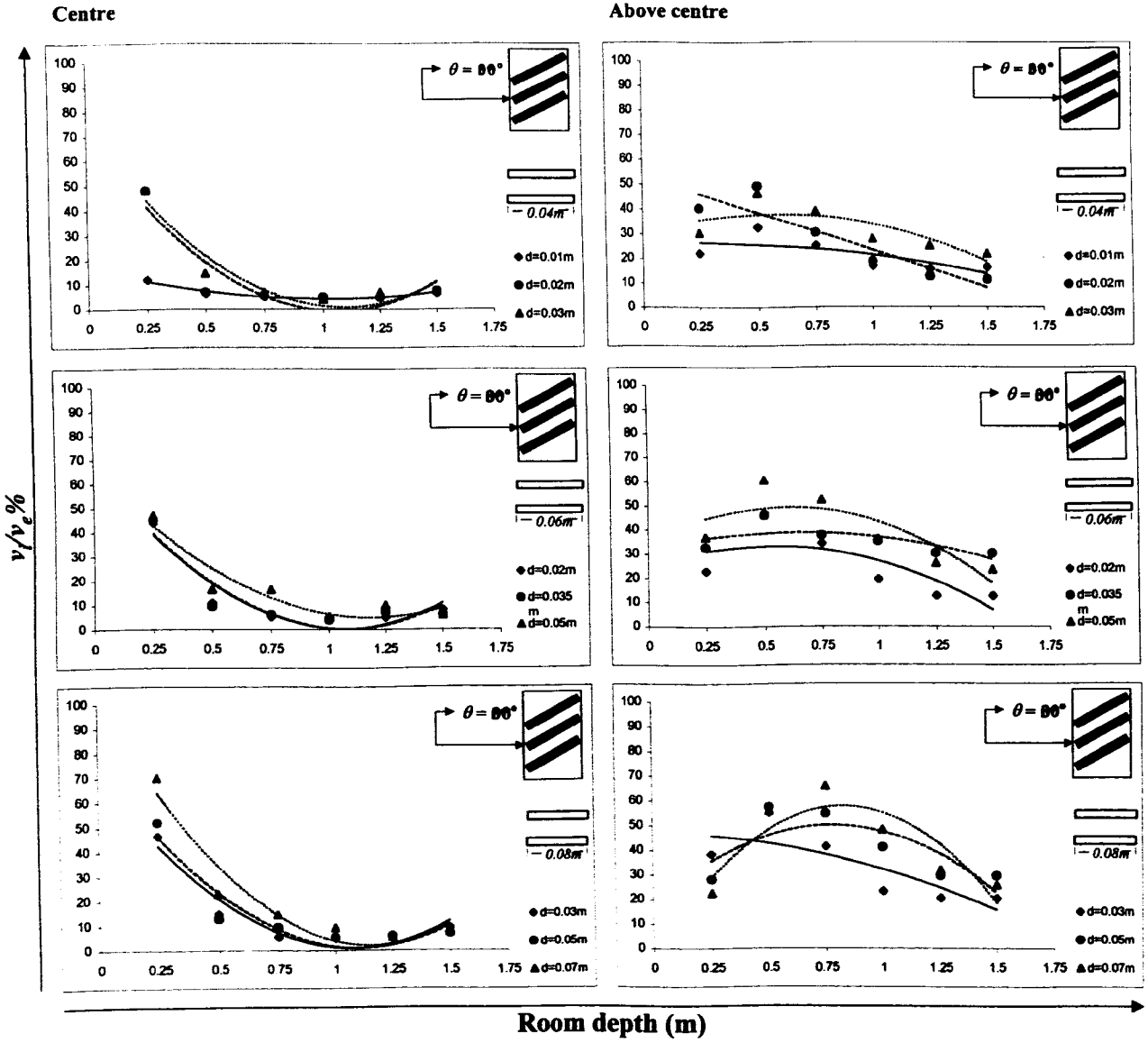

Appendix (C.8): The ratio of vi/ve as function to room depth along and above centre

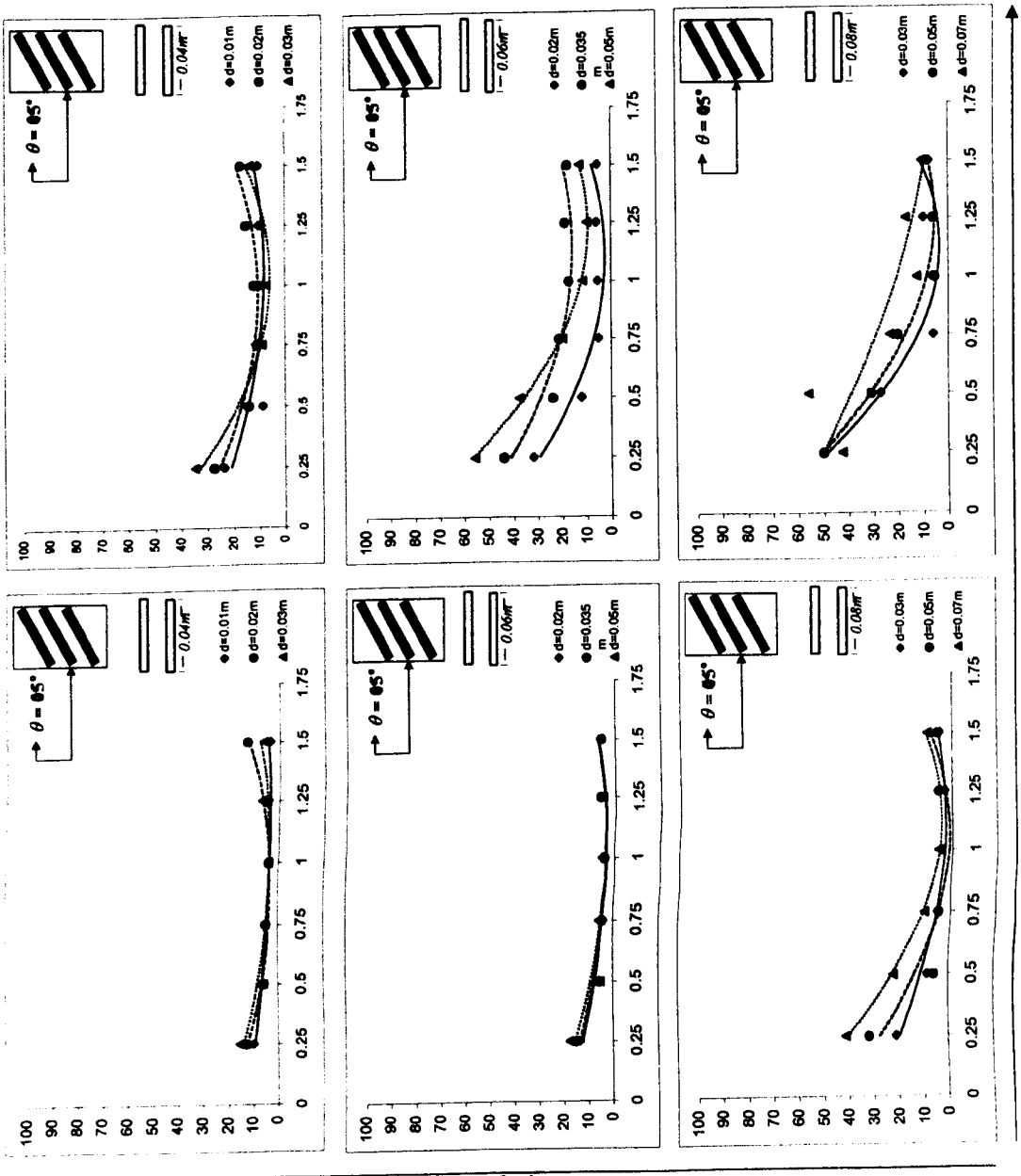

Appendix (C.9): The ratio of vi/ve as function to room depth along and above centre

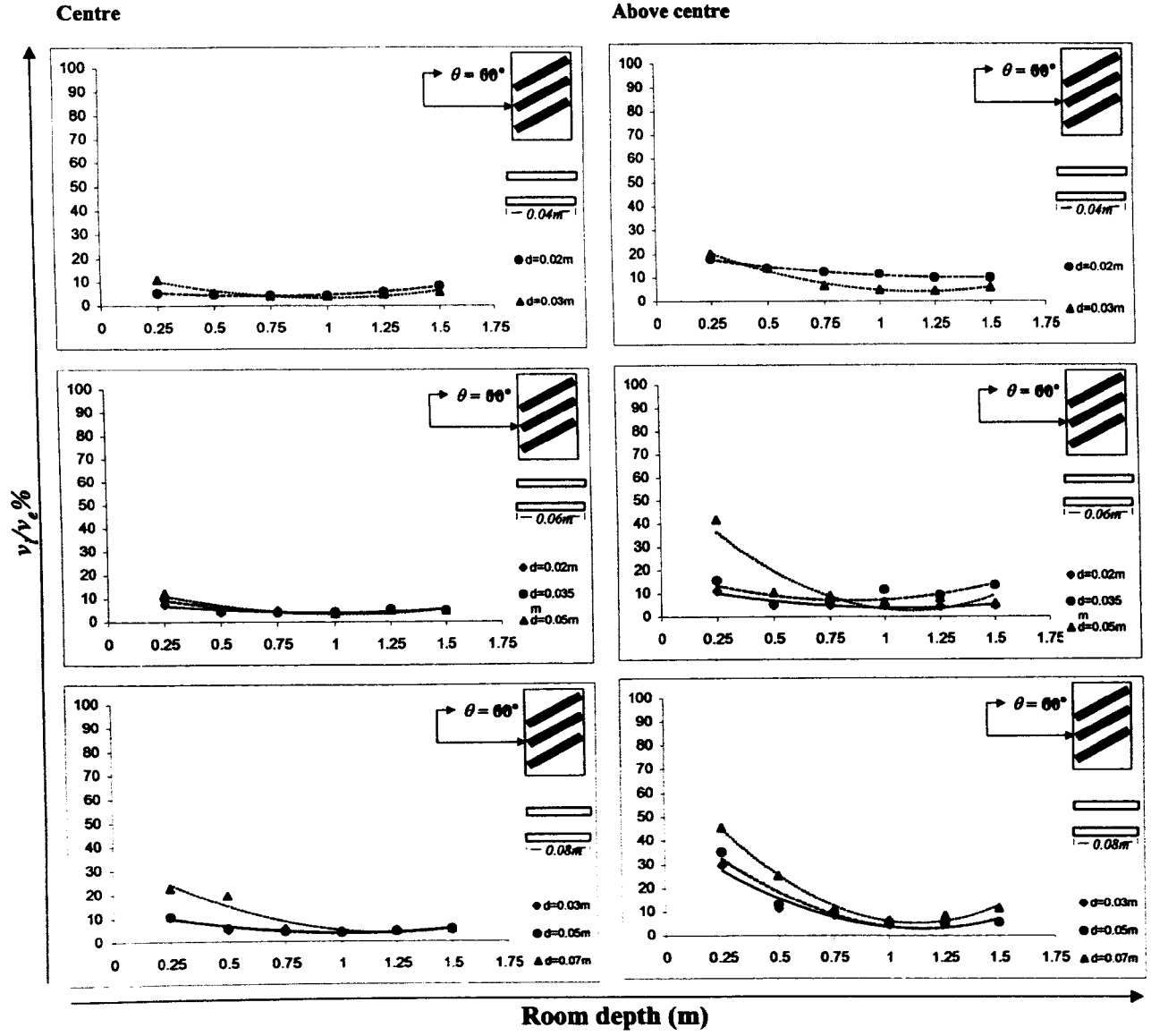

Appendix (C.10): the velocity drop across room (along the centre) for the various MLW configurations examined.

d=0.01m, L=0.04m

R_d	0	15	30	45	60
0.25	47.33788	44.00707	12.0111	10.09336	0
0.5	43.70426	18.57179	6.156952	5.500883	0
0.75	39.38935	9.084027	5.046682	4.542014	0
1	35.98284	4.693414	4.542014	3.911178	0
1.25	26.84835	3.885945	5.55135	4.491547	0
1.5	15.77088	3.971739	6.560686	3.936412	0

d=0.02m, L=0.04m

R_d	0	15	30	45	60
0.25	70.72925	64.44613	48.12011	12.66717	5.55135
0.5	67.8274	38.10245	7.065355	6.056018	5.046682
0.75	61.94802	12.11204	5.55135	5.046682	4.542014
1	57.68357	8.579359	5.046682	4.037345	4.542014
1.25	54.6051	6.056018	5.046682	5.55135	6.056018
1.5	42.03886	6.560686	7.570023	13.12137	8.579359

d=0.03m, L=0.04m

R_d	0	15	30	45	60
0.25	92.658	68.98814	48.44815	15.61948	11.1027
0.5	71.18345	49.91168	14.63538	6.056018	5.55135
0.75	71.5	36.23518	7.065355	5.046682	4.037345
1	65.2	9.109261	4.037345	4.037345	4.037345
1.25	58.6	5.828917	7.065355	7.065355	5.046682
1.5	48.3	5.248549	7.570023	6.560686	6.056018

d=0.02m, L=0.06m

R_d	0	15	30	45	60
0.25	66.06106	58.81908	43.70426	13.47464	7.570023
0.5	59.67701	55.03407	10.85037	5.55135	4.037345
0.75	59.57608	34.8978	5.187989	4.037345	5.046682
1	50.08832	5.55135	5.046682	3.986879	3.996972
1.25	36.43704	7.443856	4.935655	5.046682	5.198082
1.5	33.3838	7.645723	8.074691	5.500883	5.147615

d=0.035m, L=0.06m

R_d	0	15	30	45	60
0.25	76.4	58.31441	44.865	15.03911	10.24476
0.5	69	50.39112	9.588695	5.55135	5.046682
0.75	62.40222	45.42014	6.056018	4.542014	4.037345
1	60.56018	7.090588	4.037345	4.082766	4.390613
1.25	55.86677	5.59677	6.989654	6.056018	5.55135
1.5	46.68181	4.945748	6.106485	5.56649	5.046682

d=0.05m, L=0.06m

R_d	0	15	30	45	60
0.25	86.82816	65.90966	46.95937	17.66339	12.36437
0.5	84.75902	52.20792	16.50265	5.046682	5.046682
0.75	74.38809	43.90613	16.35125	5.70275	5.046682
1	66.51527	6.838254	5.55135	5.046682	3.532677
1.25	60.98915	7.040121	10.09336	5.046682	5.046682
1.5	53.52006	10.0429	5.879384	6.056018	5.046682

d=0.03m, L=0.08m

R_d	0	15	30	45	60
0.25	77.44133	69.94701	46.65657	21.0699	10.54756
0.5	70.93111	61.64522	14.88771	8.579359	5.046682
0.75	59.85365	28.11002	5.500883	5.55135	4.542014
1	50.44158	9.714862	5.042644	4.930608	4.536967
1.25	48.70048	6.257885	6.101438	3.028009	4.945748
1.5	31.59223	5.55135	9.437295	5.046682	5.046682

d=0.05m, L=0.08m

R_d	0	15	30	45	60
0.25	80.41887	71.61241	52.18269	31.92026	10.60308
0.5	72.94979	65.80873	12.94474	6.056018	5.55135
0.75	66.162	45.1678	9.593742	4.996215	4.542014
1	57.1789	17.31012	5.55135	4.491547	3.936412
1.25	43.25006	6.434519	6.056018	5.55135	4.542014
1.5	31.74363	8.755993	7.216755	6.061065	5.55135

d=0.07m, L=0.08m

R_d	0	15	30	45	60
0.25	95.6	73.37875	70.32551	41.10522	22.74035
0.5	91.7	69.82084	23.1895	22.2054	19.58617
0.75	87.25713	31.31466	14.73631	10.63841	5.55135
1	77.3	6.005551	9.603835	5.955085	4.491547
1.25	66.59097	6.863487	5.59677	6.056018	4.996215
1.5	48.54908	4.996215	7.74161	10.0429	5.55135

Appendix (C.11): the velocity drop across room (above the centre) for the various MLW configurations examined.

d=0.01m, L=0.04m

R_d	0	15	30	45	60
0.25	4.037345	6.863487	21.9783	23.66894	0
0.5	5.55135	21.297	32.65203	8.856927	0
0.75	5.541257	31.23896	25.23341	11.38027	0
1	7.110775	28.94272	16.72975	9.588695	0
1.25	7.570023	25.68761	15.49331	10.14383	0
1.5	10.09336	22.60913	16.25032	10.4971	0

d=0.02m, L=0.04m

R_d	0	15	30	45	60
0.25	7.065355	18.59702	40.14635	27.58012	18.16805
0.5	7.570023	30.83523	49.38178	14.13071	14.13071
0.75	11.1027	46.70704	30.45672	10.59803	12.6167
1	9.588695	50.59299	18.69796	12.11204	11.60737
1.25	11.1027	48.54908	12.59147	15.14005	10.09336
1.5	13.12137	44.865	11.35503	17.15872	10.09336

d=0.03m, L=0.04m

R_d	0	15	30	45	60
0.25	3.810245	23.23997	30.17916	34.87257	20.18673
0.5	7.191522	36.08377	46.50517	15.21575	14.13071
0.75	5.803684	44.73883	39.16225	8.983094	6.72218
1	10.69897	47.84254	27.80722	7.267222	5.036588
1.25	10.14383	41.71083	25.05678	9.866263	4.542014
1.5	8.453192	32.60156	21.85213	13.60081	6.056018

d=0.02m, L=0.06m

R_d	0	15	30	45	60
0.25	4.037345	7.141055	22.8867	31.99596	11.1027
0.5	5.299016	17.63815	46.93414	12.2382	5.198082
0.75	6.207419	36.53798	34.4436	5.122382	5.046682
1	9.588695	48.29674	19.55589	5.500883	4.774161
1.25	9.941963	47.46404	12.66717	6.091345	4.491547
1.5	11.14307	38.00151	12.66717	5.70275	5.046682

d=0.035m, L=0.06m

R_d	0	15	30	45	60
0.25	4.945748	7.191522	32.80343	43.85566	15.74565
0.5	5.147615	22.7353	46.0005	23.94651	5.55135
0.75	10.09336	37.36059	37.77441	21.42316	5.904618
1	7.065355	47.81731	35.32677	17.36059	11.65783
1.25	9.437295	47.16124	30.38102	18.95029	9.361595
1.5	10.09336	39.61645	30.38102	17.84002	13.60081

d=0.05m, L=0.06m

R_d	0	15	30	45	60
0.25	12.541	15.06435	37.09311	55.84153	41.66036
0.5	13.60081	26.69695	60.76205	37.69871	10.5728
0.75	10.7999	58.03684	52.58642	19.75776	9.084027
1	15.49331	56.90134	36.28564	11.73354	6.560686
1.25	11.4812	56.44714	26.31845	10.01766	8.074691
1.5	11.27933	53.11633	23.66894	12.79334	5.828917

d=0.03m, L=0.08m

R_d	0	15	30	45	60
0.25	3.885945	6.257885	38.43048	49.96215	29.90159
0.5	5.55135	22.38203	55.23593	27.22685	11.35503
0.75	7.998991	37.69871	41.35756	6.131718	8.579359
1	8.377492	49.25561	23.23997	6.58592	4.542014
1.25	9.99243	55.9677	20.56523	10.09336	5.006308
1.5	7.519556	48.67525	20.41383	8.024224	5.55135

d=0.05m, L=0.08m

R_d	0	15	30	45	60
0.25	9.563462	23.82034	28.18572	50.21448	35.37724
0.5	9.91673	37.62301	57.40601	30.98663	13.12137
0.75	10.9513	48.75095	54.85743	20.28766	9.588695
1	10.1943	52.40979	41.20616	5.576583	5.55135
1.25	13.34847	53.97426	29.54832	6.308352	5.046682
1.5	13.55034	49.68458	29.54832	8.478425	5.55135

d=0.07m, L=0.08m

R_d	0	15	30	45	60
0.25	6.762554	10.09336	22.60913	42.59399	45.74817
0.5	8.579359	25.86424	56.06863	55.892	25.38481
0.75	9.664396	53.36866	66.0106	23.4923	11.1027
1	9.613929	56.44714	48.37245	12.79334	6.308352
1.25	10.14383	51.37522	31.81933	17.13348	8.327025
1.5	9.714862	47.18647	25.83901	10.7242	11.4812

Appendix (C.12.a): The statistical analysis of the louver inclination effect

Tests of Between-Subjects Effects

Dependent Variable: VELOCITY

Source	Type II Sum of Squares	df	Mean Square	F	Sig.
Corrected Model	141382.018[a]	11	12852.911	75.192	.000
Intercept	165785.919	1	165785.919	969.884	.000
ROOM_D	33705.118	5	6741.024	39.436	.000
ANGLE	97131.633	1	97131.633	568.242	.000
ROOM_D * ANGLE	9804.020	5	1960.804	11.471	.000
Error	48203.306	282	170.934		
Total	355371.242	294			
Corrected Total	189585.323	293			

a. R Squared = .746 (Adjusted R Squared = .736)

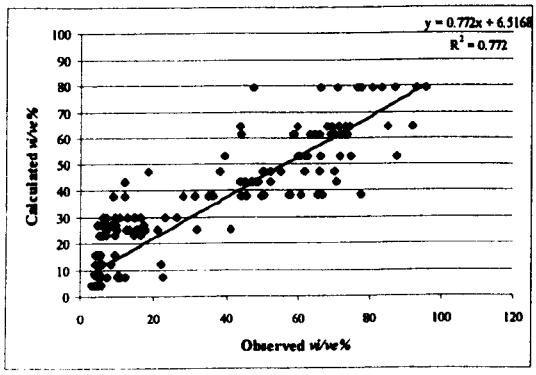

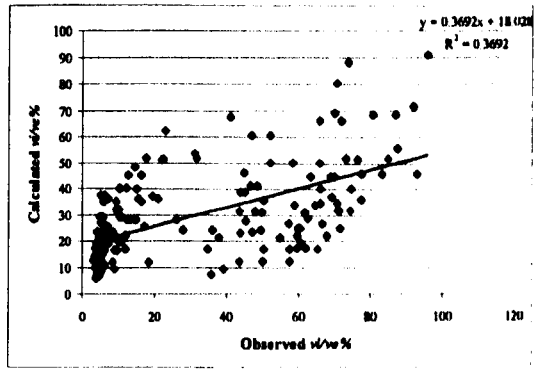

Appendix (C.12.b): The statistical analysis of the louver inclination effect

Tests of Between-Subjects Effects

Dependent Variable: VELOCITY

Source	Type II Sum of Squares	df	Mean Square	F	Sig.
Corrected Model	71286.023[a]	11	6480.548	15.448	.000
Intercept	165785.919	1	165785.919	395.198	.000
ROOM_D	809.422	5	161.884	.386	.858
APERTURE	30426.415	1	30426.415	72.530	.000
ROOM_D * APERTURE	6413.244	5	1282.649	3.058	.011
Error	118299.300	282	419.501		
Total	355371.242	294			
Corrected Total	189585.323	293			

a. R Squared = .376 (Adjusted R Squared = .352)

Appendix (C.12.c): The statistical analysis of the louver free area effect

Tests of Between-Subjects Effects

Dependent Variable: VELOCITY

Source	Type II Sum of Squares	df	Mean Square	F	Sig.
Corrected Model	118797.481[a]	11	10799.771	43.023	.000
Intercept	165785.919	1	165785.919	660.447	.000
ROOM_D	4385.152	5	877.030	3.494	.004
FREEAREA	71762.375	1	71762.375	285.882	.000
ROOM_D * FREEAREA	12588.742	5	2517.748	10.030	.000
Error	70787.842	282	251.021		
Total	355371.242	294			
Corrected Total	189585.323	293			

a. R Squared = .627 (Adjusted R Squared = .612)

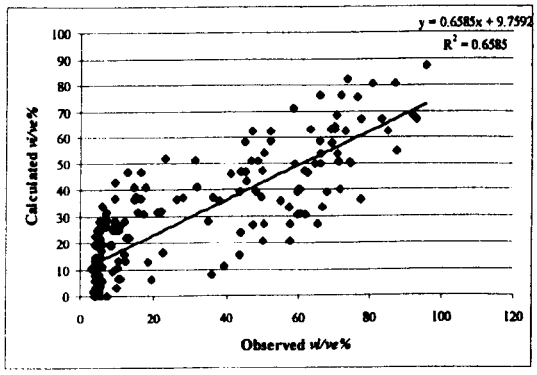

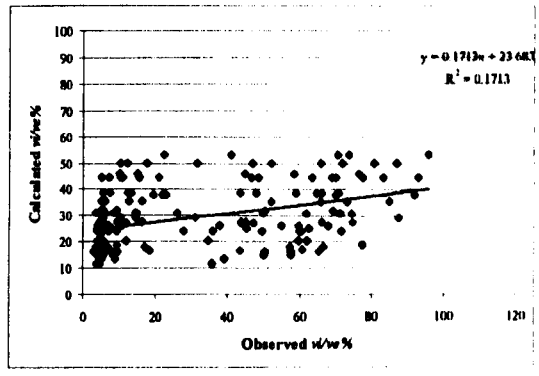

Appendix (C.12.d): The statistical analysis of the louver number effect

Tests of Between-Subjects Effects

Dependent Variable: VELOCITY

Source	Type II Sum of Squares	df	Mean Square	F	Sig.
Corrected Model	39520.447[a]	11	3592.768	6.751	.000
Intercept	165785.919	1	165785.919	311.543	.000
ROOM_D	9764.538	5	1952.908	3.670	.003
NUMBER	3820.885	1	3820.885	7.180	.008
ROOM_D * NUMBER	1253.197	5	250.639	.471	.798
Error	150064.876	282	532.145		
Total	355371.242	294			
Corrected Total	189585.323	293			

a. R Squared = .208 (Adjusted R Squared = .178)

Appendix (C.13): The statistical analysis of the integration of overall variables.

Tests of Between-Subjects Effects

Dependent Variable: VELOCITY

Source	Type II Sum of Squares	df	Mean Square	F	Sig.
Corrected Model	165453.397[a]	23	7193.626	80.486	.000
Intercept	165785.919	1	165785.919	1854.895	.000
ROOM_D	2156.929	5	431.386	4.827	.000
FREEAREA	11595.430	1	11595.430	129.735	.000
ANGLE	39302.617	1	39302.617	439.737	.000
NUMBER	18090.642	1	18090.642	202.407	.000
ROOM_D * FREEAREA	3486.253	5	697.251	7.801	.000
ROOM_D * ANGLE	2100.973	5	420.195	4.701	.000
ROOM_D * NUMBER	1576.746	5	315.349	3.528	.004
Error	24131.926	270	89.378		
Total	355371.242	294			
Corrected Total	189585.323	293			

a. R Squared = .905 (Adjusted R Squared = .892)

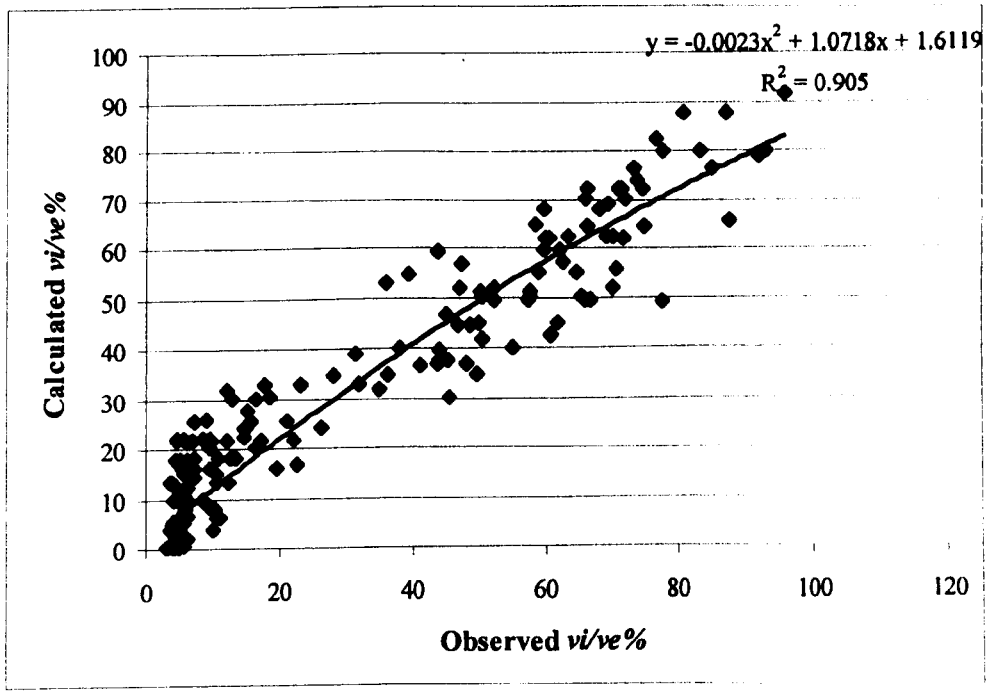

Appendix D: Computational Fluid Dynamics appraisal stage.

Appendix (D-1): The velocity profile within the louver blades at various inclinations, L=0.08m, d=0.07m θ=0°, 30°, and 60°.

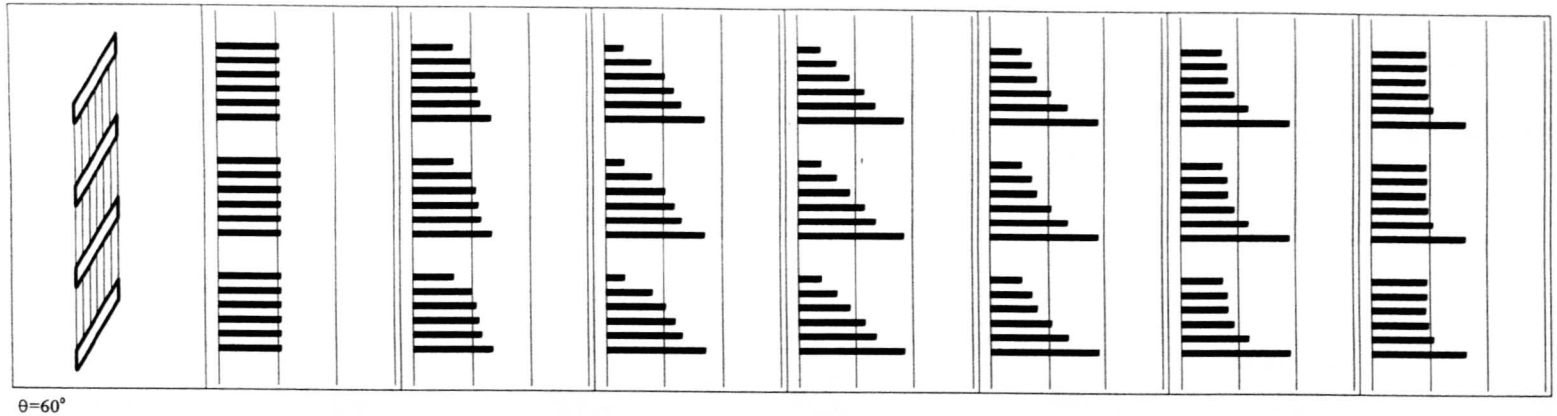

θ=60°

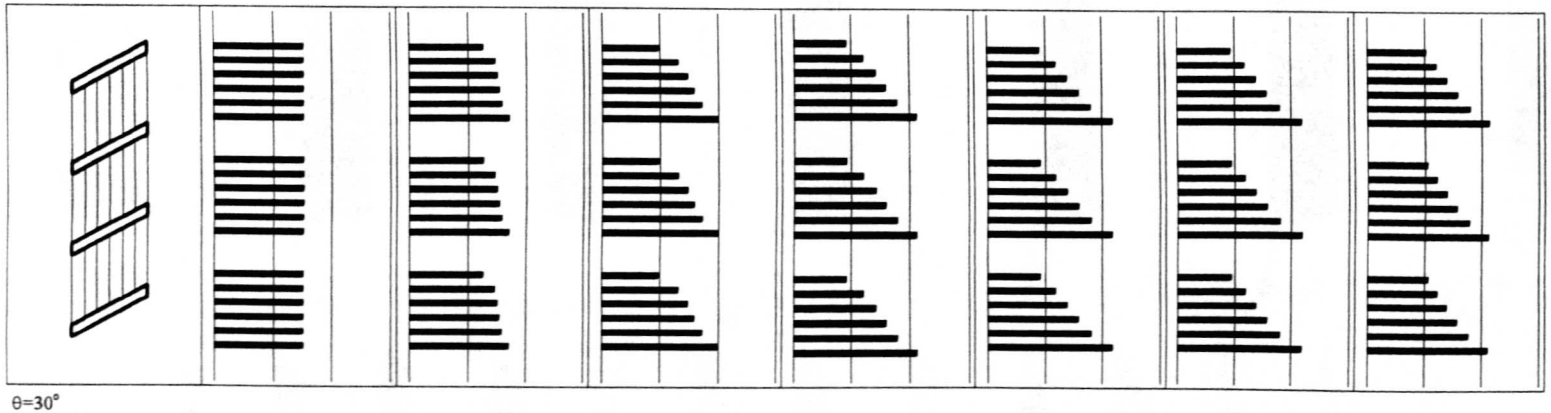

θ=30°

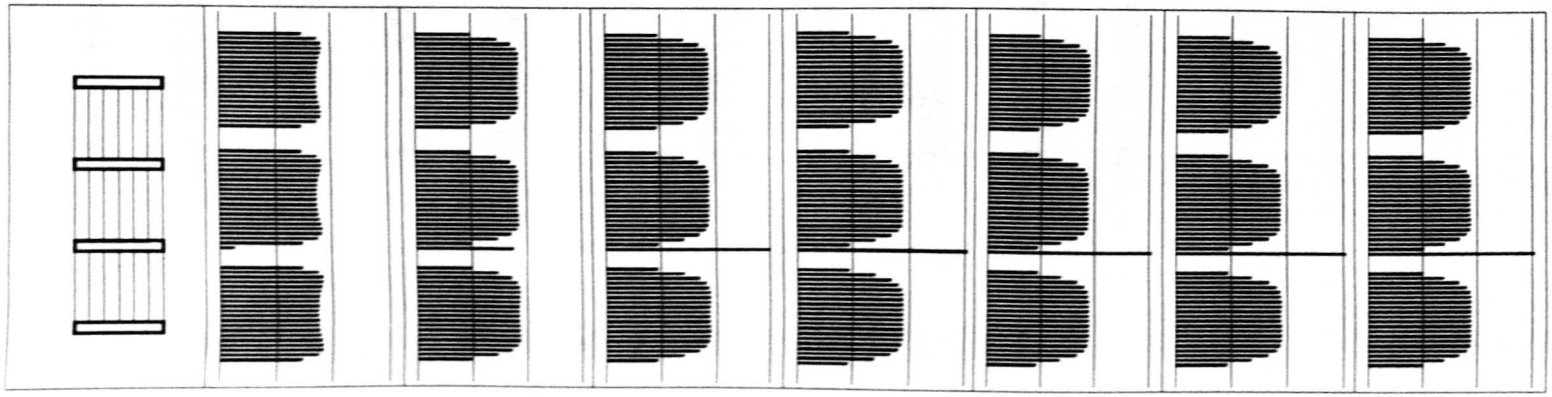

θ=0°

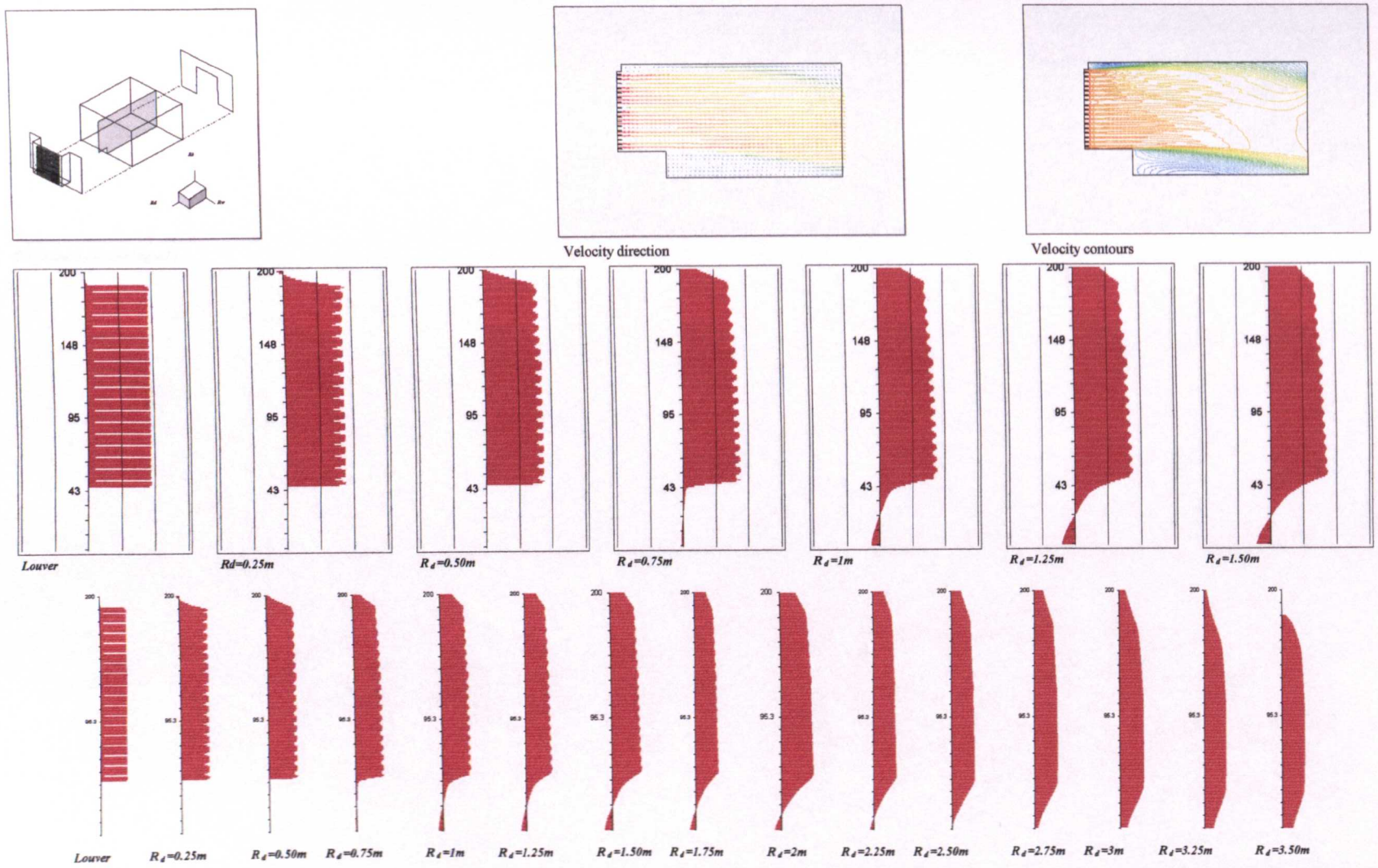

Apendix(D.2): The indoor airflow patterns at various locations along the room depths at louver inclination angle θ=0°, Projected Rowshan (inlet-II),(outlet-I), d=0.07m, L=0.08m.

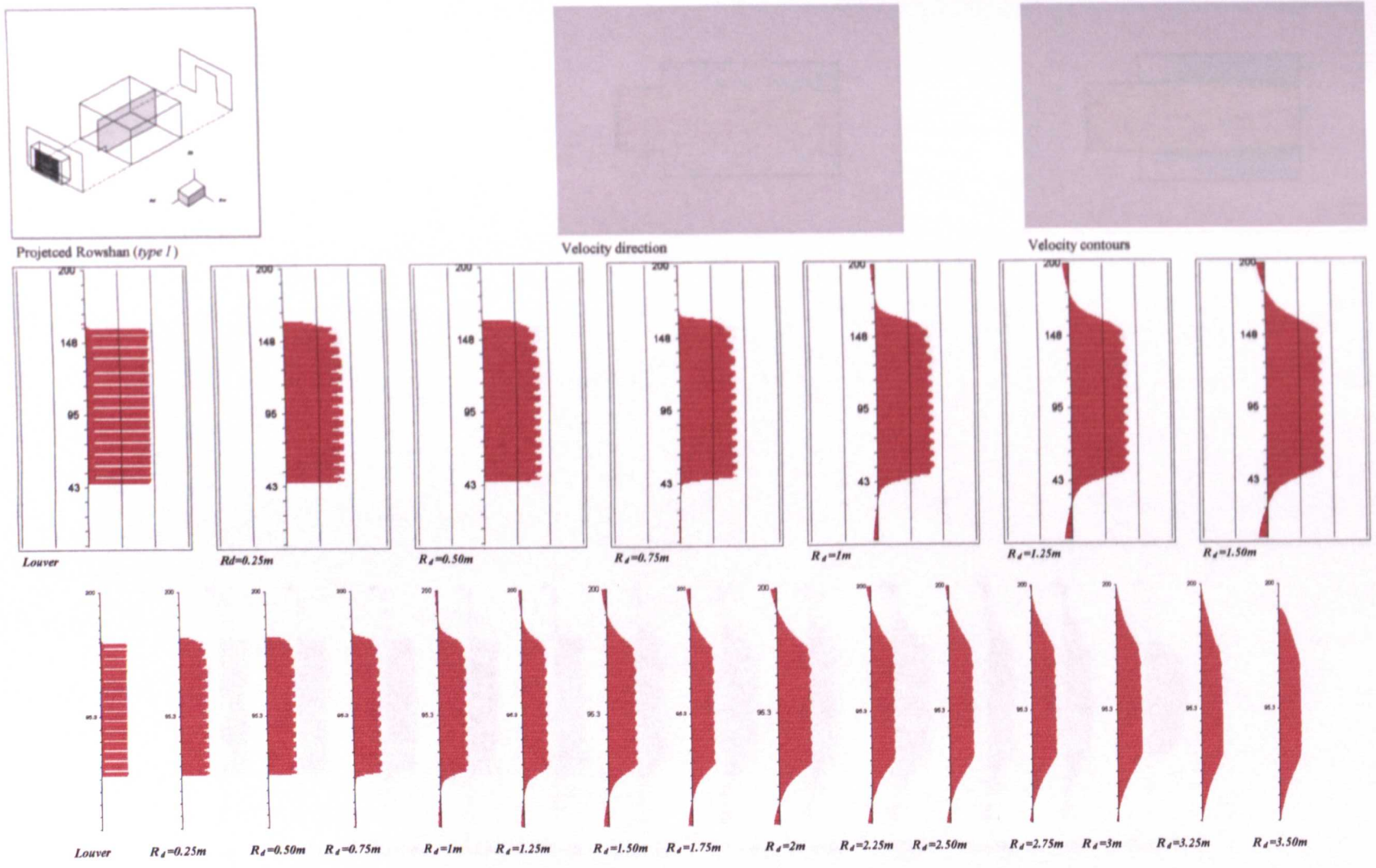

Apendix (D.3): The indoor airflow patterns at various locations along the room depths at louver inclination angle θ=0°, Projected Rowshan (inlet-II), outlet-I, d=0.07m, L=0.08m.

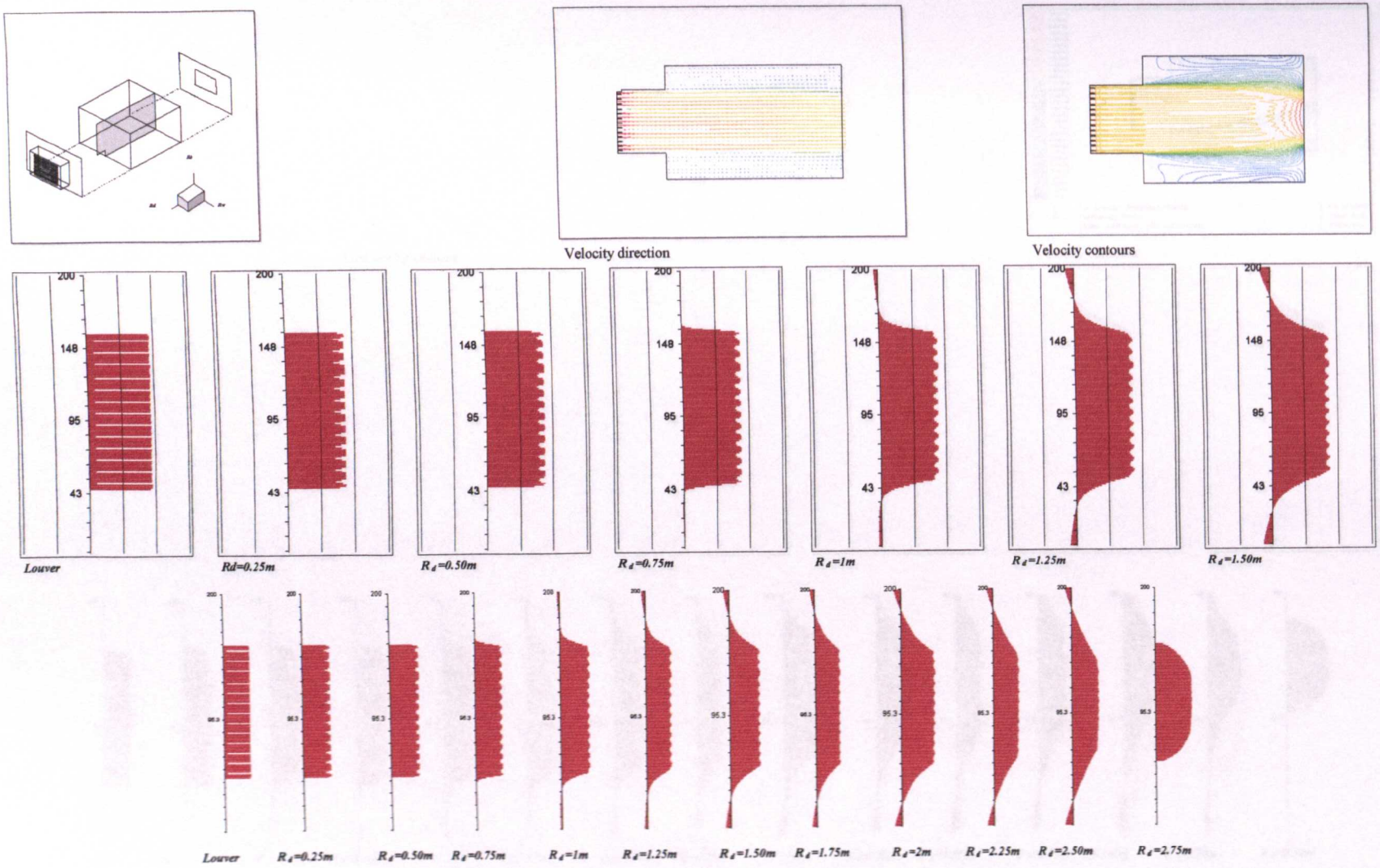

Appendix (D.4): The indoor airflow patterns at various locations along the room depths at louver inclination angle θ=0°, Projected Rowshan (inlet-V),d=0.07m, L=0.08m.

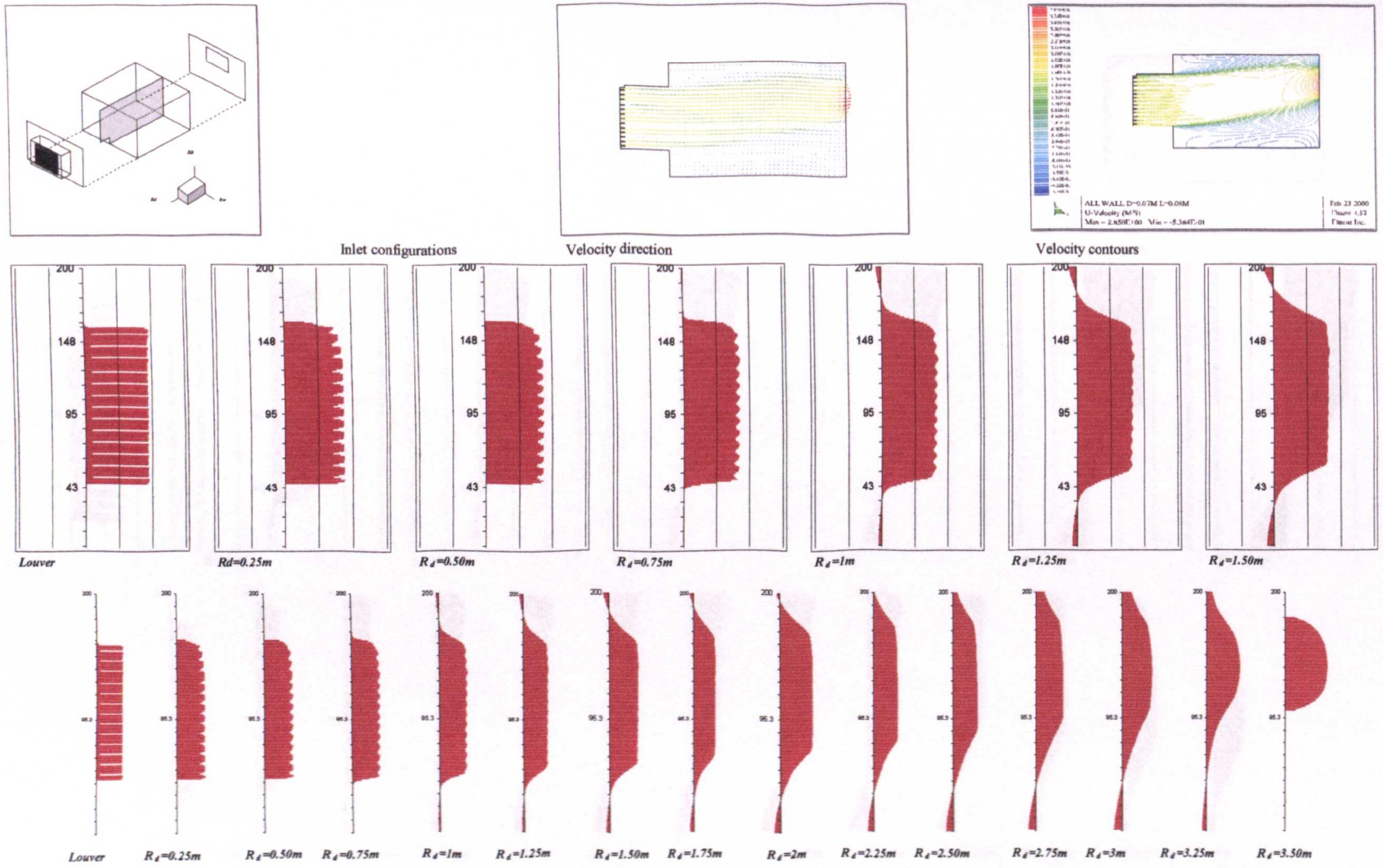

Appendix (D.5): The indoor airflow patterns at various locations along the room depths at louver inclination angle θ=0°, Projected Rowshan (inlet-V), (outlet-III), d=0.07m, L=0.08m.

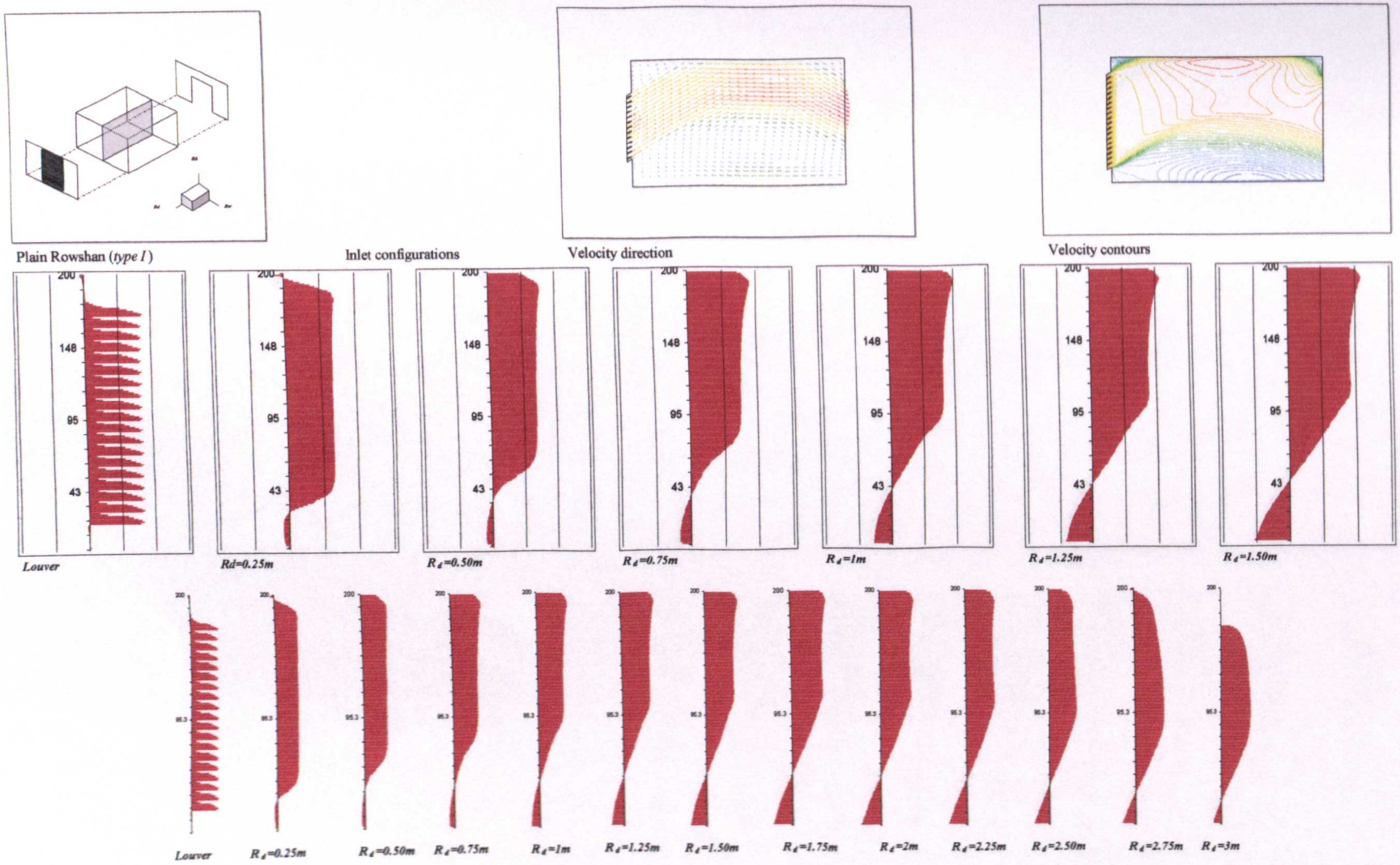

Appendix(D.6): The indoor airflow patterns at various locations along the room depths at louver inclination angle θ=30°, Projected Rowshan (inlet-I), (outlet-I), d=0.07m, L=0.08m.

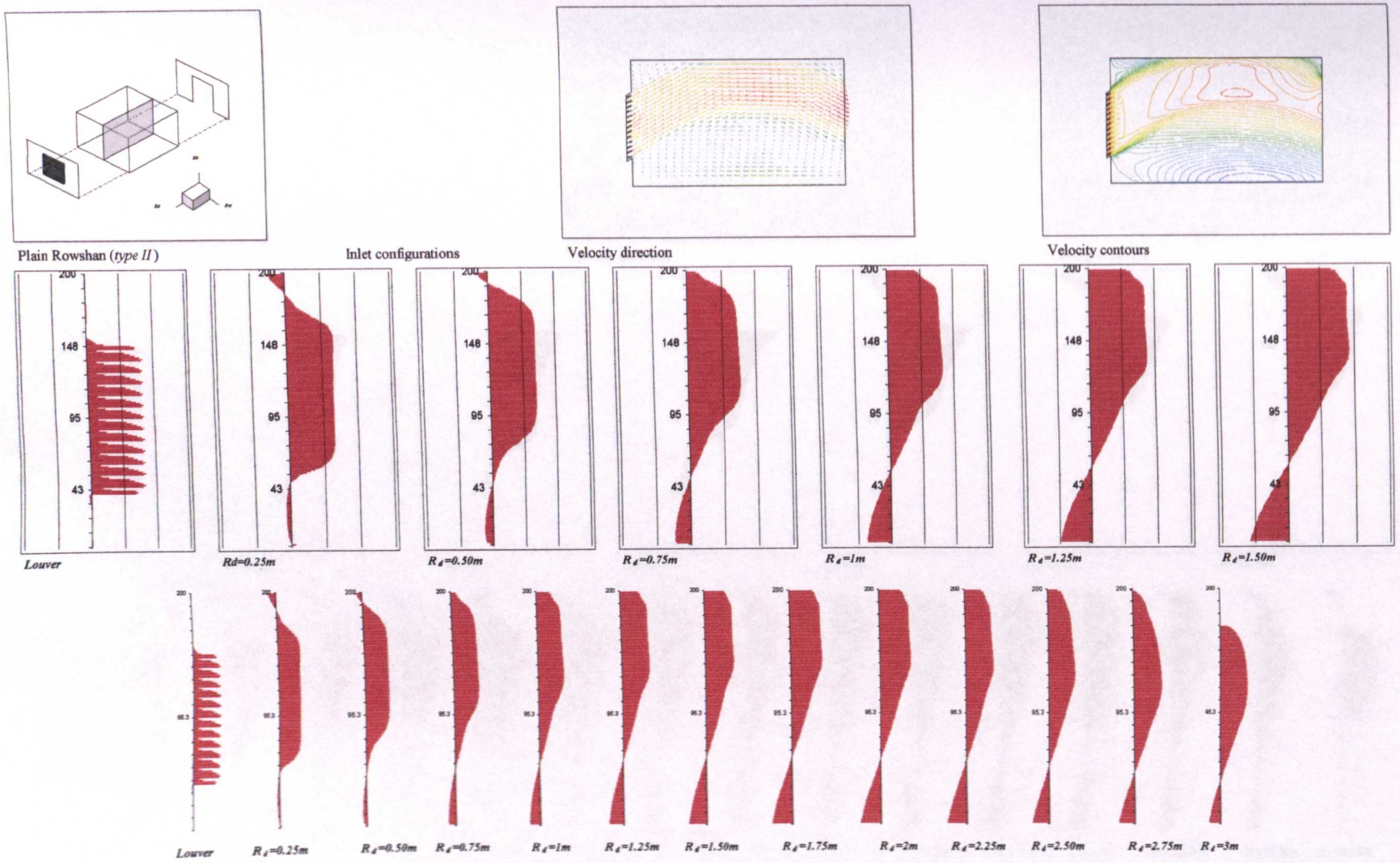

Appendix (D.7): The indoor airflow patterns at various locations along the room depths at louver inclination angle θ=30°, Projected Rowshan (inlet-III), (outlet-I), d=0.07m, L=0.08m.

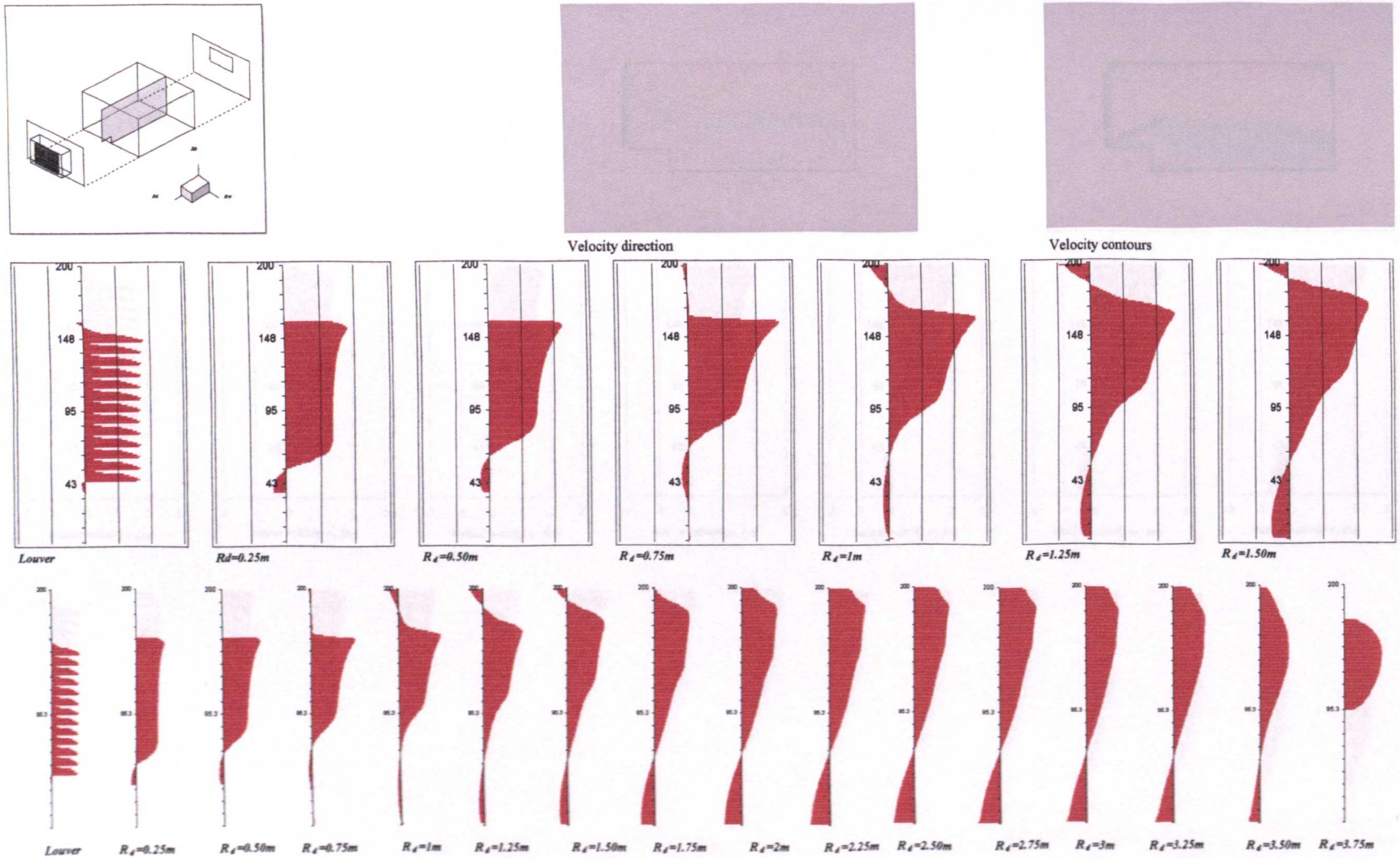

Appendix (D.8): The indoor airflow patterns at various locations along the room depth at louver inclination angle θ=30°, Projected Rowshan (inlet-V), (outlet-III), d=0.07m, L=0.08m.

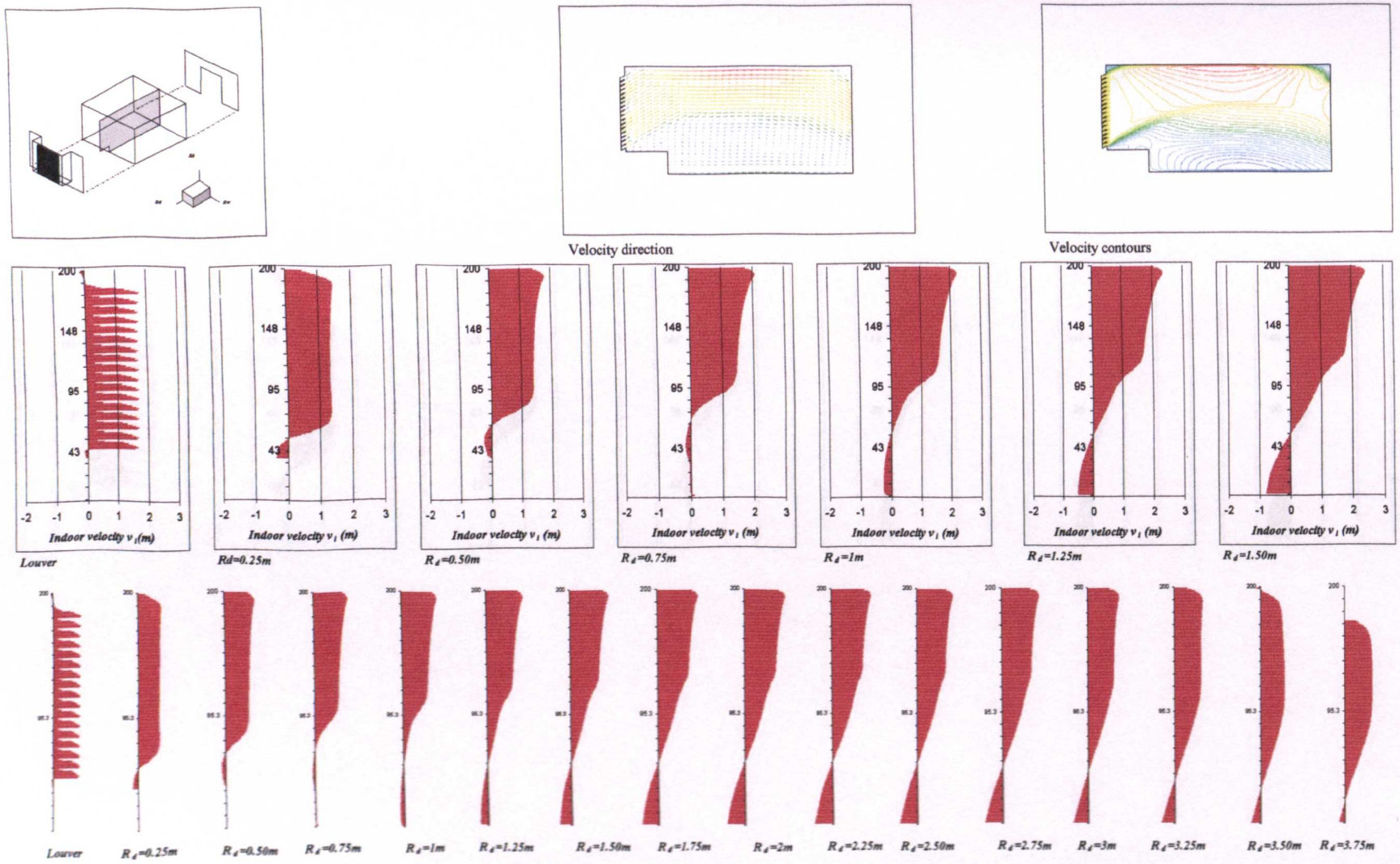

Appendix (D.9): The indoor airflow patterns at various locations along the room depth at louver inclination angle θ=60°, Projected Rowshan (inlet-II), (outlet-I), d=0.07m, L=0.08m.

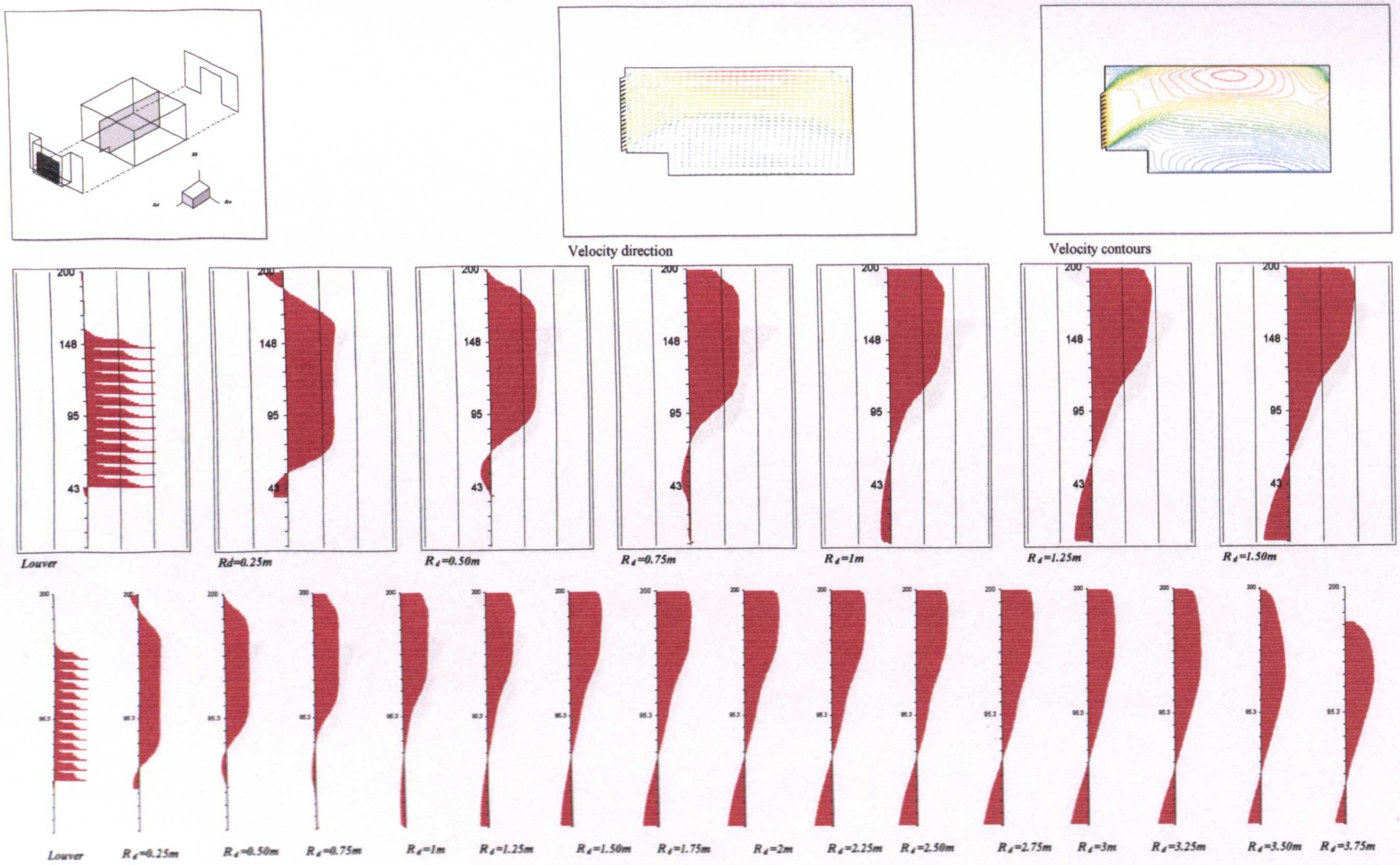

Appendix (D.10): The indoor airflow patterns at various locations along the room depth at louver inclination angle θ=60°, Projected Rowshan (inlet-IV), (outlet-I), d=0.07m, L=0.08m.

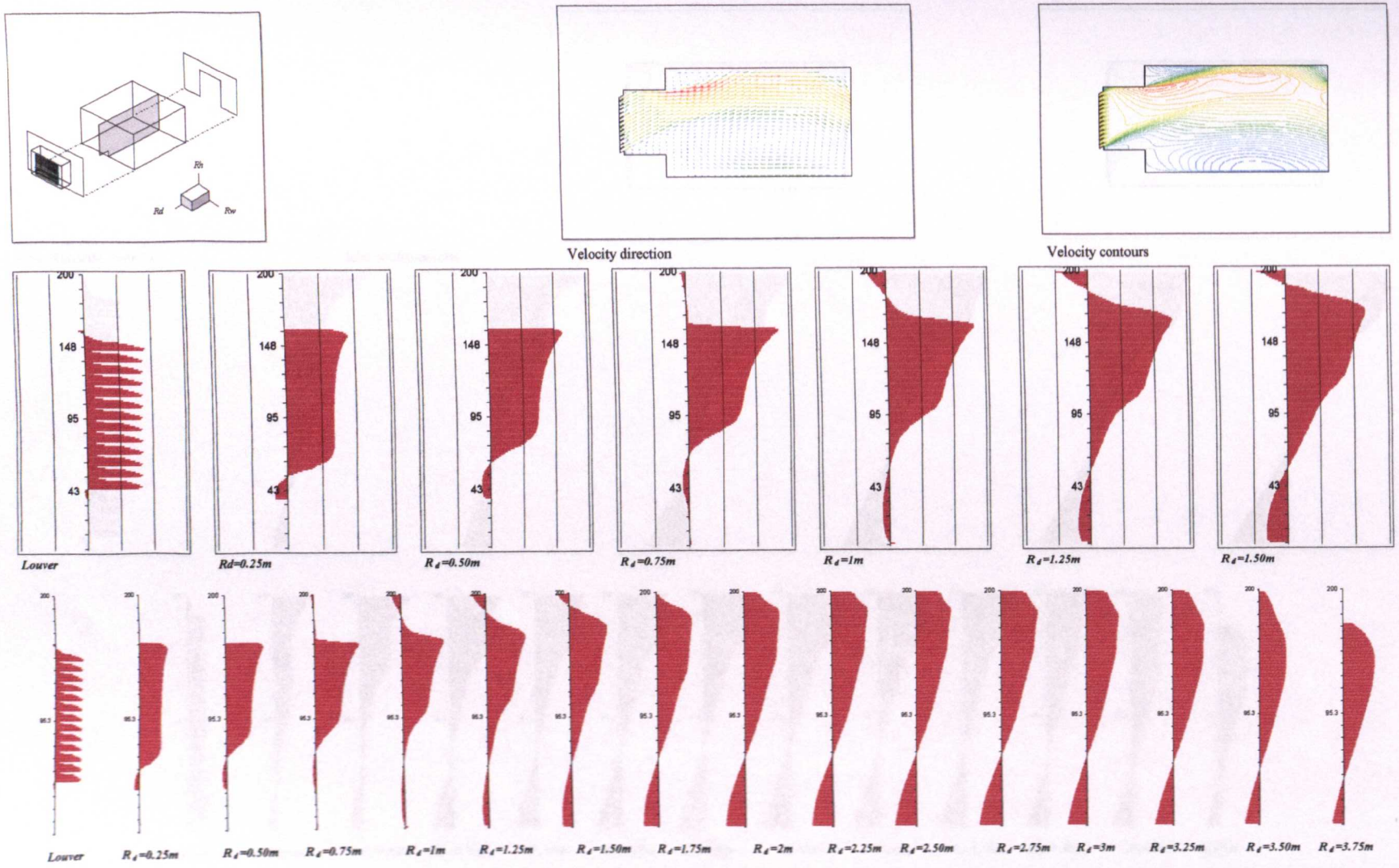

Appendix (D.11): The indoor airflow patterns at various locations along the room depth at louver inclination angle θ=30°, Projected Rowshan (inlet-V), (outlet-I), d=0.07m, L=0.08m.

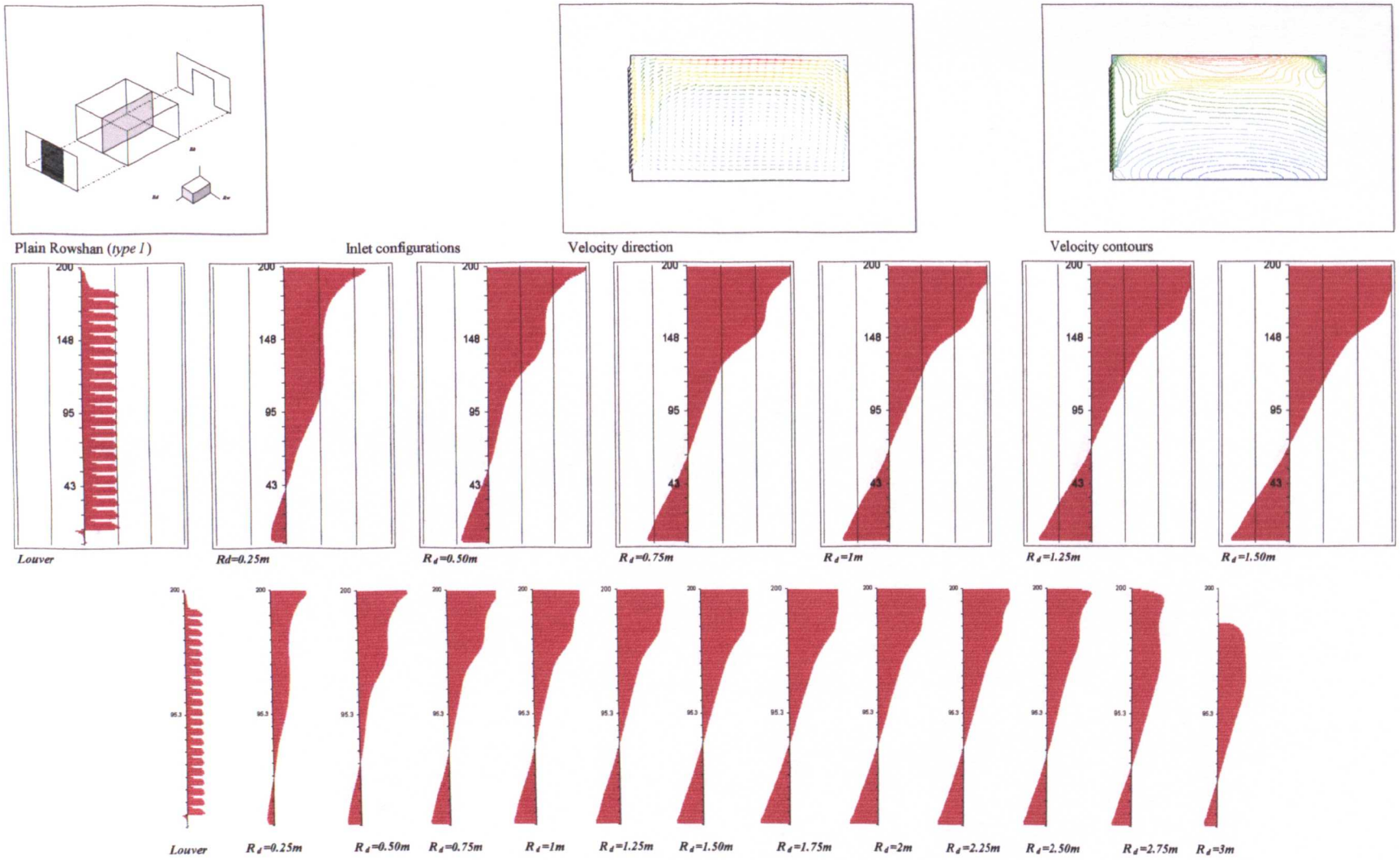

Appendix(D.12): The indoor airflow patterns at various locations along the room depth at louver inclination angle θ=60°, Plain Rowshan (inlet-I), (outlet-I), d=0.07m, L=0.08m.

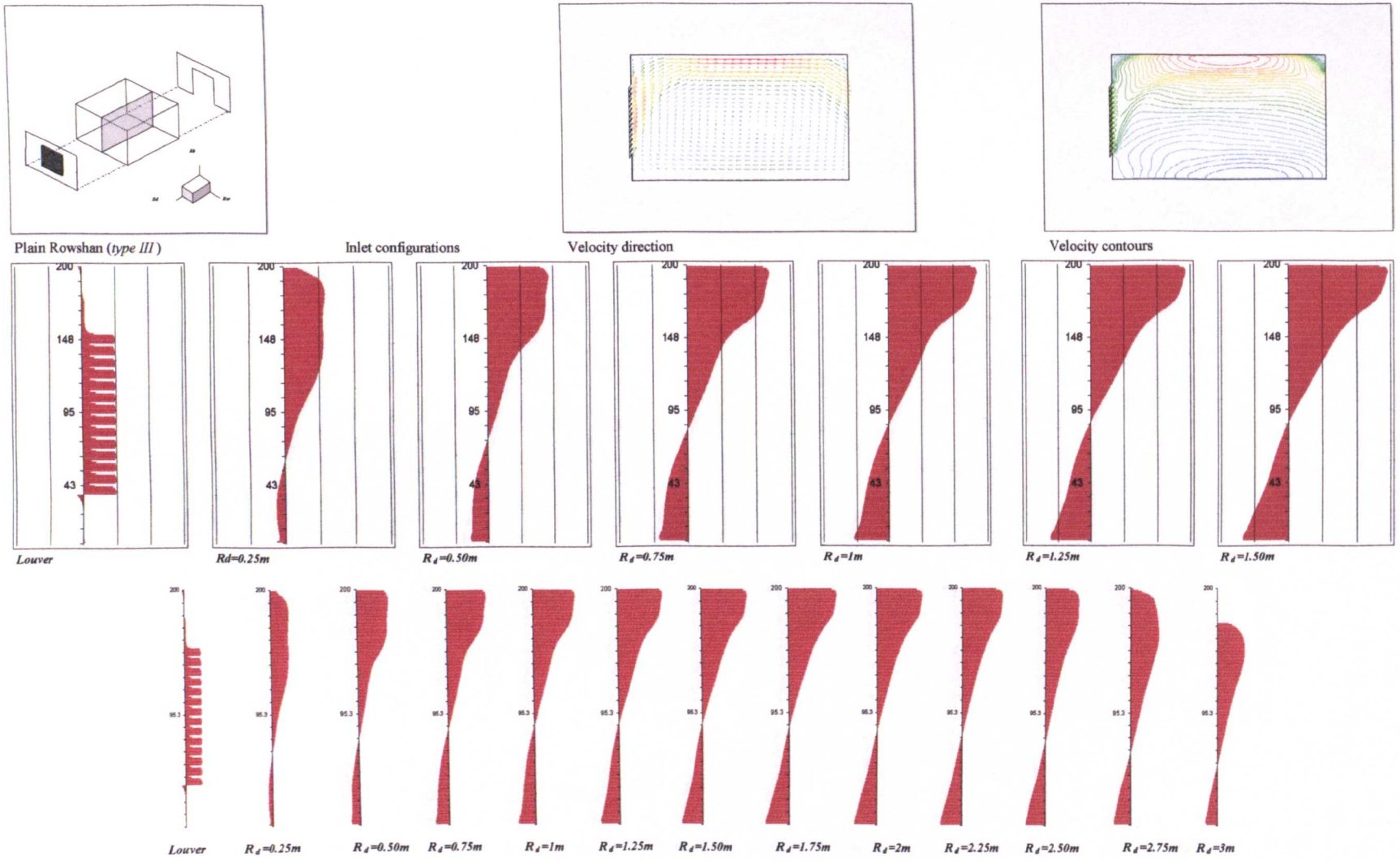

Appendix (D.13): The indoor airflow patterns at various locations along the room depth at louver inclination angle θ=60°, Plain Rowshan (inlet-III), (outlet-I), d=0.07m, L=0.08m.

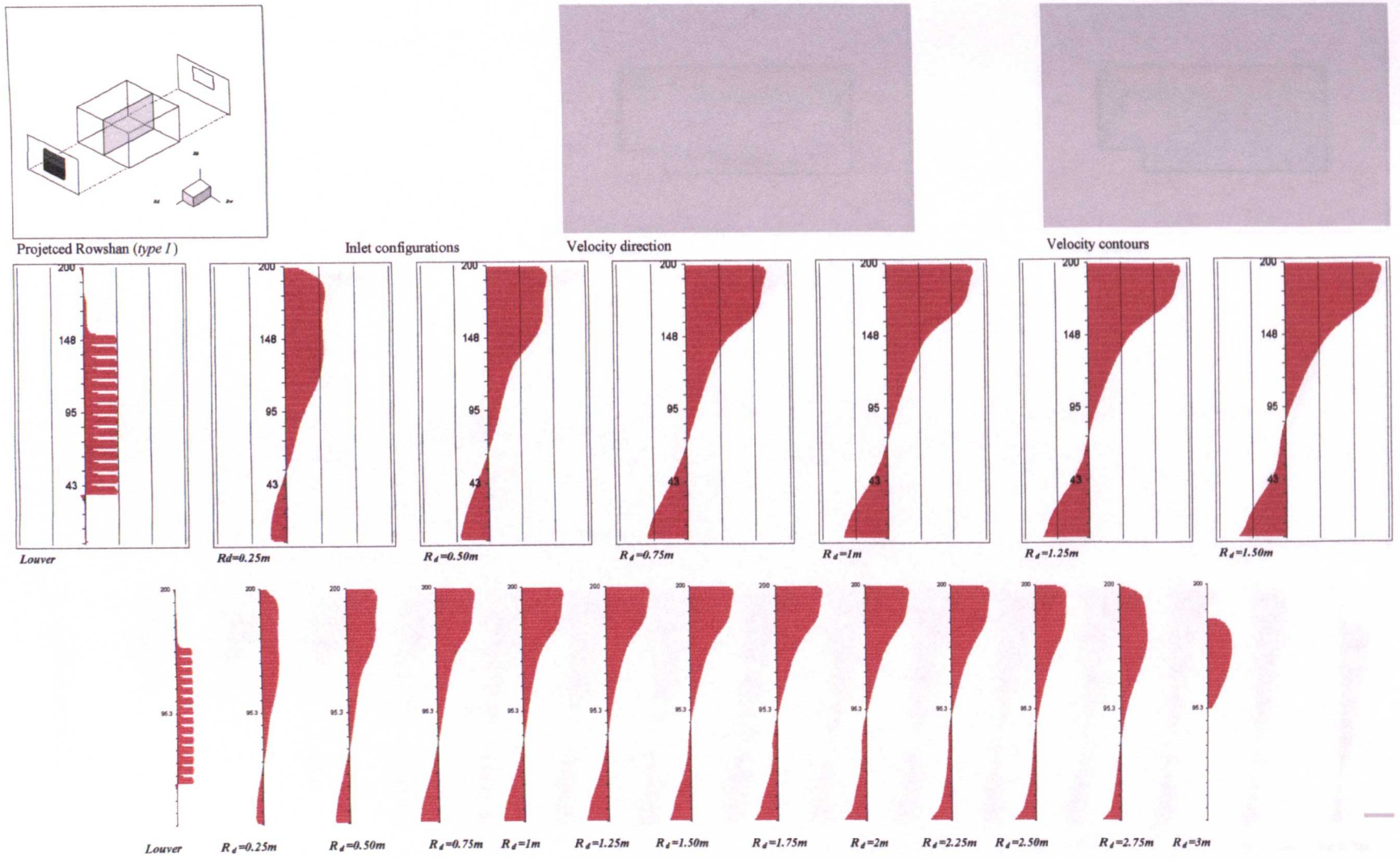

Appendix (D.14): The indoor airflow patterns at various locations along the room depth at louver inclination angle θ=60°, Plain Rowshan (inlet-III), (outlet-III), d=0.07m, L=0.08m.

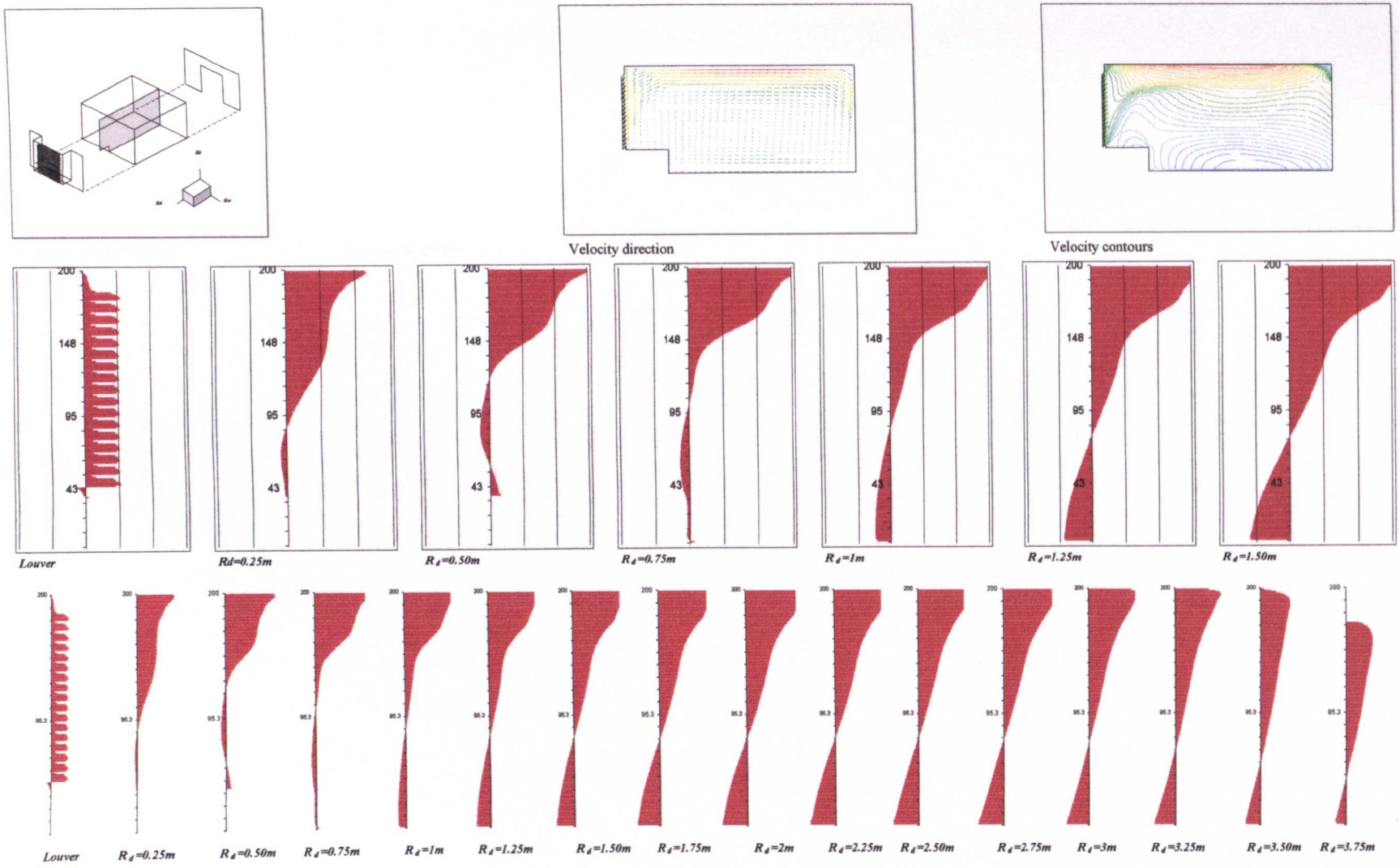

Appendix (D.15): The indoor airflow patterns at various locations along the room depth at louver inclination angle θ=60°, Projected Rowshan (inlet-II), (outlet-I), d=0.07m, L=0.08m.

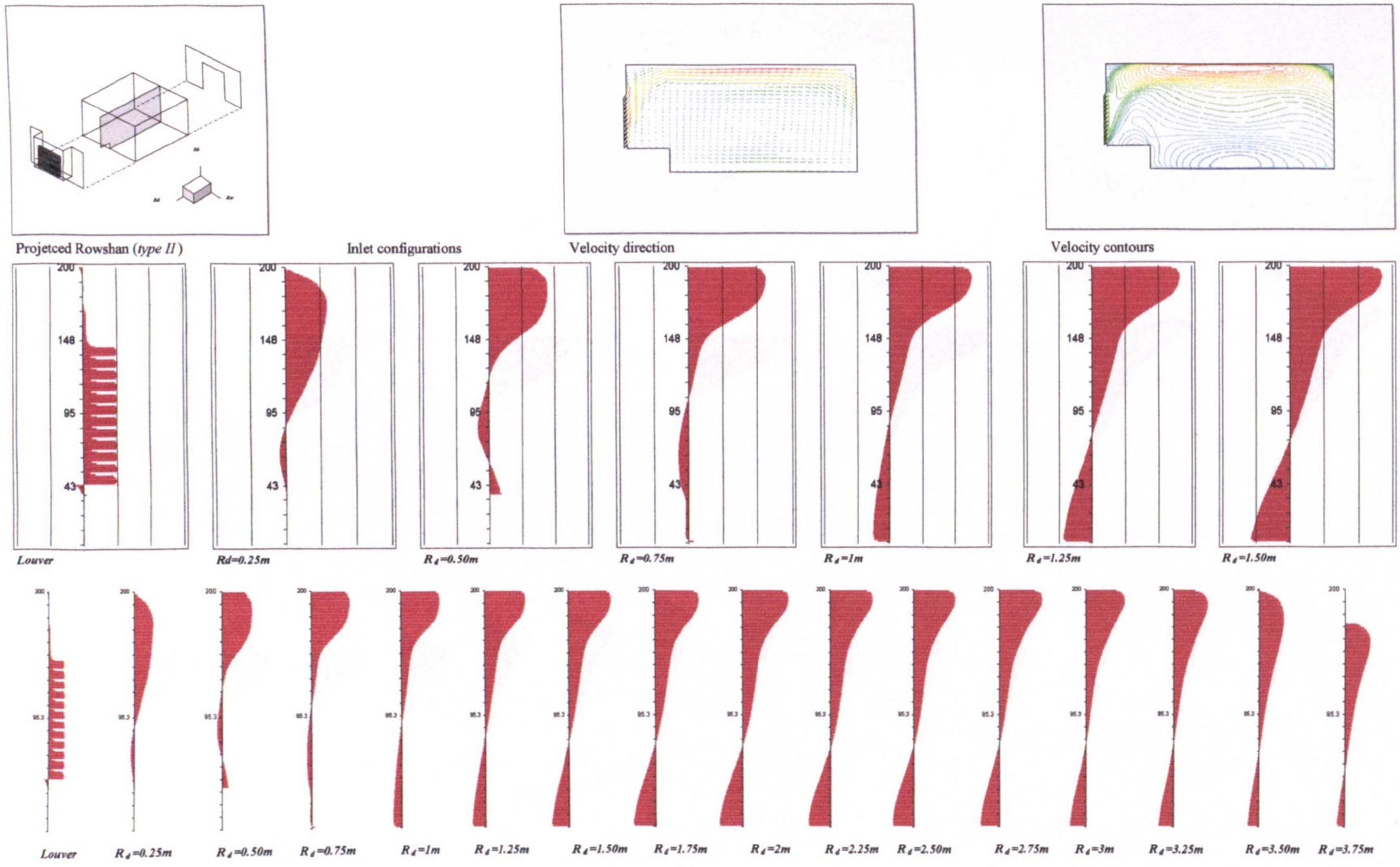

Appendix (D.16): The indoor airflow patterns at various locations along the room depth at louver inclination angle θ=60°, Plain Rowshan (inlet-IV), (outlet-I), d=0.07m, L=0.08m.

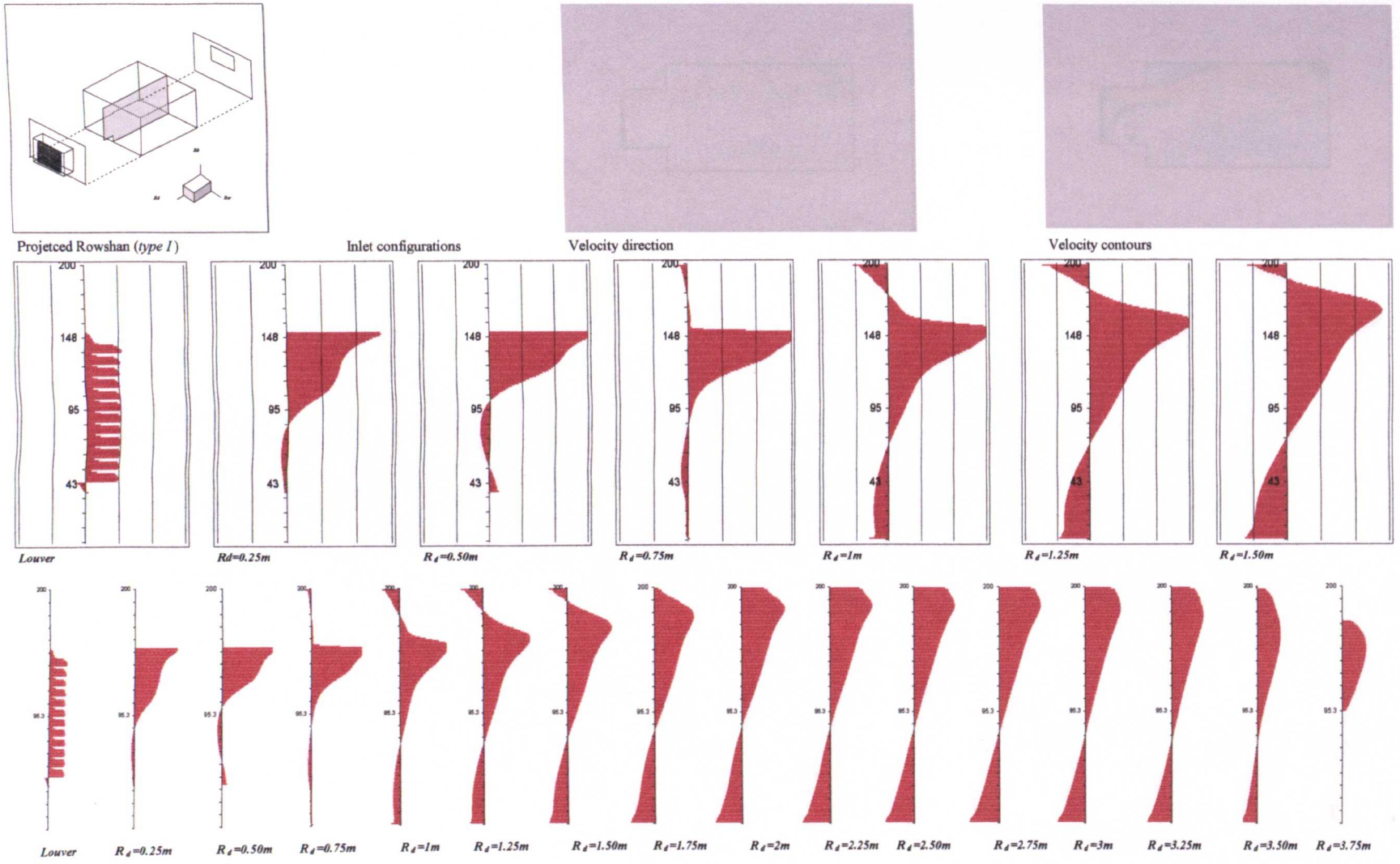

Appendix (D.17): The indoor airflow patterns at various locations along the room depth at louver inclination angle θ=60°, Plain Rowshan (inlet-V), (outlet-III), d=0.07m, L=0.08m.

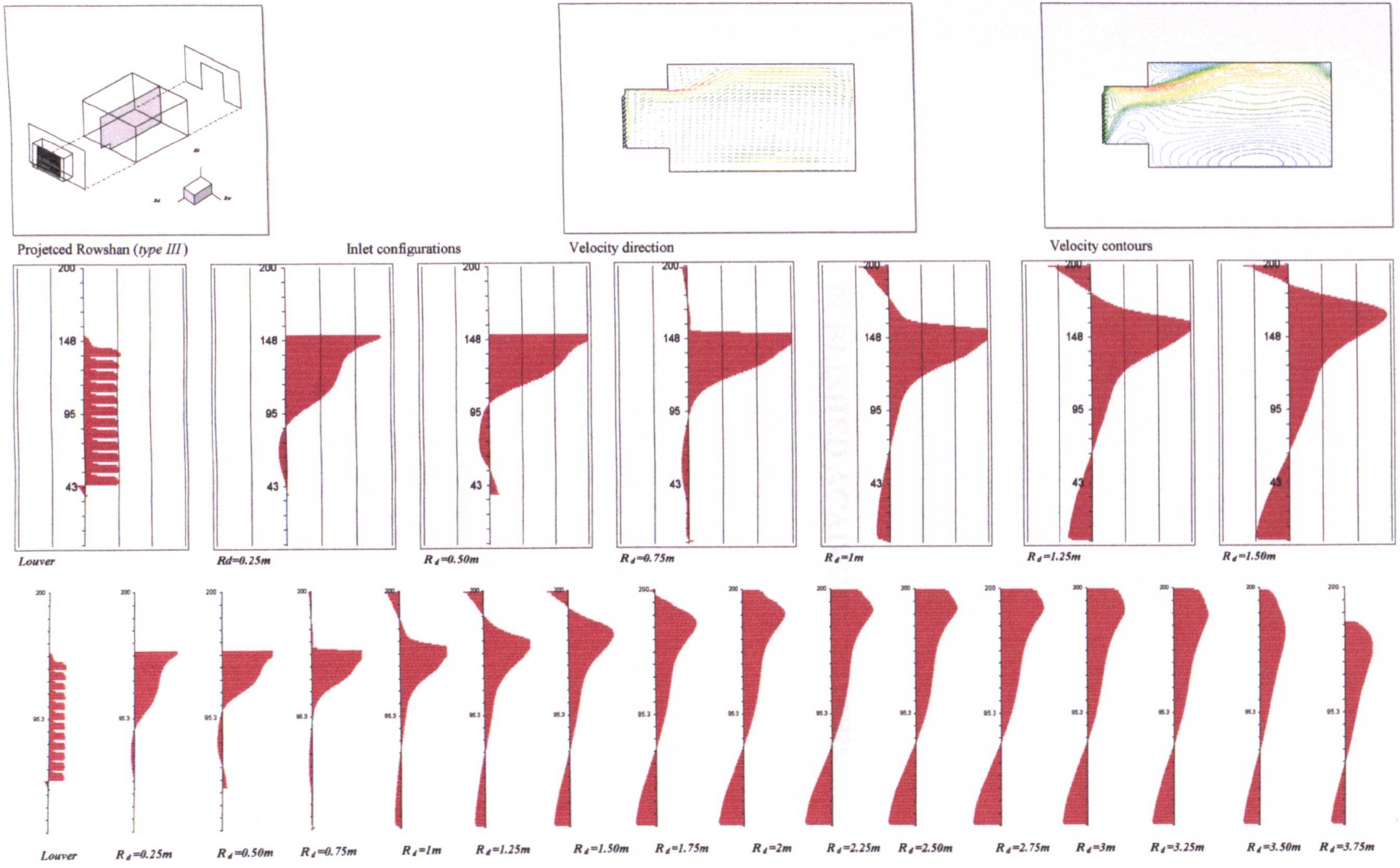

Apendix (D.18): The indoor airflow patterns at various locations along the room depth at louver inclination angle θ=60°, Projected Rowshan (inlet-V), (outlet-I), d=0.07m, L=0.08m.

PUBLISHED ACADEMIC PAPERS

ENERGY, ECOLOGY, ARCHITECTURE
PROCEEDINGS OF THE 16TH INTERNATIONAL PLEA (PASSIVE AND LOW ENERGY ARCHITECTURE)
BRISBANE, AUSTRALIA, 22-24 SEPTEMBER 1999
PLEA'99

AIR FLOW CHARACTERISTICS THROUGH MODULATED LOUVERED WINDOWS

A A Maghrabi* and S Sharples†
*School of Architecture
University of Sheffield, Sheffield, S10 2TN, United Kingdom
Tel: (0114) 222 0399
Fax: (0114) 279 8276
e-mail: apr95aam@sheffield.ac.uk

†Centre for the Built Environment, School of Environment and Development
Sheffield Hallam University, Sheffield, S1 1WB, United Kingdom
e-mail: s.sharples@shu.ac.uk

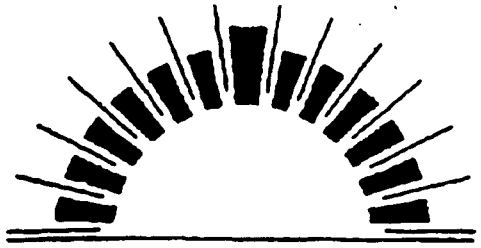

Sustaining the future

ENERGY ECOLOGY ARCHITECTURE

PLEA'99

Proceedings of the sixteenth international PLEA (Passive and Low Energy Architecture) conference
Brisbane, Australia
22-24 September 1999

volume 1

edited by
Steven V Szokolay

published by PLEA International
in conjunction with
the Department of Architecture, The University of Queensland
Brisbane

AIR FLOW CHARACTERISTICS THROUGH MODULATED LOUVERED WINDOWS.

A A Maghrabi* and S Sharples*
*Department of Architecture
University of Sheffield, Sheffield, S10 2TN, United Kingdom
tel: (0114) 222 0399
fax: (0114) 279 8276
e-mail: apr95aam@sheffield.ac.uk

*School of Construction
Sheffield Hallam University, Sheffield, S1 1WB, United Kingdom
e-mail: s.sharples@shu.ac.uk

ABSRACT This study investigated the pressure flow characteristics over a number of full-scale modulated louvered windows (MLW). The various MLW parameters included louver inclination angle (θ), depth (L), aperture (d) and the ratio of aperture/depth (d/L%). Airflow models were developed using both power law and quadratic model equations. By examining the coefficient of determination (r^2) for both model equations, it was evident that the quadratic model equation suggested the best curves fit. The pressure flow characteristics as a function of louver inclination angle (θ) in conjunction with (d/L) were presented in dimensionless form. It was concluded that the pressure flow characteristics could be controlled if proper configurations of MLW were to be chosen.

1 Introduction

Airflow within and around buildings has been a rich topic of research for many years. Hence several investigations have been carried out on the mechanism of airflow through buildings and- further - on various parameters governing air motions indoors. The Modulated Louver Windows (MLW) have been used for centuries as tool to achieve thermal comfort in buildings by natural means. Although the body of literature pertaining to the MLW dealt with its solar control performance, the optimization of its various dimensions and configurations in relation to ventilation is far from being satisfactory. On the same hand, available studies were limited in scope (Yakubu & Sharples 1991, Tsangrassoulis et al. 1997, Pitts & Georgiadis 1994). In this context, the design of window acquires special importance as air mainly flow inside buildings through its apertures. Entire parametric studies are still needed to investigate the pressure and velocity drops as functions of MLW various components.

Nevertheless, most of the available CFD packages deal with ventilation aspects in simplistic ways and may not necessarily reflect complexities occurring in physical circumstance. Furthermore, theoretical representations of airflow passing through a window could not be simplified. Calculation methods in building ventilation tend to rely upon simple experimental data and general assumptions since precise calculations of unsteady flow characteristics of openings within building are rarely known. Hence it is more preferable to undertake laboratory measurements as the *steady flow characteristic* is a significant parameter to establish any ventilation measurements (Etheridge & Sandberg 1996).

This paper presents the full-scale of pressurisation laboratory experiment carried out at the School of Architecture, University of Sheffield to investigate the influence of various MLW configurations on pressure flow characteristics (ΔP) under controlled volume-flow rates (Q). These configurations included louver inclination angle (θ), depth (L), gap between louver blades or aperture (d) and the ratio of aperture/depth (d/L). The ratio was developed to establish a non-dimensional relationship between (d) and (L). It ranged from 0.5 in which half distance of the louver depth will overlap the one underneath when MLW considered totally closed up to 1 where the outer edge of the louvre will just overlap the inner edge of the louver underneath. It will show the variations of differential pressure across inner and outer volumes as a function to the above-mentioned variables. The experimental work is reviewed and followed by the analysis and discussion of results based on quadratic and power law model equations.

2 Methodology

2.1 Modulated louvered window configurations

Ten models of full-scale MLW with different configurations were made for further analysis. Louvers could be adjusted to any pre-set inclination angle ranging from +60° to –60° at intervals of 15°. They were made of smooth pine wood with fixed frame dimensions (0.48m height and 0.32m breadth). Every model has its own mechanism that allows louvers to incline from 0° angle- when the window is totally open- up to the degree, say (θ), when the outer edge of the louver will overlap the inner edge underneath ($d \cong 0$). Three louvres' depths (L) were chosen; 0.04, 0.06 to 0.08m. The six different gap dimensions (d) chosen were 0.01, 0.02, 0.03, 0.035, 0.05 and 0.07 m (Fig.1).

No	Depth L (m)	Aperture d (m)	Number N	Ratio d/L (%)	The MLW configurations
1	0.04	0.01	24	0.5	
2	0.04	0.02	16	0.75	
3	0.04	0.03	12	1	
4	0.06	0.02	16	0.5	
5	0.06	0.03	12	0.67	
6	0.06	0.035	11	0.75	
7	0.06	0.05	8	1	
8	0.08	0.03	12	0.5	
9	0.08	0.05	8	0.75	
10	0.08	0.07	6	1	

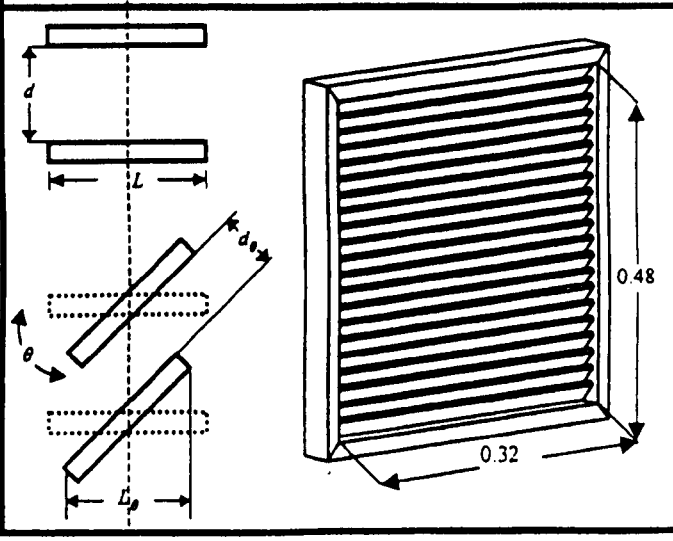

Fig.1 The modulated louvred window (MLW) various configurations

2.2 Experimental set up

A pressurisation chamber of 1x1x2 m with a volume of 2 m^3 was made to represent the environment where internal pressure would be recorded. There was no need to measure external pressure through a shield box (Baker et al. 1987). Models were fitted later on the front

panel of the chamber. The other end was equipped with a *laminar volume-flow meter device* and connected with four extraction fans from which volume-flow air (Q) was recorded. A small door on the side elevation of the box was made to enable tilting louvers to the desired inclination angle. Two digital micromanometer devices were used and adjusted to record pressure and volume-flow air at four readings per second. The first was connected to the volume flow-meter device to record the volume-flow of air passing through. Similarly, the differential pressure across the louvers was measured using other device. Both devices ranged from 0-199 *Pa* and operated with self-calibrating devices to ensure compensation for zero-drift, making them accurate enough to measure small pressure differences with an accuracy error of less ±1% as quoted by the manufacturers. A data-logger was used to transfer the data to a computer.

A number of routine measurements and calibrations were made prior to the final analysis. The proper sealing of the pressurisation chamber was intended to minimise infiltration arising from depressurisation and resulted in higher-pressure drops occurring at extremely low volume-flows. For precision, this low infiltration rate was considered to determine the actual volume-flow passing the MLW.

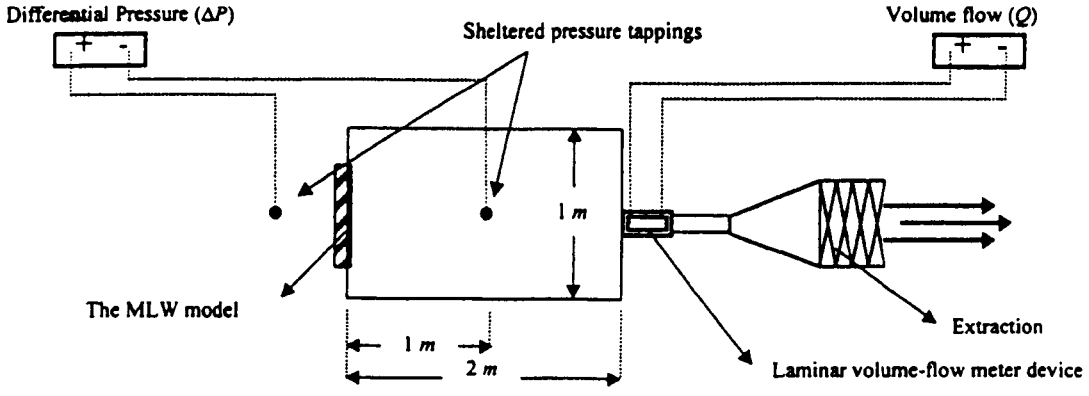

Fig.2 Schematic diagram of the experimental setup

Internal and external pressure tappings were positioned away from the influence of flow through the opening. Pressure tappings were positioned at six different locations in the pressurisation chamber before the centre location was finally recommended. Also an adjustment had been made for both micromanometers and software to give an average reading of various timings (1, 2, 3 minutes respectively), at four readings per second each. The 2 minutes was found most appropriate as positive time was given for the flow to reach its steady state and to avoid any turbulence while recording was being made. The authors compared the current results with another study (Yakubu & Sharples 1991) carried out under similar circumstances but on a much smaller range of parameters. They found that the results in both cases were similar.

2.3 Measuring principles

Readings of both pressure and air volume-flow were transferred to the computer attached when the reading had stabilised and flow was considered in a *steady state*. In measurement, *steady flow characteristic* occurs when pressure difference across an opening pressure difference does not vary with time under a specific volume of fluid (Etheridge & Sandberg 1996). The fan speed was set to various extraction rates in order to create ranges of pressures for specified volume-flow rates of air. The prior step was repeated over a range of pressure drops obtained from the combined power of the 4 axial fans. Then, louvers were adjusted to the next desired angle and the above mentioned steps were repeated for each setting. The

laboratory temperature was ensured to be about 20° C, the temperature that was programmed for both micromanometers.

3 Power law and quadratic model equations

The validity of the power law and quadratic model equations have been experienced by many researchers in ventilation studies to set standards for building envelopes, ventilation requirements and many other infiltration models. Both calculation methods have been broadly accepted and the debate as to which of the two is more valid is still on-going (Yakubu & Sharples 1991, Walker et al. 1998, Thomas & Dick 1953, Sherman et al. 1979, Dick 1950, Chand et al. 1988, Chand 1970). The power law function is expressed as:

$$\Delta P = a \cdot Q^n \tag{1}$$

where ΔP is pressure drop across crack [*Pa*], a is a constant proportional to the effective leakage area of the crack [$m^3/s\ Pa^n$], Q is the volume flow rate [m^3/s] and n is the exponent.

Alternatively, other researchers in the field apply the quadratic model equation. Etheridge (1997) prefers the quadratic equation method to determine the air infiltration. This formulation is expressed as following:

$$\Delta P = AQ + BQ^2 \tag{2}$$

where A is the flow coefficient for fully developed laminar friction losses [$(Pa\ s)/m^3$], and B is the coefficient of entry, exit and turbulent flow losses [$(Pa\ s^2)/m^6$].

Coefficients A and B are determined by the standard fluid mechanics principles:

$$A = \frac{12\mu z}{Ld^3} \tag{3}$$

$$B = \frac{\rho Y}{2d^2L^2} \tag{4}$$

where μ is the dynamic viscosity [kg/ms], z is the plate length [*m*], L is the depth of the plate [*m*], d is the gap thickness [*m*], ρ is the fluid density [kg/m^3] and Y is the a factor depending on crack geometry.

Substituting coefficients A and B into Eq. (2):

$$\Delta P = \left(\frac{12\mu z}{Ld^3}\right)Q + \left(\frac{\rho Y}{2d^2L^2}\right)Q^2 \tag{5}$$

However, inclination angle of louver (θ°) was not part of the two coefficient considerations. For MLW, pressure difference could be a function to vertical inclination angles of louver. Assuming two louver blades placed at a distance (d) with a depth (L) at initial inclination position (0°) when the two blades are perfectly horizontal as shown in Fig.1. When louvers initially were tilted positively or negatively to a determined inclination, say (θ), this would be accompanied with a decrease in the effective gap thickness between louvers (d_θ) and the depth of louver (L_θ). It is evident from the pressure difference for the parallel plate theory and when angle θ = 0° that $\Delta P = AQ + BQ^2$. Then ΔP_θ would be represented as follows:

$$\Delta P_\theta = \Delta P \cdot \frac{1}{\cos^4 \theta} \tag{6}$$

For ventilation research, some correlation is needed to identify the flow rates as a function in relation to pressure difference due to wind, stack effect, .etc, which is expressed as follows (Etheridge 1997):

$$Q = \frac{-A \pm \sqrt{A^2 + 4B\Delta P}}{2B} \tag{7}$$

These equations are called here to establish a comparison between the measured flow data with respect to theoretical formulations.

By examining the coefficient of determinations (r^2) of both model equations, it was evident that curves produced by quadratic equation were preferred particularly in models where the ratio (d/L>0.5). The coefficient of determination of latter ratios was 0.989. The smoother curves produced by quadratic formulation fitted the scattered data at both pressure limits (i.e. higher and lower ΔP). On the other hand, power law curves were gradually accepted as louvers were tilted to steeper angles ($\theta = \pm 60$) and caused an increased pressure drop due to pressurisation with a coefficient of determination (r^2) that ranged from 0.337 at $\theta = 0°$ to 0.981 at $\theta = 60°$. This Showed that power law curve fits was gradually improving from 0° to the maximum measured angle.

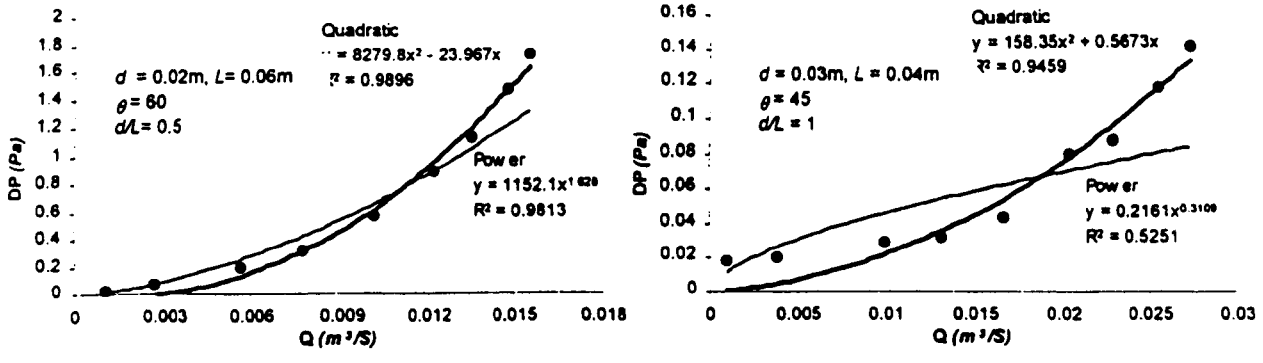

Fig.3 Regression curves produced by quadratic and power law model equations

However, representations of both coefficients evolved in the quadratic equation A (eq. 3) and B (eq. 4) could not be simplified theoretically due to number of factors. The first was related to physical complexities of flow characteristics passing through MLW various components. As mentioned earlier, these complexities could not be simplified theoretically. The second factor seemed more likely to relate to aperture of MLW. In 70% of models investigated, the aperture dimensions (d) were big enough for air to flow with no much resistance causing similar pressure drops for various d and L dimensions that are embedded in both coefficients. Similarly, the value of volume-flow of air as in equation (7) could not be simplified theoretically. This is merely due to the fact that the original format of equation was based on single crack theory. Thus it is assumed that for models with series of parallel cracks, the parallel plate theory would apply (Walker et al. 1998). Here, the total flow as the sum of number of cracks evolved could not be justified due to interference to flow caused by parallel cracks. This interference would differ from that resulted from single cracks. Another possible explanation was concerned with the inclination angle. The latter equation had no consideration to the

inclination angle of plate. These added to others embedded in the coefficients *A* and *B* could be the possible answer for discrepancies found in theoretical representation of *Q*. Such corrections is beyond the scope of this investigation, and thus, further adjustments of the quadratic model equation would be required to fit variables that might not be embedded in both *Q* and the coefficients *A* and *B* equation formats.

4 Discussion

Differential pressure was measured aiming to establish an understanding of the flow characteristics whilst passing through MLW various components. The resultant pressure drops as function of louvers inclination angles (θ) was generally not significant except at inclination angle ($-45^\circ \geq \theta \geq +45^\circ$). Fig.4 shows the gap between curves produced by inclination $\theta = \pm 45^\circ$ and those below, i.e. $-30^\circ \geq \theta \geq +30^\circ$ where curves yielded towards lower pressure drops even at the highest volume-flow rate measured ($Q \cong 0.03\ m^3/s$). This gap was even more distinguishable at inclination angle $-60^\circ = \theta = +60^\circ$ showing that inclinations at the latter pre-sets were the main parameters to cause significant pressure drop therefore. As far as the direction was concerned, variations found between positive and negative inclination angles were diminished and negligible (Fig.5).

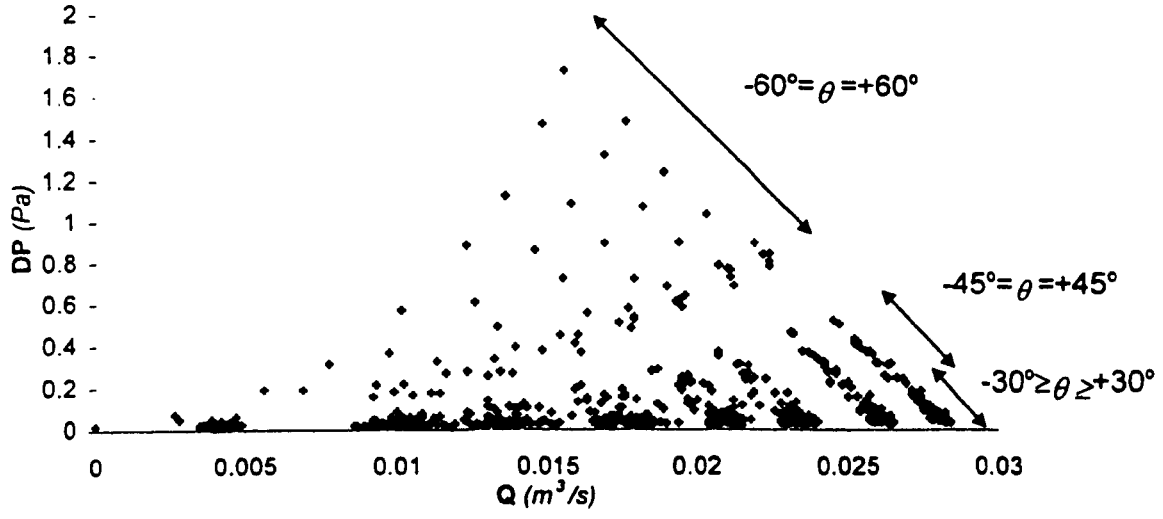

Fig.4 ΔP data as a function of inclination angles

The varieties in louvre apertures examined resulted in various pressure curves therefore. In cases where aperture $d \leq 0.035m$, higher-pressure drops was achieved compared with bigger dimensions. In the latter situation pressure records was diminished to lower readings (max. ΔP <0.45 *Pa*). Also, louvre apertures played a main role when accompanied with inclination angle. As louvers were tilted to steeper inclinations the dimension of the aperture, say (d_θ), was lessened accordingly causing reduction in pressure. As shown in Fig.5, ΔP would increase as aperture dimension would decrease. This was the fact for all MLW models examined. However, that was not the case with the variety of depths concerned. Depth of louvre was the least affecting variable in the resultant differential pressures though in some cases it positively functioned as motivate barrier to airflow (Fig.5). The number of louvres *(N)* in the same MLW model caused also some considerable pressure differences of air. As shown in Fig.5, these drops would occur as louvre number would be $N \geq 12$ blades.

Further, the relationship between *d* and *L* dimensions was established in the form of ratio *d/L*. Lower ratios of *d/L* showed an increased pressure drops than higher ones (Fig.5). At lower

ratio d/L= 0.5, significant pressure drop was at $\theta = \pm 30^{\circ}$ whilst that significance occurred at $\theta = \pm 45^{\circ}$ when bigger ratios were present. In contrary, ΔP would be dimensionless at ratio d/L=1 no matter what other configurations of MLW were. As shown in Fig.6, this dimensionless relationship could not be established at $d/L \leq 1$.

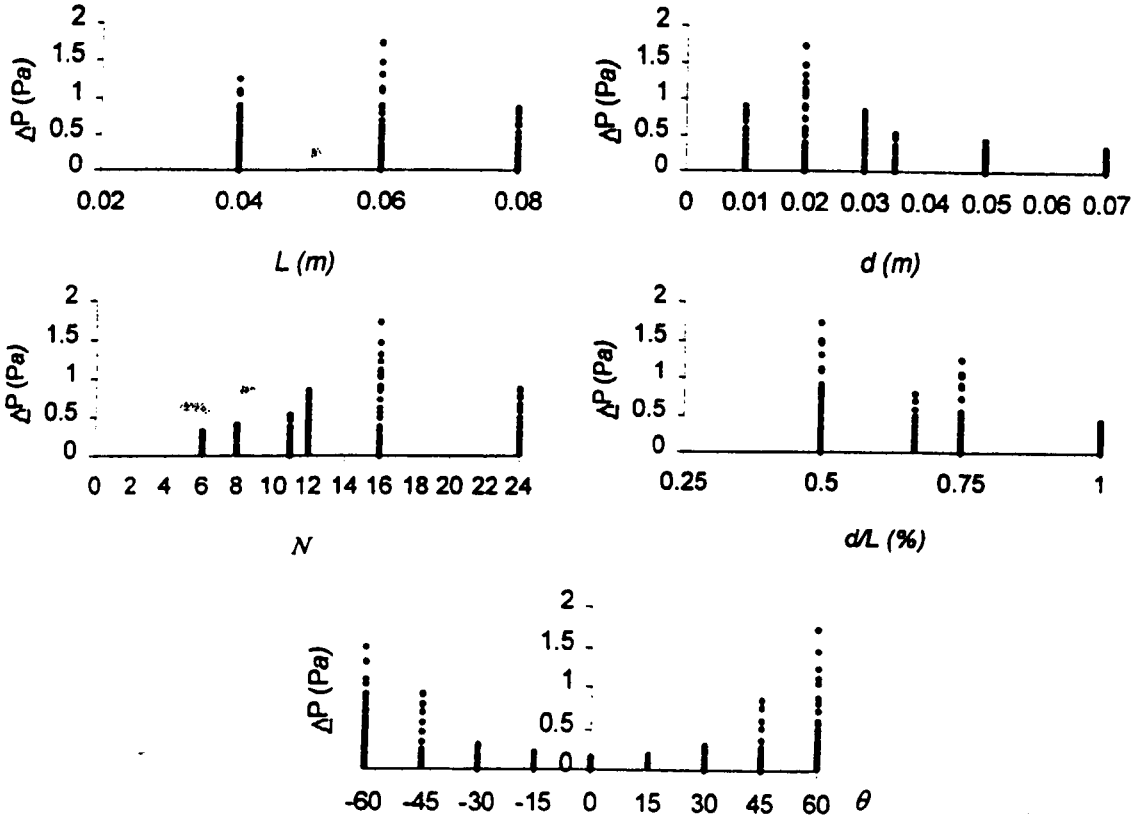

Fig.5 Differential pressures as function of various configurations of MLW

5 Conclusion

This study investigated the pressure flow characteristics over a number of full-scale MLW. The various MLW parameters included louvre inclination angle (θ), depth (L), aperture (d) and the ratio of aperture/depth (d/L %). The following points were concluded:

- The quadratic model equation suggested the best curves fits compared to that produced by power law regressions. The quadratic curves were in the form of: $\Delta P = AQ + BQ^2$. However, further adjustments of the theoretical representations of equation in the quadratic form would be required to fit other variables such as number of louvers and their inclination angles.
- The reduction in aperture area due to tilting louvre inclination angle upward or downward is the key variable to pressure drop. In contrast, louvre depth was found to be the variable with the least effect.
- Considerable pressure drop could not be achieved except at inclinations $-45^{\circ} \geq \theta \geq +45^{\circ}$. No major variations on drops were found between louvres positive and negative inclinations.
- The major enhancements in differential pressures were not due to individual variables (i.e. θ, d, L) but rather to combination of variables that would comprehensively describe ΔP. Thus, the expression of ratio (d/L) in conjunction with the inclination angles (θ) of louvers was a significant choice to comprehend the dimensionless changes in resultant pressures.

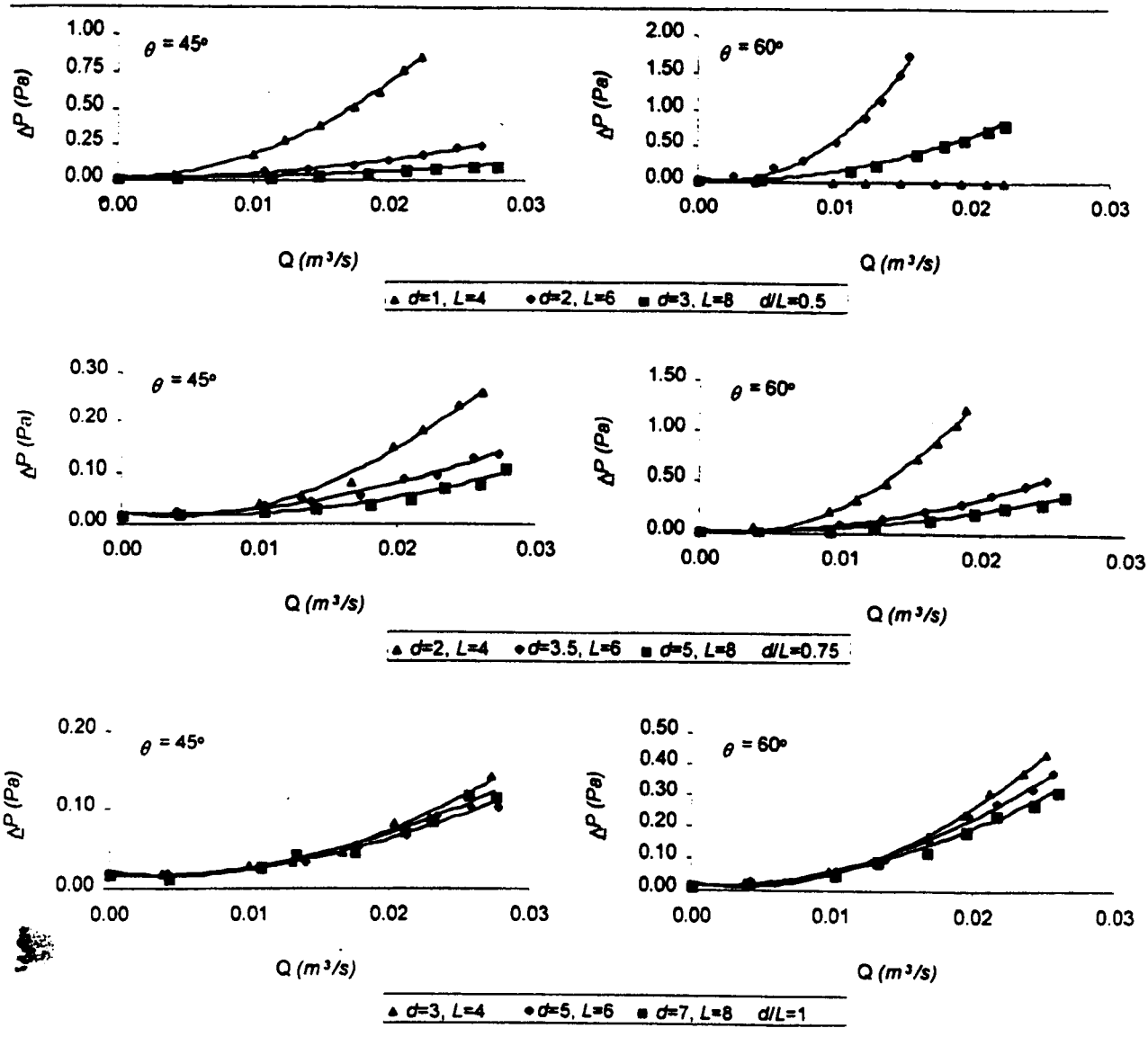

Fig.6 Differential pressures as function of various d/L ratios (0.5, 0.75, 1)

6 References

ASTM Standard E779 (1982): *Measuring air leakage by fan infiltration pressurisation method*, Annual book of ASTM standards 1418-1493.

Baker, P.H., Sharples, S. and Ward, I.C. (1987): Air flow through cracks. *Building and Environment* **22** (4):293-304. Great Britain: Pergamon Journals Ltd.

Chand, I., Bhargave, P.K., Sharma, V.K. and Krishak, N.L. (1988): Studies on the effect of mean wind speed profile on rate of air flow through cross-ventilated enclosures. *Architectural science review* **35**, 83-88.

Chand, I. (1970): Effect of the distribution of fenestration area on the quantum of natural ventilation in buildings. *Architect and Science Review* **13**, 130-133.

Dick, J.B. (1950): The Fundamentals of Natural Ventilation in Houses. *JIHVE* **18** 123-134.

Etheridge, D.W. (1997): A note on crack flow equations for ventilation modelling. *Building and Environment* 33, 325-328.

Etheridge, D. and Sandberg, M. (1996): *Building Ventilation: Theory and Measurements*, first edn. John Wiley

Pitts, A. C. and Georgiadis, S. (1994): Ventilation air flow through window openings in combination with shading devices. 15th AIVC Conference 432-439 p. AIVC.

Sherman, M., Grimsrud, D.T. and Sonderegger, R.C. (1979): Low pressure leakage function of a building. LBL-9162, Lawrence Berkeley Lab.

Thomas, D.A. and Dick, J.B. (1953): Air infiltration through gaps around windows. *JIHVE* 462-463.

Tsangrassoulis, A., Santamouris, D., Asimakopoulos, D., (1997): On the ventilation and daylight efficiency of various solar shading devices. 18th Annual AIVC Conference 225-233 p. AIVC.

Walker, I.S., Wilson, D.J. and Sherman, M. (1998): A comparison of the power law to quadratic formulations for air infiltration calculations. *Energy and buildings* **27**, 293-299.

Yakubu, G.S. and Sharples, S. (1991): Airflow through modulated louver systems. *Building Services Engineering Research and Technology* **12** 151-155.

INNOVATIONS IN VENTILATION TECHNOLOGY
21ST ANNUAL CONFERENCE
THE HAGUE, NETHERLANDS, 26-29 SEPTEMBER 2000

AIRFLOW THROUGH LOUVERS: AN EXPERIMENTAL AND CFD STUDY

S Sharples* and A A Maghrabi†

*Centre for the Built Environment, School of Environment and Development
Sheffield Hallam University, Sheffield, S1 1WB, United Kingdom
e-mail: s.sharples@shu.ac.uk

†School of Architecture
University of Sheffield, Sheffield, S10 2TN, United Kingdom
Tel: (0114) 222 0399
Fax: (0114) 279 8276
e-mail: apr95aam@sheffield.ac.uk

SYNOPSIS

In this study a series of parametric laboratory measurements were made of the velocities outside, v_e, and inside, v_i, a full-scale louver positioned in a rectangular opening located in a vertical wall forming part of a 1m x 1m x 2m deep model room. The louver parameters examined, for external incident wind speeds from 0.6 to 2.5 m/s, included louver blade depth (L), aperture (d) and distance from the louver in to room (R_d). For this initial study the blades of the louvers for each experiment were horizontal with an inclination angle θ of 0°. It was concluded that louver aperture dimensions and distance from louver both played major roles in determining the magnitude of the velocity drop, whilst the effect on v_i/v_e of louver depth dimensions was smaller. Experimental results were compared against velocity drop values predicted by the computational fluid dynamics (CFD) program FLUENT. A comparison between the experimental data and the CFD predicted results showed a generally good agreement for positions close to the internal surface of the louver. Further in to the room the comparisons showed a greater divergence.

INTRODUCTION

In recent years there has been a renewed interest in the use of natural ventilation systems in buildings as a sustainable means of supplementing or replacing mechanical ventilation and air conditioning (see, for example, NatVent[1]). For large, non-domestic buildings, in particular, the natural ventilation inlets will often consist of large wall openings with louvered covers. Night-time ventilation of buildings can also make use of secure louvered openings.

A recent study of through-the-wall ventilators was performed at the Building Research Establishment (White *et al*[2]). This indicated that interactions between components in the ventilators, such as louvers, insect screens and internal flowpaths, meant that the airflow performances of the ventilators were highly variable and not easily described by standard flow equations. One way of gaining a better understanding of these interactions is through analysis of the performance of the individual components. For louvers there is only limited design information on the airflow performance of louvers and how louver parameters (such as blade depth, blade thickness, spacing between blades and blade orientation) interact to produce the overall louver flow and velocity characteristics. This study sort to gain a better understanding of some of these interactions.

A number of researchers have investigated the effect of various window opening parameters, such as size, location and orientation, on improving indoor airflow quantity and distribution, for example Brandle and Boehm[3], Jong and Bot[4] and Sobin[5]. Others have investigated the specific mechanisms of airflow through louvers and the various parameters governing indoor air motion such as louver depth, aperture and inclination angle. Yakubu and Sharples[6] and Pitts and Georgiadis[7] focused on pressure drops across the louvers. Recently, Maghrabi and Sharples[8] investigated the influence of various louver configurations on pressure flow characteristics (ΔP) under controlled volume-flow rates (Q). They used a pressurised room chamber technique, originally developed by Baker *et al*[9], to investigate airflow through cracks. Recent louver airflow work was carried out by Oliveira and Bittencourt[10], who used louvers with dimensions similar to those of the present study.

However, in their work no consideration was given to the reduction of airflow due to the room depth and louver depth

This study describes part of a current research project to investigate the overall airflow characteristics of louvers. The louver parameters, which were examined under a series of wind speeds ranging from 0.6 to 2.5m/s, included louver depth L, aperture opening height d and room depth R_d. For this series of tests all of the louvers investigated were kept horizontal (i.e. inclination angle $\theta = 0^o$). The aim of the experimental study was to investigate any possible relationships that might exist between the velocity drops across the louver opening and the parameters given above. The laboratory results were then compared with values predicted from the computational fluid dynamics package FLUENT.

METHODOLOGY

Ten full-scale louver models with different configurations and a fixed frame measuring 0.48m high by 0.32m wide were constructed. The louver blades were 10mm thick and were made of smooth pinewood in order to reduce any surface friction effects. The louvers were adjusted to a horizontal position with an inclination angle $\theta = 0^o$. Three louvers depths (L) were chosen: 0.04, 0.06 to 0.08m. Six blade gap dimensions (d) were used: 0.01, 0.02, 0.03, 0.035, 0.05 and 0.07 m (see Table 1 and Figure 1).

Table.1: Louver configurations used in the study

Louver Number	Blade Depth *L (m)*	Blade Aperture *d (m)*	Number of Blades N	Porosity (p%)
1	0.04	0.01	24	50
2	0.04	0.02	16	66
3	0.04	0.03	12	75
4	0.06	0.02	16	66
5	0.06	0.03	12	75
6	0.06	0.035	11	77
7	0.06	0.05	8	83
8	0.08	0.03	12	75
9	0.08	0.05	8	83
10	0.08	0.07	6	87

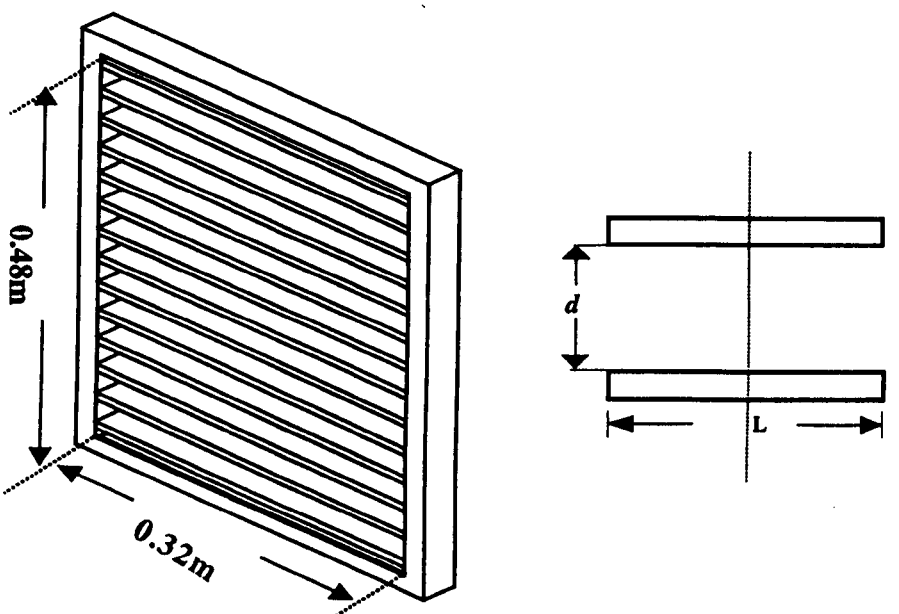

Figure 1 Louver dimensions and geometric definitions

An attempt was made to trace the flow reduction in the occupied zone along a room. For this a room chamber of 1×1×2 *m* long was constructed to represent the environment where internal velocity was recorded. Model louvers were fitted at one end of the chamber and the other end, the air-exiting side, was left open in an attempt to investigate flow patterns that were solely due to the various louver configurations. Pre-set holes on the floor of the chamber were made to represent locations where a high precision hot wire anemometer was positioned to provide a convenient readout of air velocity. Calibrations of the anemometer were carried out to provide a linear output of 0 to 5 volts DC for a velocity range of 0 to 5 m/s. The anemometer's voltage signals were logged on a computer and the software was adjusted to take three readings per second and give an average velocity reading over 30 seconds, 60 seconds and 120 seconds. The first average timing (30 seconds) was chosen to represent the mean values for velocities v_i and v_e as no major differences were found with the longer averaging times. Another hot wire anemometer was used to measure the external air velocities. This anemometer was placed outside the louver opening room chamber to measure wind velocities at pre-set distances of up to 0.75m from the louver. It was evident that the resistance to airflow caused by both the chamber and the louver resulted in discrepancies to readings taken too near to the panel. Beyond a distance of 0.50m from the louver these discrepancies were diminished and so all external velocities were measured at this distance.

For internal velocities detailed analysis of velocity drops along horizontal sections of flow was attempted. Six different locations were selected along the length of the chamber as shown in Figure 2. The pre-set distance between them was 0.25m. The inaccuracies in readings at R_d<0.25m due to the presence of jet flows led to R_d = 0.25m acting as the first measuring location inside the room.

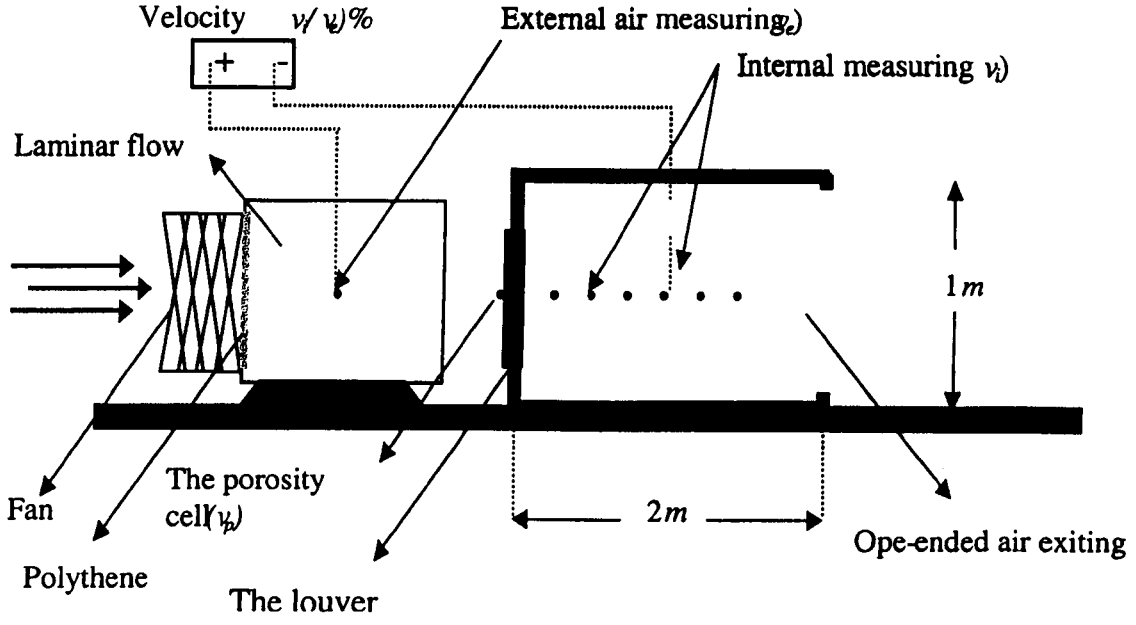

Figure 2 Schematic diagram of the experimental set-up.

Two 0.48m diameter fans placed in series and facing the front panel of the model room were used to generate the external wind velocity v_e. Initial velocity measurements showed that the fans tended to generate higher velocity profiles at the edges of the fans compared to the central axis. To produce a more uniform incident velocity field a polythene sheet (0.01m thick) was placed at the fan's air exit. Additionally, proper alterations were made to assure laminar flow towards the examined units. The measurements were then carried out after ensuring a steady flow of air using procedures detailed in Etheridge and Sandberg [11]).

RESULT

This study investigated the velocity drop across the louver model configurations given in Table 1. The louver depth L, external wind speed v_e and aperture d of the louvers were investigated, together with the effect of room depth R_d.

Louver depth L

The measured variations of the velocity ratio v_i/v_e along the room length as a function of louver depth L is shown in Figure 3.

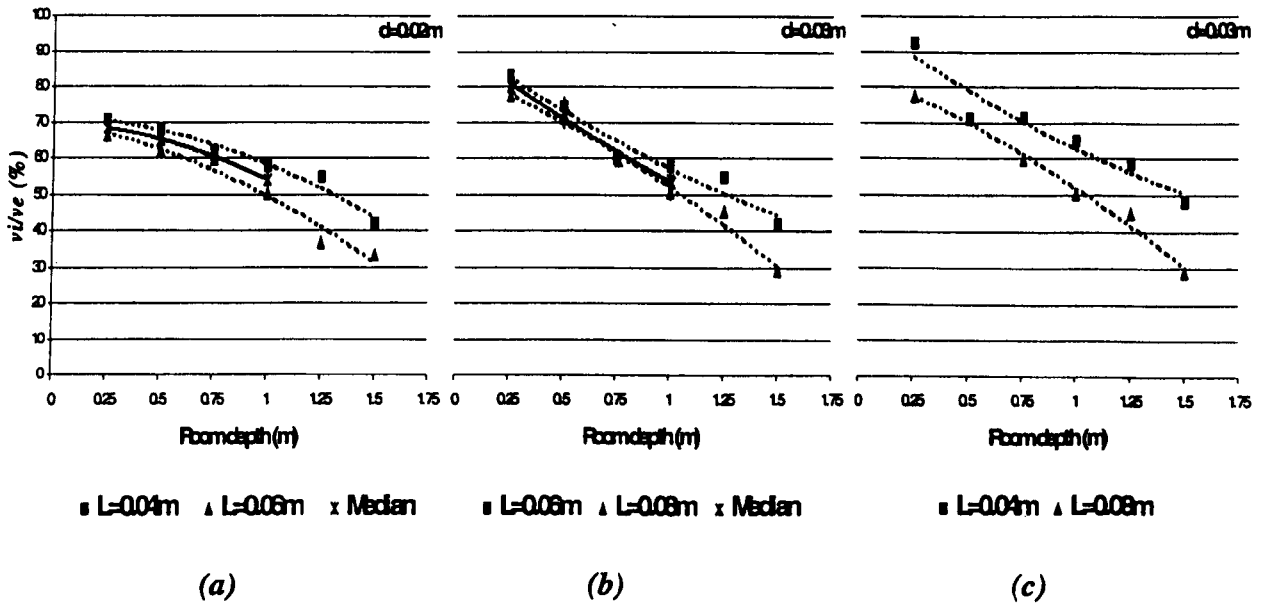

Figure 3 Variation of v_i/v_e as a function of louver blade depth L

Figures 3(a) and 3(b) show that increasing louver depths by small amounts had little effect on the velocity ratio close to the louver. However, with increasing distance in to the room the ratio values start to diverge, with the longer blade depth exhibiting a larger reduction in velocity. Figure 3(c) shows the impact of doubling the louver blade length from 0.04 to 0.08m. There is now a significant and relatively constant velocity ratio difference of 15% to 20% along the length of the room, with the 0.08m blade showing the larger reduction. The external wind speed v_e used in all of these experiments was measured as 2 m/s.

Wind speed v_e

Internal velocities at various locations along the room depth were recorded against external wind speeds that ranged from 0.6 to 2.5m/s. For the smaller louver apertures examined, i.e. $d \leq$ 0.03m, the ratio v_i/v_e was found to vary significantly with the magnitude of the external wind speed and distance R_d in to the model room. For larger apertures variations in external wind speed had much less effect on v_i/v_e close to the louvers (low values of R_d), but there were greater variations at some distance in to the room. Table 2 shows the ratio of v_i/v_e at 2.5m/s to v_i/v_e at 0.6m/s. A ratio value of 1.00 would indicate that the change in external wind speed was having no effect on the value of v_i/v_e. All values shown in Table 2 are for measurements along the centre line of the model room

Table 2 Ratio of v_i/v_e values for high to low external wind speeds

	d = 0.02 m L = 0.06 m	d = 0.03 m L = 0.06 m	d = 0.05 m L = 0.06 m	d = 0.07 m L = 0.06 m
Room depth R_d	Ratio	Ratio	Ratio	Ratio
0.25 m	1.21	1.13	1.08	1.01
0.50 m	1.34	1.24	1.08	1.03
0.75 m	1.44	1.40	1.17	1.06
1.00 m	1.47	1.37	1.32	1.14

A possible explanation of the results in Table 2 could be the resistance to airflow caused by the narrow louver spacings. For low d values the low wind speed will lose most of its kinectic energy overcoming the flow resistance of the louver gap, and so the flow on the other side of the gap inside the room will be weak. As d increases the low and high wind speeds easily push the air through the wider gaps and so the internal velocity close to the louver is higher and steadier.

Louver aperture *d*

The effect of louver aperture d on the velocity drop across the louvers v_i/v_e was investigated for several room depth locations R_d along the centre line of the room for a fixed value of louver depth L. For high wind speeds with the largest aperture (d = 0.07m) the air speed in the room at a depth of 1.0m was still nearly 80% of the external air speed. For the same location an aperture of d = 0.02m could only generate 55% of the external air speed. Figure 4 shows the experimental points and the least squares fit curves produced for the louver apertures as a function of d and R_d.

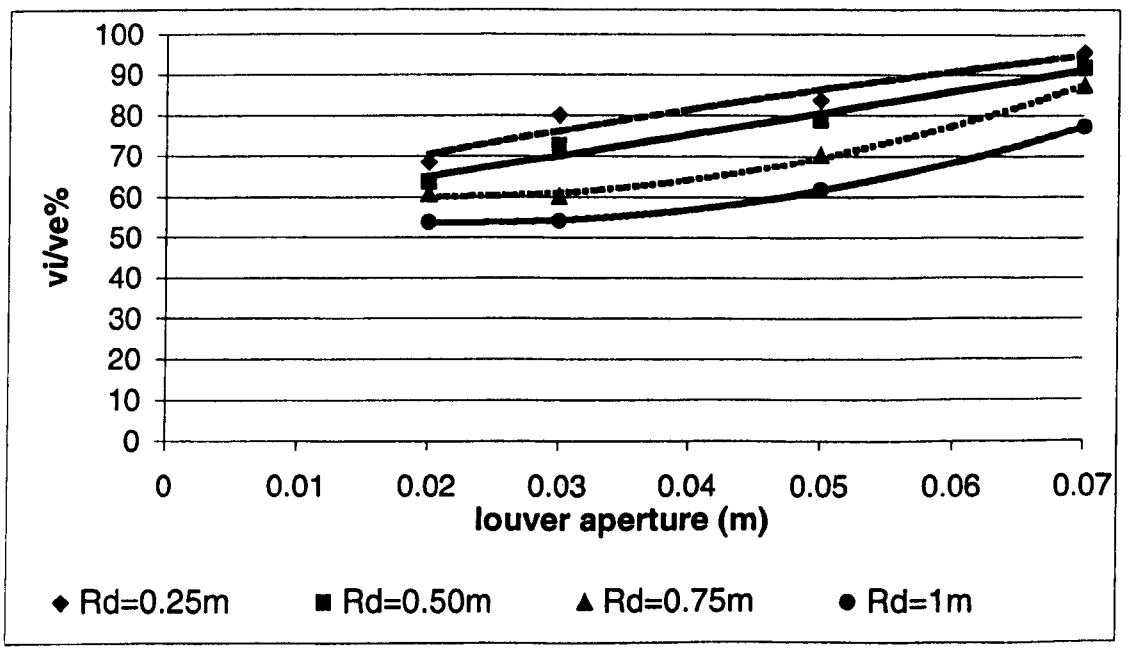

Fig. 4: v_i/v_e produced for louver apertures measured at various R_d.

CFD APPRAISAL.

Computational Fluid Dynamics (CFD) can be used to predict the indoor velocities and overall ventilation effectiveness of natural or mechanical air distribution systems. In this study FLUENT [12] software was used for the CFD simulation of the louver-room configuration. A number of case studies were tested first to simulate the laboratory work. The specification of boundary conditions was carefully established as the assumed boundary conditions play a vital role in the results predicted from the simulations. A refined grid domain of 250 x 100 nodes was established in the room and the vicinity of the louvers. The k-ε model was implemented in the simulation to represent the flow turbulence. The k-ε model is a widely used method to represent turbulence in CFD (Jones and Whittle, [13]). The results of velocity readings were taken when the simulation process was fully converged or when the global absolute residuals from the iterations reached a very low limit (approximately less than 1×10^{-4}).

The CFD analysis was used to predict the ratio of v_i/v_e for comparison with the experimental data. Two sets of comparisons were made. In the first the measured and predicted values of v_i/v_e were compared at a point close to the louver (R_d = 0.25m) for louver (L, d) values of (4, 2), (6, 3.5) and (8, 5). The results from this are presented in Figure 5. There is good agreement for the reasonably strong airflows encountered very close to the room side of the louvers, which gives encouragement that CFD can be used to predict the local air velocities around louvers. In the second comparison the room depth was varied from 0.25 to 1.5m and the v_i/v_e ratios from CFD and experiment were examined. The results for two louver settings (L=0.08, d=0.03 and L=0.08, d=0.07) are shown in Figure 6. These results are representative of the trends observed in other louver combinations The agreement is still good close to the louver, and the general form of the variation with R_d is similar. However, there is a marked divergence between CFD and experimental results as R_d increases, and towards the back of the room model the differences become very large (around 50%). The design of the room model left the back of the model open with no obstructing wall. It may be that this boundary condition needs to be better defined in future studies as the airflows in this location will be weaker and so more susceptible to large variations over small spatial distances.

CONCLUSIONS

This parametric and CFD study of airflow through louvers has highlighted the following:

- airflow velocities in a room containing a louver covered opening result from an interaction of louver geometry, room geometry and prevailing wind conditions
- the key parameters for louver performance are the aperture opening (distance between louver blades) and the distance from the louvers in to the room
- small changes in the depth of the louver blade do not have a significant effect on airflow velocities
- CFD analysis has been successfully used to predict air velocities in the region close to the room side of the louvers

- CFD analysis was less successful in predicting air velocities towards the rear of the room at some distance from the louver opening

- Further CFD simulations are required to identify appropriate boundary conditions to improve the agreement with the experimental data for all locations within the room.

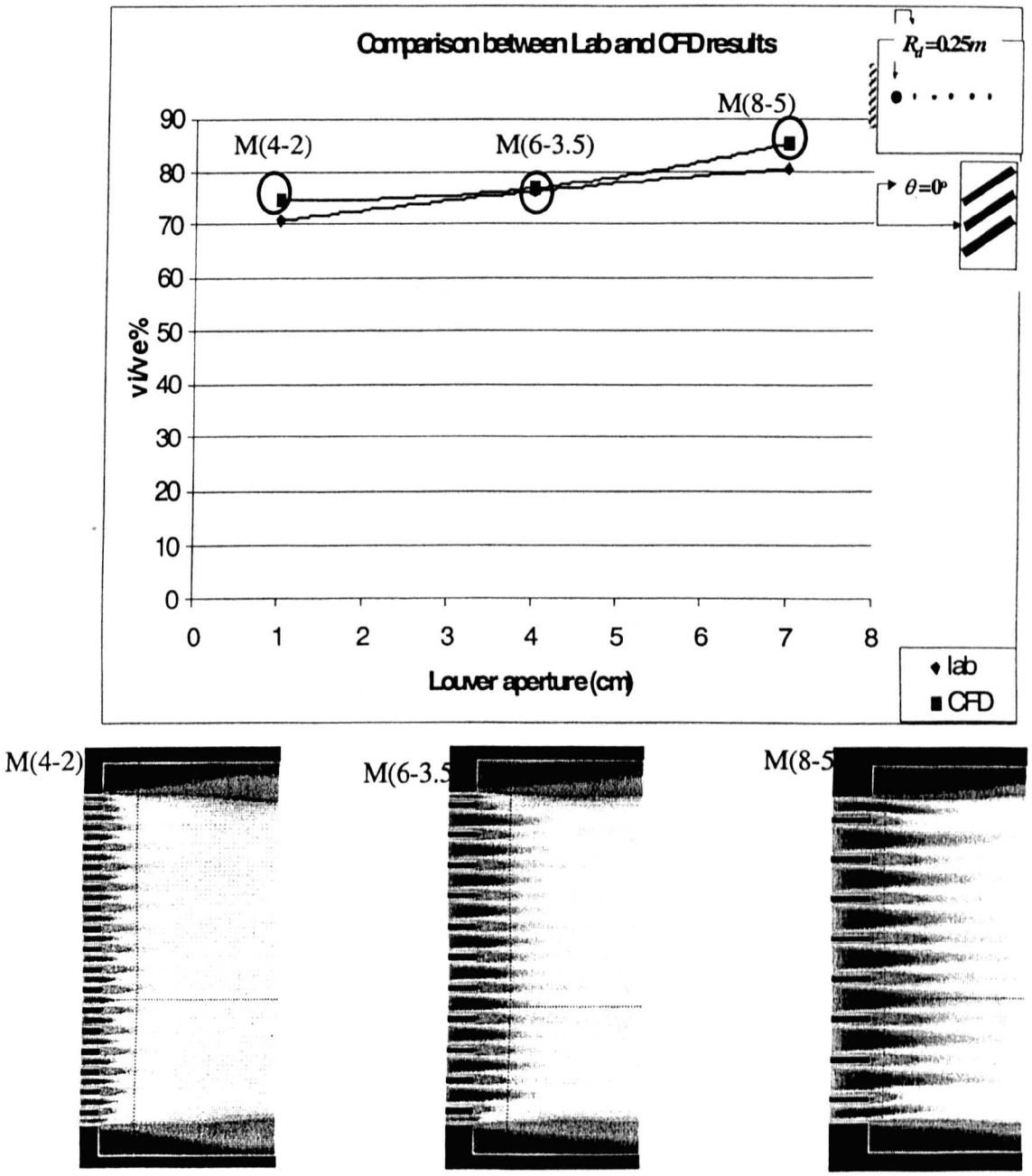

Figure 5 Comparison of CFD and experimental v_i/v_e values at R_d =0.25m

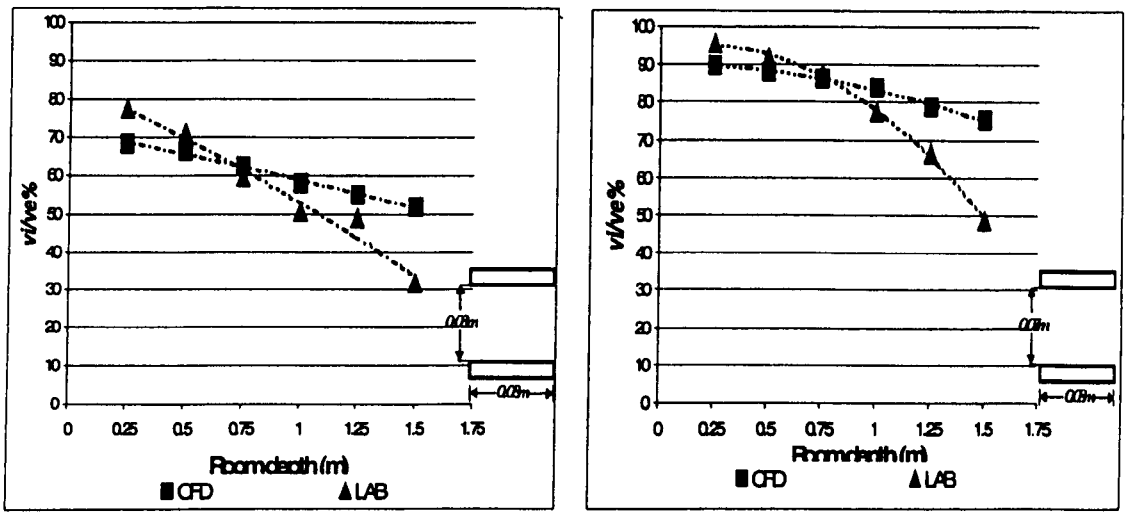

Figure 6 Comparison of CFD and experimental v_i/v_e values for two louvers configurations (a) 0.08-0.03 (b) 0.08-0.07 as a function of room depth R_d

REFERENCES

1. V. Kukadia and M D A E S Perera
NatVent™: aims and vision.
Proc. 19th AIVC Conference, 388-397, Oslo, 28th -30th September, 1998

2. M White, G McCann, R Stephen and M Chandler
Ventilators: ventilation and acoustic effectiveness.
BRE Information Paper IP4/99, 1999

3. K Brandle and P E Boehm
Airflow windows: performance and application. .
Proc. ASHRAE/DOE Conference. "*Thermal performance of the exterior envelope of the building* II", 361-379, 6th-9th December 1982

4. T Jong and G P A Bot
Flow characteristics of one-side mounted windows.
Energy and Buildings **19**, 105-112, 1992.

5. H Sobin
Window design for passive ventilative cooling: an experimental model-scale study.
Proc. International Conference on Passive and Hybrid Cooling, 191-195, Miami, 1999

6. G S Yakubu and S Sharples
Airflow through modulated louver systems.
Building Services Engineering Research and Technology **12** (4), 151-155, 1991.

7. A C Pitts and S Georgiadis
Ventilation air flow through window openings in combination with shading devices.
Proc. 15th AIVC Conference, 432-439, Buxton, UK, 27th-30th September, 1994.

8. A A Maghrabi and S Sharples
Air flow characteristics through Modulated Louvered Windows.
Proc. PLEA Conference, 507-514, Brisbane, 22nd-24th September, 1999.

9. P H Baker, S Sharples and I C Ward
Air flow through cracks.
Building and Environment **22** (4), 291-304, 1987

10. F Oliveira and L S Bittencourt
Air flow through louvered windows in small rooms.
Proc. PLEA Conference, 393-396, Lisbon, 1st-3rd June, 1998.

11. D Etheridge and M Sandberg
Building Ventilation: Theory and Measurements.
John Wiley & Sons, 1996.

12. FLUENT (version 4.51). 1999. New Hampshire, USA, Fluent Inc.

13. P J Jones and G E Whittle
Computational Fluid Dynamics for building air flow prediction-current status and capabilities.
Building and Environment **27** (3), 321-338. 1992.